D3.4 Report

Report on assessed risk and impacts in all EU case study areas

This project has received funding from the European Union´s Seventh Framework Programme for Research, Technological Development and Demonstration under Grant Agreement Nº 603663 for the research project PEARL (Preparing for Extreme And Rare events in coastal regions).

pearl
Preparing for Extreme And Rare events in coastaL regions

D3.4 Report

Report on assessed risk and impacts in all EU case study areas

Dissemination level (select one):
PU = Public
PP = Restricted to other programme participants (including the Commission Services)

Document Information

Project Number	***603663***	Acronym	**PEARL**
Full Title	Preparing for Extreme and Rare events in coastaL regions		
Project URL	http://www.pearl-fp7.eu/		
Document URL			
EU Project Officer	Denis Peter		

Deliverable	Number	D 3.4	Title	Report on assessed risk and impacts in all EU case study areas
Work Package	Number	WP3	Title	Holistic Risk Assessment

Date of Delivery	Contractual	01.06.2017	Actual	04.03.2017
Status	version 1.0		final Ĭ	
Nature	report X			
Dissemination level	public X			

Abstract (for dissemination, 100 words)	This report describes the work conducted in the EU case studies and some international case study areas of PEARL to determine the level of risk due to extreme events occurred in the past. Each chapter describe the data used to conduct the analysis of hazard and vulnerability assessment. For vulnerability analysis, PEARL has developed a flexible methodology to be able to be applied in a wide variety of cases with different levels of information. Finally each chapter presents a description about the methods used to aggregate the information and produce risk maps.
Keywords	Hazard assessment, Vulnerability assessment, Impacts, Risk

Version Log				
Issue Date	Rev. No.	Author	Change	Approved by

Disclaimer

The research leading to these results has received funding from the European Union Seventh Framework Programme (FP7/2007-2013) under Grant agreement n° 603663 for the research project PEARL (Preparing for Extreme And Rare events in coastaL regions).

Summary

This report describes the work conducted in the EU case studies and some international case study areas of PEARL to determine the level of risk due to extreme events occurred in the past. Each chapter describe the data used to conduct the analysis of hazard and vulnerability assessment. For vulnerability analysis, PEARL has developed a flexible methodology to be able to be applied in a wide variety of cases with different levels of information. Finally each chapter presents a description about the methods used to aggregate the information and produce risk maps.

This report is structured in the following way: each PEARL partner responsible for the case study area have documented the work that has been conducted so far in relation to the methods and tools used to estimate Hazards, Vulnerabilities and Risk. Chapters 2- 10 presents the description of each case study area.

Contenido

List of figures

List of tables

Abbreviations

Glossary

1 Introduction

Task 3.4 have conducted the risk assessment in EU case studies (and in some international case studies such as St Maarten and/or Thailand). The integrated modelling and holistic risk assessment framework and tools have been applied to the case studies for evaluation of risks of multi-hazard scenarios. The work performed in the case studies generates different scenarios that are used to support decision makers.

This means that the outcomes from simulation runs, which will start from a range of initial parameter settings, will tend to converge to a specific and very limited set of outcomes. By systematically exploring a wide range of initial parameters and scenario values, which will provide insight into which types of actor decisions, parameterisations and scenarios will lead to which types of end states. Model simulations will be carried out offline and incorporated into the platform developed in WP5 for stakeholder use. Displaying relevant simulation output data, initial conditions and end states within the platform will enable stakeholders to explore the collective effects of their individual decisions and whether they will lead to more or less desirable futures.

Additionally, the lessons learned and experiences gained in the international case studies that are collected in Task 6.4 are analysed and where it was possible have been cross-referenced with the outcomes from the EU case studies.

2 Case Study Marbella

2.1 Description of the study area

2.1.1 *Main geomorphologic, social and economic features*

Marbella is a city that belongs to the province of Malaga and it is part of the ñCosta del Solò It is located in the south of Spain, in the region called Andalusia. The city extends for 117 km^2 and 138,679 (according the Spanish Statistical Office in 2015) inhabitants live there with a density of almost 1,200 inh/km^2.

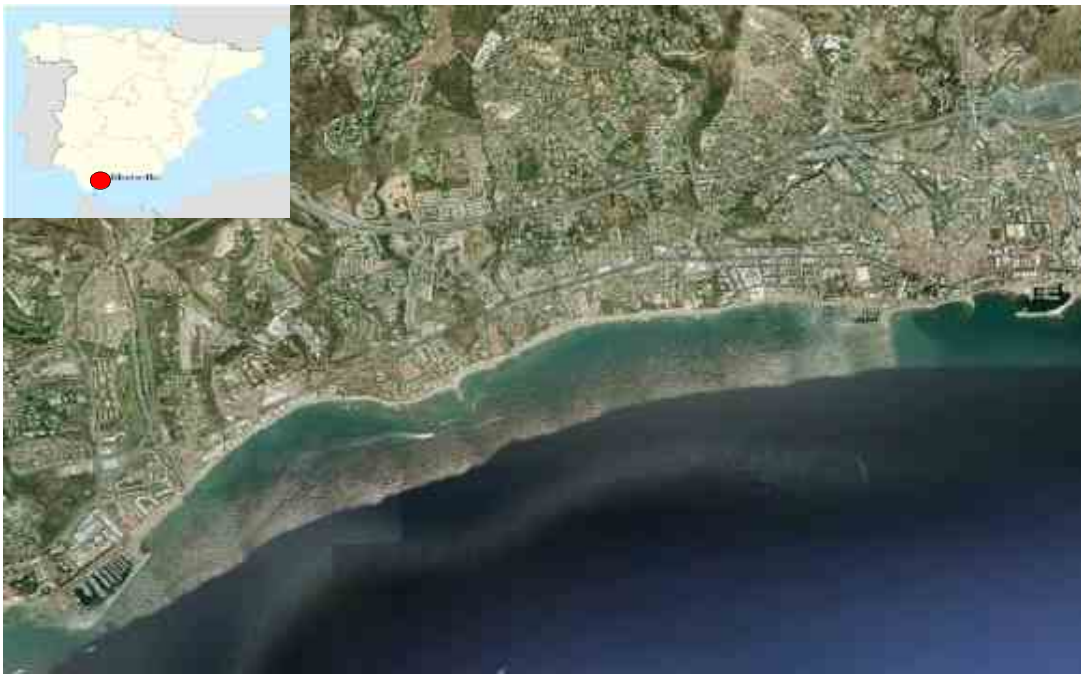

Figure 2-1. Marbella map and location.

Marbella is characterized by a significant slope gradient, which decreases from the highest part of the city until it reaches the Mediterranean Sea. Three main river streams affect the area: Guadalmina (28 Km, 68 Km^2), Guadaiza (22 Km, 45 Km^2) and Rio Verde (35 Km, 150 Km^2).

Marbella shows a significant amount of rainfall per year. The mean annual value is 625 l/m^2, which the main part occurs during the months of summer and autumn.
The climate conditions are the Mediterranean typical ones, with a mean annual temperature of 18 °C, dry hot summer and wet warm winter.

Since the city involves maybe 44 Km of coastline, many beaches and recreational ports are present in the city. The main economic activity is the tourism, which mainly involves wealthy people, therefore assets and properties are characterized by high economic value. An example is given by the presence of high-class resorts, recreational ports, golf clubs and many other luxurious facilities.

2.1.2 *Main challenges that affect the case study*

Main challenges that threaten Marbella are due to its particular topography. In fact, the city is characterized by various kinds of morphological elements like extensive coastal plains that come from previous mountains eroded during the centuries and high mountain elements like Sierra Blanca Mountain that contrasts to its flat morphology.

These different morphological elements promoted the development of short rivers along the city, characterized by steep banks that put Marbella at risk of flash floods.

Situation results even worse because of the irregular nature of rainfall events in Marbella. ñGota fríaò is a significant meteorological phenomenon that characterizes the case study. It is generated by cold air fronts that penetrate into warm air ones at high altitude. The consequence is given by high intensity precipitations and strong storms, which mainly take place in fall.

These rainfall events provoke urban flood events characterized by short lead times, therefore significant runoff values that are not manageable by the existing drainage network, which does not have such a capacity to drain the whole runoff.

Furthermore, because of the presence of many small fluvial streams that cross the city, many flash flood events may occur under ñgota fríaòconditions.

Another challenge for the city is given by storm surges, which often provoke important problems in recreational ports and increase erosion activity in the several beaches of the city. Therefore, the main challenges that have been identified in Marbella city are flash flood and storm surge and they are characterized by high potential to create huge damages to people, assets and natural landscape.

The risk is even increased when both phenomena occur at the same time because, in this case, water runoff cannot be discharged into the sea. The main consequences are higher water depth and velocity values, so higher damages to assets and people.
Some effects of climate change has been already identified, like the jellyfish bloom, which has been jeopardizing tourism in recent times.

2.2 Data collection and analysis for hazard assessment

2.2.1 *Rainfall data sources*

Application of the hydraulic model to get depth and velocity values implies the knowledge of rainfall data in Marbella to obtain project storms for all return periods considered in this analysis.

Rainfall data has been collected from the AEMET (Agencia Estatal de Meteorologia), which is the national meteorological agency to deal with design storms in Spain.
AEMET provided maximum daily rainfall series for durations of: 10, 20, 30, 60, 360, 720 and 1440 minutes, corresponding to six gauge stations located close to Marbella.
It has been chosen to use just data corresponding to Malaga airport station because it resulted characterized by many years of observations and its data resolution has been considered

suitable for the purpose of this study. Available data consists of 34 years of record for short duration (from 10 minutes to 12 hours) and 72 years for long duration (24 hours).

Several comparisons have been done in order to verify that Malaga Airport can represent properly the study area.
Besides the historical rainfall series, analysis has been conducted for two climate scenarios corresponding to regional climate model RCP4.5 and RCP8.5 (both for the period 2006-2100). Furthermore an additional set of historical model data has been provided for the period 1960-2005.

These data has been provided by the Max-Planck-Institut, which deals with climate change modelling.

2.2.2 *Rainfall data elaboration*

Current rainfall analysis has been done through Log-Pearson Type III distribution, from which expected probable rainfall has been computed.

Empirical intensities have been calculated for the wanted return periods, which are: 1, 2, 5, 10, 20 and 100 years.

Since Marbella study area is characterized by the probability of flash flood events, intensities corresponding to short durations have been obtained through Shermanîs formula.

In this way, it was possible to create IDF curves suitable to build project storms with intervals of 10 minutes.

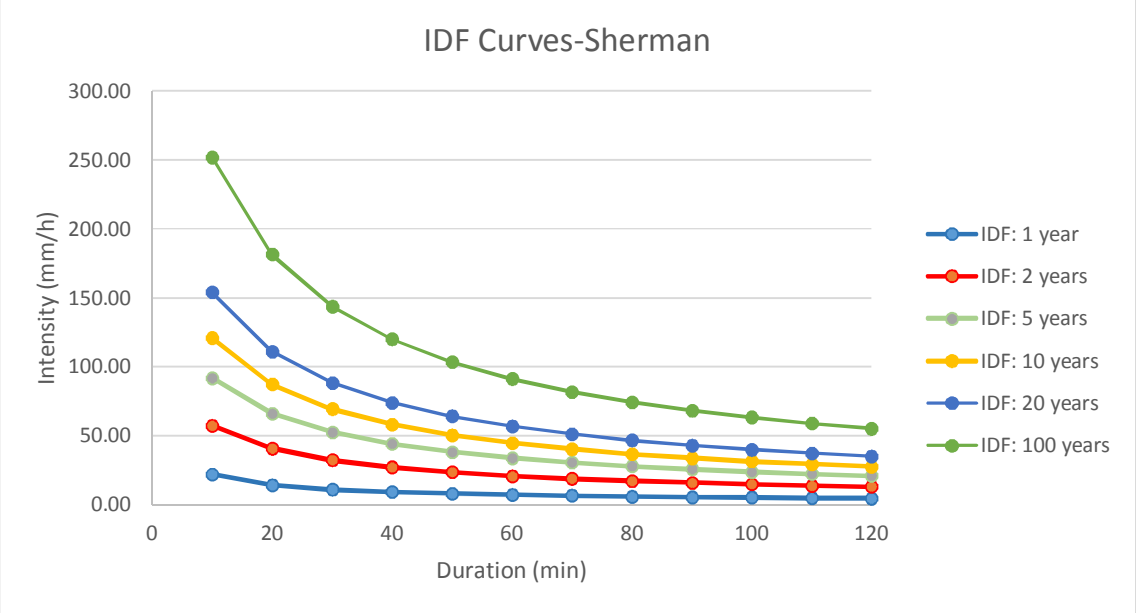

Figure 2-2. IDF Curves ï Sherman per each return period studied.

Through these intensity values, alternating block method has been applied to get project storms. Two examples, corresponding to 10 and 100 years return periods are reported.

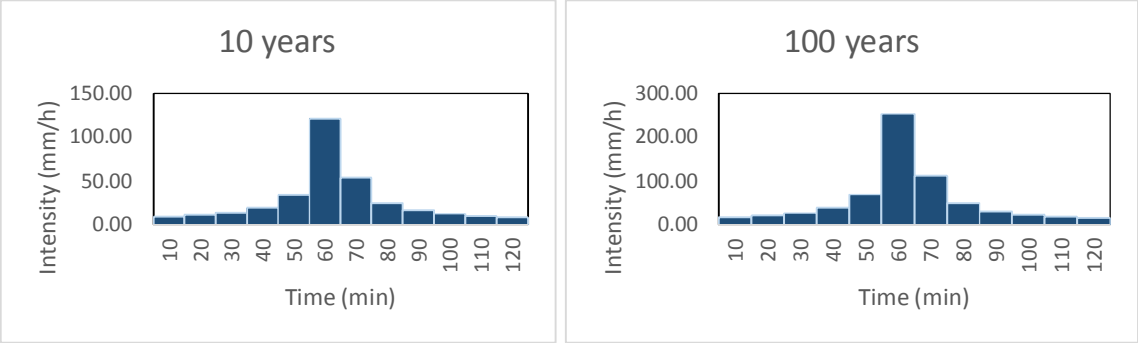

Figure 2-3. Projected storms intensities for 10 and 100 years return period.

In order to obtain project storms for the three data sets provided by the Max-Planck Institute, a temporal downscaling process has been applied to compute intensity values corresponding to short durations.

In this case, GEV distribution has been chosen to conduct the analysis. Distribution parameters for short durations have been obtained using the scale parameters and distribution parameters corresponding to 6 hours:

$$\square = \square_{\square\square\square}$$

$$\square = \square^{\square} \cdot \square_{\square\square\square}$$

$$\square = \square^{\square} \cdot \square_{\square\square\square}$$

Where $\square^{\square}$ is called scale parameter and has been computed as ratio between the first no-central moments of higher and lower durations.

IDF curves involving short duration intensities have been compared to IDF curves obtained through GEV distribution. Results show a good correspondence:

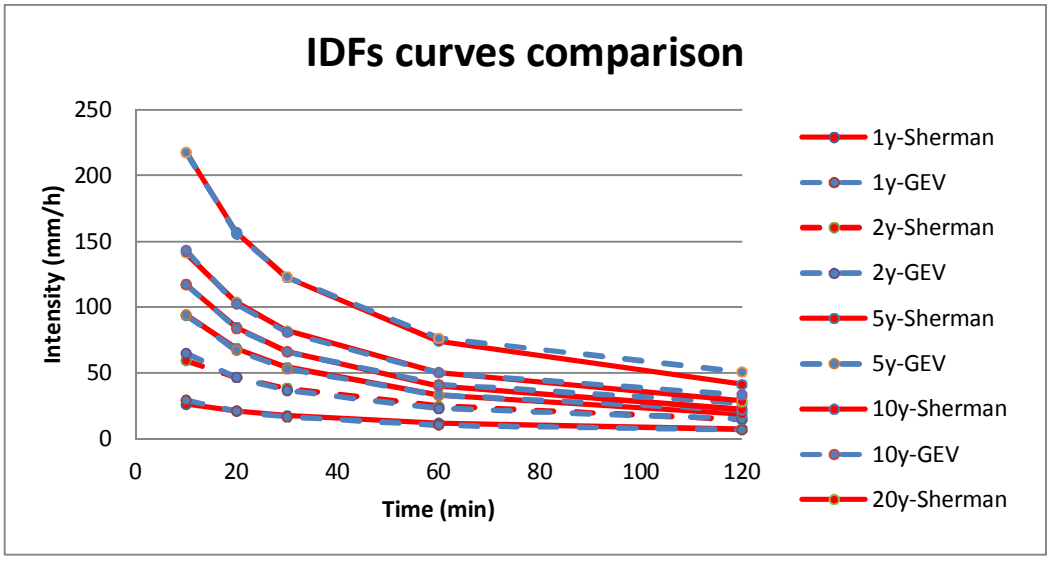

Figure 2-4. Comparison between IDFs obtained through GEV distribution and Sherman method

2.2.3 *Data collection and calibration*

Hazard assessment has been done through a coupled 1D/2D model of Represa's subcatchment. The model covers 10.6 km^2 of the municipality land involving 68 km of sewers. A 2D unstructured mesh with more than 60 thousand cells was created on the basis of a detailed digital terrain model (DTM). For this study, a specific 2 m2 resolution DTM model has been used. This DTM was generated by a LIDAR (laser imaging detection and ranging) flight with a minimum density of 0.5 points /m2 and a precision of 20 cm in terms of ground elevation provided by the National Geographic institute of Spain. The model is being calibrated using a set of sewer sensors (3 water level sensors and 1 rain gauge) of well-recorded flooding events that occurred during the last months. DTM, catchments limits and the location of these sensors can be observed in the following figure.

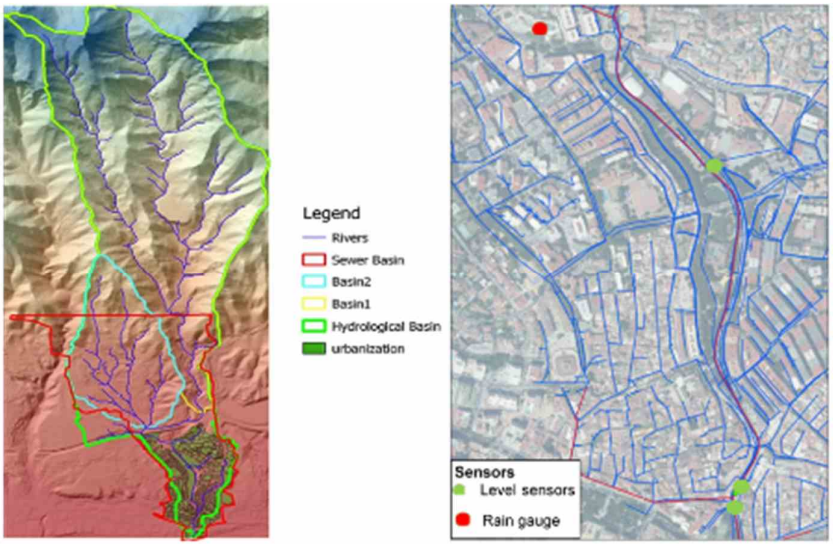

Figure 2-5. DTM and main basins affecting Marbella case study (left). Location of the sensors within the sewer network (right).

Two different type of data type are being collected to calibrate the model. On one hand, rainfall data of a rain gauge located downstream of the main highway crossing the city and, on the other hand, water level time series collected by 3 water level sensor distributed along the sewer network (**Error! Reference source not found.** right). One of them is located inside an 800 mm conduit of diameter at the upper part of the city. The two others are inside the Represa channel, upstream and downstream the Huelo river junction. Represa channel was executed to convey storm water produced in the peri-urban catchment and transport it directly to the sea.

Both data types are processed with the purpose of run different past scenarios and calibrate the developed model.

Regarding the calibration for 1D/2D model being developed in Marbella Case, the main processes identified for the modelling are rainfall-runoff transformation and flow propagation in the sewer network. The main parameters studied are:

- Hydrological initial losses: In this case, the totality of the runoff generated on roofs and roads has been directly connected to the sewer network has been considered.
- Surface roughness coefficients: Two different coefficients have been taken into account depending on the type of surface considered: streets and roads (0.016) and rural areas (0.025).
- Hydrological losses (in pervious areas): Horton method is being implemented whose parameters have been calibrated in similar experiences (initial infiltration=20mm/h, residual infiltration=7.2mm/h, decay constant=0.043h^{-1} and recovery constant=0.108h^{-1}).
- Routing parameters: Cells characteristics and representation of the area excluded by 2D domain, which are building and other infrastructures (roads and train railways) that suppose an interruption of the surface flow and most of time have their own and independent drainage structures.

Calibration is the procedure for ensuring an acceptable level of confidence in a modelôs ability to accurately represent the real system. It refers to the whole process of ensuring that a model behaves a similar to the real system as possible. For urban surface runoff models, it is recommended that at least three events are used (DHI 2002). By the moment, 4 events have been used for parameter estimation in this case (**Error! Reference source not found.**).

Date event	Cumulative rainfall (mm)	Maximum rainfall intensity in 10 minutes (mm/h)	Function of the event
25/11/2016	77	34.8	1D/2D calibration
04/12/2016	198.5	56.3	1D/2D calibration
14/12/2016	15	33.4	1D calibration

Table 2-1. Events selected for calibration of 1D/2D flood model (Marbella Case Study).

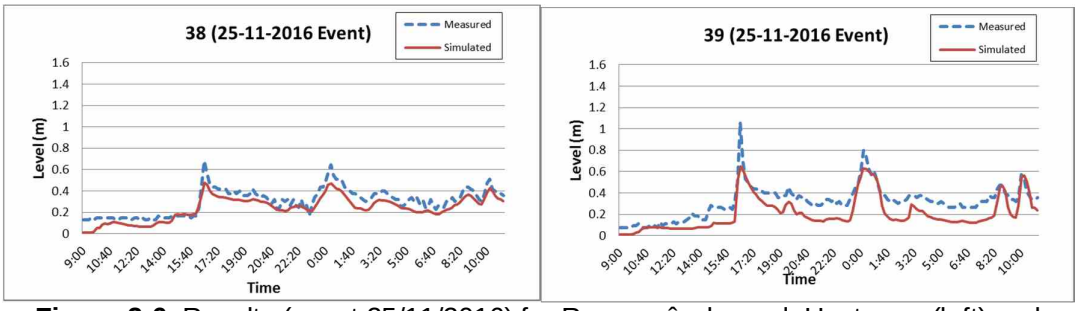

Figure 2-6. Results (event 25/11/2016) for Represaôs channel. Upstream (left) and downstream (right) Huelôs river junction.

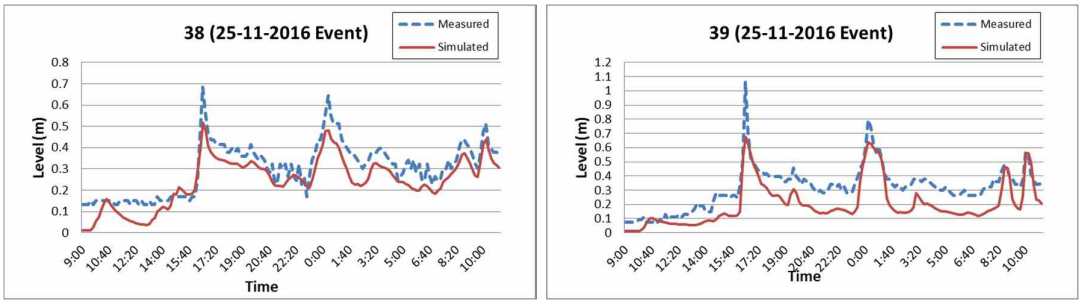

Figure 2-7. Results (event 25/11/2016) for Represas channel. Upstream (left) and downstream (right) Huelos river junction.

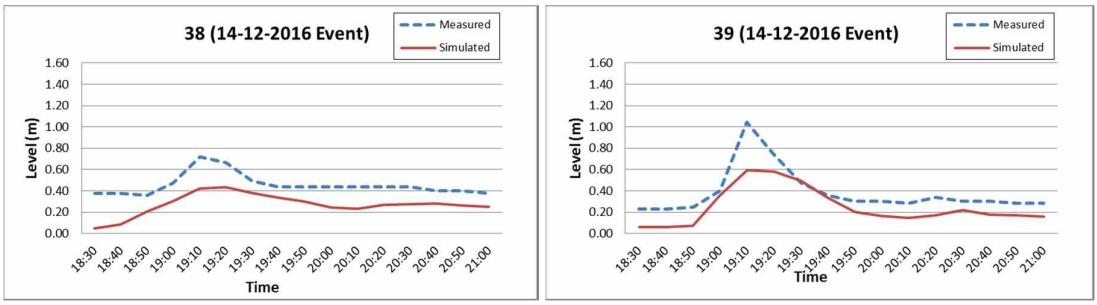

Figure 2-8. Results (event 14/12/2016) for Represas channel. Upstream (left) and downstream (right) Huelos river junction.

Common statistical analysis was carried out in order to evaluate the calibration processes (**Error! Reference source not found.**).

Code	Location	Coeficient of determination R^2	Root mean squared RMSE	Measured peak level (m)	Simulated peak level (m)	Peak Error (m)	Time to Peak Error (minutes)
Calibration event: 25/11/2016							
38	Upstream Huelos river junction	0.92	0.07	0.68	0.47	0.21	0
39	Downstream Huelos river junction	0.92	0.11	1.07	0.65	0.41	0
Calibration event: 04/12/2016							
38	Upstream Huelos river junction	0.62	0.23	1.33	1.15	0.18	30
39	Downstream Huelos river junction	0.56	0.29	1.50	1.28	0.22	40
Calibration event: 14/12/2016							
38	Upstream Huelos river junction	0.75	0.20	0.72	0.43	0.29	10
39	Downstream Huelos river junction	0.88	0.17	1.05	0.60	0.45	0

Table 2-2. Statistical parameters related to calibration processes for the sewer facilities used in this study.

Other sources of information, such as emergency reports from police officers, firefighters and the affected population during the heavy storm events, were also used for the calibration/validation processes. This type of data is a very useful information for the calibration of the model in case of surface flooding as well as for the detection of critical points of the network where the there are no surface water level sensors (as commonly in urban drainage).

Figure 2-9. Calibration results for Navedul Avenue. Flow depths provided for the model for the event of 25 November 2016 were compared to images recordered during this event. On the right, it is possible to observe the water depth map in the cells arround Navedul Avenue. On the left, in photo from a local newspaper where can be observed water depths just above the kerb.

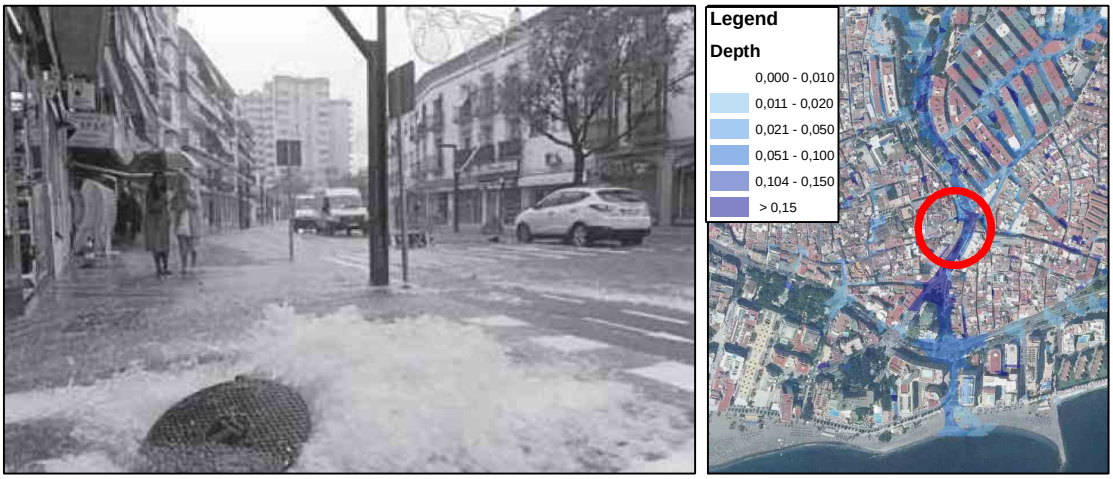

Figure 2-10. Calibration results for Navedul Avenue. Flow depths provided for the model for the event of 04 December 2016 were compared to images recordered during this event. On the right, it is possible to observe the water depth map in the cells arround Navedul Avenue. On the left, in photo from a local newspaper where can be observed runoff over the roadway and overflow from the sewer network.

2.2.4 *Hazard assessment*

A consensus has been reached within the field of urban drainage and storm water management that hazard for pedestrians can be assessed taking into account two specific flow parameters: water depth and velocity.

In the studies of Russo *et al*. (2009; 2013) (as a first experimental campaign) and in Martínez-Gomariz *et al*. (2016a) (as a second campaign), the most common flows with low flow depth and high velocities (commonly found during urban storm events) were reproduced through a physical model in real scale. These tests aimed to establish general hazard levels (low, medium or high) for pedestrians when attempting a street crossing under various combinations

of water depth and velocity. This hazard classification would allow for a threshold to be established. Hydrodynamic conditions which result in a low hazard posed to pedestrians should be allowed to occur in the urban environment while medium and high hazard conditions should be more carefully considered and mitigated if possible. In the last experimental campaign carried out by Martínez-Gomariz *et al*. (2016a) a sample of 26 subjects was tested considering different conditions and exposure combinations (i.e. types of shoes, hands busy or free, and visibility conditions). The lower function threshold for all the assessed instability points is given by the product $(v \cdot y) = 0.22\ m^2 \cdot s^{-1}$. This study offers a revised and most updated stability threshold, which concentrates on acceptable levels when operating under low depth and high velocity conditions, the most common conditions in flooded streets during storm events. Also, new aspects such as the critical first step from a dry footpath into fast flowing water and the assessment of subjectsô emotional response and perceptions have been considered in the hazard analysis.

The proposed limits for hazard delimitation are: Low Hazard below the product $(v \cdot y) = 0.16 m^2 \cdot s^{-1}$, Medium Hazard for the values $(v \cdot y)$ compressed between 0.16 $m^2 \cdot s^{-1}$ and 0.22 $m^2 \cdot s^{-1}$, and High Hazard beyond $(v \cdot y) = 0.22\ m^2 \cdot s^{-1}$. The maximum accepted water depth is proposed to be 0.5 m according to Cox *et al.* (2010), who considered that threshold as a limiting depth for children. Therefore, Low and Medium Hazard hydraulic conditions are both found below a water depth of 0.5 m (**Error! Reference source not found.**).

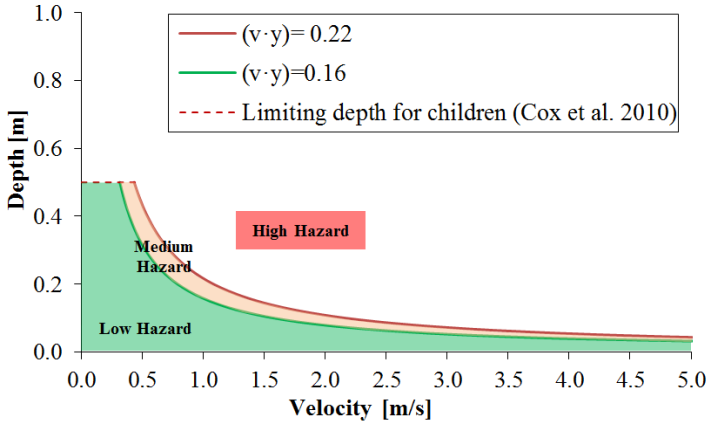

Figure 2-11. Hazard levels proposed based on the results of Russo et al. (2009; 2013) and Martínez-Gomariz et al. (2016b).

Taking all mentioned above into account, the maps of the water depth are reported below for the three considered return periods:

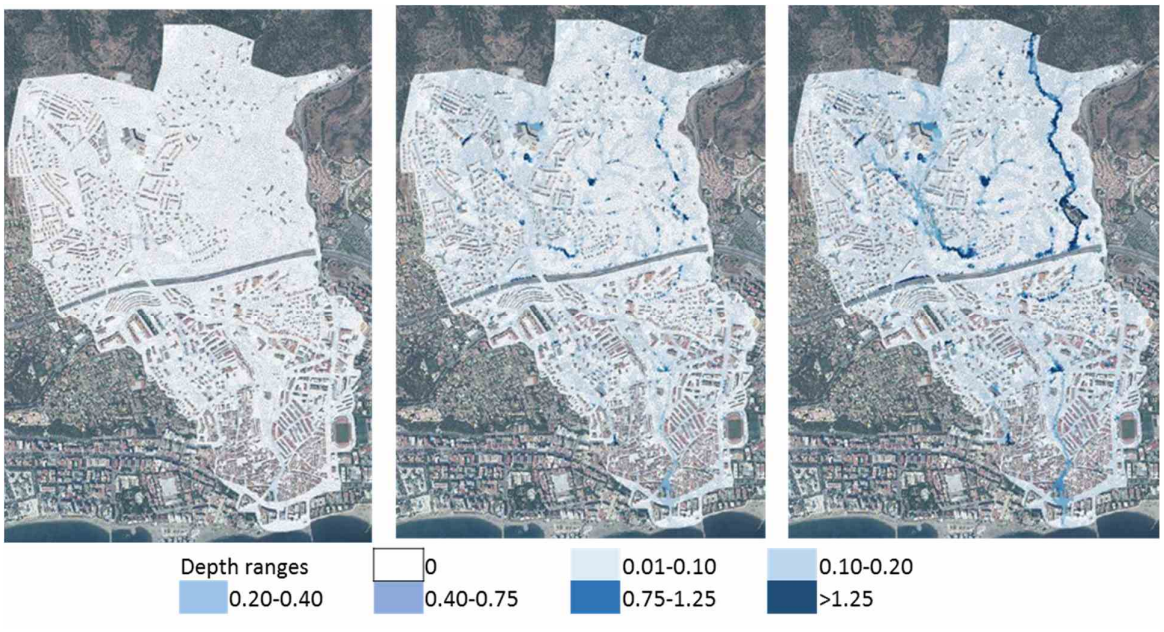

Figure 2-12. Depth maps for Marbella Case Study for 1 (left), 10(centre) and 100 (right) years of return period.

Finally, the hazard maps were produced using depth and velocity of the surface water resulting in the maps reported below for the three considered return periods:

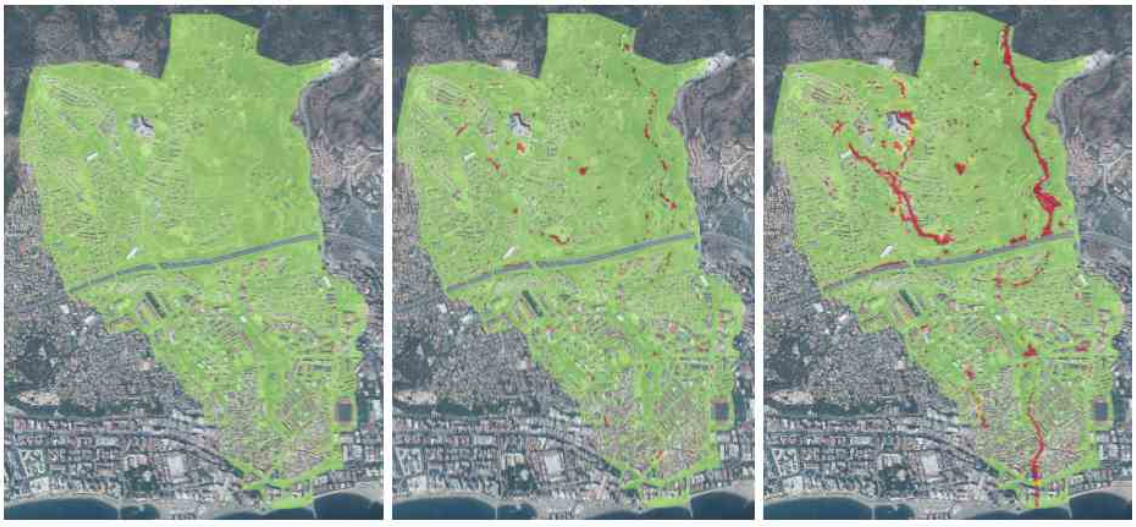

Figure 2-13. Hazard maps for Marbella Case Study for 1 (left), 10 (centre) and 100 (right) years of return period. The high hazard corresponds with the color red, medium hazard with yellow colour and low hazard with green colour.

As can be seen in Figure 12 the most dangerous zones are the stream paths, that within the downtown corresponds to main roads of the city.

2.3 Data collection and analysis for vulnerability assessment

In order to assess the human vulnerability in Marbella, we followed the methodology developed in CORFU project and reflected in D3.4 of that project (Hammond et al. 2014). INE, the

National Institute of Statistics, provide us statistical data of current population per census area that were used in the assessment. The information used is collected in the following table.

ID	Census area (m^2)	Total inhabitants (2015)	People density	<15 years	>65 years	Foreign people
001	81.509,30	1.029	12.624	156	181	268
002	34.551,91	1.170	33.862	193	208	225
003	45.371,61	1.805	39.783	306	324	351
004	242.003,53	2.226	9.198	306	401	456
005	113.526,71	1.547	13.627	241	233	208
006	19.652,77	1.298	66.047	190	214	317
007	20.486,08	1.404	68.534	175	271	239
008	26.438,06	1.211	45.805	171	205	227
009	18.233,97	1.130	61.972	177	199	147
010	60.423,78	1.897	31.395	354	235	326
011	76.364,53	2.001	26.203	303	315	285
012	69.199,31	973	14.061	119	191	110
013	26.632,38	910	34.169	133	144	174
014	81.201,87	1.671	20.578	246	293	292
015	49.368,52	1.607	32.551	197	222	179
016	144.022,58	2.040	14.164	280	359	446
017	41.893,71	1.145	27.331	145	230	328
018	5.637.684,74	2.647	470	430	223	260
019	18.986,21	756	39.818	82	163	130
020	191.787,29	1.181	6.158	122	238	222
021	131.769,62	1.726	13.099	163	396	450
025	60.424,29	937	15.507	117	95	63
026	56.023,22	1.189	21.223	161	245	196
027	29.769,72	1.509	50.689	175	281	243
028	288.521,11	1.775	6.152	452	90	88
029	106.586,04	2.544	23.868	473	216	247
032	132.633,38	1.692	12.757	268	194	248
033	691.207,24	1.596	2.309	294	197	233
034	34.185,40	1.135	33.201	135	149	124
037	54.613,65	1.573	28.802	346	145	159
038	46.198,55	1.769	38.291	325	160	384
039	202.690,77	1.363	6.725	287	132	129
040	313.853,08	1.670	5.321	349	112	156
041	261.214,00	1.278	4.893	208	152	107

Table 2-3. Current population data for the vulnerability assessment.

The next step on the methodology application was to set the thresholds that allow us to assess the vulnerability in each census area. Three thresholds were defined according to the three indicators used. First, the threshold for the people density was set using the medium density of the studied area of Marbella (5463 inh/km^2) and the definition of the National Institute of Statistics of urban area defined as a group of minimum 10 houses in a distance less than 200 m (equivalent to 1273 inhabitants per Km^2). Then, thresholds regarding the percentage of foreign people and the most vulnerable, people less than 15 years old and over 65, were defined. The whole thresholds are shown in **Error! Reference source not found.**.

The final vulnerability index was defined as the average value between the three indicators explained above. The final vulnerability level was achieved according to the formulations proposed in the **Error! Reference source not found.**.

Vulnerability index	C % people age < 15 or > 65 years old	F % of foreign people	D People density
1 (low)	Ò33%	Ò33%	Ò1273
2 (medium)	33% < X Ò50%	33% < X Ò50%	1273<XÒ5463
3 (high)	> 50%	> 50%	> 5463

Table 2-4. Thresholds to assess human vulnerability according to different criteria.

Vulnerability level	Formulation
Low	(D+C+F)/3 < 1
Medium	1< (D+C+F)/3 < 2
High	(D+C+F)/3 > 2

Table 2-5. Formulation to compute the total vulnerability index.

Following the criteria established above, the vulnerability map is produced per each building (in the left image there is the studied area without building boundaries while the second one the boudnaries are highlighted in black):

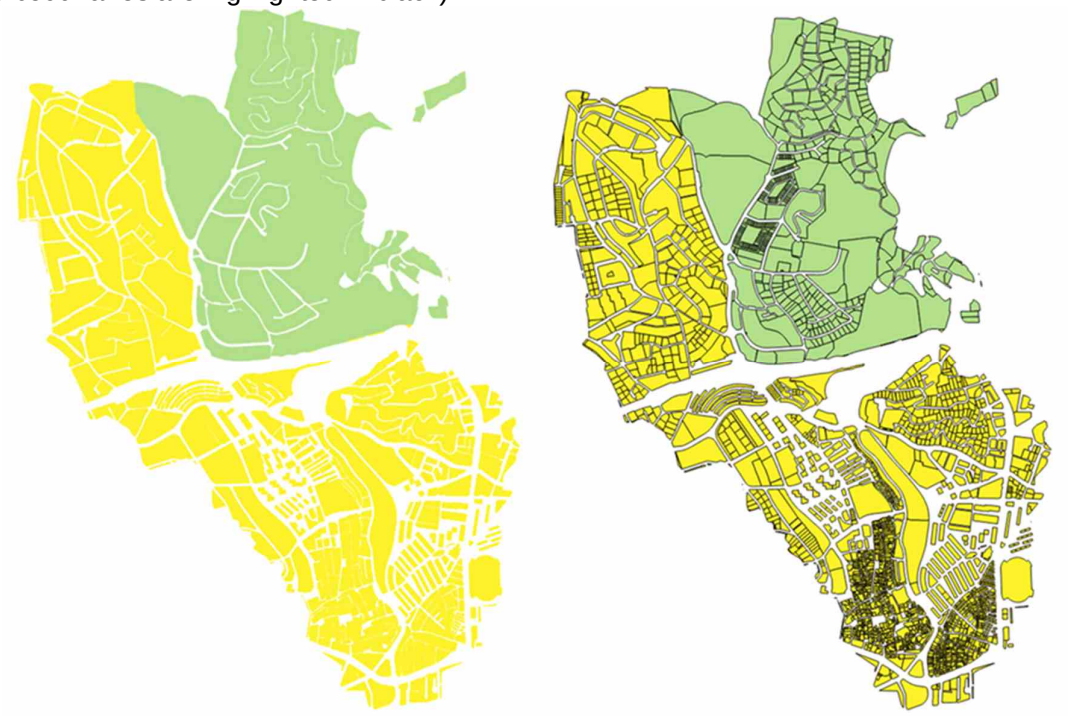

Figure 2-14. Vulnerability maps for Marbella per building.

2.4 Risk assessment

In a context of climate change flooding and CSOs, problems can produce significant social and economic risks in urban and peri-urban areas. Methods for risk determination can be qualitative or quantitative, both having limitations. If we define risk as the probability or threat to a hazard occurring in a vulnerable area, flood risk can be assessed through a risk map related to a determined scenario and return period by combining hazard and vulnerability maps (as shown in **Error! Reference source not found.**). These maps can be used to evaluate potential impact on urban elements (i.e. pedestrians, vehicles, properties, etc.).

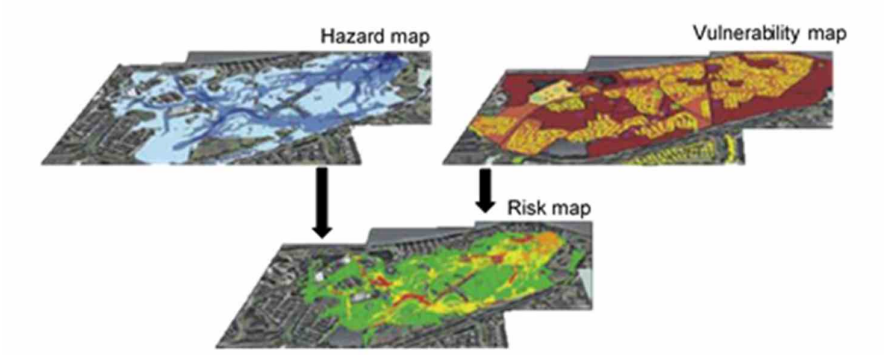

Figure 2-15. Combination of hazard and vulnerability maps to produce a flood risk map.

Qualitative assessment defines hazards and vulnerability and risk levels by significance levels such as ñhighò, ñmediumòand ñlowòand evaluates the resultant level of risk against qualitative criteria. In this case, hazard and vulnerability maps are generally elaborated through specific criteria and indexes, so risk maps are created multiplying the vulnerability index (1, 2 or 3, corresponding to low, moderate and high vulnerability) by the hazard index (1, 2 or 3, corresponding to low, moderate and high hazard). Finally the total risk varies from 1 to 9 where higher levels indicate higher risk. This approach can be summarized in the following risk matrix shown in Figure 15.

Risk Matrix				
		Hazard		
		1	2	3
Vulnerability	1	1	2	3
	2	2	4	6
	3	3	6	9

Figure 2-16. Risk matrix obtained by multiplying vulnerability and hazard indexes.

Finally, the maps that have been obtained through this study are reported below:

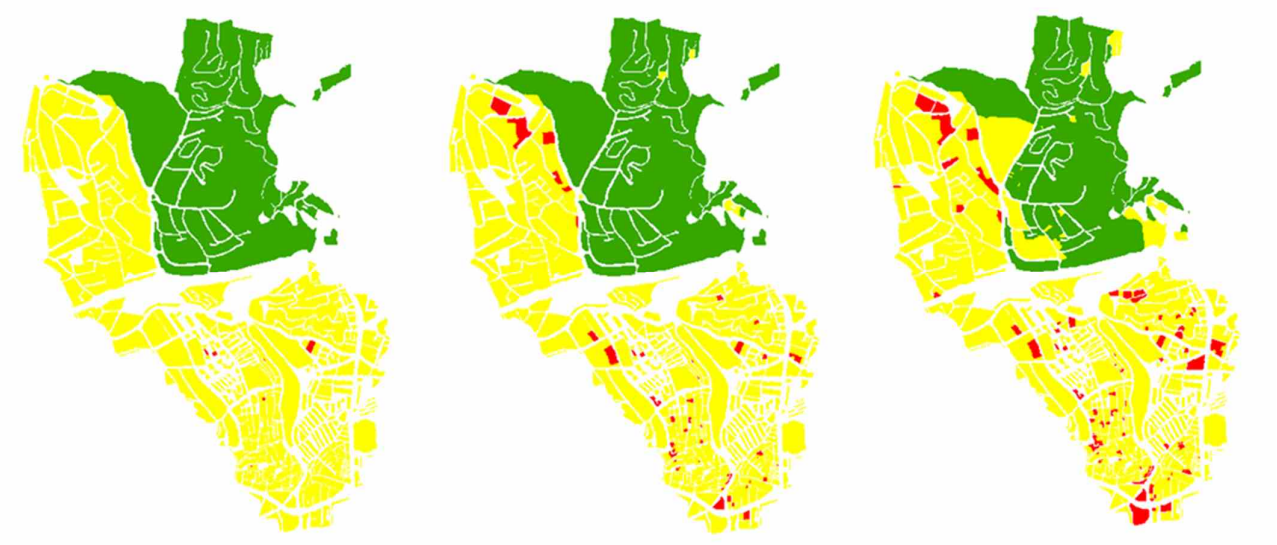

Figure 2-17. Risk maps obtained for Marbella case study for 1 (left), 10 (centre) and 100 (right) return period.

As it can be seen in the risk maps, the most dangerous parts correspond to the streams of rio Huelo and Represaõs channel. In contrast, the less dangerous parts are in the highest part of the case study.

2.5 How risk analysis benefit local stakeholders

Nowadays, Marbella is facing and increase in risk by its two components. Firstly, the hazard is increasing due to climate change. Secondly, vulnerability is growing due to the increasing urban population. And, moreover, exposure is rising due to the higher concentration of assets, goods and people. This environment makes even more necessary to use more detailed and accurate tools by decision makers.

So that, risk analysis is set up as an essential tool for all people, municipalities, organizations and companies that are involved in Marbella city and that have an interest in it.
In fact, as it was introduced in the previous paragraphs, Marbella city shows a significant predisposition to flood risk and storm surge risk.

In the recent periods, flood and storm surge events have taken place with more and more high frequencies. Furthermore, it is now clear that climate change has been playing a key role in provoking higher intensities and frequencies, therefore also a significant exacerbation of damages caused by those events. Moreover, the damages are not increasing linearity as the intensity and frequency increase, but exponentially.

The most direct and concerning consequence affects tourism and other main economic activities, which result surely at risk. They will be subjected to grave economic damages that will have heavy economic consequences on all stakeholders of the city. These damages are going to increase more and more if adequate measures wonôt be defined and applied.

Therefore, a detailed risk analysis is essential to plan adequate measures to contrast flood and storm surge effects, in order to attenuate consequences and damages that result from those kinds of event.

According to this point of view, identifying properly the risk is a necessary analysis in order to minimize losses and avoid new investments to recover previous conditions.

Thus, this work is set up as the baseline for future measures analysis in order to attenuate the impacts caused by the increasing risk. The 1D-2D hydraulic model becomes essential for the correct decision of the solutions that will be applied in the coming years.

2.6 References

Cox R., Shand, TD., Blacka, MJ. (2010). Australian Rainfall and Runoff (AR&R). Revision Project 10: Appropriate Safety Criteria For People. New South Wales (NSW), Australia.

Danish Hydraulic Institute (DHI) 2002. Calibration of MOUSE Urban Surface Runoff Models. Final Report, Waiatkere City Council New Zealand.

Hammond, M.; Chen, A.; Djordjevic, S. 2014. Flood Damage Model Case Study Results. Deliverable 3.4 of the CORFU (Collaborative research on flood resilience in urban áreas) Project.

Martínez-Gomariz, E., Gómez, M., Russo, B. (2016a). Experimental study of the stability of pedestrians exposed to urban pluvial flooding. Natural Hazards (Submitted).

Martínez-Gomariz, E., Gómez, M., Russo, B. (2016b). A new experimental-based methodology to obtain the stability threshold for any real vehicle exposed to flooding. Journal of Hydraulic Research (Submitted).

Russo, B. (2009). Design of surface drainage systems according to hazard criteria related to flooding of urban areas. PhD Thesis. Technical University of Catalonia, Barcelona, Spain.

Russo, B., Gómez, M., Macchione, F. (2013). Pedestrian hazard criteria for flooded urban areas. Nat Hazards 69:251ï 265. doi: 10.1007/s11069-013-0702-2.

3 Case Study Genova

3.1 Description of the study area

The case study concerns the city of Genova, and specifically the coastal area and the Bisagno river basin. The focus of the case study is on the Bisagno final reach (last 5km of the river), streaming into urban area.

Extreme events affecting the Bisagno river basin are heavy precipitation, cyclones, flash floods, pluvial and coastal floods as well as combination of floods. The Mediterranean region is a clear example where large-scale flows and topography are contributing factors to the occurrence of heavy precipitation events. In the study area of the Liguria region, localized extreme precipitation is produced by large-scale flow interaction with regional topography. Cyclones relate with a low pressure area, also referred to as Genova low, insisting on the Genova gulf. The depression bear rain, often intense, on the Liguria coast.

Recently Genova was hit by two major flash floods in November 2011 and October 2014, both resulting in fatalities, displacement of people and high financial damage.The Genova case study is aimed to address the issue of in urban areas. Flooding in urban areas can be caused by flash floods, coastal floods or river floods, but there is also a specific flood type that is called urban flooding (http://www.floodsite.net/). This kind of flood is specific in the fact that the cause is a lack of drainage in an urban area. Heavy precipitation can cause flooding when the city sewage system does not have the necessary capacity to drain away the amounts of rain that are falling.

All these phenomena occurred in Genova in the November 4, 2011 and in the October 9, 2014 events.Urban flooding is the most frequent floods occurring in Genova. Their impact though is less severe than flash floods, but there are many areas that, in correspondence with heavy precipitation, flooded regularly for the lower floors and basements of buildings. Heavy rainfall can overwhelm the sewage system. When this happens, sewage can overflow from manholes and rainfall water flowing into city roads. For example these phenomena occurred before, during and after flood event of Fereggiano stream (drainage area 5 km2), of Bisagno torrent (98 km2) and of other small streams (e.g., Noci, Rovera, Chiappeto) in November 4, 2011.

Urban flooding are a great disturbance of Genova daily life. Roads can be blocked; people can't go to work or to schools. Some areas are on flat terrain and so the flow speed is low and you can still see people driving car or scooter through ponding water. Other areas of the city are on sloping terrain and it's common that the water quickly flowing on the city streets due to high slopes. The streets become drainage networks and this flow doesn't go into the river due to banks or other obstacles. It's happen that water depth is not deep but velocity doesn't allow citizens to walk. The economic damages are high but the number of casualties is usually very limited, because of the nature of the flood. The propagation and extent of urban flooding in Genoa are obviously a function of the intensity of the event, but it is a fact that is sufficient a rainfall that does not cause a riverine flood.

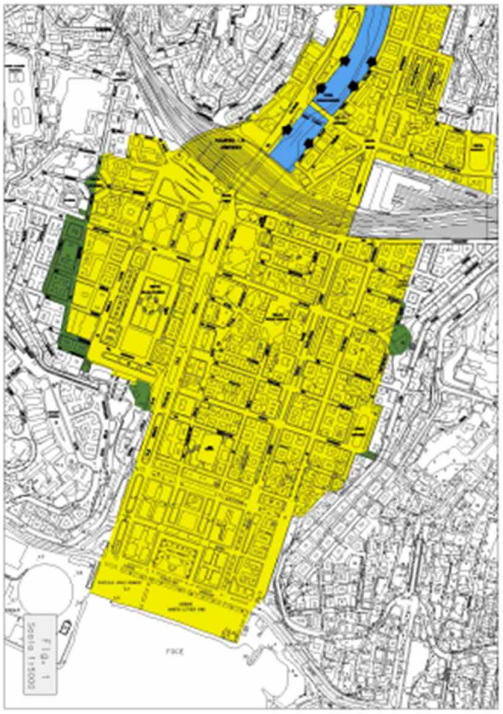

Figure 3-1 Bisagno drainage basin. Flood prone areas for different return period (T=50 yellow; T=200 orange; T=500 green)

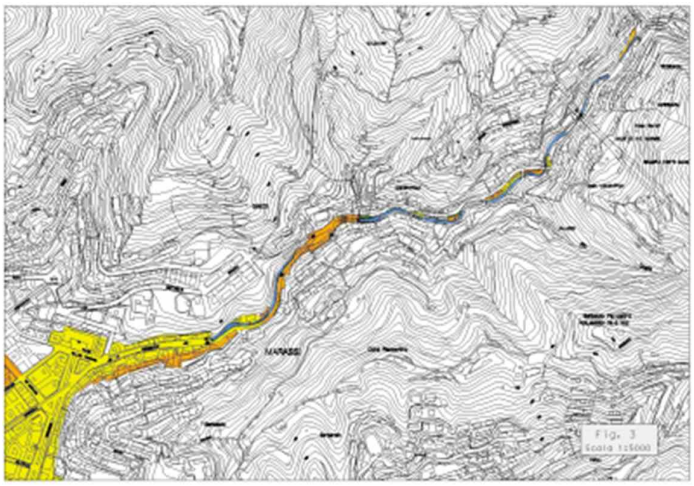

Figure 3-2 *Fereggiano drainage basin. Flood prone areas for different return period (T=50 yellow; T=200 orange; T=500 green)*

The Bisagno Basin Plan identifies a number of hydraulic structures and maintenance works to be performed to minimize the risk in urban areas. In brief, works for the complete re-building of the Bisagno cover in its final reach will be soon completed, sensitively increasing the maximum discharge of the river. Then, works for the diversion of Fereggiano river (a triburary of Bisagno) are also started, collecting waters from Fereggiano basin to the sea, avoiding in such a way to overload the Bisagno river discharge.

3.2 Data collection and analysis for hazard assessment

3.2.1 *Collected data for hazard assessment*

Timeseries of rainfalls
Event:9-10 October 2014 in Genova
Time step: 10 minutes.
Data owner: Regional Environmental Agency - ARPAL

Timeseries of Discharge
Events: October 2014 in Genova
Time step: 10 minutes
Data owner: Regional Environmental Agency - ARPAL

Flood prone areas
Return period = 50, 100, 200 years
Data owner: River Basin Authority

Digital Elevation Model
Geographical scale: 1:5000
Data Owner: Regione Liguria

River profile sections
Data owner: River Basin Authority
November 4, 2011 observations
Details: rainfall, discharge, ground effects
Data owner: Regional Environmental Agency - ARPAL

Census
Details: 2011 data
Data owner: ISTAT

Municipal technical map
Geographical scale: 1:2000, 1:1000
Data owner: Municipality of Genoa

3.2.2 *Analysis of data for hazard assessment*

Technical activities of GISIG (in collaboration with University of Genoa - DICCA) mainly focused on the study of the event that hit the city of Genoa (Liguria, Italy) on October 9, 2014. The workgroup also focused on October 25, 2011 event of Cinque Terre, modelling this extreme rainfall event in the Bisagno area.

In particular, on the topic of October 9, 2014 event, the workgroup focused on:

a) Data collection in terms of rainfall measurements for the Bisagno basin (CMIRL network), water level observed, discharge measurements, flooded area observed and Basin Authority flood prone areas, cross-sections for the part of the Bisagno river streaming in culvert and vectorial data to build a DEM model for 2D analyses.

b) Meteorological and statistics analysis in term of study of the evolution of the event, mapping of the rainfall fields and valuation of the return period of the event and comparison with main flood events of the past such as the 2011 event
c) Hydrological analysis using a rainfall-runoff model named DriFt, developed by the University of Genoa, aims to estimate the flood hydrograph of October 9, 2014 event for some sub-catchments of interest and comparison with available discharge measurements.

d) Hydraulic model using Hec-Ras tools and the results of hydrological analysis in terms of flood hydrograph of the event. The aims was to simulate the floods event and create water depth maps to describe the evolution of the event.

e) Creation of flood maps by using a script developed into an ESRI environment calculating water depth for each point of the grid and in different time steps.

Meteorological and statistics analysis of October 9, 2014 event

The meteorological event of Genoa on October 9, 2014 is due to a frontal system able to generate a number of rainfall cells starting on the sea and rapidly moving from south-east to north-west, hitting the natural barrier formed by the mountainous of Liguria. The high amount of rainfall released by these sequences of thunderstorms is to be associated to an anomalously (for the season) high temperature of the Mediterranean, to the orographic lifting due to the mountains, and, for this specific event, to the ñV-shapedò aspect of winds converging toward the city of Genoa. The centre of the storm was located on the Bisagno and Sturla basins.
The collection of rainfall measurements for the area are available from the professional (CMIRL) network. Stations are subject to regular maintenance, their location is decided following international standards and quite long time series are available.

Figure 3-3 CMIRL network and Bisagno basin in red.

The CMIRL network recorded a maximum of 400 mm for a 24 hours duration cumulated rainfall and 135 mm for a 1 hour duration (Geirato station). These values can be quickly compared to the maximum recorded for the November 4, 2011 event: 605 mm for the 48 hours duration, 411 mm/12 hrs, and 181 mm/hr (Vicomorasso station).

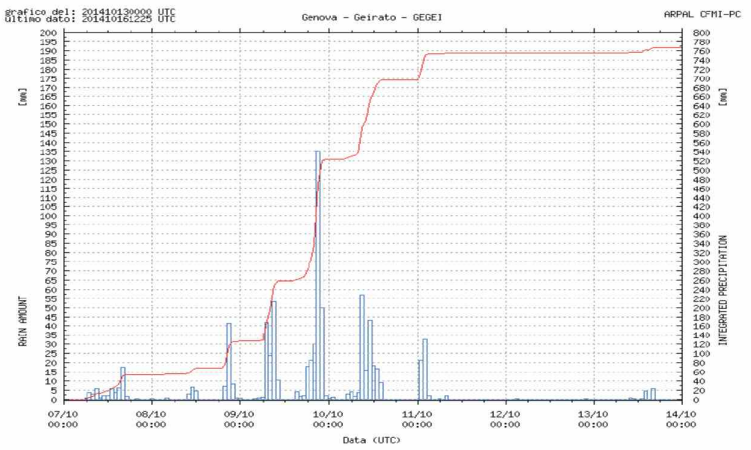

Figure 3-4 October 9, 2014: rainfall record at Geirato raingauge station, CMIRL network.

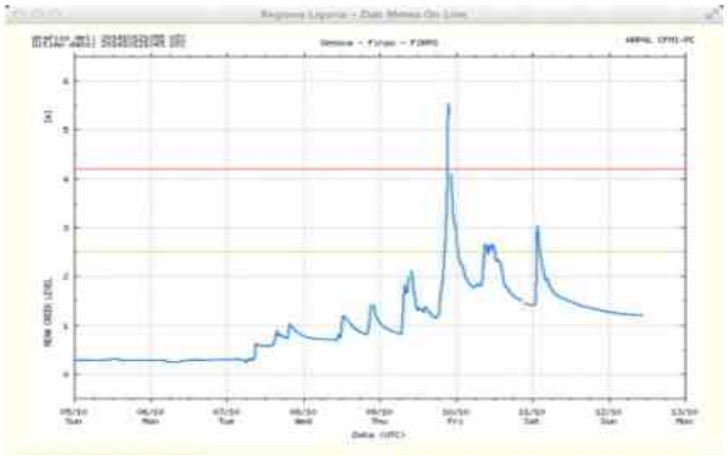

Figure 3-5 October 9, 2014: Water depth record at Firpo station in the Bisagno River, CMIRL network.

In the following pages some of the results of the analyses performed:

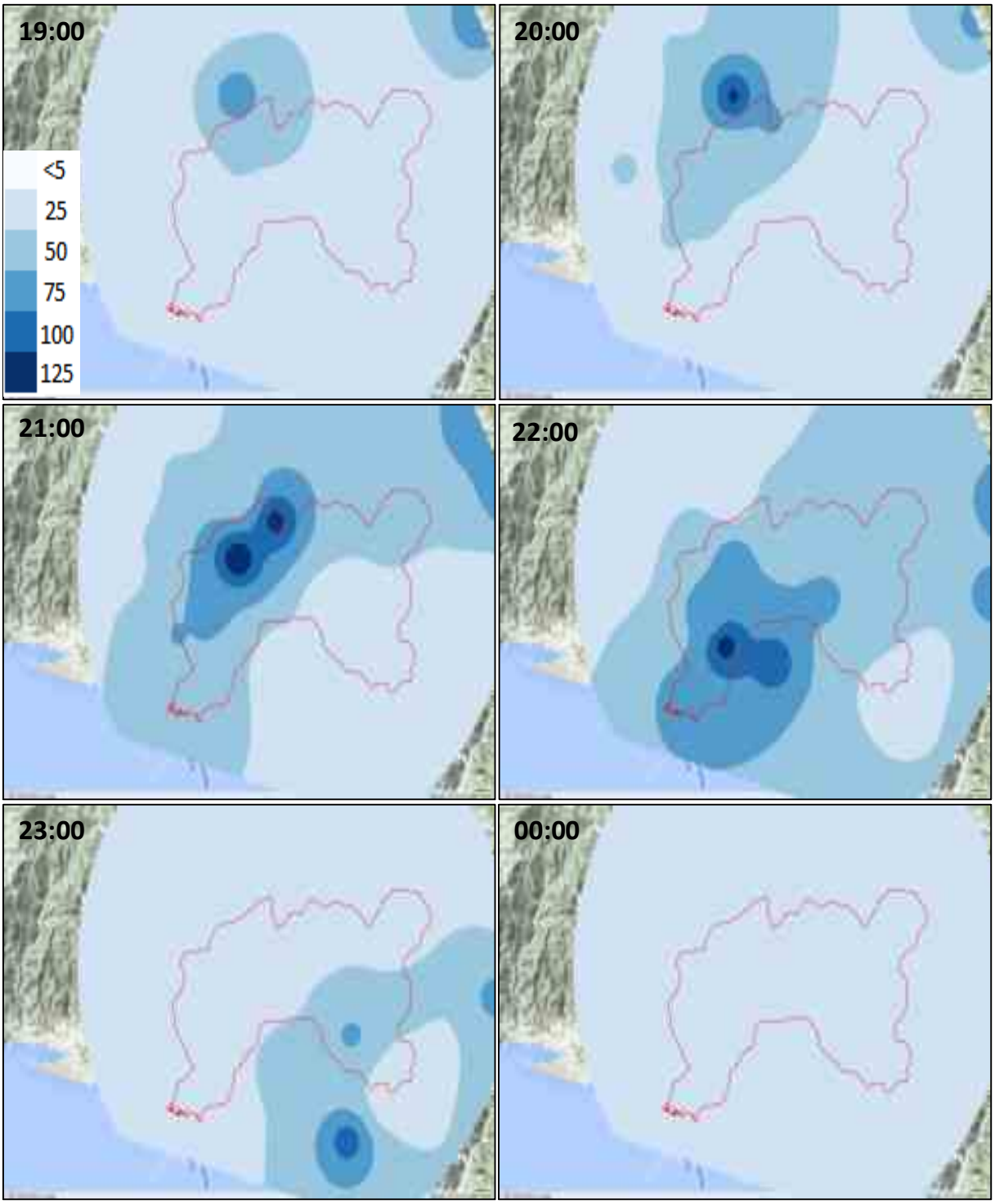

Figure 3-6 Cumulated rainfall (mm) for 1 hour of duration starting from 19:00 pm on October 9, 2014 and finished at 00:00 am on October 10, 2014.

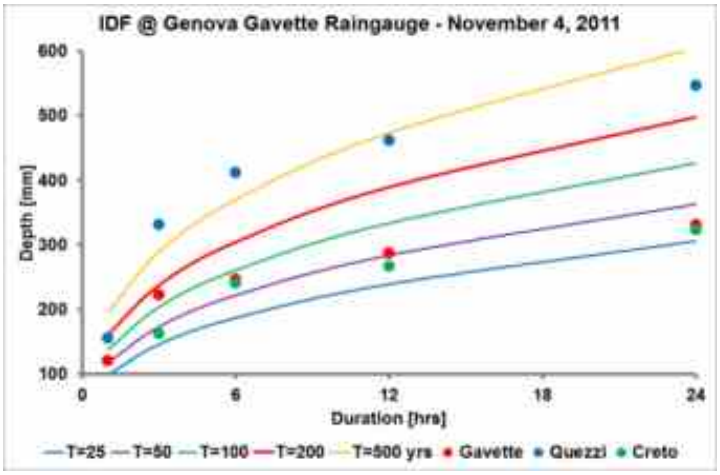

Figure 3-7 Intensity-Duration Frequency curves for Genova Gavette Raingauge and comparison with November 4, 2011 event.

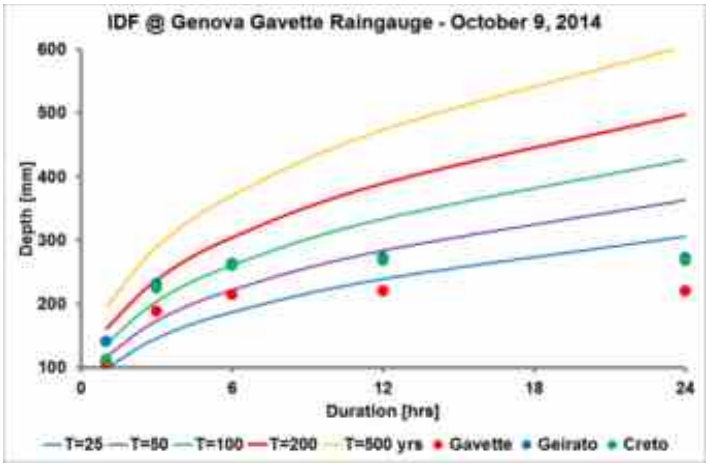

Figure 3-8 Intensity-Duration Frequency curves for Genova Gavette Raingauge and comparison with October 9, 2014 event.

Hydrological modelling of October 9, 2014 event

The Hydrologic model used for this study is DRiFt (Discharge River Forecast), a semi-distributed event model based on a geomorphologic approach. This model is focused on the efficient description of the drainage system in its essential parts: hillslopes and channel networks are addressed with two kinematic scales, which determined the base of the geomorphologic response of the basin. The geomorphologic module is coupled with a simple distributed representation of soil infiltration properties, while the rainfall event is schematized with its variability in time and space. The runoff volume is routed with a time variant TUH (T-hour Unit Hydrograph) technique, which takes into account the runoff production variability. Parameters calibration and validation have been carried out using different intense rainfall events in different size basins. This robust and parsimonious model is able to predict consistently the main features of the hydrograph; the observed parameter invariance allows the reliable utilization for flood forecasting, especially in regions where many small non-

gauged basins are present. DriFt was developed by University of Genoa (see: Giannoni F., Roth G. e R. Rudari, A procedure for drainage network identification from geomorphology and its application to the prediction of the hydrologic response, Advances in Water Resources, 28(6), 567-581, 2005. AA. VV., DRiFt, 239-246. In: MIKE 11 - A modelling system for rivers and channels, User Guide, DHI Software, 430 pp., 2003.Giannoni F., Roth G. e R. Rudari, A semi-distributed rainfall-runoff model based on a geomorphologic approach, Physics and Chemistry of the Earth (B), 25(7-8), 665-671, 2000).

Figure 3-9 Bisagno River - Channel networks of Bisagno basin determined on the base of the geomorphology of the basin, using a slope & area filter.

In the following, an example of result obtained by the hydrological modelling activity and related to the Firpo station along the Bisagno River.

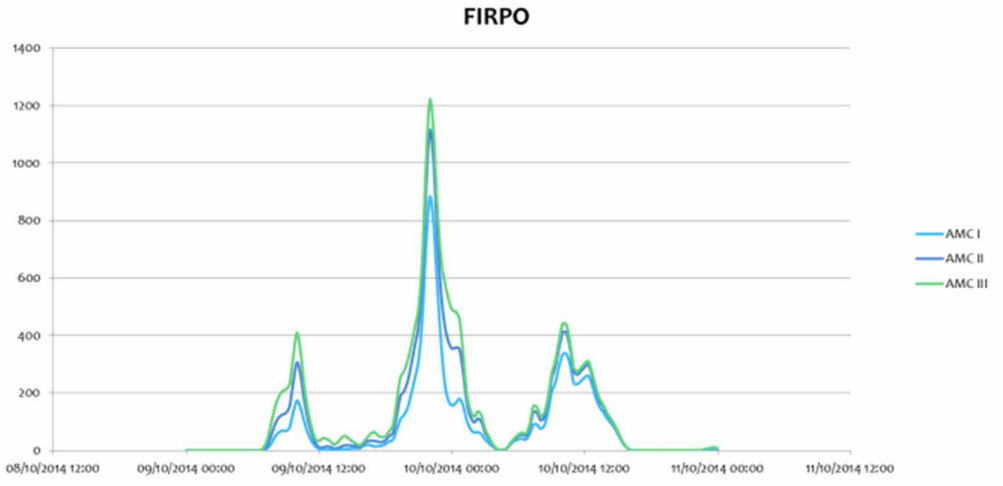

Figure 3-10 DRiFt model result: Hydrograph of October 9, 2014 event at Firpo (Bisagno stream)

Hydraulic modelling of October 9, 2014 event

The Hydraulic model used for simulating the Bisagno River is HEC-RAS. It is designed to perform one-dimensional hydraulic calculations for a full network of natural and constructed channels.

Figure 3-11 Bisagno River - Planimetry of cross section of Bisagno river used to develop the Hydraulic model in Hec-Ras of pilot case.

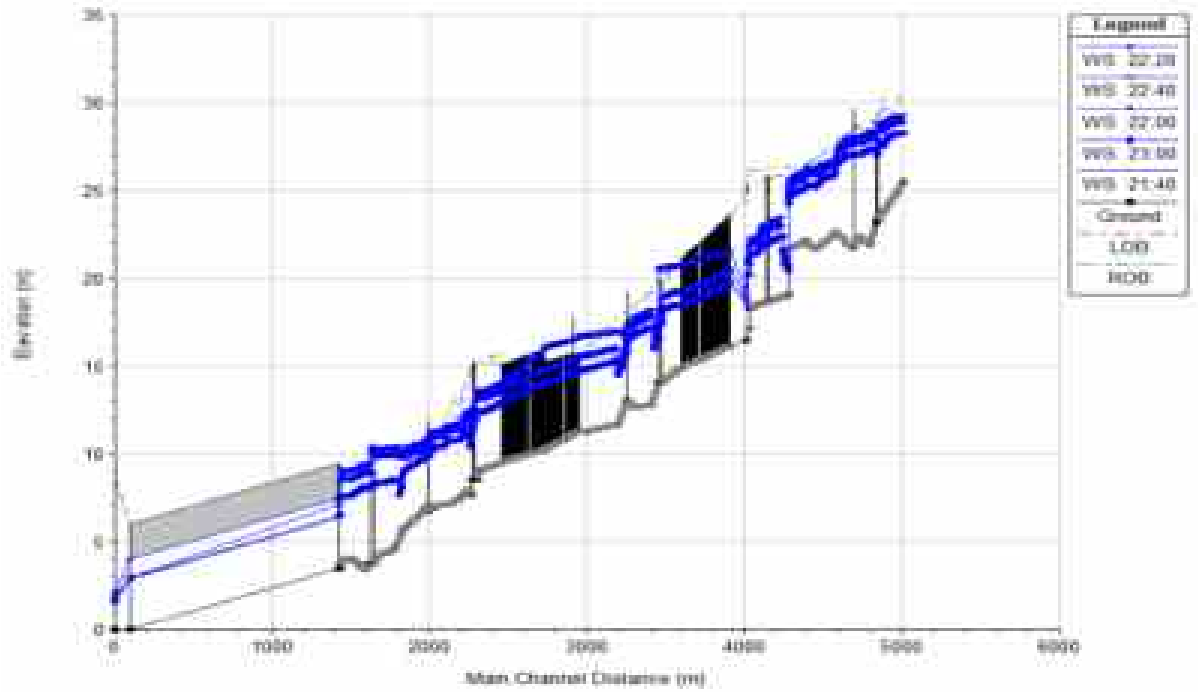

Figure 3-12 Bisagno River - October 9, 2014 event. Water profiles for the final reach of October 9, 2014 event at different time.

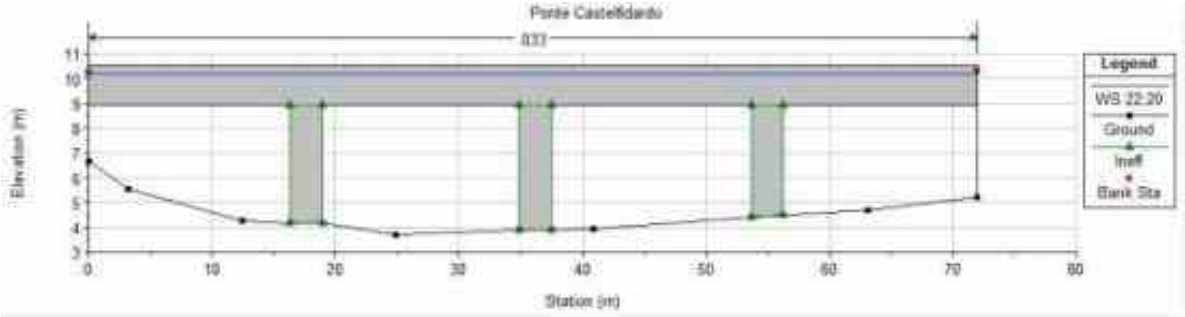

Figure 3-13 Bisagno River - October 9, 2014 event. Water level, river section at Castelfidardo bridge at 22:00 p.m.

Generation of the flood maps for the October 9, 2014 event

For two-dimensional analyses it was used a GIS tool developed in an ESRI environment by GISIG, very similar to Hec Geo Ras tool. Water depth is calculated as the difference between the water height above the channel bottom and the value of the DEM in each cell of the grid. Flood maps have been generated with a time step of 20 minutes and delivered in raster format (geotiff).

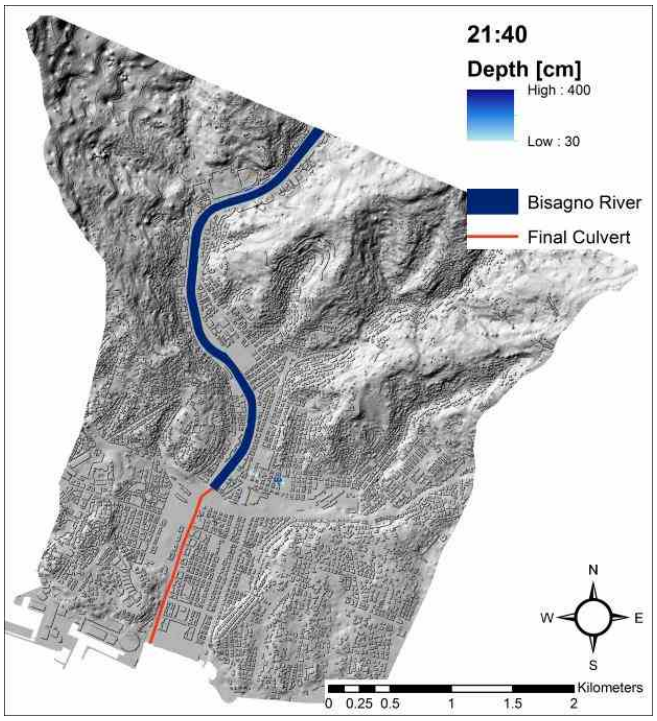

Figure 3-14 Bisagno River - October 9, 2014 event. Water depth map at 21:40 p.m.

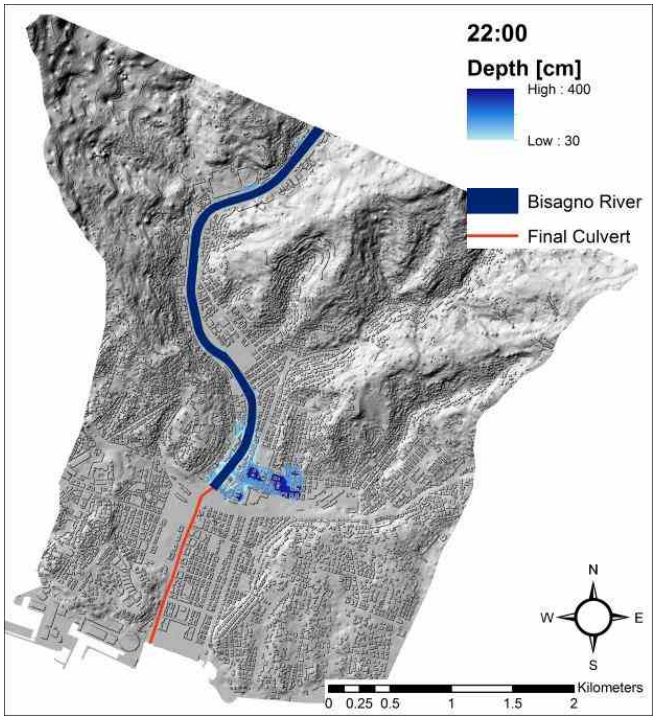

Figure 3-15 Bisagno River - October 9, 2014 event. Water depth map at 22:00 p.m.

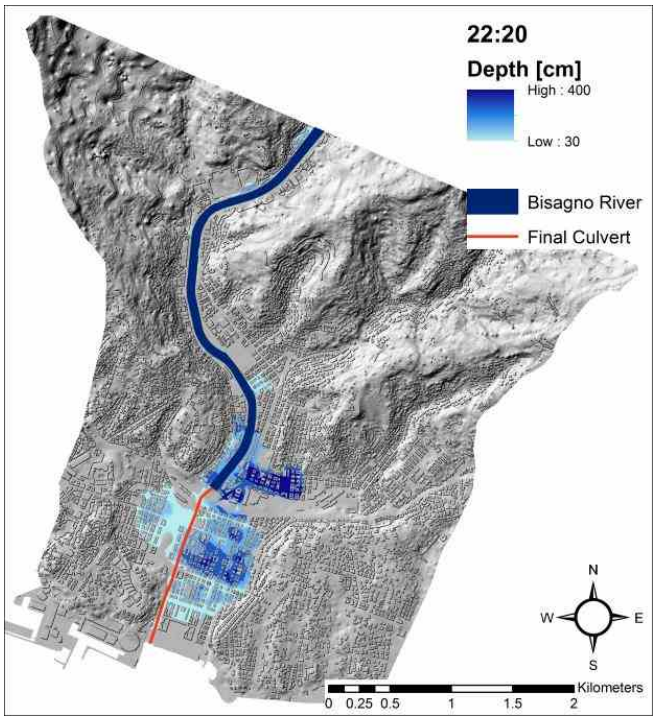

Figure 3-16 Bisagno River - October 9, 2014 event. Water depth map at 22:20 p.m

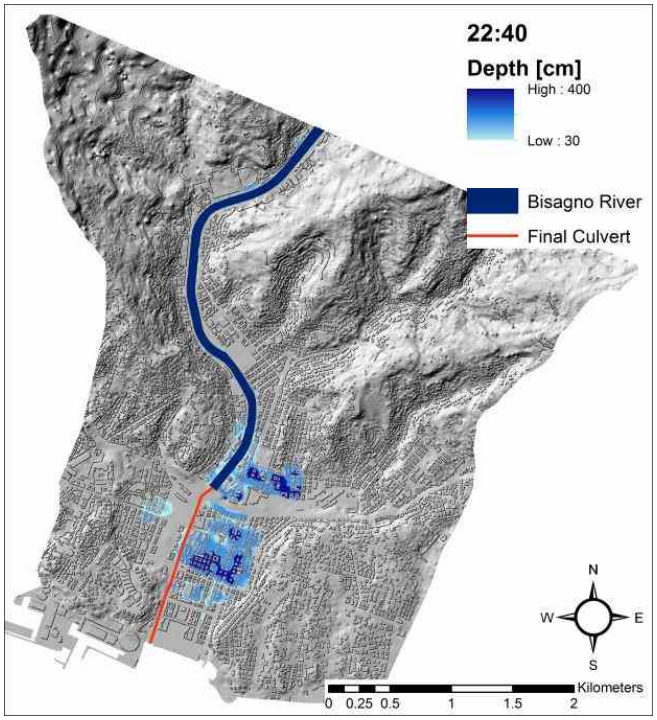

Figure 3-17 Bisagno River - October 9, 2014 event. Water depth map at 22:40 p.m.

The 1D and 2D models implemented for the final reach of Bisagno River (around last 5km, corresponding to the most urbanized area) have been moreover calibrated with the map of flooded area observed for the event of 9 October 2014.

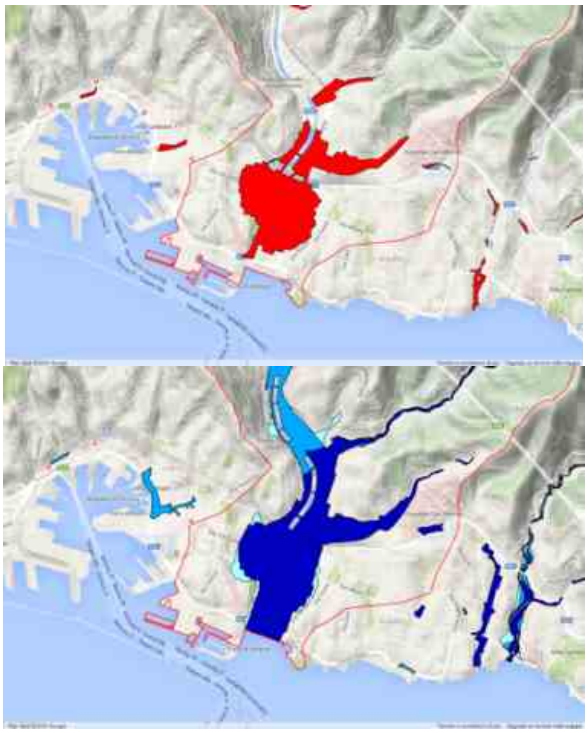

Figure 3-18 Comparison with flooded area observed in October 9, 2014 event (red) and the Basin Authority flood prone areas (blue).

Generation of the flood maps for the October 25, 2011 rainfall event

On October, 25, 2011 heavy rainfall affected Cinque Terre and Val di Vara (Eastern Liguria, Italy). A cumulative daily rainfall of 539 mm was recorded by the Brugnato rain gauge, with intensity up to 153 mm/h and 328 mm/3h (CMIRL network.), a truly record for Liguria Region. This event triggered several slope movements and floods, causing 13 casualties, severe structural and economic damages.

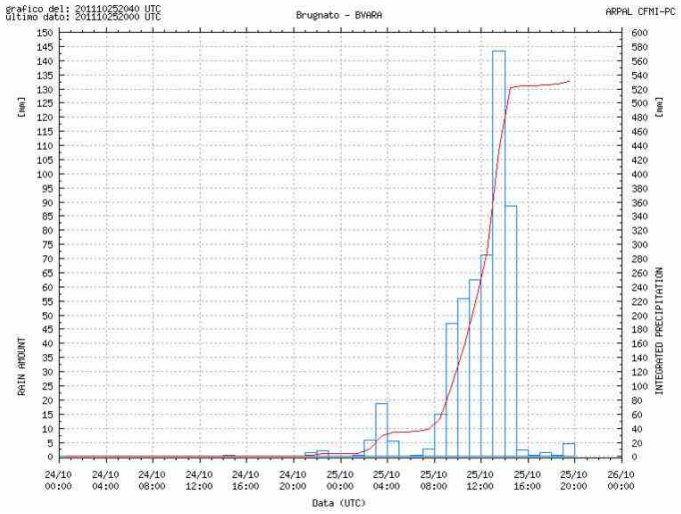

Figure 3-19 October 25, 2011 - Rainfall record at Brugnato raingauge station, CMIRL network.

In the PEARL research activities, rainfall event of Cinque Terre was analyzed and applied to the Bisagno Basin. The aim was to develop water depth maps for this the event and simulate the behavior of Bisagno Basin towards the most important extreme rainfall event occurred in Liguria Region in the last decades.

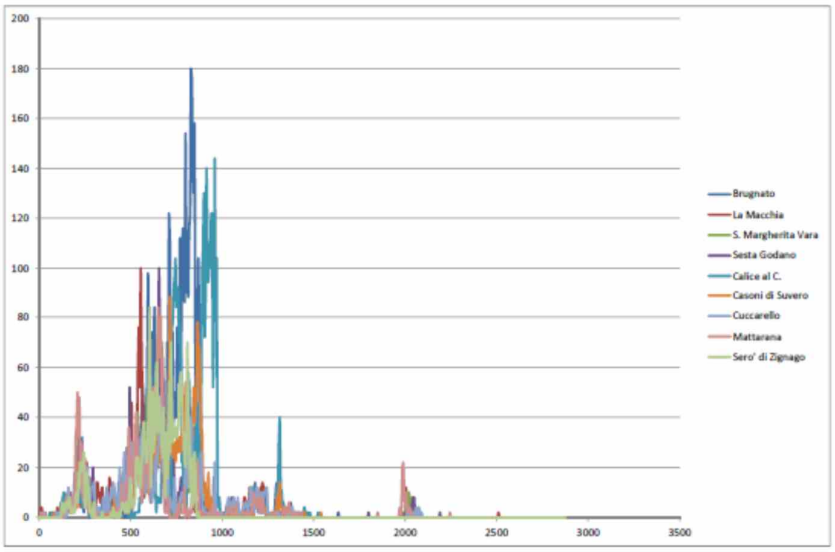

Figure 3-20 October 25, 2011 - Rainfall record at different stations, used for analyses.

Flood maps have been generated for the whole duration of the event, with a time step of 1 hour. In the following pages some of the results of the performed analyses, where it is evident a really high water depth (around 4m) specially in the left side of the river.

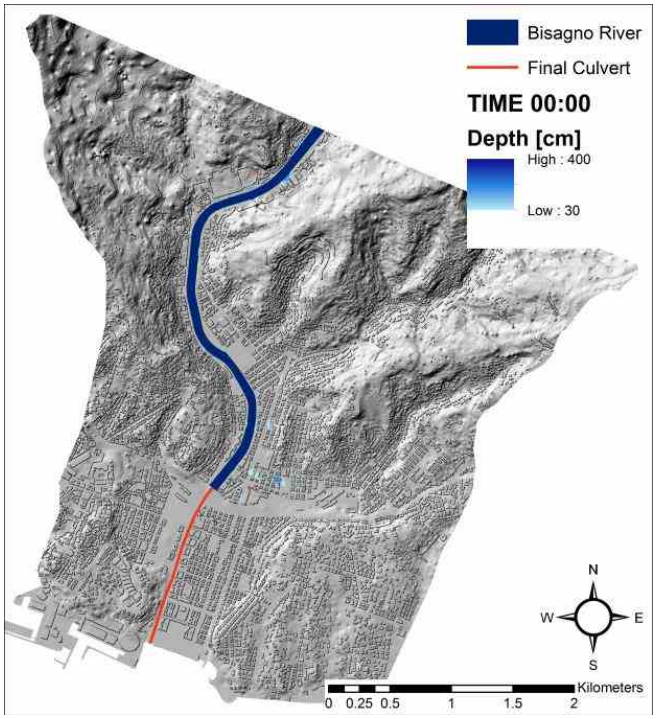

Figure 3-21 Bisagno River - October 25, 2011 event. Water depth map at time 00:00

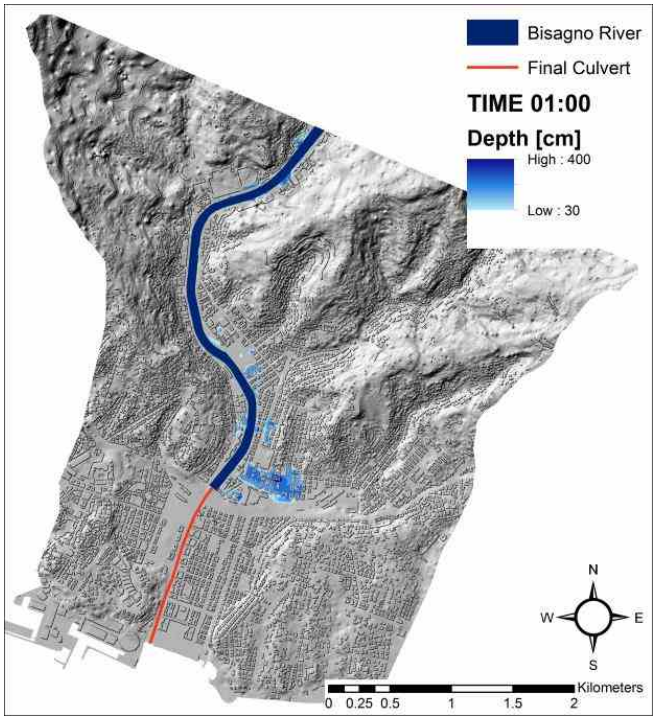

Figure 3-22 Bisagno River - October 25, 2011 event. Water depth map at time 01:00

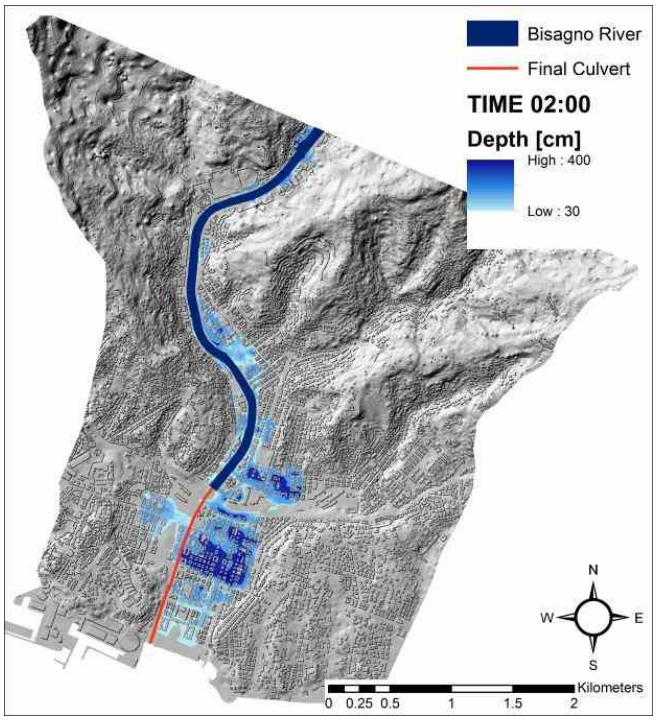

Figure 3-23 Bisagno River - October 25, 2011 event. Water depth map at time 02:00

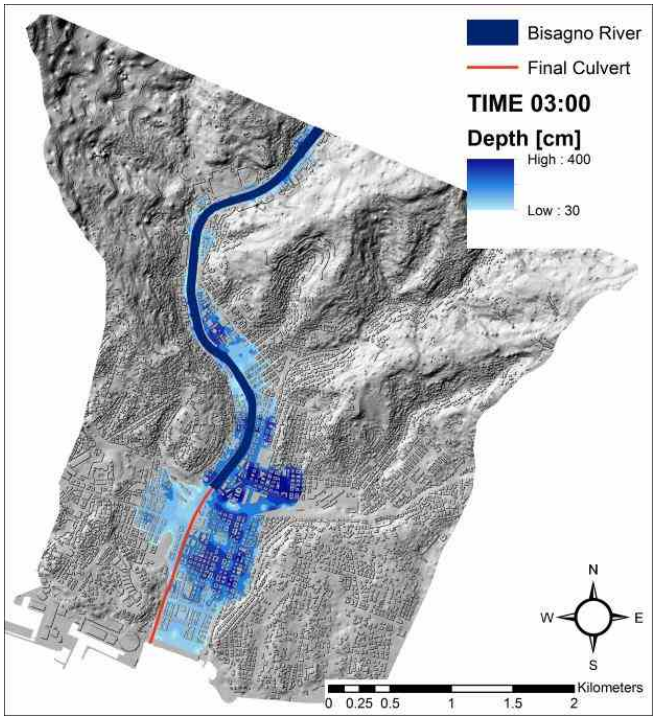

Figure 3-24 Bisagno River - October 25, 2011 event. Water depth map at time 03:00

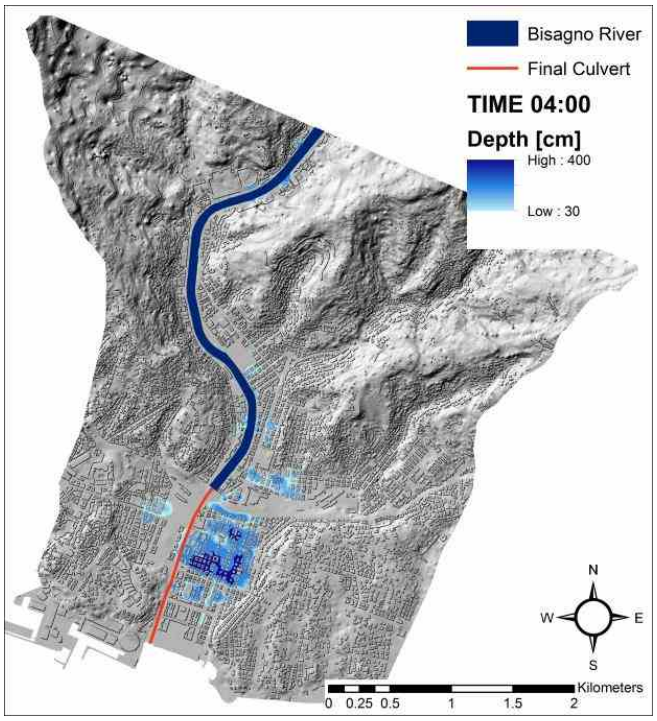

Figure 3-25 Bisagno River - October 25, 2011 event. Water depth map at time 04:00

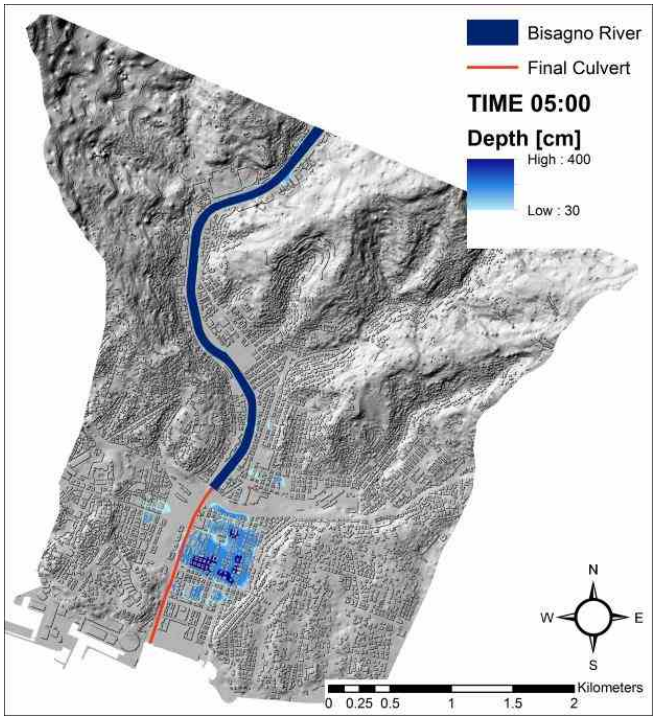

Figure 3-26 Bisagno River - October 25, 2011 event. Water depth map at time 05:00

3.3 Data collection and analysis for vulnerability assessment

3.3.1 *Data collection for vulnerability assessment*

First step in vulnerability assessment consisted in the collection, by the University of Stuttgart, of data about the pilot area and its main characteristics.

Collected data mainly refers to two following categories:

Territorial data ï they are data taken in particular by the regional maps, and consist of:

- DEM ï Digital Elevation Model (resolution 5m), from Liguria Regional Authority
- CTR ï Regional Technical Map (geographical scale 1:5000), from Liguria Regional Authority, with reference to the layers: Buildings (Private and Public), Cultural Heritage, Electricity Network, Railways and Stations, Streets.

Statistical data ï they are taken in particular by the ISTAT web site (National Statistical Institute), and consist of:

- Census tract
- Population distribution and social structure

Data which were not available in territorial and statistical databases, were moreover collected door to door through a series of interview carried out at 500 households in the pilot area.

3.3.2 *Methodology applied to the vulnerabity assessment*

The vulnerability assessment (carried out in the WP1) comprises a household survey, as well as a methodology for spatial vulnerability assessment with the calculation of a compound vulnerability index. The PEARL vulnerability index is based on a modular structure with three elements (susceptibility, coping capacity and adaptive capacity). These three elements in turn consist of several sub-indices.
Starting point of the vulnerability assessment in the Genova pilot was the Risk and Root Causes Assessment (RRCA), performed as well in the WP1. Furthermore, an approach for vulnerability assessment was developed.

Household survey

The vulnerability assessment by means of the household survey conducted through the population of the pilot area can be considered as a stand-alone part of the work. The aim of this survey was to deduce vulnerability patterns of local households and to gather information on how the households respond before, during and after a hazard, in order to get an understanding on local risk management strategies. Results and conclusions from the vulnerability analysis in the Genova pilot are included into the milestone report 25, WP1.
The survey was conducted by 10 interviewers, selected by students from Earth Science and Engineering schools of the University of Genova, and interested 500 households in the pilot area.

The students were properly trained for the purpose by a researcher of the University of Stuttgart and by an officer of the Municipality of Genova ï Civil Protection Department ï on how to approach people and communicate to them. Pilot area was divided into ten districts, homogeneous for number of inhabitants (see the map below) and each interviewer was assigned to a district. The map was derived through a GIS analysis, taking into consideration the flooded area in the October 2014 event and the population distribution by the census data.

Each interviewed household was provided with an hard copy of the questionnaire, and the answer directly noted on that.The household survey was conducted in December 2015 and had the patronage of the Municipality of Genova, of the University of Genova and of IREN Group, the multiutility in charge for the management of water and energy networks in Genova.

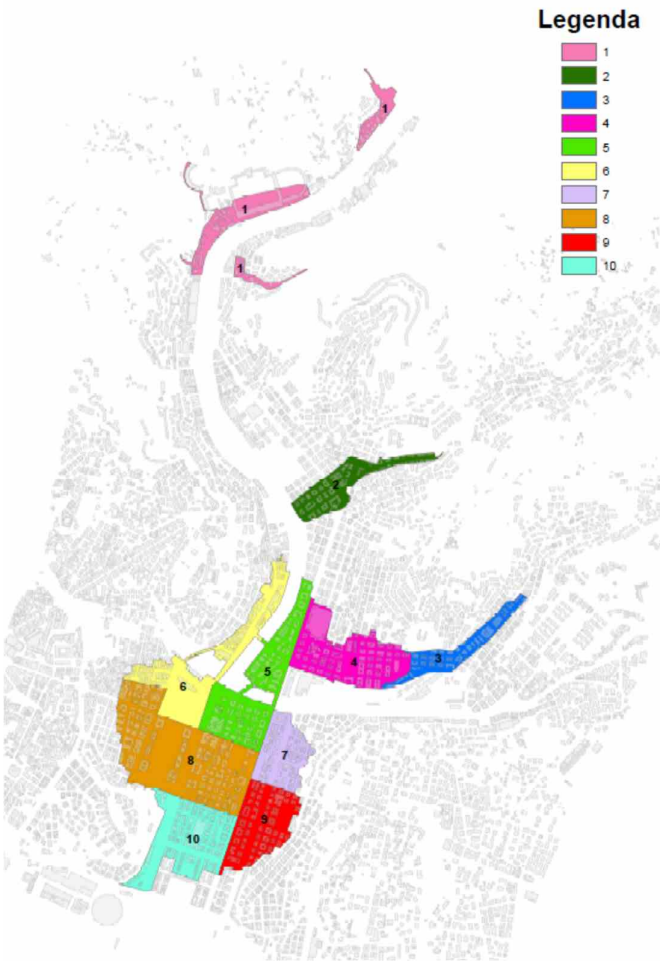

Figure 3-27 Map of the 10 districts assigned to the interviewers for the household survey in the Genova pilot area

Risk and Root Cause Analysis (RRCA)

Root Cause Analysis was conducted for Genoa and the analysis drew on 17 semi-structured telephone interviews with key stakeholders to supplement a review of the vast existing literature in Italian on the floods and flood history in Genoa, including technical reports, planning documents, legal documents and scientific reports and articles as well as analysis of relevant media reports, which covered more than 150 articles published online between 2010 and 2015.

The RRCA focused on the flooding events of 2011 and 2014 in Genoa, Italy points up the vital role of early warning systems and structural mitigation works in protecting against rapid-onset flooding due to the complex morphology and climate of the city ï which contains multiple river catchments with steep slopes and a small coastal fluvial plain. In particular, the analysis highlighted the governance issues that prevented structural mitigation projects planned as far back as the 1990s from being realised. The interplay between legal and financial issues generated a deadlock that prevented local authorities from effectively reducing risk. The progressive increase of extreme events and the presence of a flexible institutional structure allowed this root cause to be addressed through a change in the criteria for funding allocation and by creating new institutional units to reduce hydrogeological risk. The holistic nature of the Root Cause Analysis brought to the fore issues often hidden from local narratives about the

flooding disasters, namely the human resources constraints for the authorities in charge of disaster risk management.

Vulnerability assessment

As mentioned above, the vulnerability assessment in PEARL comprises a survey on household level for Genoa, as well as an approach for spatial vulnerability assessment, including the calculation of a compound index.

A geo-referenced vulnerability assessment approach was developed. The purpose of the spatial vulnerability analysis is to display the results on maps, either as a compound index or parts. The advantage of this method is that all sub-indices can be represented separately or as a combination. In this way, a better understanding of the vulnerability structure can be achieved. The aggregation of numerous components into a single index allows to draw conclusions at one glance, because every spatial entity is assigned to one value. For the calculation of indicators information is required, starting with (1) geo spatial data and (2) spatially explicit statistical data on the respective scale. The results of the vulnerability assessment aim to be tractable to policy-makers and can be integrated in ongoing or future spatial planning or management processes. The vulnerability assessment in PEARL includes a methodology which is flexible in terms of the data and as such it can be applied for every case study area with regard to the availability of data. The concept and outcome is furthermore explained in Deliverable 1.3. To ensure optimal use of information, IREUS and UNESCO-IHE developed an extended approach of vulnerability assessment, which makes it possible to incorporate findings from the household survey in Genoa into the general vulnerability assessment scheme. It therefore comprises the combination of statistical data, deriving from the Census data in Genoa, geo-statistical data and information on household level.

Two maps where used for the vulnerability component of risk. The first map consist on the assessment of vulnerability purely based on census data for the region at the geographical scale selected for this project whereas the second method combine information of the census data with data collected using a field survey campaign (household enriched method). The vulnerability maps are shown in Figure 3-28.

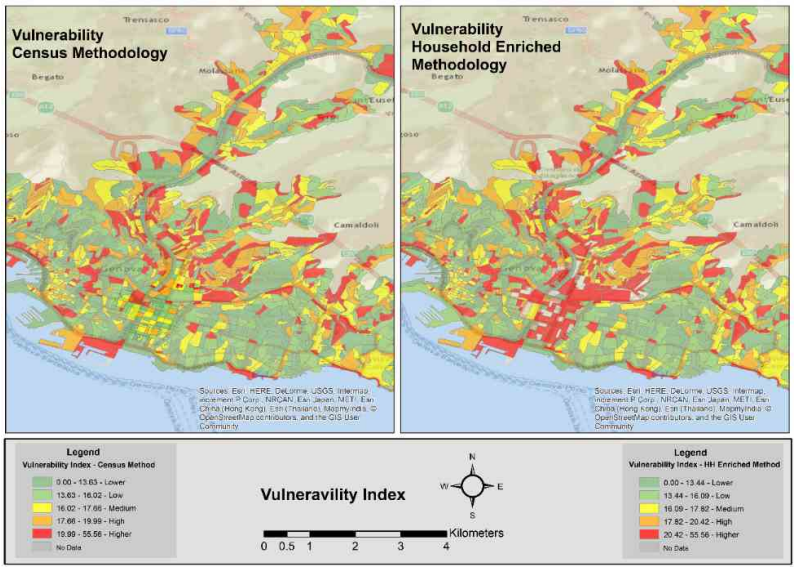

(a) (b)

Figure 3-28 Vulnerability Index Genoa Case Study. (a) Household enriched methodology. (b) Census based Methodology.

3.4 Risk assessment

The overall risk assessment consist in compound index based on the vulnerability assessment performed by the project partners IREUS (Stuttgart university) and UNESCO-IHE and the flood inundation maps generated by GISIG as project partners in the study area. For the purpose of this case study Risk is defined as:

$$\text{Risk} = \text{Vulnerability} \times \text{Hazard}$$

For vulnerability, the two methodologies above mentioned classify the vulnerability of the study area into 5 categories and due to the inherent characteristics of vulnerability it was decided to not define thresholds to be able to properly illustrate disparities within a case study site, therefore the quantile method was used for spatial display into the five selected categories: Lower, low, medium, high and higher vulnerability.

In the case of the hazard component, two major flood events were used in this study: Flood of 2011 and flood of 2014. For the event in 2011 the peak of the flood in terms of water depth was at 3:00 hours in the simulation and for the 2014 event the peak corresponds to the 22:20 hours (Figure 3-29).

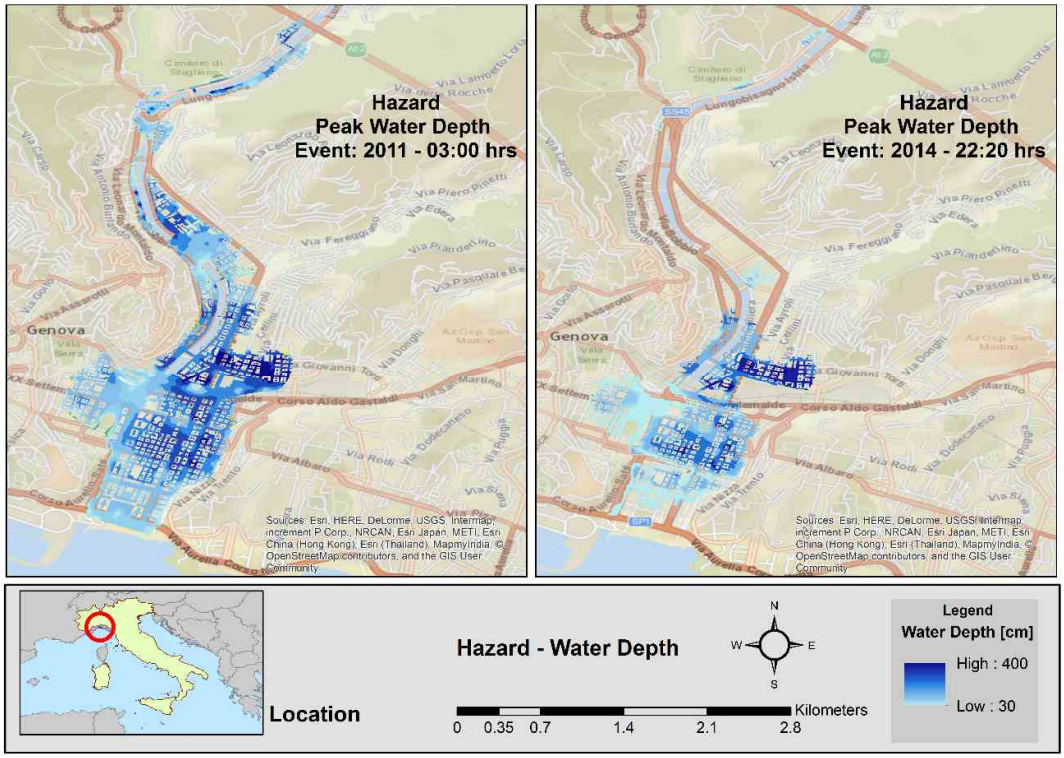

(a) (b)

Figure 3-29 Water depth ï Flood Hazard Genoa Case Study. (a) 2011 event. (b) 2014 event.

In order to compute the risk index the two maps of vulnerability and the two maps of hazards were reclassified and be converted into the same scale, this in order to be able to operate with them. The scales for reclassification used in the case of Genoa are shown in Table 3-1 for vulnerability and Table 3-2 for hazards. The reclassification of maps was done using the reclassify command of ArcGIS based in raster files of the files.

Table 3-1 Reclassification of Vulnerability

Vulnerability Index			Map Category
Category	Census Data	Census + Household	
[Lower]	0.00 – 13.63	13.95 – 16.26	1
[Low]	13.63 – 17.52	16.26 – 17.52	2
[Medium]	17.52 – 18.02	17.52 – 18.02	3
[High]	18.02 – 18.75	18.02 – 18.75	4
[Higher]	18.75 – 19.65	18.75 – 19.65	5

The respective reclassified map is presented here below in figure 3-30

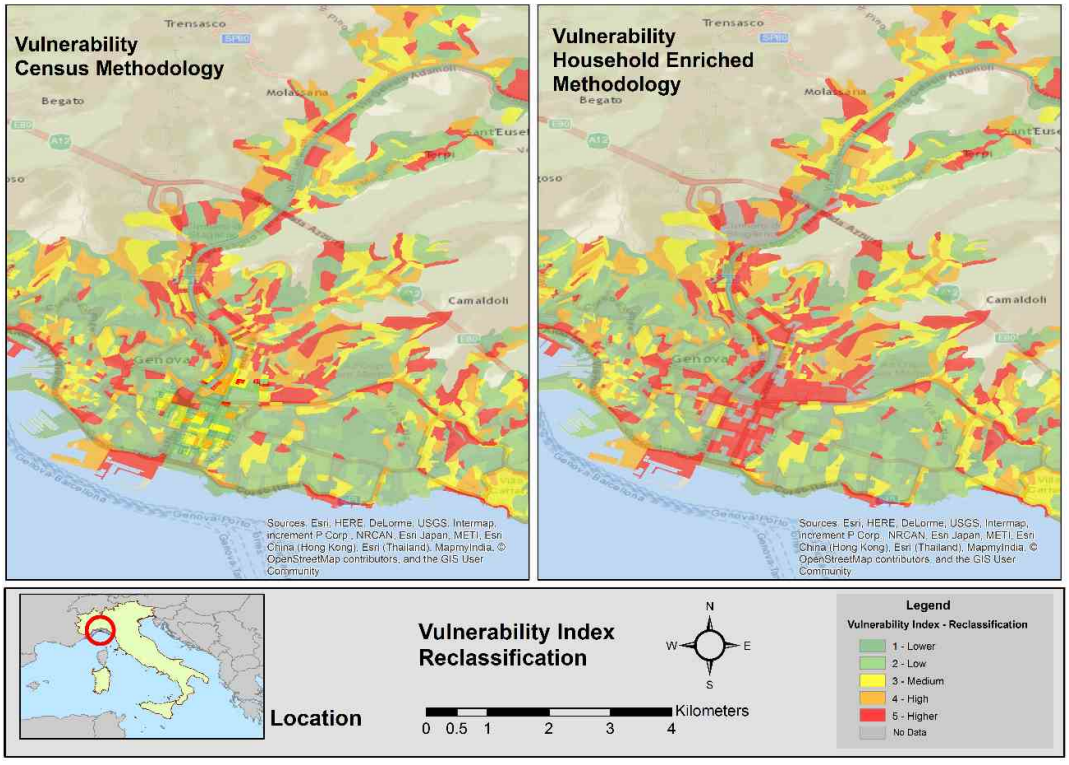

(a) (b)

Figure 3-30 Reclassification of Vulnerability. (a) Household enriched methodology. (b) Census based Methodology.

Table 3-2 Reclassification of Hazards/Water Depth classes

Hazard		Map Category
Category	Water Depth [cm]	
[Lower]	0.00 – 30	1
[Low]	30 – 50	2
[Medium]	50 – 75	3
[High]	75 – 100	4
[Higher]	> 100	5

The reclassified maps for the flood maps (hazard) is shown in Figure 3-31.

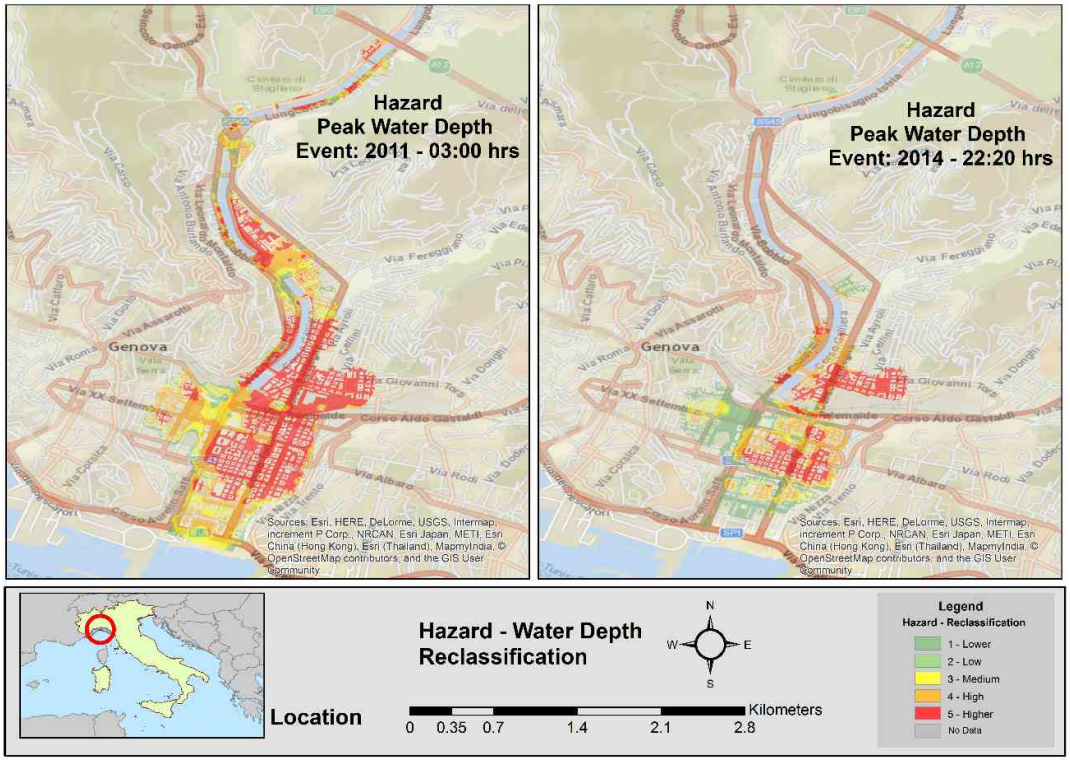

(a) (b)

Figure 3-31 Reclassification of Water depth ï Flood Hazard. (a) 2011 event. (b) 2014 event

Having all the maps in raster format and reclassified into the 5 categories mentioned above the next step in the risk computation was to multiply this maps. Due to the nature of the operation the output maps will range values between 0 and 25, where the lowest the number the less risk for that area in particular. An extra Reclassification of this maps was done to have a five category scale for risk and preserve the integrity with the other maps scale (Table 3-3).

Table 3-3 Final Reclassification of Risk.

Risk		Map Category
Category	Vulnerability x Hazard	
[Lower]	0 - 5	1
[Low]	6 – 10	2
[Medium]	10 – 15	3
[High]	15 – 20	4
[Higher]	> 20	5

The resulting risk maps are presented in figures 3-32 and figure 3-33

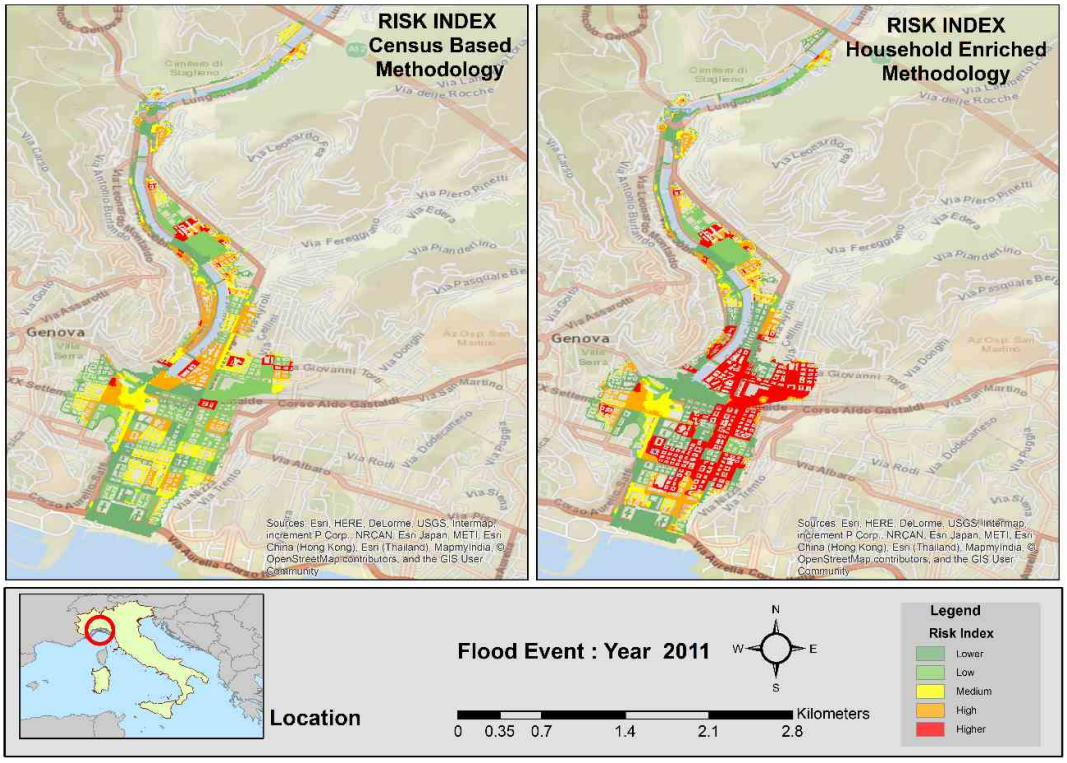

(a) (b)

Figure 3-32. Risk Index Genoa Case Study ï 2011 Flood Event. (a) Census based Methodology (b) Household enriched methodology

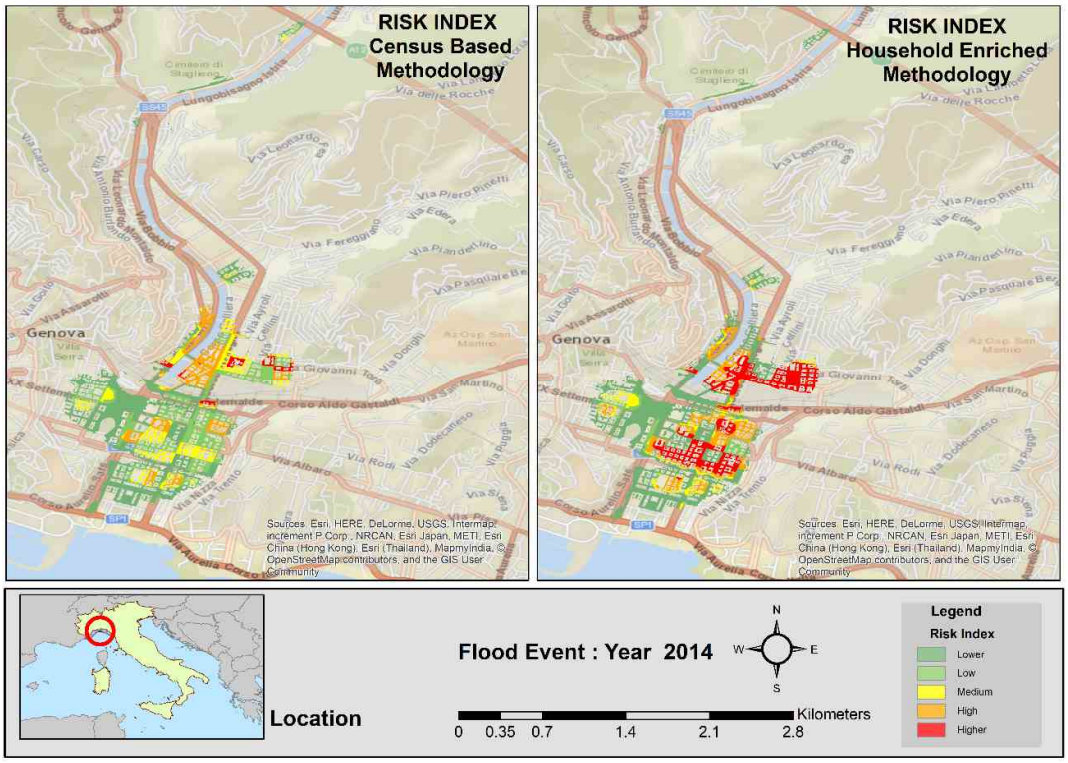

(a) (b)

Figure 3-33. Risk Index Genoa Case Study ï 2014 Flood Event. (a) Census based Methodology (b) Household enriched methodology

3.5 How risk analysis benefit local stakeholders

Local stakeholders didnôt receive yet any information regarding the risk analysis, this activity will be included in the next meeting of the LAA.

4 Case Study Hamburg, Elbe Estuary

4.1 Introduction

This report describes the research activities in WP3 until the due date of the deliverable 3.4, which is the 31st December, 2016. The research activities for the Elbe Estuary/ Hamburg case study will be updated during 2017.

The impact and risk assessment is focussed on the flood prone area of the largest urban area in the Elbe Estuary being the city of Hamburg (Figure 1, marked in blue) and encompass the following activities:

- damages to the built environment focusing on a densely populated Hamburg district of Wilhelmsburg, which is undergoing an intensive urbanisation process in the recent years (IBA, 2012). Here, PEARL is building upon the research outcomes from the EU project CORFU and the project XtremeRisK funded by the German Ministry for Education and Research, in which the impact assessment has been performed as of the year 2010. This is taken as a baseline for the investigations described in this report. Due to the development of the urban area of Wilhelmsburg, which mainly took place after 2010 (see chapter 1.5.2) it is the objective of this study to assess the temporal development of the impacts and flood risk in the area, mainly triggered by an intensive urban development process (in further text***: the District of Wilhelmsburg***)
- direct and indirect damages for critical infrastructure, for the port of Hamburg and the public and private transportation sector (are still an ongoing research, where the activities so far the intermediate results are thoroughly documented in Gkliati (2015), Blaj (2016), Zhamo (2016) and PEARL D6.2. The updated results will be reported in the final version of this deliverable). (In further text: ***Critical Infrastructure***)

A overview of the impact assessemnt activities for the City of Hamburg is given in **Error! Reference source not found.**.

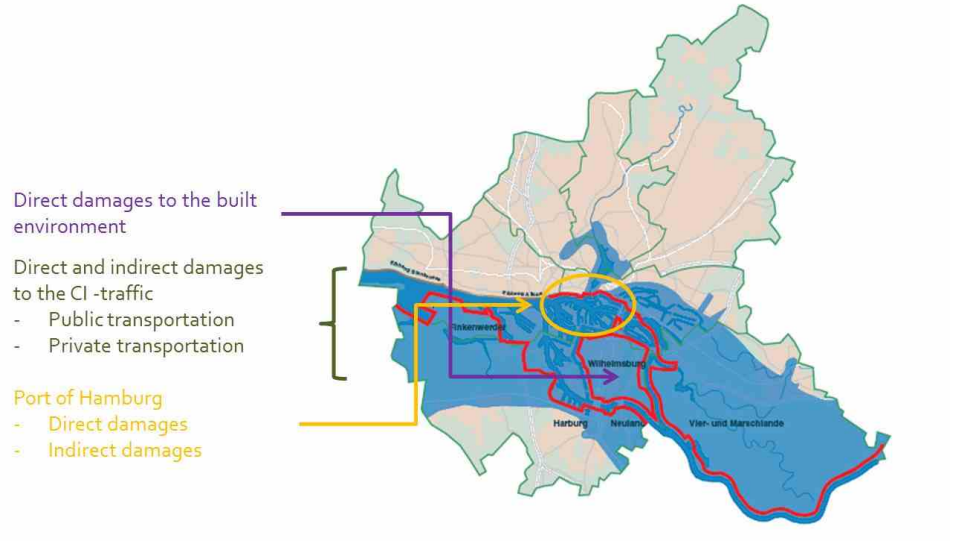

Figure 4-1 Actual overview of the research acitvities for the Elbe estuary/Hamburg case study (red line indicates the public flood protection infrastructure)

Expected updates of the study by the end of 2017:

- Finalised impact assessment for the District of Wilhelmsburg, based on the updated flood hazard maps and different scenarios (performed and defined in WP2) to asseess the temporal development of the flood risk
- Finalised impact assessment on the Critical Infrastructure
- Holistic risk assessment (applying the ósimplifiedô holistic risk assessment approach (D3.1) i.a. taking into account the temporal development of the flood risk

4.2 Description of the study area

The city of Hamburg and the Elbe estuary are located in the North German Plane with a direct connection to the North Sea and the German Bight. Storm surges evolving in the German Bight can move in the direction of the river Elbe and hit the city of Hamburg. In the recent past a number of storm surges hit the city. The storm surge causing highly severe impacts occurred in 1962. In total, 315 people died during the storm surge and entire districts have been flooded, especially Hamburg Wilhelmsburg suffered from the storm surge (LSBG, 2012, Hötte, 2012). Several years later, a storm surge occurred, which caused large damages to the seaport of Hamburg, but caused less damage to the rest of the city (Laucht, 1977). As a result of the storm surges flood protection infrastructure has been redesigned and reinforced and is today considered to be in good condition (LSBG, 2012). Nevertheless, there is a certain flood risk, which has to be assessed, especially in the light of City of Hamburgôs strategy to enhance the urban growth and development.

4.3 Data collection and analysis for hazard assessment

Extreme hydro-meteorological events characterized by i) storm surge water levels, ii) precipitation and iii) river run-off represent hazards to the case study area. Together with the corresponding probabilities, both univariate and bivariate, these parameters are the input for the hazard assessment. Relevant loads for the Hamburg case study have been analysed in work package 2. Details on the analyses can be found in the PEARL deliverables D2.1 and D2.2. Based on multivariate statistical analyses in WP2 different hydro-meteorological scenarios can be defined. Figure 4-2 shows an example of storm surge scenarios characterized by water levels and fullness (T = 200 years).

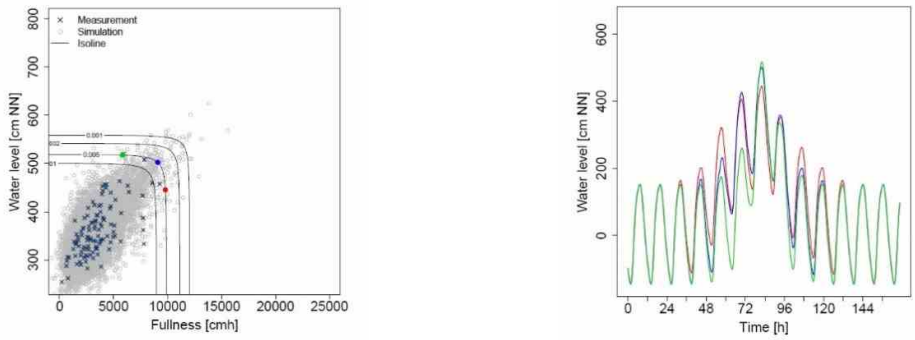

Figure 4-2: Example for defined storm *water scenarios with a return perios of 200 years.*

The district of Wilhelmsburg: For the risk assessment in the area of Wilhelmsburg, the flood hazard assessment and the considered scenarios are based on the results of the projects Corfu and XtremRisK, being described in the following.

In a first step, the storm surge scenarios have been derived on the basis of recorded storm surge hydrographs from the recent past. These storm surge hydrographs have been superimposed by phenomena like bores and extreme spring tide set-up. Investigations of storm surges of the recent past have shown, that bores can increase the storm surge water levels significantly (Heerten et.al. 1977, Laucht 1978). Adding a high spring tide set-up leads to storm surge scenarios with extreme water levels representing adverse storm surges, which may result in high damages and flood risk. The methodology for the derivation of the storm surge scenarios and the respective storm surge scenarios hav been developed for the tidal gauge of Cuxhaven (Gönnert et.al. 2012). In order to transfer the storm surge hydrographs to Hamburg St. Pauli the numerical model UnTRIM has been used (Rudolph, 2011, in: Oumeraci, 2012). The simulation work has been carried out the Federal Waterways Engineering and Research Institute (BAW) (Oumeraci et.al. 2012). A detailed description can be found in Oumeraci et.al. 2012 and Rudolph 2011 (in: Oumeraci, 2012).

In the following, the three derived storm surge scenarios are described. The first scenario, HH_XR2010A, is based on the storm surge of January 3rd, 1976 representing the highest storm surge that has occurred in the recent past. The storm surge hydrograph, at the tidal gauge of Cuxhaven, was superimposed by a bore with a height of 77 cm and a maximum spring tide set-up of 61 cm (Oumeraci et.al., 2012). The superimposed storm surge has been transferred to the tidal gauge of Hamburg St. Pauli using a numerical hydrodynamic model. Additionally, the highest measured river run-off of the Elbe of 3600m³/s and the wind field over the Elbe of January 3rd, 1976 has been considered (Figure 4-3, red line).

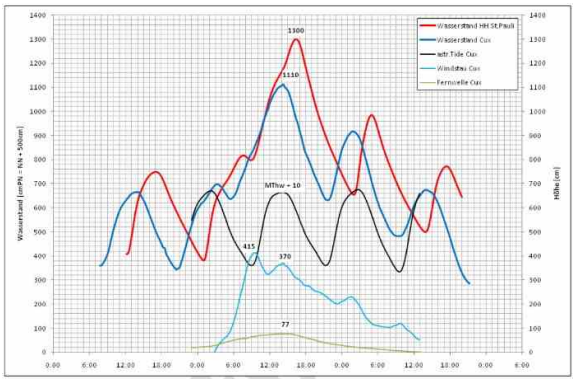

Figure 4-3: Storm surge hydrograph for the scenario HH_XR2010A

The second storm surge scenario, HH_XR2010B, is based on the storm surge of February 27th/28th, 1990 representing a chain of three consecutive storm tides. Considering a river run-off of 3600 m³/s as well, high tide water levels between NN + 6,5 m and NN + 7,08 m have been reached (Figure 4-4, red line) (Oumeraci et.al., 2012).

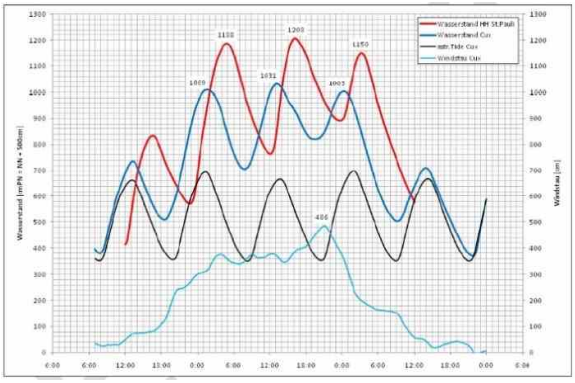

Figure 4-4: Storm surge hydrograph for the scenario HH_XR2010B

The storm surge of January 3rd, 1976 has been the basis for the storm surge scenario HH_XR2010C as well. The difference from the scenario HH_XR2010A lies in the underlying climatic and meteorological conditions. The scenario HH_XR2010A has been derived for present climatic conditions. Whereas, a potential increase of the mean sea level for the time horizon until 2100 and changed climatic conditions have been considered in the scenario HH_XR2010C. The storm surge is a chain of three consecutive storm tides, as well, with high tide water levels between NN 5,51 m and NN + 8,64 m (Figure 4-5, red line) (Oumeraci et.al., 2012).

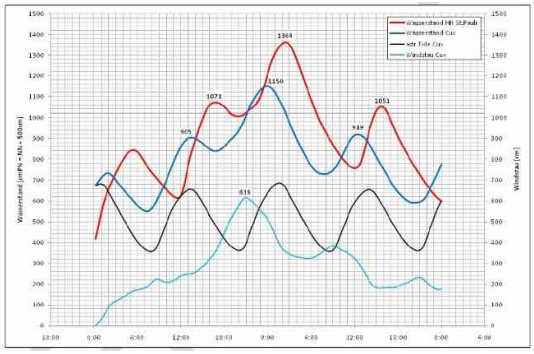

Figure 4-5: Storm surge hydrograph for the scenario HH_XR2010C

All three scenarios have been statistically analysed using multivariate models in order to assign a probability of occurrence to each of them (Oumeraci, 2012). The following table gives an overview of the scenarios.

Table 4-1: Characteristics of the considered storm surge scenarios (Oumeraci, 2012, modified)

Scenario	HH_XR2010A	HH_XR2010B	HH_XR2010C
Peak water level [cmNN]	610	531	650
Fullness [-]	537	770	767
P_e [1/a] (bivariate)	$3{,}17*10^{-4}$	$7{,}20*10^{-3}$	$4{,}27*10^{-4}$
Fresh water discharge [m^3/s]	3600	3600	3600

$P_{e, Oberwasser}$ [1/a]	$2{,}50*10^{-2}$	$2{,}5*10^{-2}$	$2{,}5*10^{-2}$
P_e, Hamburg [1/a] (trivariate)	$7{,}72*10^{-6}$	$8{,}09*10^{-8}$	$5{,}3*10^{-8}$

The described scenarios are the basis for a hydrodynamic model, leading to the hydraulic input parameters for the impact assessment assuming a functional failure, namely overtopping, of the dike line. In a further step, an inundation model was set-up to simulate the flood propagation using Mike 21 by DHI. A digital terrain model is generated using a combination of laser scanning point data, breaklines and polygons of the channel beds, describing the canals, in order to establish the hydrodynamic model. The influence of changing roughness is considered based on the prevailing land use categories and breaklines are derived from the dataset.

The combination of the digital terrain model and the breaklines from both the digital terrain model and the roughness polygons is used to generate the calculation mesh for the hydrodynamic model. The storm surge hydrograph, described above, are used as hydrodynamic boundary conditions.

The results from the inundation model are analysed to derive the maximum water depth, as this is the decisive input parameter for the assessment of the tangible damages and the calculation of the flood risk (Figure 4-6).

Figure 4-6: Results of the inundation modelling for the considered scenarios (Ujeyl, 2012)

The subsequent spatial modelling of the tangible damages use a cell based approach (see chapter 1.4). Therefore, it is necessary to convert the results from the hydrodynamic model into regular grids of uniform size (10 m, 50 m, 100 m) (Ujeyl, 2012).
Within 2017 the flood hazard assessment will be carried out based on the derived hydro-meteorological scenarios from WP2, using the TUHH Kalypso model suite.

4.4 Data collection and analysis for vulnerabiltiy assessment

The district of Wilhelmsburg: As given in Section 4.1 the research results from the projects Corfu and XtremeRisk form the baseline for the investigations described in this report describing the temporal development of the flood risk. Within the Corfu and XtremeRisk projects vulnerabilities for i) residential buildings, ii) commercial objects and iii) infrastructure

with respect to direct damages are assessed and described in the following. The investigations have been carried out on a micro scale (i.e. on building scale with a spatial resolution of 10 m x 10 m).

The objects that are potentially exposed to storm surges have been identified and geo-processed; the residential objects are represented by polygons based on the data of the cadastral map. For the commercial objects point data is used, which has been generated from data collected from the chamber of trade. This data contains addresses and further information (e.g. number of employees) on the commercial objects.

The elements at risk (residential buildings, commercial objects, infrastructure areas) have been divided into categories of equal characteristics, based on the gathered data. For the representation of the residential objects representative building types have been defined, based on a multi-criteria analysis considering i) the type of the building, ii) the occupancy of the ground floor and iii) the wall construction. On-site surveys, available construction drawings and floor plans of the buildings as well as home visits have been used to gain an overview of the existing building stock and to define the representative building types. I totoal, a catalogue of 25 representative building types has been created. Figure 4-7 shows exemplarily the representative building types for detached houses.

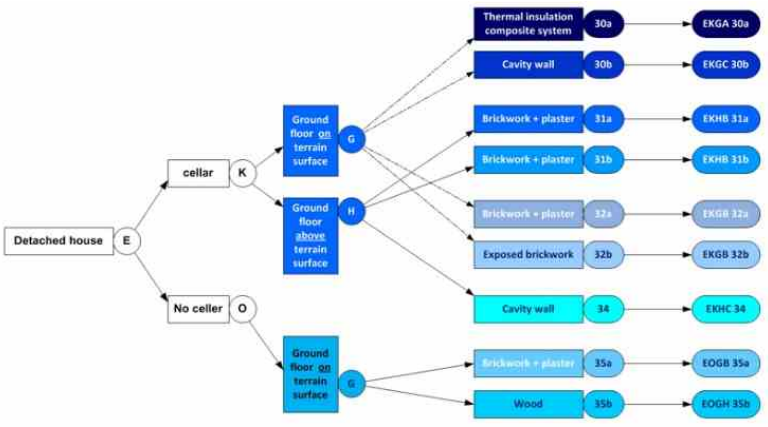

Figure 4-7: Representative building types for detached houses (Ujeyl, 2012)

Thereby, it is possible to assign a representative building type to each residential object in the area under investigation, which are represented using ArcGIS (Figure 4-8).

Figure 4-8: Assignment of representative building types to residential objects, (Ujeyl, 2012)

Classification of the commercial objects is made on the basis of the respective branches of economic activities represented by the firmôs industry classification (NACE Code, Figure 4-9). By this, the economic activities are represented in a uniform manner and it is possible to link the number of employees, which represents a measure of the businessôsize, with the branches of economic activities.

Figure 4-9: Representation of the commercial objects based on the NACE codes (Ujeyl, 2012*)*

After the residential and commercial objects have been classified, the evaluation of the asset values and the derivation of the depth-damage curves is carried out. Concerning the residential objects, the vulnerability has been assessed with regard to the following potential damages considering the respective costs (Ujeyl, 2012):

- Damages to structural elements: replacement costs for the inner walls, floor and floor covering, doors, windows etc.
- Costs for cleaning-up: cost for cleaning and drying in dependence of the material and the duration of flooding
- Damages to the inventory: replacement cost of the fixed and dismountable furnishing of residential houses

Damage curves for each representative building type have been calculated for both the building itself and the inventory. An example is shown in Figure 4-10. These curves have been implemented into a geoprocessing tool for a GIS based spatial modelling approach (Burzel, 2012).

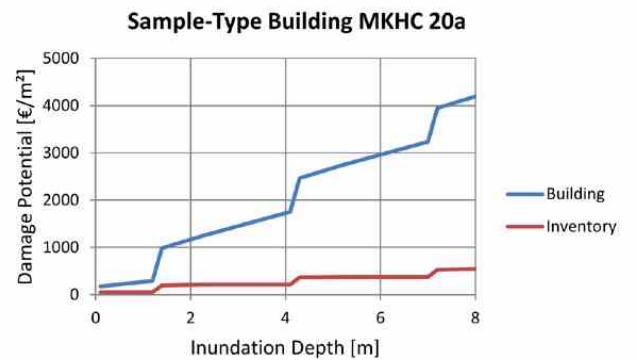

Figure 4-10: Damage curves for building and inventory for a representative building type, (Ujeyl, 2012)

Relative depth-damage curves for the building and equipment are derived for the commercial sector. Necessary data has been gathered on the basis of direct inquiries and visits with local businesses. The assets are downscaled to Wilhelmsburg from national accounts defined for fixed assets, divided into buildings and equipment. A detailed description can be found in Oldhafer, 2012. The toolbox mentioned above, is applicable for the calculation of the damages of the commercial sector as well, by adjusting the input files and the damage curves.
During 2017, the assessment of the temporal development of the vulnerabilities will be finished. Furthermore, the assessment of the impacts on the critical infrastructure and the indirect damages (see 4.1) will be finalised.

4.5 Risk assessment

4.5.1 *The district of Wilhelmsburg*

Assessment as of the year 2010 (XtremRisK/CORFU)

The following calculation of the damages is carried out within an ArcGIS, based on the results of the hazard and impact assessment. A cell based risk assessment approach is used to calculate the direct tangible damages and subsequently the flood risk. Water levels, resulting from the hazard assessment are intersected with the objects at risk resulting from the vulnerability analysis (see chapter 4.4). Thereby, the affected objects are localized. In a next step, the water level relevant for the calculation of the damages is calculated depending on the results of the inundations modelling, the representative building type and the number of storeys. With the help of the derived water levels, the resulting damage potential can be calculated from the damage curves (see Figure 4-10). By multiplying the damage potential with the area of the affected cells, the resulting damage due to the flooding is gathered. Figure 4-11 give a general overview of the operating principle of the toolbox for the calculation of the direct damages for residential houses. Table 4-2 gives an overview of the damages caused by the considered storm surge scenarios and the corresponding flood risk (Ujeyl, 2012).

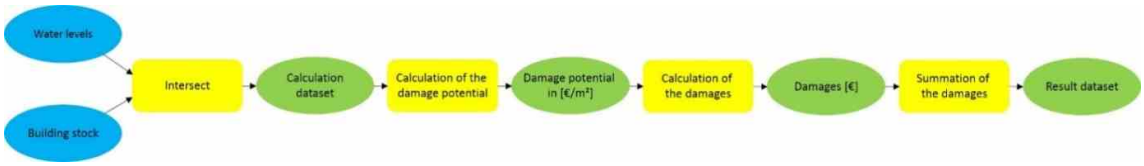

Figure 4-11: Overview of the operating principle of the geoprocessing tool

Table 4-2: Calculated damages and flood risk based on the considered scenarios (Ujeyl, 2012, modified)

Scenarios	Damages in Mio. €					$P_{e,\ Hamburg}$ [1/a]	Risk [€/a]
	Residential		Commercial		Total		
	Buildings	Inventory	Buildings	Equipment			
HH_XR2010A	572,47	67,57	87,15	311,29	1038,48	$7{,}72*10^{-6}$	7477,06
HH_XR2010B	0,26	0,03	2,12	1	3,14	$8{,}09*10^{-8}$	0,25
H_XR2010C	2297,04	323,47	824,53	1907,47	5252,51	$5{,}3*10^{-8}$	278,38

4.5.2 *Assessment of the temporal development of the flood risk (2010- 2016)*

The disctrict of Wilhelmsburg : The district Wilhelmsburg, the largest and one of the central districts of the city of Hamburg, was conceived as central working-class district and emigrant districts back in the 1920s. This image hasnôt change for decades. Wilhelmsburg has been neglected in the urban development for a long time. Nevertheless, it is a district with a high potential for urban development. In recent years, politics have discovered this potential and launched a new development program in 2003 called ñLeap over the Elbeò aiming at the improvement of quality of life and living in megacities by developing sustainable strategies for urban development (FFH, 2005). In the scope of this development program and the International Building Exhibition Hamburg (IBA) 2013 a large number of new and innovative urban development project have been evolved and realized. Amongst others, residential districts have been rebuilt or have been newly built using innovative construction methods as happened in the district Wilhelmsburg Central (Figure 4-12 - yellow circle, Figure 4-13).

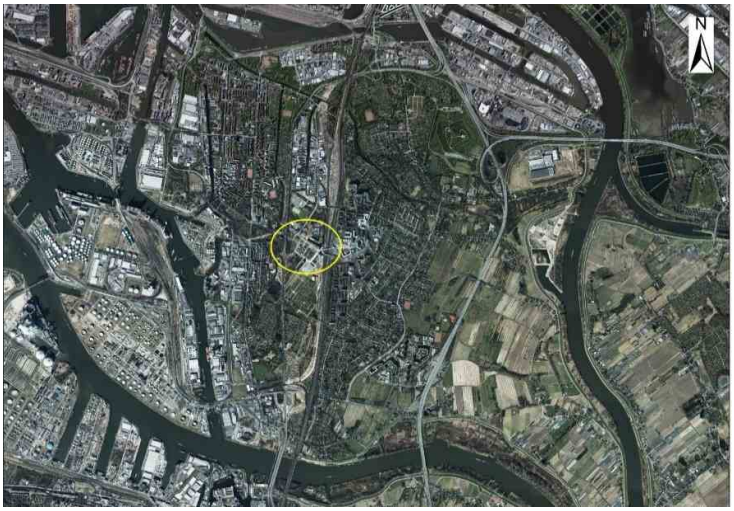

Figure 4-12: Location of the district Wilhelmsburg Central

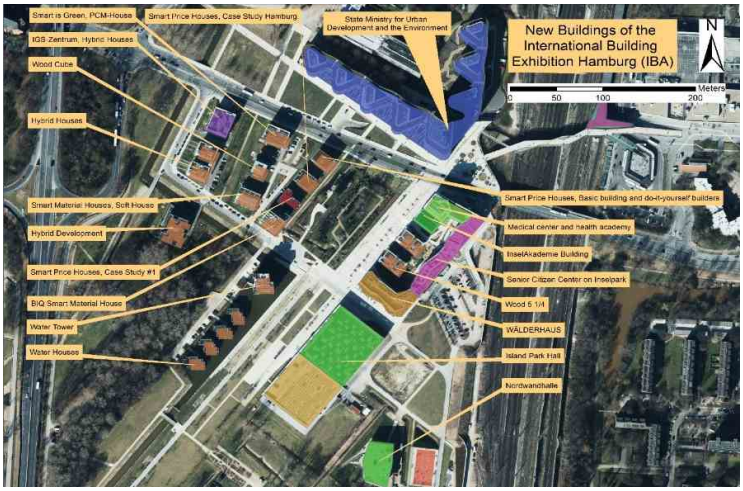

Figure 4-13: Overview of the IBA projects in Wilhelmsburg Central

A comparison of the available building stock on the basis of the data of the cadastral map from 2010 (results from the XtremeRisK project) and 2016 showed that, besides the buildings in Wilhelmsburg Central, a number of other mostly residential buildings have been newly built all over Wilhelmsburg.

In order to derive the magnitude of change of the flood risk the methodology developed during the XtremeRisK project and described above is applied. As mentioned above both conventional and innovative house construction can be found in the building stock. The damage curves are assigned to the new buildings depending on the construction types. Existing damage curves, developed during the XtremRisK project, are assigned to buildings of conventional construction technique. Due to the innovative construction technique of the residential houses in Wilhelmsburg Central (see Figure 4-13) new damage curves must be

developed, based on the respective building specifications and available floor plans. Figure 4-14 shows exemplarily the damage curves of the ñSmart Material House BIQò for both the building and the inventory. Similar damage curves will be developed for the other IBA projects. It is expected that the overall vulnerability will significantly increase, due to the new created asset values.

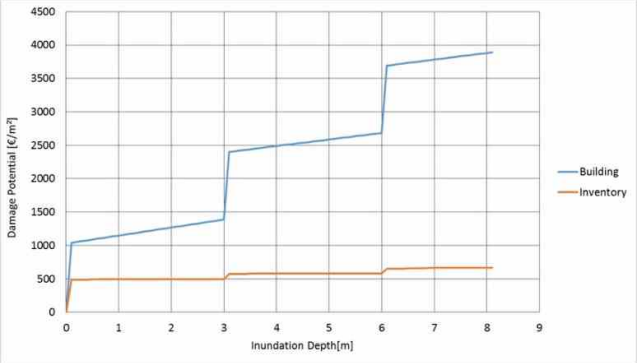

Figure 4-14: Damage curve of the ñSmart Material House BIQò

Once the damage curves have been developed, the damages resulting from the storm surge scenarios described in chapter 4.3 will be calculated. To this, the developed geoprocessing tool (see chapter 4.5) will be used. Before the tool can used, the toolbox and the respective scripts have to be recoded to make it executable in the latest ArcGIS version. Furthermore, the geoprocessing tool has to be extended by the new developed damage curves. It is expected that the calculated damages will have significant magnitudes. Whereas, the damages to the buildings are expected to be higher than the damages to the inventory. This is due to the specialized building services located on the ground floor of each building and the specialized construction technique (e.g. WoodCube: mere wooden construction).

4.6 How risk analysis benefit local stakeholder

The investigations carried out and described above represent the baseline for the assessment of the temporal evolution of the flood risk in a constantly growing and developing city. With the help of the initiated investigations it will be possible get an overview of the effect of urban development plans like the ñLeap over the Elbeò program on the flood risk. Furthermore, the results of the investigations could be used as the basis for a risk-based revision of the flood protection infrastructure. It is possible to identify potential hot spots of the urban area, which might receive enhanced flood protection because of planned developments of the respective urban area. On the contrary, in urban areas in which assets or object should be dismantled the flood protection may be dismantled as well and give space to the nature.

4.7 Influence of adaption measures on hazards and consequently on the risks

The Elbe Estuary and the City of Hamburg have a high level flood protection infrastructure composed of dikes, walls, gates and pumping stations, which consequent reinforcement and improvement has been established in response to the devastating storm surge event of 1962. The flood location and extent of the public flood protection infrastructure is given in **Error!**

Reference source not found.. In Wilhelmsburg, the current dike crest elevation varies between +7.70m and +8.35m, well above the design stage level, i.e. +7.30m. However, due to the enhanced urbanisation with the associated changes in the flood risk over time (for the scope of this work given for the district of Wilhelmsburg) the current flood protection infrastructure may be not appropriate in the future and new adaptation and mitigation measures, including the nature-based solutions, are to be developed. In PEARL, different adaptation strategies have been identified and analysed in their potential to mitigate the flood risk and are given in (Table 4-3).

Table 4-3: An overview of the adaptation measures including their types, short description/location and the status in respect to their modelling in WP5

Catalogue of adaptation measures					
Type of adaptation measure	**Adaptation Measure**		**Description**		**Status**
Static	M1	Narrowing of the cross section	M101	90% Narrowing near Brunsbüttel	In Progress
			M102	60% Narrowing near Brunsbüttel	In Progress
			M103	75% Narrowing near Brunsbüttel	In Progress
	M2	Re-aligment of dikes	M201	100m	In Progress
			M202	250m	In Progress
			M203	500m	In Progress
			M204	750m	In Progress
			M20X	>750m	In Progress
Dynamic	M3	Flood protection polder	M301	Location/Size A	
			M30X	Location/Size B	
	M4	Elbe flood barrier	M401	Closing time A	
			M40X	Closiing time B	
	M5	Integration of old tributaries	M501	Historical conditions (1930)	In Progress
			M502	Wischhafener Süderelbe	
			M503	Haseldorfer Binnenelbe	
			M504	Borsteler Binnenelbe	
			M505	Alte Süderelbe	
			M506	Dove-Elbe	
			M507	all	
	M6	Integration of tributaries	M601	Oste	
			M602	Stör	
			M603	Krückau	
			M604	Pinnau	
			M605	Schwinge	
			M606	Lühe	
			M607	Este	
			M608	all	

In order to assess the hydrodynamic effects on the Lower Elbe in case of storm surges, the adaptation measures are incorporated into the 2D HDN model of the Elbe estuary (see D6.2, D4.1). Storm surges hydrographs derived in WP2 or measured Storm surges hydrographs (e.g. Xaver in 2013) are used as hydrodynamic boundary conditions. Hitherto, the historic condition, re-alignment of dikes and the narrowing of the river cross section are under investigation or preparation. A preliminary assessment of the historic situation, without the continuous dike line along the Elbe estuary assuming the storm surge event ñXaverò showed on the one hand, that the water level at the gauge Hamburg St. Pauli are significantly lower compared to the recent situation (Figure 4-15).

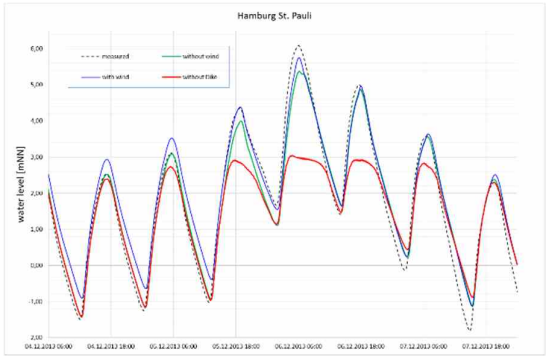

Figure 4-15: Comparison of the water levels at the gauge Hamburg St. Pauli for the historic situation without a continuous dike line (red line) and the recent situation and additional flood protection infrastructure (black dashed line)

On the other, the water levels along the Lower Elbe during a storm surge event (e.g. Xaver) are higher than the average ground level of the hinterland (Figure 4-16) resulting in large inundated areas.

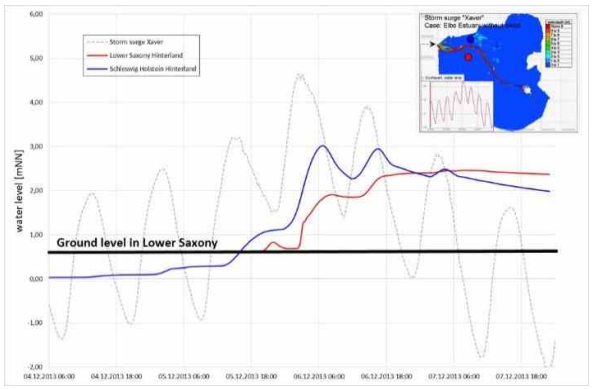

Figure 4-16: Comparison of the water levels at two randomly selected points in the hinterland of the Elbe estuary (dark blue ï Schleswig-Holstein, red ï Lower Saxony) with the water levels of the storm surge Xaver.

These preliminary results illustrate advantages and disandvantages of the recent flood protection infrastructure along the Elbe estuary. Protection of low lying hinterland areas in Schleswig-Holstein and Lower Saxony against large scale inundations is beneficial (see Figure 4-16). On the contrary, the high level flood protection infrastructure along the Elbe river leads to higher storm surge water levels in the Hamburg city area (including the District of Wilhelmsburg) (see Figure 4-15), due to missing space for the river in case of high water levels in the river. Therefore, it is still a matter of research to identify and develop the appropriate adaptation measures (see Table 4-3).

Re-alignment of the continuous dike line by 250 m and 500 m have been investigated (Figure 4-17). The preliminary results shows that a re-alignment of the dikes lead to a decrease of the water levels (Figure 4-18).

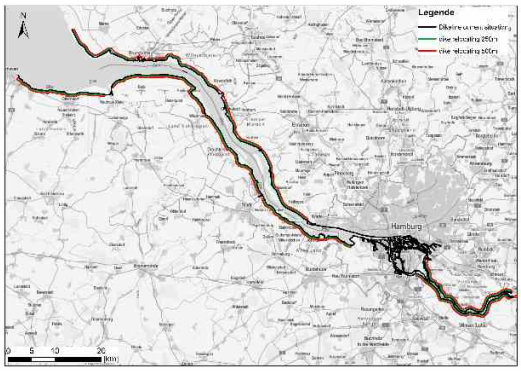

Figure 4-17: Investigated re-alignment scenarios i) 250 m – green line, ii) 500 m – red line

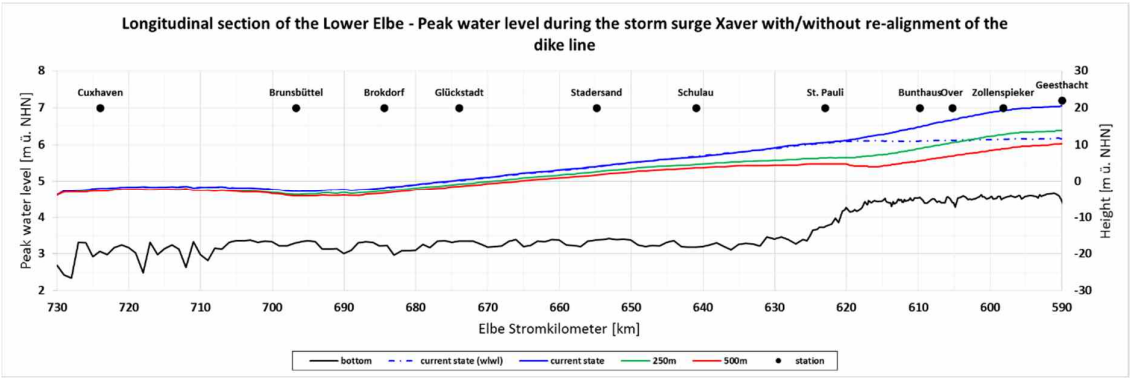

Figure 4-18: Longitudinal section of the Lower Elbe showing the peak water levels during the storm surge Xaver 2013

In 2017 the investigation of the adaptation measures is being continued and will be related to the assessed flood risk and updated flood hazard maps.

4.8 Summary and Outlook

Assessing the development of the flood risk is the aim of the investigations described in this report. During the finished project XtremRisK risk assessment has been already carried out for the district Hamburg-Wilhelmsburg. The assessment of the flood risk was based on a vulnerability analysis for residential and commercial objects and infrastructure as well as a hazard analysis to assess the inundation propagation and the resulting inundation depths. Input data from 2010 formed the basis for investigations in the project XtremRisK. Since then, in the scope of an urban development launched in 2003 (ñLeap over the Elbeò) plan and the IBA Hamburg in 2013 a number of projects have been realised, contribute to the urban development of the Wilhelmsburg district. Due to the new objects and the corresponding asset values, flood risk is expected to increase. In order to assess the current flood risk, the developed methodology is applied. Once, the investigation of the residential objects is finished, commercial objects and the infrastructure is considered as well. Applying the described methodology will lead to the current flood risk here as well and an overall flood risk with the status 2016 will be derived.

4.9 References

Blaj, I. A.: Development of a methodology for economic damage assessment for the critical infrastructure traffic and transportation and application to the case study of the city of Hamburg, Master Thesis, Hamburg University of Technology, 2016

FHH (2005): Sprung über die Elbe, Hamburg auf dem Weg zur internationalen Bauaustellung ï IBA Hamburg 2013, Eds.: Freie und Hansestadt Hamburg, Behörde für Stadtentwicklung und Umwelt, 2005. http://www.iba-hamburg.de/fileadmin/Die_IBA-Story_post2013/051030_sprung_ueber_die_elbe.pdf, Last access: December 8th, 2016

Gkliati, C.: Development of a mehtodology for econmic damage assessment of sea ports and application to the port of Hamburg, Master Thesis, Hamburg University of Technology, 2015

Gönnert, G.; Gerkensmeier, B.; Sosside, K.; Thumm, S. (2012): Extremesturmfluten ï Teilprojekt 1A ï Abschlussbericht, Final Report, 2012, https://www.tu-braunschweig.de/Medien-DB/hyku-xr/04_goennert_et_al_xtremrisk_gesamtbericht.pdf, Last access: December 8th, 2016

Hötte, H., et.al.: Die Große Flut ï Katastrophe Herausforderungen Perspektiven, edt.: Hötte, H., Accompanying book of the exhebition in the Hamburg Town Hall (50. Anniversary of the storm surge 1962), Landeszentrale für politische Bildung, ISBN: 978-3-929728-72-9

Laucht, H.: Der Sturmflutschutz im Hafen Hamburg nach der Sturmflut vom 3. Januar 1976, In:Jahrbuch der Hafentechnischen Gesellschaft, Vol. 36, pp. 157-171, Springer-Verlag, 1977/1978

LSBG: Landsbetrieb Straßen, Brücken und Gewässer: Sturmflutschutz in Hamburg Gestern-Heute-Morgen, Report Nr. 10/2012, 2012 (In German)

Oldhafer, N. (2012): Damage Calculation and Assessment at Open Coasts and Estuarine Areas as a Consequence of Extreme Storm Surges ï Case Study of Hamburg (Wilhelmsburg) and Sylt (Hörnum), Diploma Thesis, in German, 2012

Oumeraci, H.; Gönnert, G.; Jensen. J.; Kortenhaus, A.; Fröhle, P.; Gerkensmeier, B.; Wahl, T.; Mudersbach, Ch. Naulin, M.; Ujeyl, G.; Pasche, E. À; Dassanayake, D.R.; Burzel, A. (2012): Extremsturmfluten an offenen Küsten und Ästuargebieten ï Risikoermittlung und ï beherrschung im Klimawandel (XtremRisk) ï Abschlussbericht, Final report, 2012, https://www.tu-braunschweig.de/Medien-DB/hyku-xr/50_oumeraci_et_al_xtremrisk_abschlussbericht.pdf, Last access: December 8th, 2016

Ujeyl, G.; Fröhle, P.; Pasche, E. À (2012): Evaluating direct damages of residential and commercial assets on a micro scale ï Results of the XtremRisk Project, In: Comprehensive Flood Risk Management, Research for Practise and Policy, Eds.:Schwenckendiek, T., CRC Press, DOI: 10.1201/b13715-82, 2012

Rudolp, E. (2011): Modellierung von Extremsturmfluten im Elbeästuar am Beispiele des Sturmflutszenarios HH_XR2010C, Vortrag beim XtremeRisK-Arbeitsstreffen vom 30.05.2011

Zhamo, M.: A contribution to the development of a method for flood impacts assessment of the public transportation network as an element of the critical infrastructure. Lessons learned from NYC, USA, Master Thesis, Hamburg University of Technology, 2016

5 Greve Case Study

Greve is a municipality in eastern Denmark. It is a sub-urban area located around 20 km southwest of the Danish capital Copenhagen (Figure 4). The Municipality has a total area of around 60 km^2, with 9 km of coast to the southeast bordering the Baltic Sea at Køge Bay. The coastal boundaries stretch from Hundige Beach Park in the north to the sandy coast of Kalstrup Beach Park in the southwest. The beaches in this area are mainly sandy and very flat-bottomed. The coastal area is the most densely built-up part of Greve, and is characterized by relatively flat terrain with elevations between 2 and 6 m (above MSL).

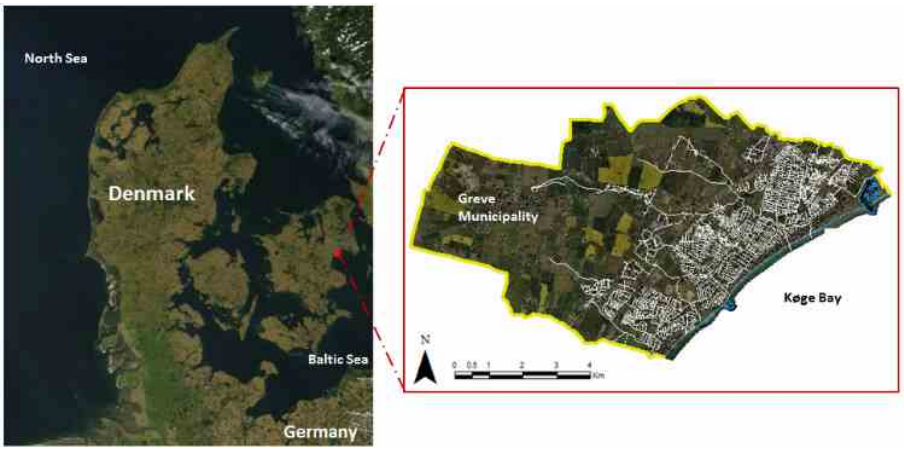

Figure 5-1 Location of the Greve case study area in eastern Denmark.

The sandy beaches, as well as the natural ecosystems of marshes and shallow lagoons in the area, attract local and tourist populations, which has led to the development of numerous holiday and detached houses near the coast. In addition, Greve is in part of a highly-industrialized area in the south of Copenhagen, where four municipal wastewater treatment plants and several industries are located. The municipalities in the northern part of Køge Bay, which includes Greve, have some of the largest population densities in Denmark (Økonomi- og Indenrigsministeriet, 2013), and residential settlements are densely built up along the coast.

Past Flooding in Greve

The main climate change threats to Denmark are increased rainfall and cloud bursts (EC, 2009). The sewer systems are unable to cope with large amounts of water as was demonstrated in Greve during the storms of 2002 and 2007. In August 2002, a rain event of 1000 years return period caused damages in the city centre, inundating important facilities such as the city hall and the local high school (Sto. Domingo et al., 2010). And in July 2007, a series of rain events with a joint probability of occurrence of 500 years caused severe flooding in Greve, necessitating evacuation of citizens due to widespread flooding in the area (Greve Kommune, 2007). The serious flooding in Greve in 2002 prompted formation of a Technical Committee to evaluate the performance of the storm- and wastewater systems in the Municipality and implement adaptation measures. However, the flood of 2007 showed further actions were needed (Greve Kommune, 2007).

Greve is considered one of the most flood-prone areas in Denmark (EC, 2009). It is located along the Baltic Sea, and has been deemed vulnerable to coastal flooding. In addition to

extreme rainfall and cloud bursts, the region is at risk from coastal flooding due to storm surges and general water level increase because of its location in Køge Bay (Vestergaard, 2011).

There have been 28 documented high sea level events in Køge Bay with magnitudes greater than 1.52 mð the highest water level observed in the area for the period 1955-2002. But the most extreme coastal flood in Køge Bay ever recorded was in 13 October 1760 with an estimated maximum water level of 3.7 m. Also, extreme storm surge flooding happened the night between the 12 and 13 November 1872, where water levels reached 2.8 m (Madsen, 2008; Colding, 1881). This flood event was described in detail by Colding (1881) in the report ñ*Nogle Undersøgelser over Stormen over Nord- og Mellem-Europa af 12te-14de november 1872 og over den derved fremkaldte vandflod i Østersøen* (Some studies of storms over northern and central Europe on 12th -14th November 1872 and flood consequences around the Baltic Sea)ò Estimates of these historical extreme coastal flood events using simple Terrain (GIS) Analysis are shown in Figure 5-2 below.

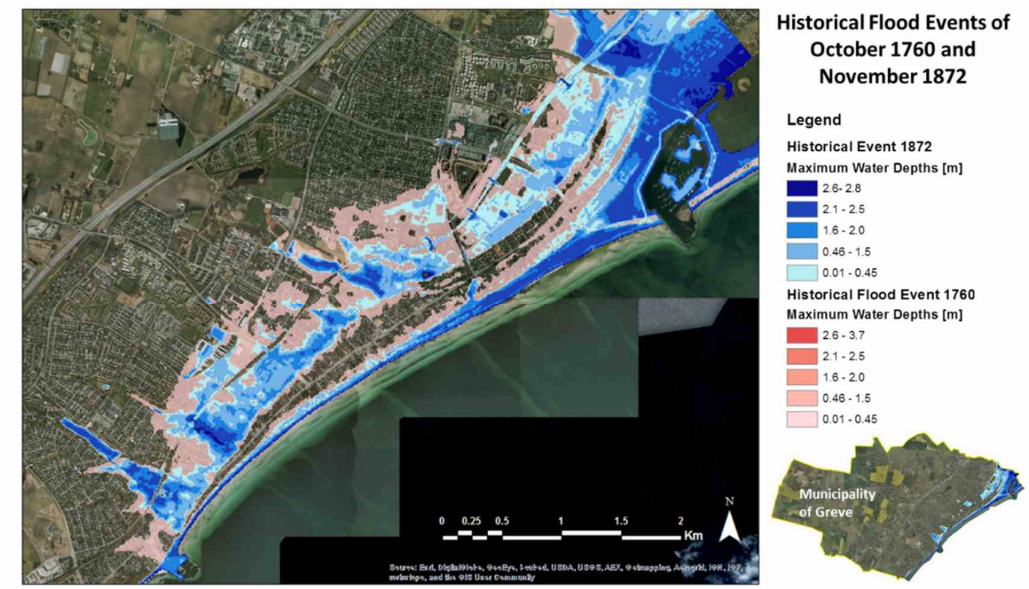

Figure 5-2 Plots of historical flood events in Greve in October of 1760 with an estimated maximum water level of 3.7 m and November of 1872 with an estimated water level of 2.8 m estimated using Terrain Analysis (Berbel Roman, 2014).

Case Study Objectives

Coastal flood risk assessment in Greve was performed as a case study in the PEARL Project. It was conducted as part of a Master Thesis project by Berbel Roman (2014).

Traditionally, flood risk assessments are performed considering isolated extreme events, but several studies have demonstrated that this is not realistic (Lian et al., 2013; Zheng et al., 2013; Zhang et al., 2014). Given the identified vulnerabilities of Greve to both pluvial and coastal flooding, flood risk assessment based on concurrent occurrence of extreme rainfall and storm surge events was performed. A joint flood risk analysis methodology was developed and applied to quantify flood damages for single as well as combined events in present and future (climate change) extreme event scenarios.

5.1 Data collection and analysis

Data for relevant coastal flood forcing event(s) in formats that may be used as boundary conditions to subsequent flood modelling were derived for the study. In addition, Joint Probability Analysis was performed in the derivation of event data to consider the occurrence of concurrent events.

Extreme Sea Level Data

In Køge Bay, an 8-cm increase in mean sea level has been observed in the period 1891 to 1990 (Kystdirektoratet, 2002). This rate of increase is expected to continue in the future (Madsen, 2008), and GEUS and DMI (2012) estimated that mean sea level rise around Denmark will be 0.8 ± 0.6 m, up to 1.5 m by 2100 (Figure 5-3). In Køge Bay, estimated mean sea level rise values range from 0.75m to ± 0.6m.

Figure 5-3 Estimates of mean water level increase in year 2100 compared to today. The location of Køge Bay, near Greve, is shown. (Source: GEUS and DMI, 2012)

Synthetic extreme sea level event time series near Greve were derived from earlier climate change studies (Madsen, 2008; DHI, 2012). In ñ*Vandstandsstatistik i Køge Bugt under klimaændringer*ò (Water level statistics in Køge Bay under climate change), Madsen (2008) analysed sea level statistics in Køge Bay to derive future projections for extreme sea levels in the area under climate change conditions. Regional climate and hydrodynamic modelling were employed to derive extreme sea level statistics. Wind and pressure data from regional climate modelling (RCM) were used in a 3D hydrodynamic model of the seas around Denmark to obtain long-term sea level values around Køge Bay (RiskChange, 2015). Statistical analysis of these sea level results, and comparison against observed statistics, were performed to determine appropriate change factors for scaling actual extreme sea level statistics into future scenario estimates. In the study, 100-year extreme sea levels were projected to increase by 69 cm in the future (from 153 cm to 222 cm) under the A1B climate scenario. DHI (2012) updated this study based on additional observed data, and revised estimates from an ensemble of Regional Climate Models (RCMs) for modelling future sea levels, obtaining new estimates of changes to extreme sea level statistics in Køge Bay (Table 5-1).

Table 5-1 Changes in storm signal [m] in Køge Bay in 2100 based on the three RCM/GCM projections for different return periods (DHI, 2012).

Return Period [yrs]	HIRHAM_ARPEGE	HIRHAM_ECHAM5	HIRHAM_BCM	Average
10	-0.14	0.14	-0.06	-0.02
50	-0.17	0.19	-0.07	-0.02
100	-0.18	0.21	-0.08	-0.02

This information was then combined with updated estimates for mean sea level rise in Denmark by GEUS and DMI (2012) (Figure 5-3), giving total storm signal change estimates for the most extreme future scenario projections as shown in Table 5-2 below. For the most extreme future scenario, a 100-year extreme sea level event is projected to increase by 1.56 m considering the highest storm signal change estimate.

Table 5-2 Calculation of most extreme (Upper) estimates for sea levels in Køge Bay considering changes in storm signal and mean sea level rise for different return periods T

[yrs]	Current Extreme Statistics [m]	Year 2100 Upper Estimates [m]	2100 Upper Change [m]
10	1.35	2.84	1.49 *(0.14 + 1.35)*
50	1.47	3.01	1.54 *(0.19 + 1.35)*
100	1.52	3.08	1.56 *(0.21 + 1.35)*

To derive the event time series patterns, the change factors for storm surge heights (Table 5-2) were directly applied to selected records of observed extreme water level events, as illustrated in Figure 5-4 below.

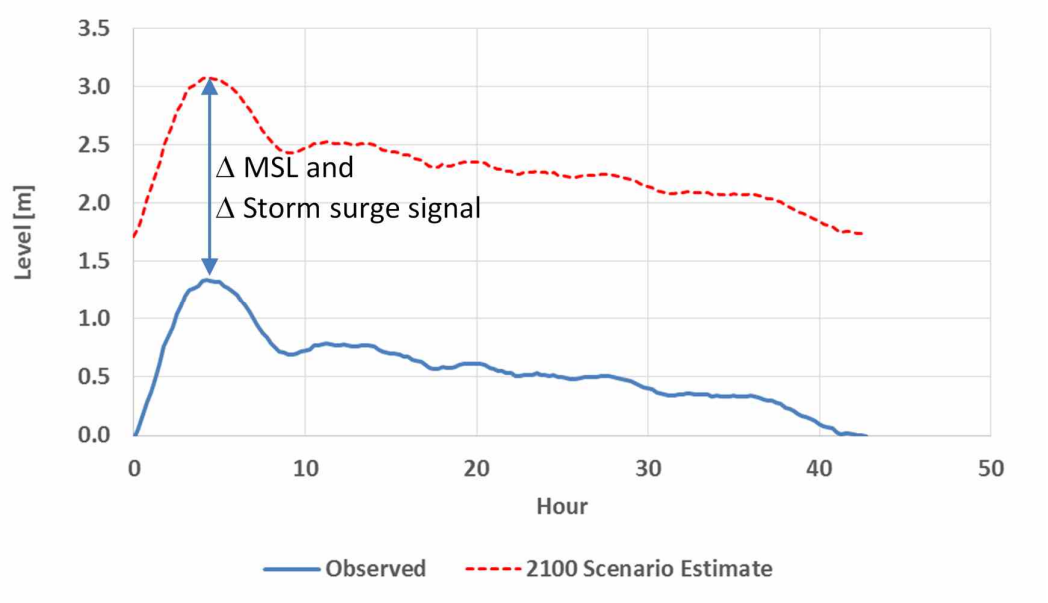

Figure 5-4 Future extreme water level event time series (red dotted line) estimated based on an observed extreme event pattern (blue solid line). The future event time series has been derived from observations by scaling to a given return period and adding estimates of mean sea level (MSL) rise and change in storm surge signal.

Two sets of future extreme sea level event time series were derived and used in the case study are shown in Figure 5-5. They were based on actual observed extreme event time series (see ñObsò in Figure 5-5), with Event 1 having a duration of 42.5 h, and Event 2, lasting 24 h. Figure 5-5 plots time series values for 100-year extreme sea level event projections.

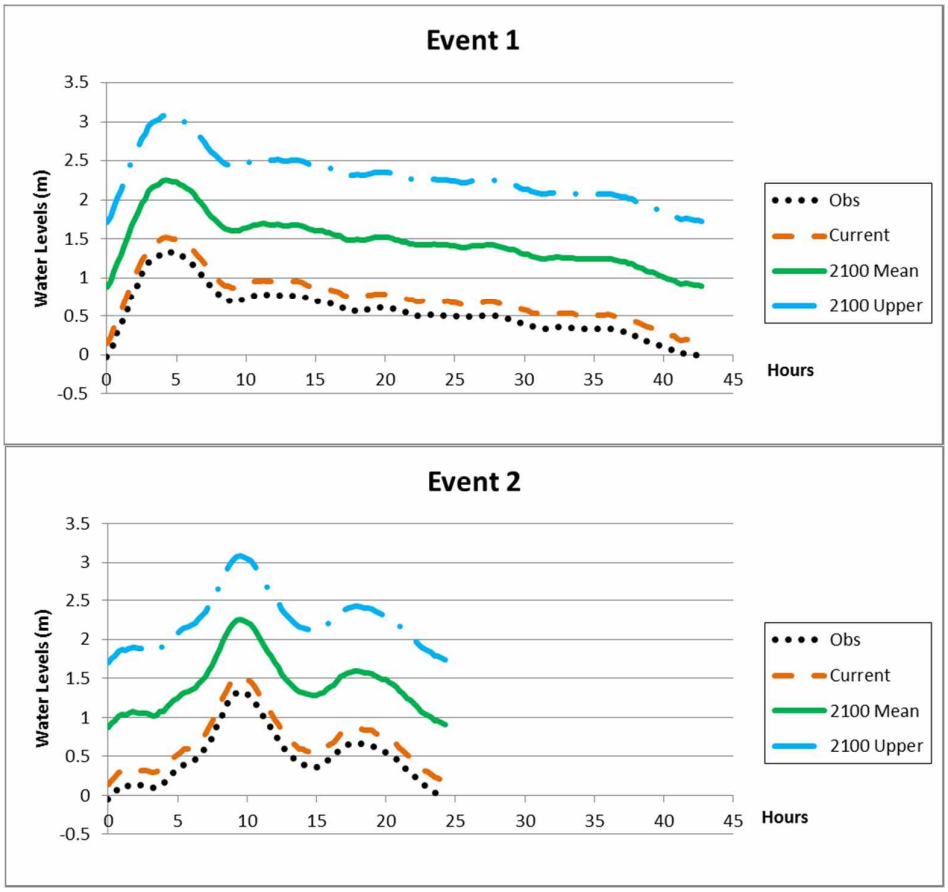

Figure 5-5 Future (2100) projections of mean and upper extreme sea level event time series for 2 events in Køge Bay with 100 years return period.

Extreme Rainfall Data

Synthetic rainfall hyetographs derived based on a regional statistical model for extreme precipitation (Madsen et al., 2002) using the Chicago Design Storm (CDS) method were used in the case study (see Figure 5-6). According to the Intergovernmental Panel on Climate Change (IPCC), more intense and frequent extreme rainfall is expected in Denmark in the future, especially during summer periods (IPCC, 2007). Therefore, extreme design rainfall used in the case study should include climate change impacts. Climate factors were thus applied to the CDS rain time series to account for increased precipitation due to climate change. A guideline document has been published in Denmark recommending climate factors to scale extreme rainfall data for climate change impact assessments (Gregersen et al., 2014), and a summary of the recommendations are shown in Table 5-3 below.

Table 5-3 Recommended climate change factors for extreme rainfall events in 2100 in Denmark (Gregersen et al., 2014)

Return Period (years)	2	10	100
Mean Climate Factor	1.2	1.3	1.4
High Climate Factor	1.45	1.7	2.0

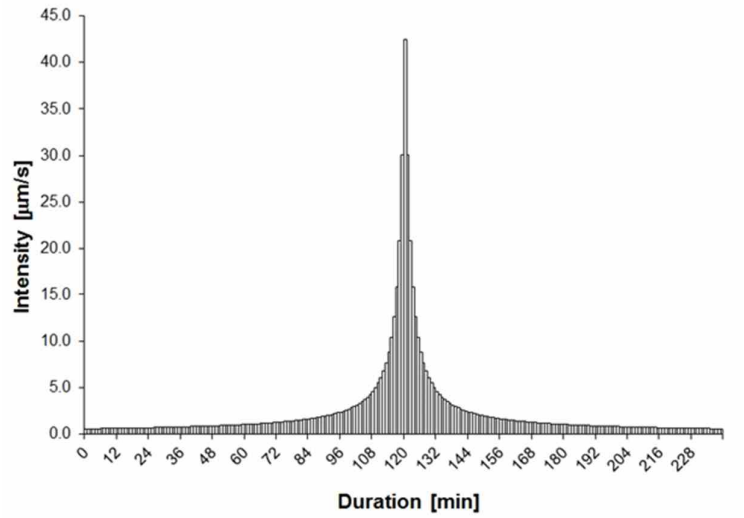

Figure 5-6 Future CDS design rainfall time series derived for a 10-yr return period event considering a climate factor of 1.3.

Joint Probability Analysis

Joint probability analysis was performed to assess the correlation between the relevant flood-driving events in the case areað i.e. rainfall and sea levels, and investigate the threshold conditions for flooding under their combined impacts. It involved frequency analysis with long term observed data for derivation of corresponding marginal probability distributions of extremes (e.g. extreme rainfall and extreme water levels), and the estimation of probabilities for different concurrent conditions of the extreme events. Information about the concurrence probabilities of combinations of events was used to select the event time series data for flood modelling.

5.2 Urban coastal flood hazards

In coastal cities, flooding may be from runoff generated by extreme rainfall, elevated sea levels, or a combination of both occurring simultaneously or in close succession (Zheng et al., 2013). However, most flood risk analyses have been performed considering only extreme rainfall or high sea levels individually. For some areas, the combined effect of both events and the joint probability of extremes should be considered for better flood risk assessment (Lian et al., 2013).

A 1D-2D hydrodynamic model was used for flood hazard analysis in the coastal area of Greve. It was built using MIKE Flood FM, a modelling system integrating one-dimensional and two-dimensional models into one dynamically coupled model (DHI, 2014). It comprises of a 1D model of the drainage system representing stormwater sewers and streams, coupled to a 2D surface flow mesh model of the inland and sea areas along the coast. The drainage network

is included in the flood model to ensure simulation of pluvial and fluvial flooding, as well as consider the influence of the drainage network in conveying flooding from the sea further inland.

The 1D network model is relatively comprehensive and detailed, covering most of Greve Municipality and consisting of around 7 000 nodes, 6 500 links and 9 outlets to the sea. MIKE 21 FM, a 2D modelling system based on a flexible mesh approach, was used to build the 2D model in Greve. The model covers 53 km2 of the area made up of sea and inland regions along Greveås coast. It uses a flexible computational mesh to represent the terrain surface.

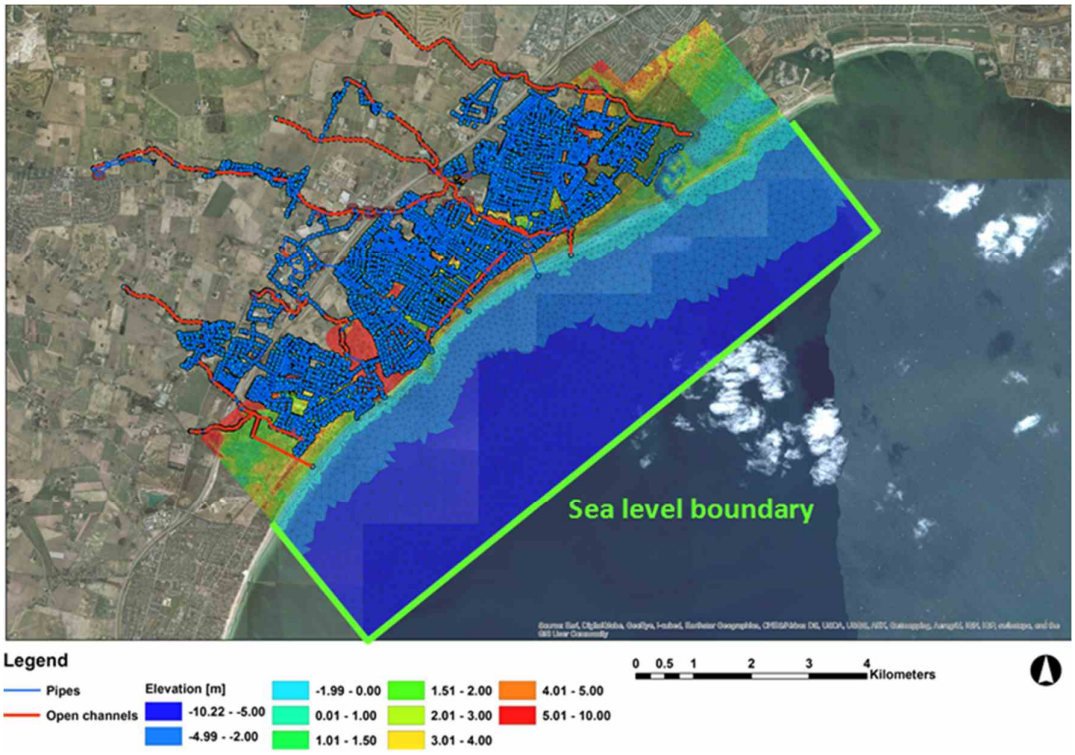

Figure 5-7 A map showing the 1D-2D coastal flood model for Greve. A 1D model of the drainage system comprising of streams (red lines) and stormwater sewers (blue lines and points) is linked to a 2D mesh model of the coast (coloured areas). The triangular elements of the terrain mesh and open boundaries of the 2D model are also shown.

Coupled 1D-2D hydrodynamic models are the state-of-the-art in analysing flooding from the sea in urban coastal areas (Henonin et al., 2013). 1D-2D models are able to simulate flows in the pipe network, flows over the land surface, as well as the interactions and flow exchanges between the two systems. In this approach, the urban coast and topography are represented in the 2D model, which simulates water levels and flows over surfaces based on computations solving the 2-dimensional shallow water equations. The underground drainage system is represented by a 1D pipe model, which simulates flows through the network using equations of flow in one dimension (i.e. along sewers).

Modelling either individual or concurrent events using 1D-2D models is done through specification of appropriate boundary conditions in the respective model systems. Rainfall, or sea water levels, or both, can be applied as driving or boundary conditions to both systems in the coupled model. Rainfall may be specified as input to the conceptual runoff model component of the 1D model to simulate runoff over the urban area. Rainfall may also be applied

as a ósourceôto the 2D model. Sea water level and flux time series boundaries may also be applied along open boundaries of the 2D model. In addition, water level boundaries may be specified at outlets of the 1D network model to the receiving body of water (i.e. the sea).

Summaries of the different individual and concurrent flood events analysed in the case study are shown in Table 5-4 and Table 5-5 below.

Table 5-4 Summary of individual flood forcing events analysed in the case study.

	Return Period [years]		
	100	**10**	**2**
Sea level	x		
Rainfall	x	x	
			x

Table 5-5 Summary of concurrent flood forcing events analysed in the case study.

		Sea level
	Return Period [years]	100
Rainfall	100	x
	10	x
	2	x

Figure 5-8 shows a plot of one of the flood events analysed in the case study. It shows the maximum calculated flooding for an individual future extreme sea level event (upper estimate) with 100 years return period (Event 2) (see also time series plot in Figure 5-5).

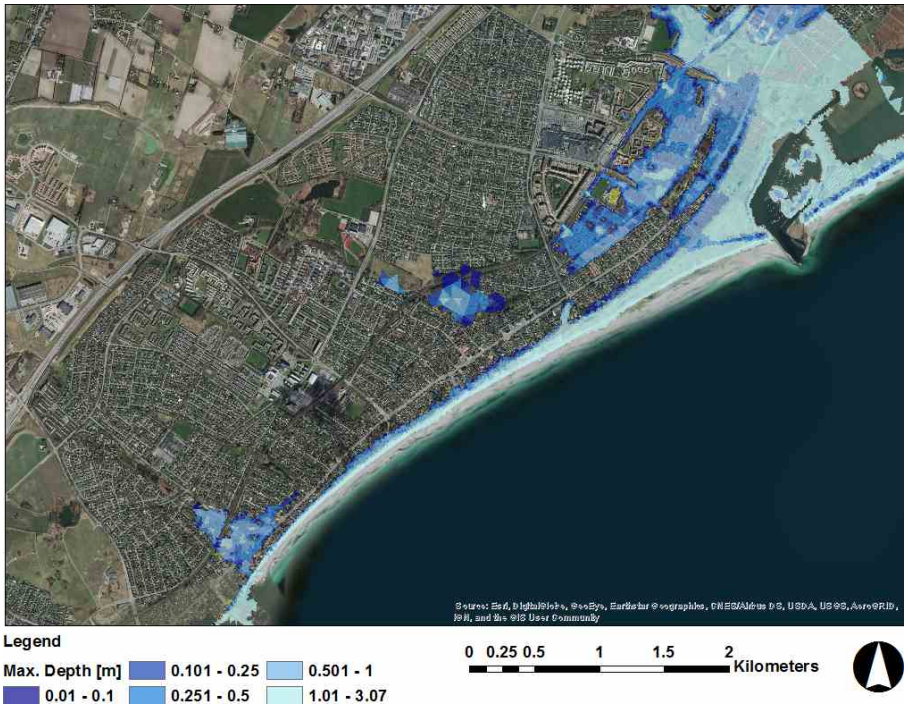

Figure 5-8 Calculated maximum flooding in Greve for future 100-year extreme sea level event scenario. (Source: Berbel Roman, 2014)

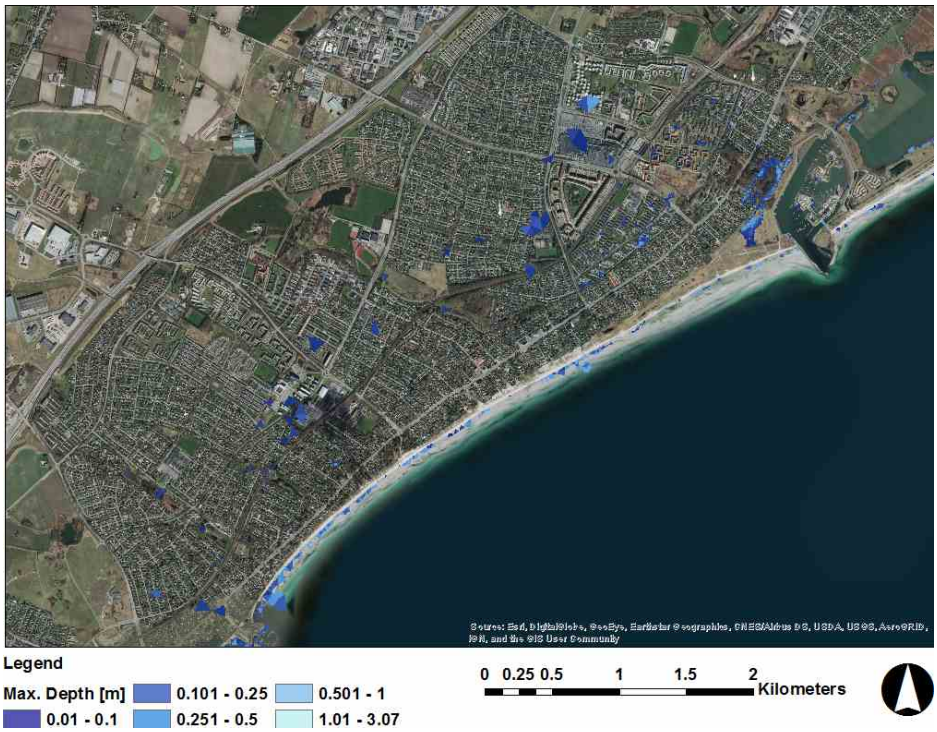

Figure 5-9 Calculated maximum flooding in Greve for future 100-year rainfall event scenario. (Source: Berbel Roman, 2014)

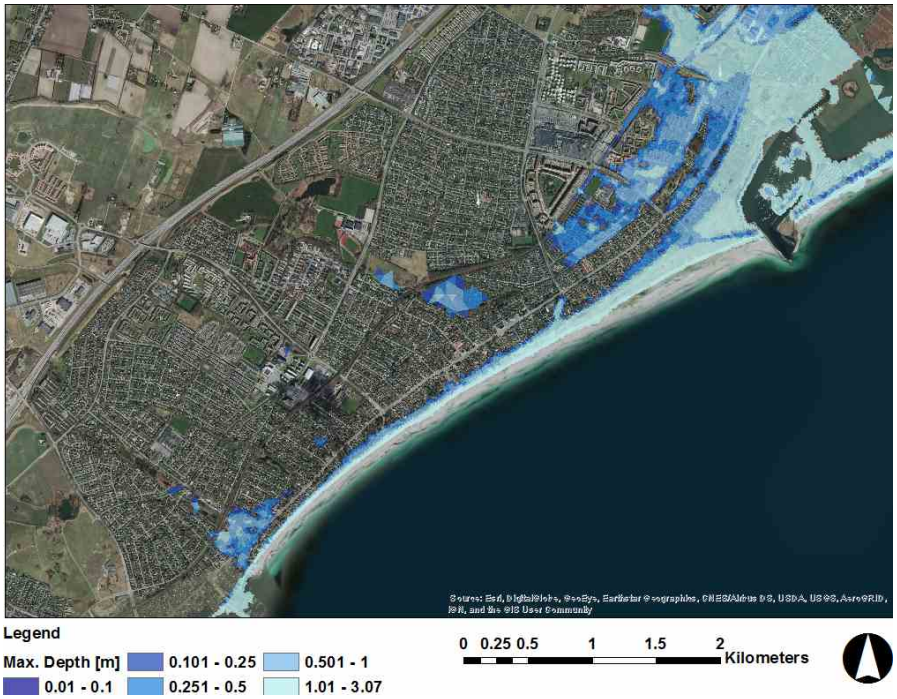

Figure 5-10 Calculated maximum flooding in Greve for future concurrent 100-year extreme sea level and 2-year rainfall events scenario. (Source: Berbel Roman, 2014)

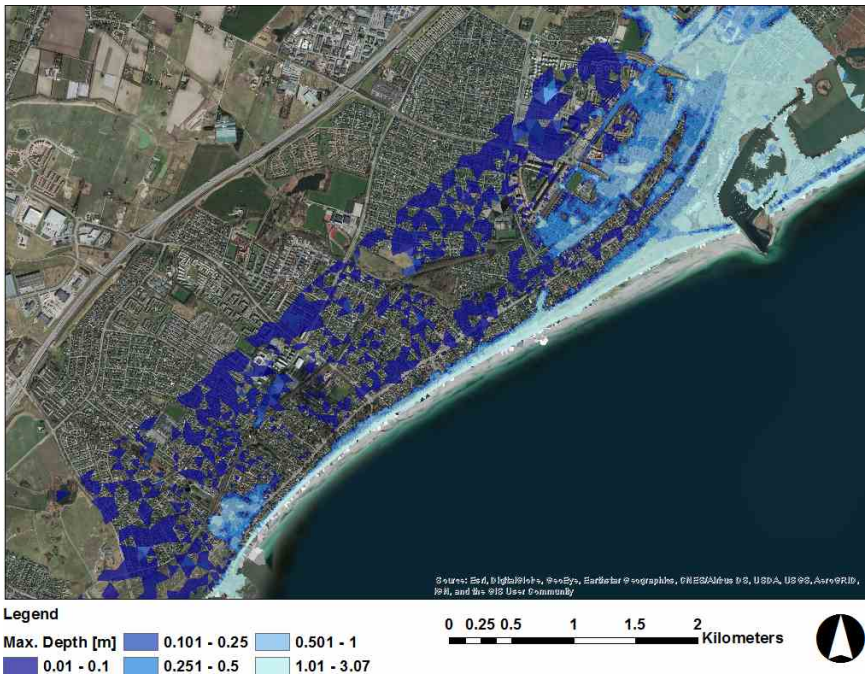

Figure 5-11 Calculated maximum flooding in Greve for future concurrent 100-year extreme sea level and 100-year rainfall events scenario. (Source: Berbel Roman, 2014)

5.3 Flood damages and risks

Two different approaches were used to estimate flood damages in the case area. The first one used a value mapping technique where flood damage was estimated based on aggregated gridded values of properties in the case area (i.e. value maps or *værdikort*). The value maps are grid data containing information on the total aggregated value of properties (land and buildings), and property area sizes, within each grid cell. The other method used a flood depth-damage curve, which defined damage costs for different flood depths.

Collection of the necessary data and their pre-treatment were very important steps in the analyses. Both methods required flood maps of maximum water depths, flood durations, and spatial data on valued properties in the study area. Geo-spatial data on buildings/properties (Figure 5-12) and value maps (*vaerdikort*) (Figure ***5-13***) were obtained from the Danish Data Agency, while flood depth-damage data were obtained from the Municipality of Greve.

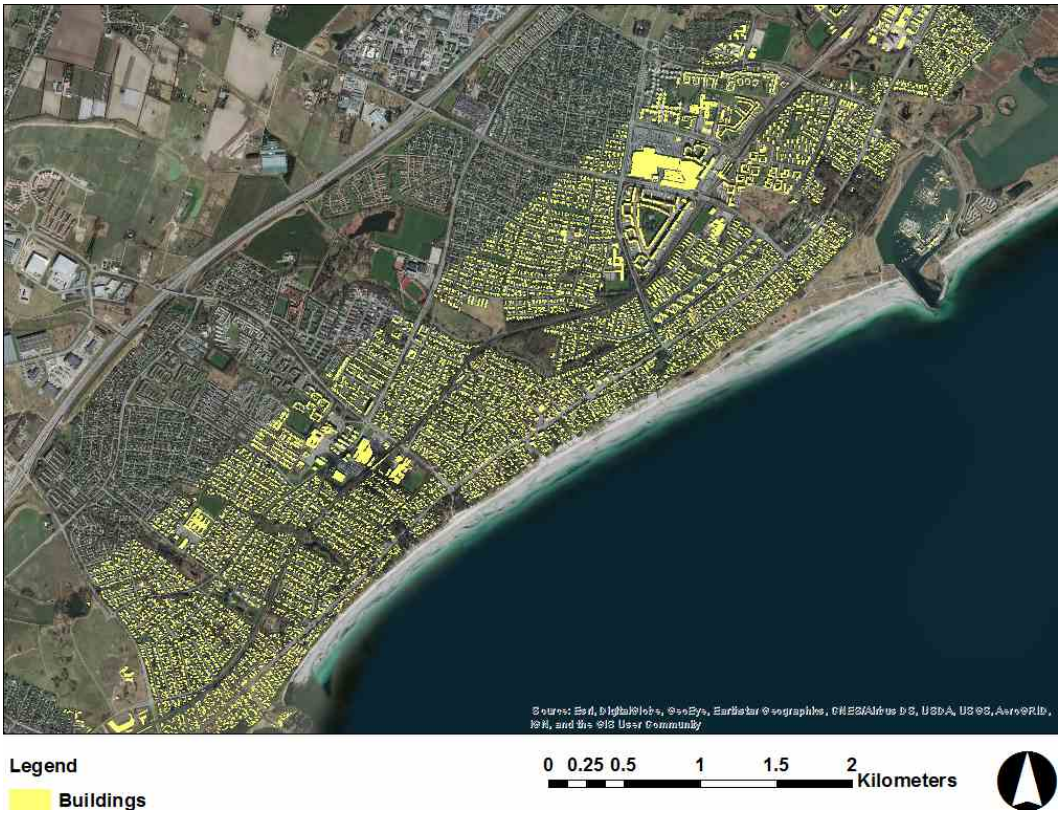

Figure 5-12 Geo-spatial data on buildings/properties in the study area.

Value map (vaerdikort) grid approach

Value map grids were downloaded from the Danish Data Agency website (http://download.kortforsyningen.dk). The value map grid had a resolution of 100 x 100 meters, and each cell contained information on the total value of buildings, land, and total property area (in m^2) within each grid cell.

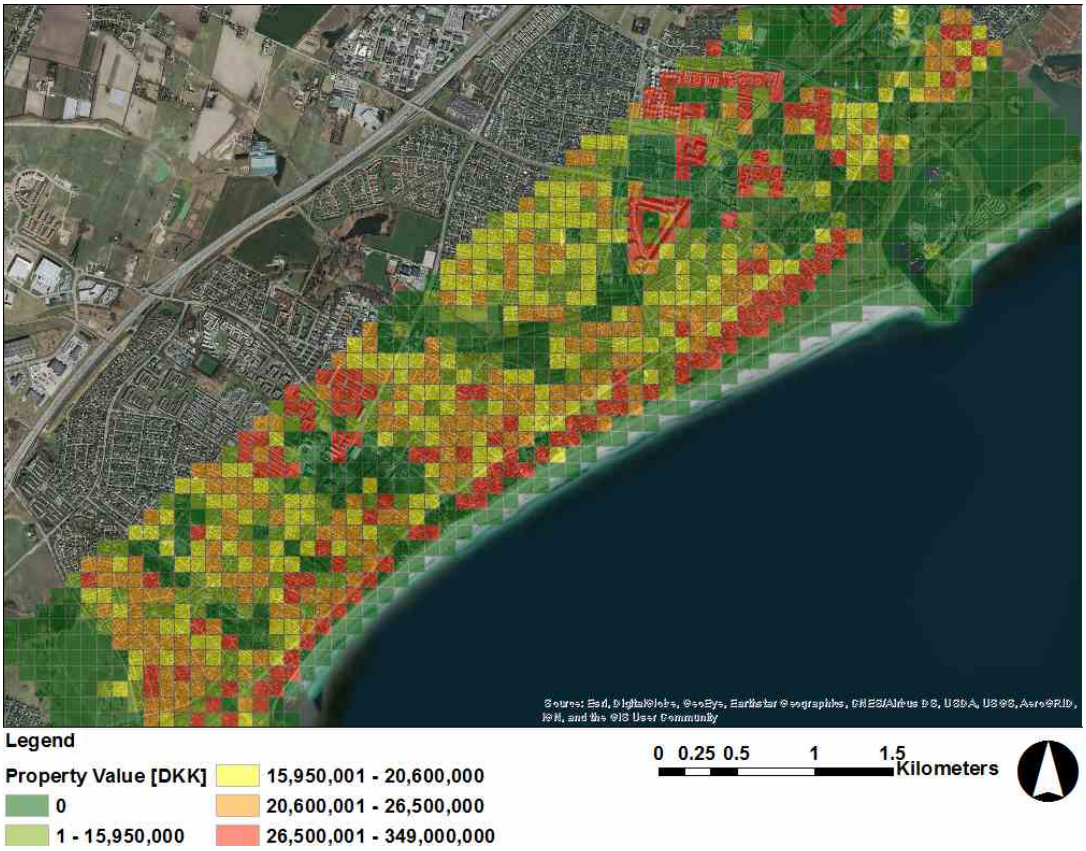

Figure 5-13 Value Map showing data on aggregated property value in 100 x 100 m cells in the study area.

Flood depth-damage curve approach

Flood risk was analysed in areas flooded for more than 5 hours. The 5-hour duration criterion was set based on the definition of the flood-depth damage curve obtained from Greve Municipality, and shown in Table 5-6 below. The same depth-damage table was used for all types of buildings in the case area.

Table 5-6 Flood depth-damage table used in the case study.

Water Depth [cm]	Cost per square meter [DKK/m^2]	Type
> 0	500	Only Basement
> 20	2500	All
> 40	6500	All

Results from the flood damage analyses using the Value Map Approach are shown in Figure 5-14, Figure 5-15, and Figure 5-16 below.

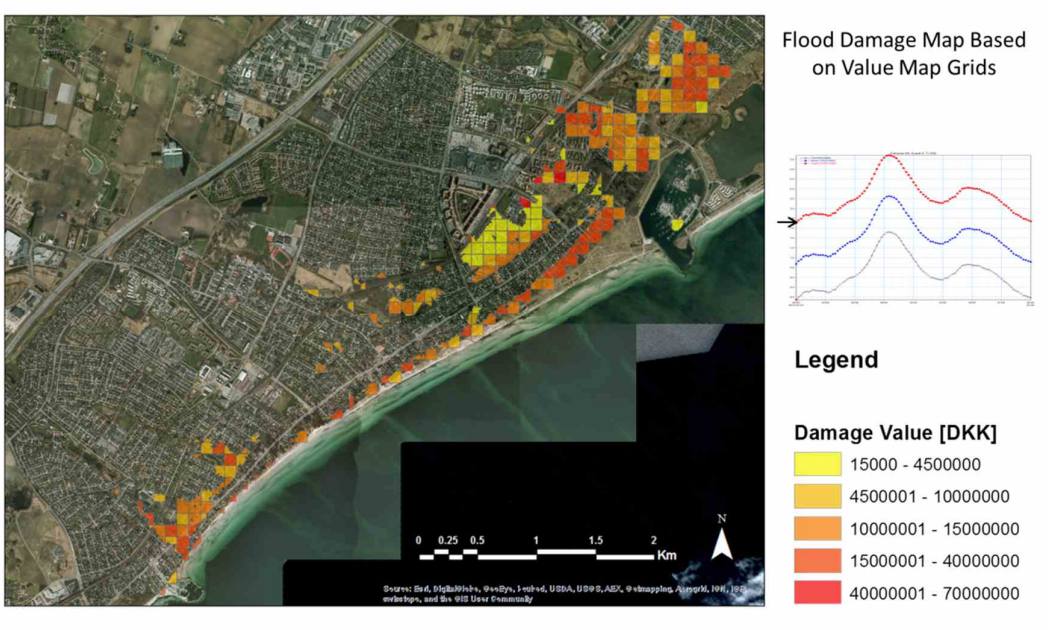

Figure 5-14 Flood Damage Map for an extreme 100-yr sea level event considering climate change. (Source: Berbel Roman, 2014)

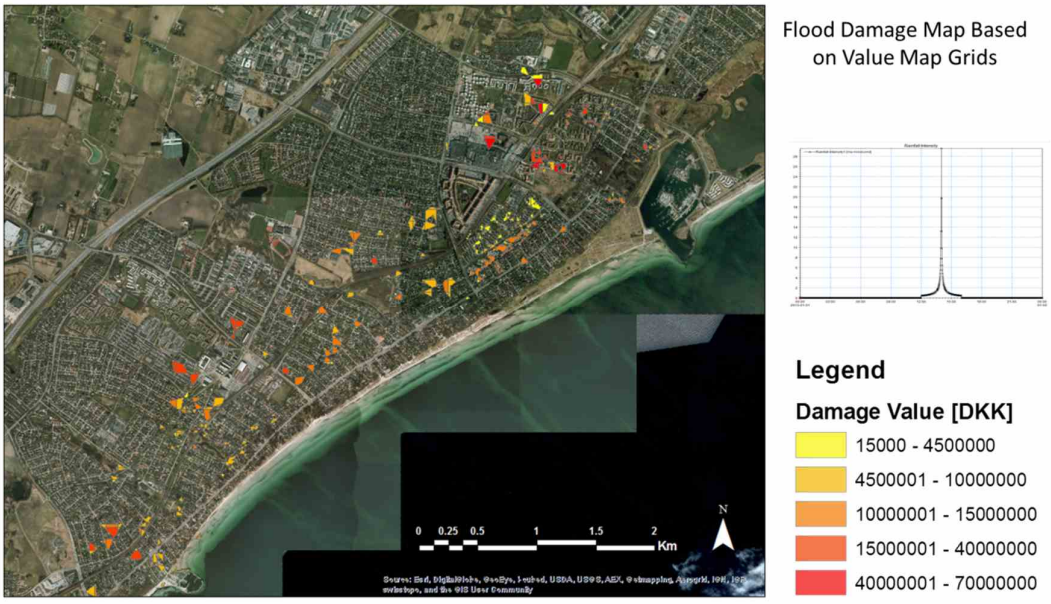

Figure 5-15 Flood Damage Map for future extreme 100-yr rainfall event considering climate change. (Source: Berbel Roman, 2014)

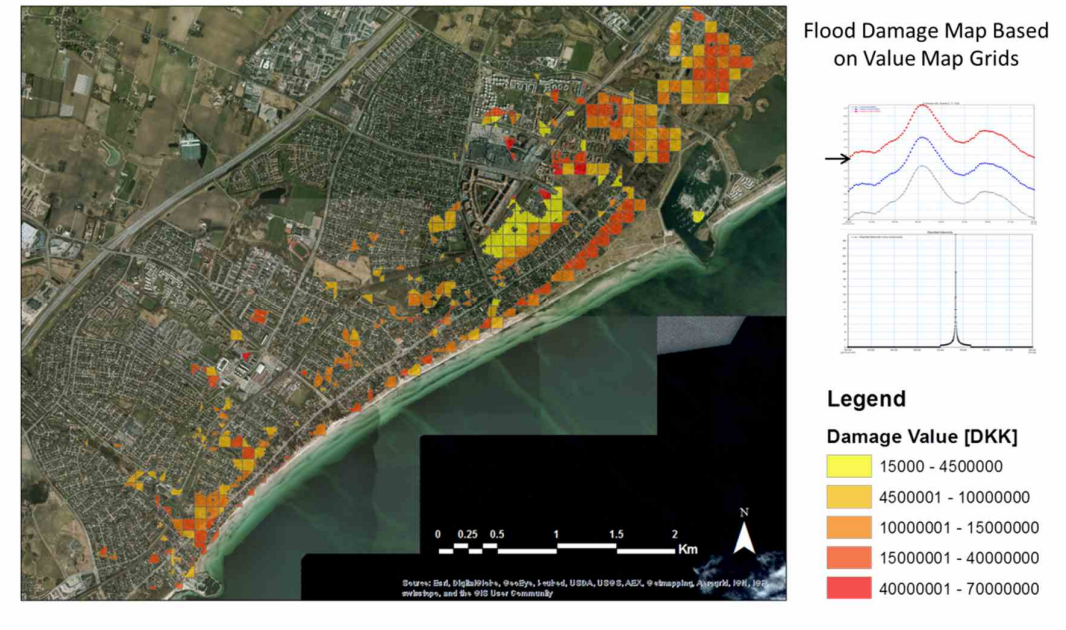

Figure 5-16 Flood damage map for concurrent future extreme 100-yr sea level and 2-yr rainfall considering climate change. (Source: Berbel Roman, 2014)

Flood damage analysis results using the Damage Curve Approach are shown in Figure 5-17, Figure 5-18, and Figure 5-19 below.

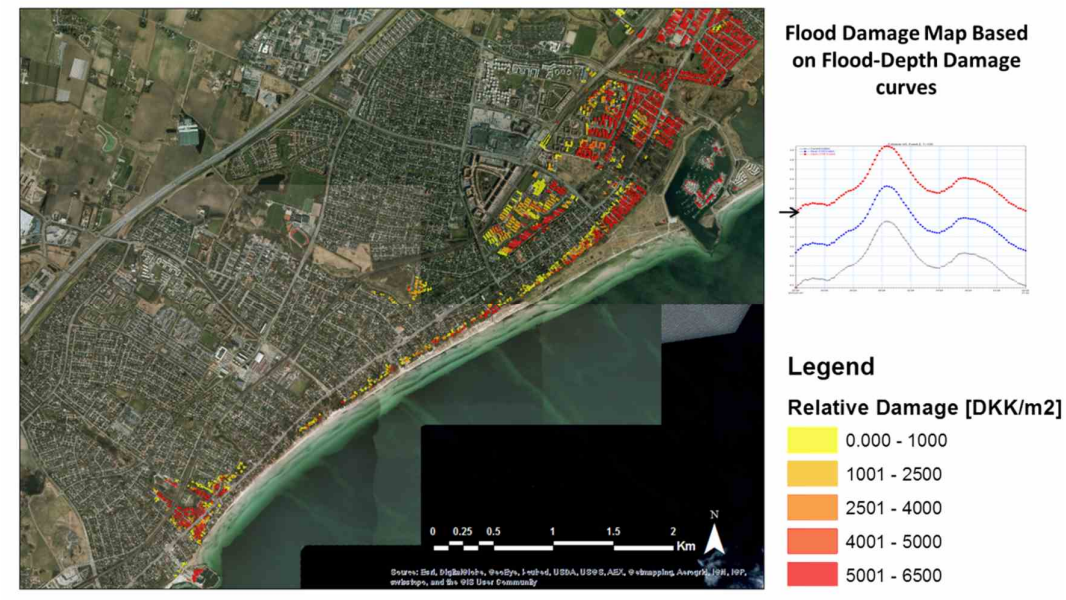

Figure 5-17 Flood damage for extreme 100-yr sea level event considering climate change. (Source: Berbel Roman, 2014)

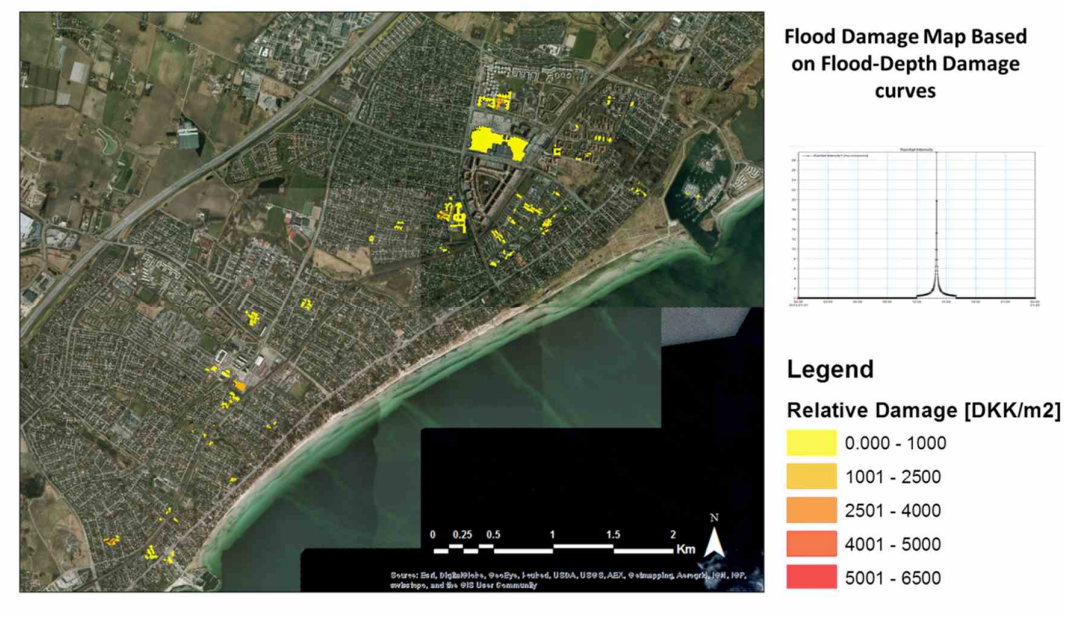

Figure 5-18 Flood damage for extreme 100-yr rainfall event considering climate change. (Source: Berbel Roman, 2014)

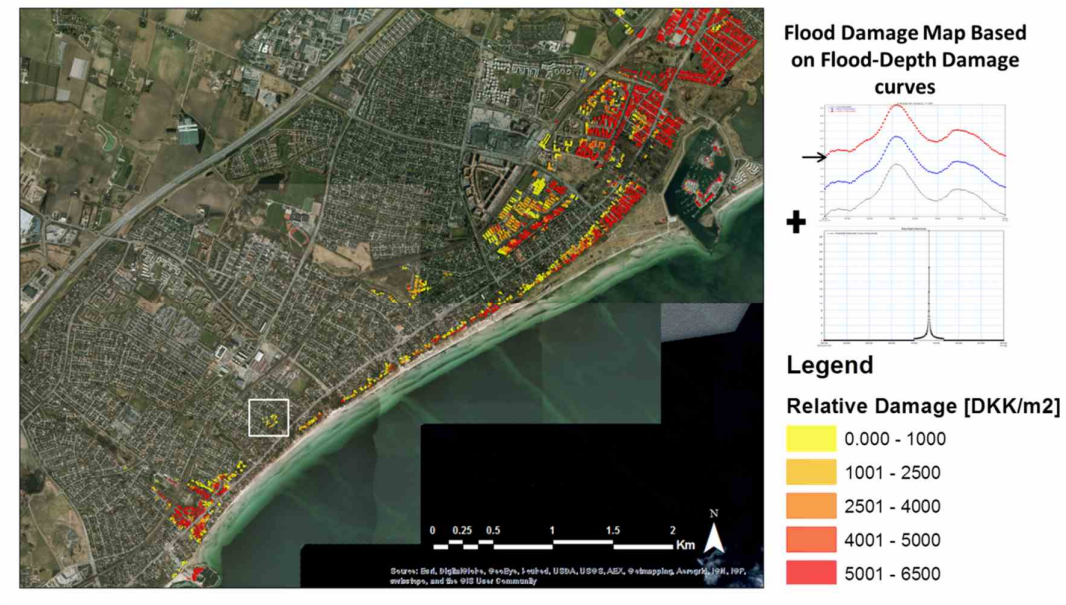

Figure 5-19 Flood damage for concurrent extreme 100-yr sea level and 2-yr rainfall events considering climate change. (Source: Berbel Roman, 2014)

Below are summary tables of results from each damage calculation method with expected total damages for each return period. Table 5-7 and
Table 5-9 summarise damage assessment results for single events, and
Table 5-8 and Table ***5-10*** show results for concurrent events.

Table 5-7 Expected total flood damages for single events using the Value Map Approach.

	Return Period [years] 100	10	1	Expected Total Costs [Million DKK]	Expected Occurrence per year [%]	Return Period [years]	Risk
Sea level	x			3072.12	1	100	30.72
	x			93.95	1	100	0.94
Rainfall		x		65.32	10	10	6.53
			x	28.86	50	2	14.43

Table 5-8 Expected total annual costs for concurrent events using the Value Map Approach.

	Return Period [years]	Sea Level 100	10	2	Expected Total Costs [Million DKK]	Expected Occurrence per year [%]	Return Period (Concurrent Event) [years]	Risk
Rainfall	**100**	x			4769.67	0.10	1000	4.77
	10	x			3954.48	0.63	160	24.72
	2	x			3617.59	2.86	35	103.36

Table 5-9 Expected total costs for single events using Depth-Damage Curve Approach.

	Return Period [years] 100	10	2	Expected Total Costs [Million DKK]	Expected Occurrence per year [%]	Return Period [years]	Risk
Sea level	x			1561.90	1	100	15.62
	x			37.32	1	100	0.37
Rainfall		x		6.63	10	10	0.66
			x	1.57	50	2	0.79

Table 5-10 Expected total costs for concurrent events using Depth-Damage Curve Approach.

	Return Period [years]	Sea Level 100	10	2	Expected Total Costs [Million DKK]	Expected Occurrence per year [%]	Return Period (Concurrent Event) [years]	Risk
Rainfall	**100**	x			1588.43	0.10	1000	1.59
	10	x			1578.01	0.63	160	9.86

2	x	1567.46	2.86	35	44.78

The event probabilities were estimated based on joint probability analysis results of extreme rainfall and extreme storm surges. The probability of a flood event being exceeded in one year was computed to estimate the risk associated to each event. For example, a flood event with 100 years return period has an expected occurrence of 1% within a year. Flood risks were quantified using the following:

Risk = Damage [DKK] x Probability

5.4 Summary

The first approach calculated flood damages using Value Maps (*vaerdikort*) over the Municipality of Greve. The damage was estimated taking into account the flood area and the financial value of properties within each cell, and a total aggregated damage value was obtained for each cell. The disadvantage of this method is that it does not specifically identify buildings potentially affected by flooding. The expected total damages obtained with this method are extremely high since the method does not consider the spatial distribution of affected buildings/properties within a value cell. On the other hand, the second approach using a depth-damage curve provided information on which specific buildings are potentially flooded, and estimates of affected area extents for each flooded property could be obtained.

The study analysed flood damages and risks not only from single-forcing flood events, but also for concurrent events. Analysis results revealed that the most potentially affected areas by coastal flooding are those around the northern harbour and southern harbours in Greve. Moreover, it was found that flood damages are more distributed over the city when (pluvial) flooding from extreme rainfall is considered. Nevertheless, it was found that a significant percentage of potential damages was due to flooding from the sea, as total costs due to single rainfall events were consistently significantly less than when floods from extreme sea level events were considered.

Active stakeholder involvement in the Greve Case Study being conducted under the PEARL Project is limited. The Municipality and local utility company operating the drainage system in the city provide great support (e.g. in terms of data and information provision) and express high interest in the case study; but they nevertheless also actively and continuously conduct their own analyses for improving their system. For example, stemming from past flood events in 2002 and 2007, it was politically decided to upgrade the drainage system in the city to handle a maximum flooding frequency of only once every 10 years. A vulnerability map was prepared for the city using GIS, and climate adaptation plans for implementation over the next 12-15 years was developed (EC, 2009; Kelder, 2011). The city has taken advantage of the use of hydraulic modelling tools, together with measurement campaigns, for detailed evaluation of prioritisation areas in their climate adaptation plans. And in August 2010, several locations in Denmark was affected by very heavy rainfall far exceeding Danish design standards, and subsequently, severe flooding. But in Greve, knowledge and learning from past events allowed the Municipality and local utility company to manage and handle this extreme rainfall event and avoid major flood damages in the city (Kelder, 2011).

5.5 References

Berbel Roman, S. (2014). Modelling flooding from the sea interacting with the drainage system under the influence of combined flood hazards to develop risk management strategies for the coastal region of Greve, Denmark. Master thesis, Hydroinformatics and Water Engineering, Ecole Polytechnique Universitaire, Universite de Nice-Sophia Antipolis, France.

Colding, A. (1881) Nogle Undersøgelser over Stormen over Nord- og Mellem-Europa af 12te-14de November 1872 og den derved fremkaldte vandflod i Østersøen, Vidensk. Selsk. Skr., 6. Række, Naturvidenskabelig og Matematisk Afdeling I4.
Colding, A. (1881) Nogle Undersøgelser over Stormen over Nord- og Mellem-Europa af 12te-14de November 1872 og den derved fremkaldte vandflod i Østersøen, Vidensk. Selsk. Skr., 6. Række, Naturvidenskabelig og Matematisk Afdeling I4.
DHI (2012). Projektioner af højvandsstatistik for Køge.
DHI (2014). MIKE FLOOD, ID-2D Modelling, User Manual. DHI: Hørsholm, Denmark.
European Commission (2009). The economics of climate change adaptation in EU coastal areas. Country Reports: Denmark. Executed by Policy Research Corporation (in association with MRAG). Retrieved from http://ec.europa.eu/maritimeaffairs/documentation/studies/climate_change_en.
GEUS and DMI (2012). *Ændringer af havniveauet i Danmark de næste 100-200 år*, Notat til Klima-, Energi- og Bygningsministeriet, GEUS og DMI, Udarbejdet af Karen Edelvang, Andreas Ahlstrøm, Camilla Snowman Andresen, Signe Bech Andersen, Ole Bennike, Jens Morten Hansen, Antoon Kuijpers og Birger Larsen fra De Nationale Geologiske Undersøgelser for Danmark og Grønland (GEUS) og Erik Buch, Katrine Krogh Andersen og Kristine S. Madsen fra Danmarks Meteorologiske Institut (DMI), 29. februar 2012. Retrieved from https://www.dmi.dk/.../notat_vandstand_geus_dmi.pdf.

Gregersen, I.B., Madsen, H., Linde, J.J., & Arnbjerg-Nielsen, K. (2014). Opdaterede klimafaktorer og dimensionsgivende regnintensiteter. (In Danish: Updated Climate Change Factors and extreme precipitation used for design intensities). Paper no. 30, The Water Pollution Committee of The Society of Danish Engineers. Retrieved from https://ida.dk/sites/prod.ida.dk/files/svk_skrift30_0.pdf.
Greve Kommune (2007). *Oversvømmelserne i Greve Kommune Juli 2007*. Technical report. Retrieved from http://www.gsforsyning.dk/sites/default/files/oversvommelserne_i_greve_kommune_juli_2007.pdf
Henonin, J., Russo, B., Mark, O., & Gourbesville, P. (2013). Real-time urban flood forecasting and modelling ï a state of the art. Journal of Hydroinformatics, 15(3).
IPCC (2007): Climate Change 2007: The Physical Science Basis. Contribution of Working Group I to the Fourth Assessment Report of the Intergovernmental Panel on Climate Change. [Solomon, S., D. Quin, M. Manning, Z. Chen, M. Marquis, K. B. Averyt, M. Tignor and H. L. Miller (eds.)]. Cambridge University Press, Cambridge, United Kingdom and New York, NY, USA, 996pp.
Kelder, T. (2011). Flood action plan of Greve. Retrieved from http://www.eukn.eu/e-library/project/bericht/detail/flood-action-plan-of-greve/.
Kystdirektoratet (2002). Højvandsstatistikker 2002, Kystdirektoratet, Trafikministeriet.
Lian, J. J., Xu, K., & Ma, C. (2013). Joint impact of rainfall and tidal level on flood risk in a coastal city with a complex river network: a case study of Fuzhou City, China. Hydrology and Earth System Sciences, 17(2), 679ï 689.
Madsen, H. (2008). *Vandstandsstatistik i Køge Bugt under klimaændringer*. Report by DHI for Greve Kommune. Retrieved from http://www.greveforsyning.dk/dokumenter/Klima/Vandstandsstatistik%20i%20K%C3%B8ge%20Bugt%20under%20klima%C3%A6ndringer%20dec08.pdf.
Madsen, H., Mikkelsen, P.S., Rosbjerg, D., Harremoes, P. (2002). Regional estimation of rainfall-intensityduration-frequency curves using generalised least squares regression of partial duration series statistics. Water Resources Research 38 (11), 1239.
Økonomi-og Indenrigsministeriet (2013). Befolkningstæthed. Statisticalmapsbasedoninformation from Danmarks Statistik, Kort og Matrikelstyrelsen and Geodatastyrelsen.
RiskChange (2015). RiskChange ï Risk-based design in a changing climate. Retrieved from http://riskchange.dhigroup.com/.

Sto. Domingo, N. D., Paludan,B.,Hansen, F., Madsen, H., Sunyer, M., Mark, O., (2010). Modeling of sea level rise and subsequent urban flooding due to climate changes. In E. &. DHI Water (Ed.), SimHydro 2010: Hydraulic modeling and uncertainty, (p. 9). Sophia Antipolis.

Vestergaard, L. F. (2011). *Analyse af oversvømmeslesmønstret ved havvandsstigning i Køge Bugt ud for Greve*. Note to agenda item for meeting in ôTeknik og Miljøudvalgetô, Copenhagen Municipality. Retrieved from http://www.gsforsyning.dk/sites/default/files/havstrategi_politiskvedtaegt_bilag.pdf.

Zhang, S., Wang, T., & Zhao, B. (2014). Calculation and visualization of flood inundation based on a topographic triangle network. Journal of Hydrology, 509, 406ï 415.

Zheng, F., Westra, S., & Sisson, S. a. (2013). Quantifying the dependence between extreme rainfall and storm surge in the coastal zone. Journal of Hydrology, 505, 172ï 187.

6 Rethymno Case Study, Crete

6.1 Description of the study area

Rethymno city is sited at the Region of Crete in Greece and its population stands at 32,468 inhabitants (Census 2011) with a density 140.12 population/km^2. As the 3rd most populous urban area in the island of Crete, commercial, administrative, cultural and tourist activities are being developed along the north coast where the city is located (Makropoulos C. et al., 2014). Population growth during the last ten years is high since it is estimated around 12.1% (permanent population according to Census 2001 is 28,959 inhabitants and 32,468 according to Census 2011). A rough estimate of the floating population would be between 20%ï 30% of resident population especially during summer month due to tourism.

Although Rethymno is not a provincial capital where a large number of decision makers live the city is a major centre of economic activity in the Region of Crete. Tourism is the sector concentrating major economic activity since according to the Municipality of Rethymno 19% of the economically active population is employed in activities directly related to tourism. Public services of the Regional Unit of Rethymno are also located in the city.

The mean absolute altitude is 15 m and the length along the coastline of the area under study is approximately 8 km (Figure 6-1, a). At the coastal area in a zone of approximately 500 m, the area consists of flat terrains i.e. value of area slope 0 ï 5% which is gradually increased around 10 - 20% (moderate slope) while moving towards the inland area. Apart from the low-lying coastal area, 13 ephemeral streams cross the city of Rethymno before reaching the sea making it more vulnerable to multiple stressors. Within PEARL project, the urban area under study where the flood risk is being assessed is about 16 km^2 but for hydrologic analysis purposes a total area of 145 km^2 is being examined covering the river basins from the origins while trying to estimate the total amount of stormwater that flows through the city of Rethymno (Figure 6-2).

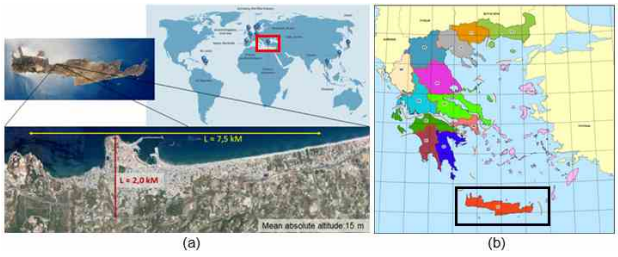

Figure 6-1: Rethymno city, Crete, Greece, sited in the 13th water district of Greece

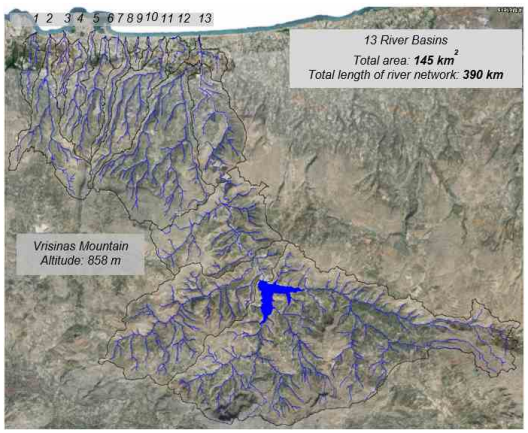

Figure 6-2: River basins and river network of Rethymno case study

Multiple stressors have always posed flood threats for the city of Rethymno in Crete. The flow of stormwater through the city, the large number of streams that cross it and the rapid transition from the steep slopes at the upstream rural areas to the flat urban zone imposed significant pressure to flood defences. The coastal zone is also exposed throughout the years to strong N and NW winds resulting in the development of waves, which often overtop the harbour infrastructure and erode recreational beaches. Historic flood events led to adverse human, material, economic and environmental effects and eventually to the selection of engineering prevention and mitigation measures. Major historic flood events with high impact to the cityôs life and infrastructure occurred on *February 29th, 1968, February 6th, 1984, October 28th, 1991 and November 10th, 1999* (Archontakis D., 2013). Primary cause of those flood events was heavy precipitation along with insufficient flood protection infrastructure. Nevertheless, the multiple forcing variables from the urban and coastal area still result in flood problems as it was evidenced by recent flood events. On January 1st and 13th, 2015 and on February 10th, 2015 the flood problems took place at the adjacent areas of the port and in parts of the Old Town of Rethymno as a result of storm surges and extreme violent wave overtopping of port infrastructures.

Desk based study, data collection and field visits enabled the researchers to initiate flood risk assessment of Rethymno case study, but understanding flood problems through the stakeholdersôperspective was of primary importance for the actual comprehension of flood risk. While hosting the 1st official LAA workshop in Rethymno (October 1st and 2nd, 2015, please refer to Gourgoura P., Lykou A., and Koutiva I. (2015)) an activity was carried out aiming at ñestablishing factsò and grasping stakeholdersôrisk perception. By marking on a cityôs map along with comments, information was gathered in terms of hazards e.g. places where flood problems occur, types of flood, frequency, etc.

below depicts the areas which are under risk today according to stakeholders' perspective and

Table 6-1 provides the type of problem, the area of occurrence and a brief description. Analysis of the information provided in the aforementioned table is being provided in Deliverable 6.2 under the paragraph ñHazard and risk situation in the case study are whereas further information in terms of existing flood defence measures is provided in the section of ñCurrent institutional and governance practiceòof the document.

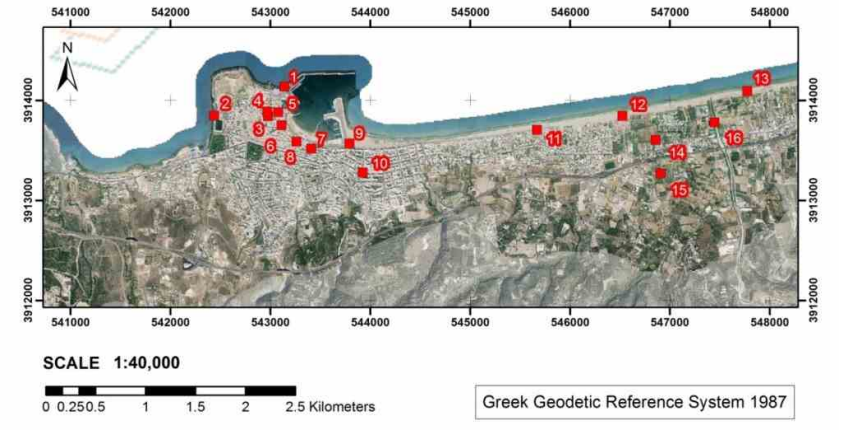

Figure 6-3: Rethymno flood problems as described and identified by stakeholders

Table 6-1: Area of occurrence and flood problems of Rethymno as described and identified by stakeholders

ID	Problem	Area of Problem	Brief description provided by authorities
1	Wave Overtopping	Parking Area of Port Facilities	Inundation of the Old Town of Rethymno
2	Wave Overtopping	Sochora Area, Peripheral Road	Inundation of Peripheral Road
3	Pluvial Flooding	Old Town of Rethymno	Coverage of drainage inlets, low lying areas
4	Pluvial, Drain & Sewer Flooding	Loggia Area	Elevation +0.60, coverage of drainage inlets
5	Pluvial, Drain & Sewer Flooding	Museum Area	Low lying areas & low capacity of drainage network
6	Pluvial, Drain & Sewer Flooding	Arkadiou str.	Low lying areas & low capacity of drainage network
7	Pluvial Flooding	Agnostou Stratioti Square & Arkadiou str.	Low lying areas, accumulation of stormwater
8	Fluvial, Drain & Sewer Flooding	Outlet of Kamaraki - Kallergi & Arkadiou str.	Old Lavirinthos, 06/02/1984 & 1999 flood event
9	Pluvial, Fluvial & Coastal Flooding, Sedimentation	Delphini building, Technical Department premises	Flooding of the building, sedimentation of outlet
10	Fluvial, Drain & Sewer Flooding	Sinatsaki stream	Overflow during high discharges
11	Coastal Flooding	Perivolia, west area of Pearl Hotel	Flooding of houses & plots
12	-	Interchange of Amari	Concerns for future flood problems that might occur due to new road infrastructures
13	Coastal Flooding	Missiria & Platania area	Sea intrusion, construction of small sand dikes
14	Pluvial Flooding	Missiria area, upstream & downstream of National Road	Low lying areas, gentle slopes, no flow
15	Pluvial Flooding	Missiria area, upstream & downstream of National Road	Low lying areas, gentle slopes, no flow
16	Fluvial	Platanias river	Overflow at river at the part between the National Road to the sea

Starting the research activities at the beginning of the PEARL project, several challenges and difficulties were encountered. In terms of hazards, the multiple flood problems that Rethymnoôs community experiences highlight the need for the estimation of hazards due to combined roots and causes, therefore, coupling of several models in different spatial and temporal scale was necessary. Missing data imposed additional difficulties in the setting up of all models, data such as discharge measurements for model calibration, digitised sewerage and stormwater network for coupled simulations, plans of infrastructures of closed conduits crossing the urban area and leading stormwater from open channel riverbeds to the sea. Another challenge faced was the long computational times of hydrodynamic models while working on a city scale with high resolution data such as the DSM of 0.8 m or the DEM of 2.0 m used in sophisticated coupled 1D-2D models. Last but of primary importance, was the challenge of engaging the stakeholders while comprehending in depth, the flood risk management procedures, the authorities engaged within the flood risk and the level of citizenôs and authorities awareness of flood related issues. Absence of an authority dedicated to flood management and lack of flood management plans, unclear jurisdictions among existing authorities, low preparedness and flood risk awareness of citizens, civil engineers and authorities were some of the difficult tasks that later on researchers would have to work on.

6.2 Data collection and analysis for hazard asssessment

Trying to face all the above challenges and while having the primary aim to assess hazards in Rethymno, different type of data from multiple sources was collected from the very first day of the project and an integrated modelling framework to be able to estimate the impact of all type of stressors was developed.

6.2.1 *Data collection*

Within the case study work, information and data has been harvested by several sources serving most of the time several purposes and used within different research activities. Especially for the modelling work and the general hazard assessment of Rethymno, different geospatial data were collected and utilised while setting up the different models. Examples of this data and where it was utilised are listed below:

- Digital Elevation Models (DEMs), Digital Surface Models (DSMs) and Bathymetries of the coastal area were used in order to build up the topography/morphology/terrain of the area under study necessary for hydrologic and hydraulic simulations (at the inland and coastal area)
- Existing topographic maps (with contours and rivers lines, of scale 1:5000) such as those produced by the Hellenic Military Service which were used for digitisation purposes when modification of DEMs/DSMs was needed e.g. at the area of the reservoir of Potamon Dam or for the river network delineation which was derived from DEMs spatial analysis (while defining different values of thresholds)
- Shapefiles of Corine 2000 land use were collected and used in order to derive manning values i.e. roughness values per type of land use for hydrologic and hydraulic purposes. Further, these files were used with the urban growth modelling work.
- General Urban Planning maps of Rethymno were provided by the Municipality of Rethymno and used in the Cellular Automata model of urban growth and in the process of understating future plans of local municipal authorities on future cityôs spatial expansion.
- Precipitation data collected by several open access databases and local and national organisations were used to identify major past flood events occurred due to heavy precipitation and also in different model simulations by setting them up as boundary loads in hydrologic and hydraulic simulations. The location of existing hydro-meteorological stations was of interest too.
- Wind data, was one of the main input in coastal simulations and used for the identifications of past storm events and the corresponding simulations
- Road network and buildings were used for the mesh creation in 2D MIKE 21FM model
- Drawings and cross section of geometries e.g. of port facilities were used as additional data in setting up geometry of models
- Report, books, existing studies and textual information in general was of primary importance too, since completed the knowledge related to flood events, problems and their impact as well as the existing or future infrastructure of flood defence. Examples of those sources of information are conducted coastal engineering studies for the creation of reef breakwaters, studies related to the design of stormwater network or the dam breach of Potamon dam or the Standard Operational Procedure document provided by the Fire Service describing the areas which are considered to be more at risk along with the necessary actions that need to be done during the occurrence of a flood event
- Information collected through online surveys completed by local authorities, technical meetings with them or the LAA workshops that were organised enriched researchers knowledge at all aspects of flood risk and its management procedures and enabled the exchange of knowledge between research community and local authorities and as well as the creation of common images

Data which was collected in order to conduct the vulnerability assessment is being described in section 1.3 of the current document.

Emphasis on the sources from where data and information has been harvested, instead of the actually data and the purposes of collecting it, is being provided in paragraph 7.1.4 (ñAvailable data used for research activitiesò) of Deliverable 6.2.

6.2.2 *Integrated modelling framework*

Having as primary objective the hazard assessment for multiple stressors for the city of Rethymno, an integrated modelling framework has been developed which combines different models and methodologies utilised in the simulation of flood risk. The primary components of this framework are comprised of the followings (Figure 6-4):

1. Estimation of atmospheric variables and development of climate change scenarios
2. Estimation of Wave Characteristics (4-level downscaling approach)
3. Modelling of nearshore response to hurricane impacts and storms (e.g. storm surges, wave propagation, sediment transport, erosion, wave diffraction and refraction, etc.)
4. Catchment hydrological modelling (incl. hydraulic calculations of natural channels networks)
5. Urban flood modelling (incl. surface flow & stormwater network)
6. Comparing alternative solutions and suggesting interventions for damage repair & protection

Figure 6-4: The integrated modelling framework applied in Rethymno

While trying to understand downstream stressors from the coast, the components of this framework include a sequential process working on different spatial and temporal scales (Figure 6-5), starting from the level of climatic analysis at a regional level and ending with the simulation of wave overtopping at port facilities and wave run-up at the shore.

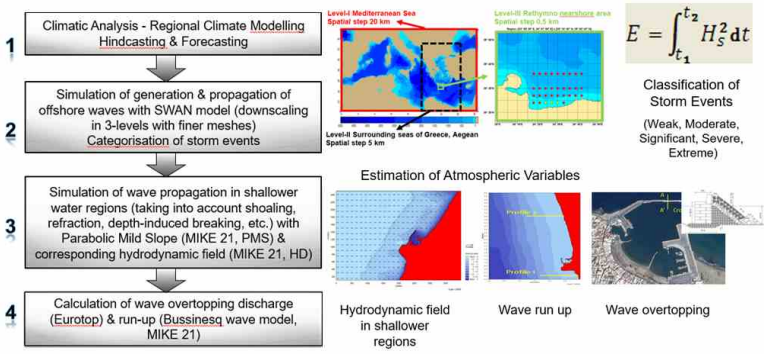

Figure 6-5: Schematic of integrated modelling framework for the comprehension of coastal stressors (adopted from (Tsoukala V. et al. (2016))

Starting with the coastel pressures, a storm is defined as the event exceeding a minimum significant wave height (H_S=2 m) and with a minimum duration of 6 h (De Michele, Salvadori, Passoni, & Vezzoli, 2007; Li, van Gelder, Ranasinghe, Callaghan, & Jongejan, 2014). The threshold of significant wave height (H_s) is considered to be 2 m in order to describe rare events with only 10% of total wave heights and thus defined as the 90th percentile of the data set (Rangel-Buitrago & Anfuso, 2011). The analysis and classification of stormevents is done for the North, Northeast and Northwest wind direction, since it is considered that generates incident waves to the Rethymno coast. In case of the direction or the H_s falls below the threshold for one record and returns above this, remains to be one event.

Following the definition of the storms through the energy content as proposed by Dolan and Davis (1992) and (Dolan and Davis (1994)) a classification of storm events can be derived with a cluster analysis based upon the energy and the average peak period, in order to combine the most important variables of a storm event (Hs ï Duration and Tp). Hierarchical agglomerative clustering techniques were used, employing the average linkage method (Mendoza et al., 2013) as well as the Ward method but with the same results and finally the classification is accomplished into five classes (I - Weak, II - Moderate, III - Significant, IV - Severe, V - Extreme).

The results of the average wave height, period and duration for each storm class are given in the Table 0-1 - Table 0-6 of Annex 1 for each direction N, NE, NW and for two periods: 1960ð 2000 (past climate) and 2000ð 2100 (future climate).

Extreme Value Theory and Block Maxima method (Friederichs & Thorarinsdottir, 2012) is used in order to analyse extreme wind wave heights of the Rethymno estimate levels that are more extreme than observed. The wave condition that is used for the extreme value analysis occurs from the primary data of the meteorological stations of the Hellenic National Meteorological Service and the National Observatory of Athens between the years 1957 and 2014. By using the SMB (Sverdrup-Munk-Bretschneider) method the winds are matched to the significant waves that appear in the offshore. The datasets consist of the annual maxima of wave heights for a period of 57 years, in order for return levels of 25 and 50 years to be estimated, by means of R programming language (R Core Team, 2015) and the use of «extRemes» package (Gilleland & Katz, 2006). The Generalized Extreme Value Distribution (GEV) is fitted to the annual maxima time series of Hs and the parameters estimation is done by method of L ï moments. Finally the MIKE 21 ï PMS model is used for the transformation of offshore wind waves in nearshore areas, according to the bathymetry of coastal area. The results (some of them provided in Annex 1) confirm that the increase of the significant wave height affects the increase of wave overtopping, which can cause catastrophic consequences in coastal zone of Rethymno, especially in the future where the stormsôfrequency is also expected to increase due to climate change.

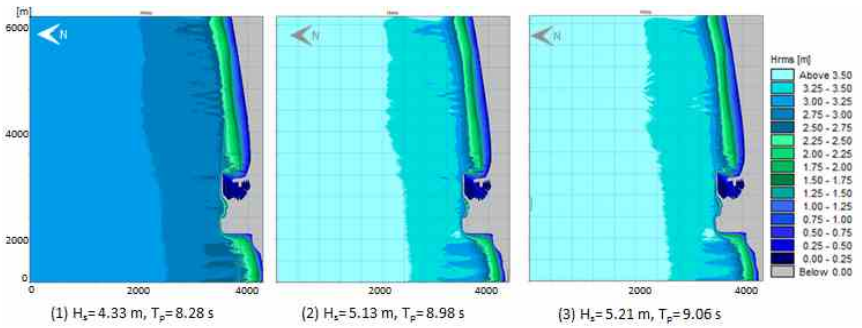

Figure 6-6: Wave propagation of study area

The bathymetry of Rethymno coastal area is constructed into a grid with dimensions 5.5 km * 6.2 km in x and y axes respectively. The spatial step is chosen dx = dy = 5 m. The bathymetry

has been rotated counter clockwise at 900 due to requirements of MIKE21 PMS. The average values of wave height and period of each storm class are adopted as input data and numerical simulations with MIKE21 PMS are carried out to estimate the spatial evolution of these quantities in the whole coastal area. Consequently, the resulting radiation stresses serve as input to the hydrodynamic module with MIKE21 HD to investigate the spatial evolution of the velocity. The results are obtained from MIKE 21 HD concern the hydrodynamic circulation, and more precisely the velocity components u, v along x and y axes, for the total of five storm categories (Ιδ V) in case of north wind direction and for the two storm categories in case of northwest wind direction (I, II).

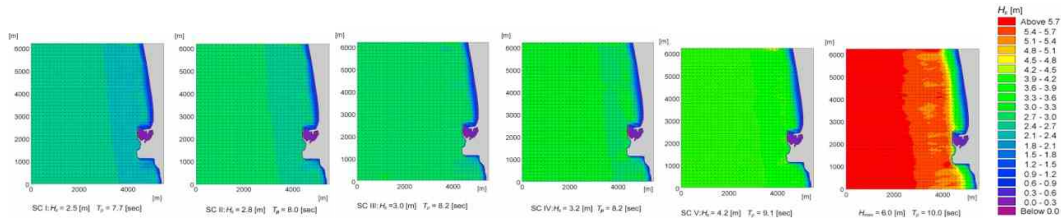

Figure 6-7: Spatial distribution of significant wave height (Hs) for storm classes (SC) I to V and for the maximum occurred incident wave Hmax = 6.0 m for the north direction. Arrows denote the mean wave direction. The colour legend of wave height contours is identical for all classes.

For a more precise analysis of the wave and hydrodynamic conditions the bathymetry of Rethymno is arranged into an unstructured mesh, consisting entirely of triangular elements. The spatial discretization of this complex geometry provided important benefits of flexibility, with different level of density depending on the distance from the shore (Figure 6-8 - a). Having as input this flexible mesh the MIKE21 FM SW, a directional spectral wave model, is applied for the description of the wavefield including refraction, wave breaking, bed friction, wind forcing, and an approximate representation of diffraction (Figure 6-8). After the flow module MIKE21 FM HD , which solves the Saint-Venant equations, is used in coupling with MIKE21 FM SW to include driving forcing from wave breaking, current refraction, and flow resistance taking wave-current boundary layer interaction into account [Fredsøe, 1984]. Finally, the MIKE21 ST model is applied for the investigation of the transport of sand under combined waves and current, considering the vertical distribution of the turbulence with interaction between the wave and current boundary layers [Fredsøe, 1984] and turbulence generated by wave breaking [Deigaard et al., 1986]. The hydrodynamic calculations of the worst case scenario i.e. Scenario 2 (N-direction storm event with the highest identified significant wave height Hs=4.95 m and storm duration D=72 h) are presented in Figure 6-8 and Figure 6-9. The output concerns the wave height H (m) and velocities u and v (m/s) on x- and y- axes respectively. As it is obvious, from the below figures, one can notice the effect of refraction, as waves approaching the shallower region. The most striking feature is that the wave height in front of the windward breakwater is approximately 2.5m, which may cause a wave overtopping in that area. Furthermore, diffraction phenomenon is satisfactorily simulated inside the port basin with the wave disturbance being close to 0.5m. Concerning the velocities, in the sub area of the port and the area west of it, considerable values take place for both current directions. Moreover, it is also worth pointing out there is an intense longshore hydrodynamic movement to the west which is a dominant factor for the motion of sediment.

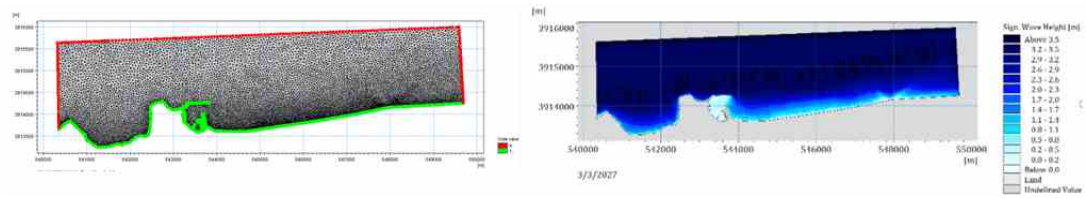

Figure 6-8*: The* computational grid of MIKE 21 for the coastal area and spatial distribution of wave height (H) for Scenario 2

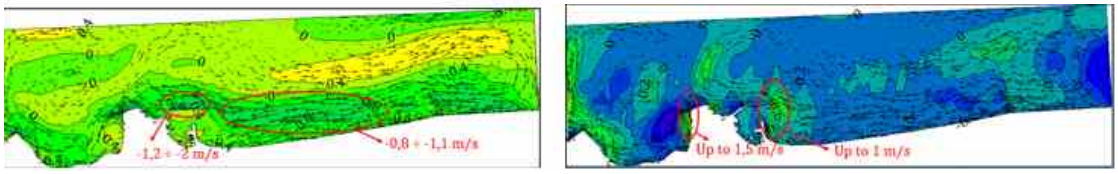

Figure 6-9: Spatial distribution of velocities u, v (m/s) on x- and y- axes respectively for Scenario 2

Moving forward, XBeach is a two-dimensional morphological model which applied in the region of Rethymno for the simulation of near-shore processes, and consequently the evaluation of the hydrodynamic conditions, the sediment transport and the wave run-up during time varying storm conditions. The computational grid for the existing bathymetry and topography is constructed with dimensions 1500x5160 m in x- and y- axes respectively and the spatial steps are chosen dx=dy=5m. The wave run-up level is investigated in twelve cross-shore transects per 300m with the first one being located 100 m to the right of the port (Figure 6-10). The sediment properties are selected uniform sand with porosity of 0.4 and size of 0.2 mm. XBeach is applied here in hydrostatic mode for the four different storm scenarios , which are simulated using the 2D instationary mode of XBeach. This mode is based on a sequence of time-varying wave groups generated using a Jonswap spectrum (keyword: wbctype=jons_table). The results obtained are evaluations of wave height, velocities and sediment transport. Concerning the profiles for each storm event, they are investigated using the 1D transect mode for instationary conditions as well in order to estimate the bed update and wave run-up level (Table 0-10). The wave run-up height estimations are given by Ru2%.

Figure 6-10: Investigated profiles of the case study area

Finally, a combination of MIKE21 BW, EurOtop and empirical formulas are utilized for the computation of wave overtopping and wave run-up. Wave run-up is the extreme vertical height of the wave on a beach, and itis affected by the wave setup and swash. This quantity is estimated using the following tools: i) the above XBeach application, ii) the empirical formula derived by Stockdon et al. (2006) iii) the irregular wave run-up Equation of Coastal Engineering Manual (CEM, 2008), iv) the numerical simulation with the 1D version of a Boussinesq-type wave model (MIKE21 BW).

Moving to the inland area and the comprehension of the upstream pressures, the research activities were initiated with the pre-processing of geospatial data which enabled the sub-catchments and river network delineation (Figure 6-11), the estimation of stream and sub-catchments characteristics such the concentration times, the estimation of hydrological parameters and finally the derivation of necessary input data for hydrologic and hydraulic calculations.

After performing research on several commercial or open access existing models for hydrologic and hydraulic simulations such as SOBEK[1] (Deltares), MIKE models[2] (DHI), HEC-HMS[3] and HEC-RAS[4] (The Army Corps of Engineers), SWMM[5] (EPA) and Hydrogeios[6] (ITIA), the MIKE models of DHIôs were selected. Initials runs were also performed by using HEC-HMS and HEC-RAS products, but since they gave no option of creating combined simulations and not having 2D component were soon abandoned.

A combination of 1D-2D MIKE models (MIKE 11, MIKE 21FM and MIKE Urban) has been setup and coupled through MIKE Flood (Figure 6-12) for the simulation of flood events and their propagation in space and time. The total area under study is defined by all the river catchments that cross the urban area of Rethymno (145 km^2). This area has been taken into consideration for the hydrologic simulation and the calculation of the total volumes of water that drain through the city. Parts of the main river beds with open channel cross section at the upstream areas or all the way down to the sea (e.g. Gallianos River) have been set up in the 1D model MIKE 11. The parts of river with closed cross sections that cross the city have been simulated with MIKE URBAN in order to enable interactions between the subsurface drainage network and the surface runoff. MIKE 21FM is the 2D model used for the simulation of surface runoff by using its hydrodynamic component. All three models have been coupled with MIKE Flood enabling combined 1D-2D simulation of flood phenomena. The coupling of models has been achieved by using 4 types of links for the exchange of volumes of water among models (Figure 6-12). Since the flood impact is important mainly for the urban area (where cityôs functions and services are), the domain of the urban area covers an area of 10.7 km^2, having as boundary the national road at the upstream, the boundaries of the sub-catchments at the east and west boundary of the domain and finally the contour of -20 m as the downstream coastal boundary. The total area of the 2D domain for which mesh has been created is equal to 15.5 km^2 (including the coastal part). But the difficulties encountered due to the large area of interest and the level of desired accuracy (DEM of 2m spatial resolutions) led to the creation of 2 different modelôs set ups in order to lessen computational demands (Figure 6-13). Focusing on Area 1, the 2D model covers a 6.06 km^2 of Rethymnoôs west area comprising of both sea and inland regions, and its mesh consists of 774,619 elements varying in size from 0.064 m^2 to 500 m^2. The most demanding part in modelling set up has been the creation of mesh files. Road network, building polygons, river network and boundaries of sub-catchments where the geometrical entities based on which mesh was created. Figure 6-14 depicts the conceptual model of Area 1.

[1] Sobek, official web site: https://www.deltares.nl/en/software/sobek/
[2] MIKE Flood, official web site: http://www.mikepoweredbydhi.com/products/mike-flood
[3] HEC-HMS, official web site: http://www.hec.usace.army.mil/software/hec-hms/
[4] HEC-RAS, official web site: http://www.hec.usace.army.mil/software/hec-ras/
[5] SWMM, official web site: https://www.epa.gov/water-research/storm-water-management-model-swmm
[6] Hydrogeios, official web site: http://hydroscope.gr/software/hydrogeios.html

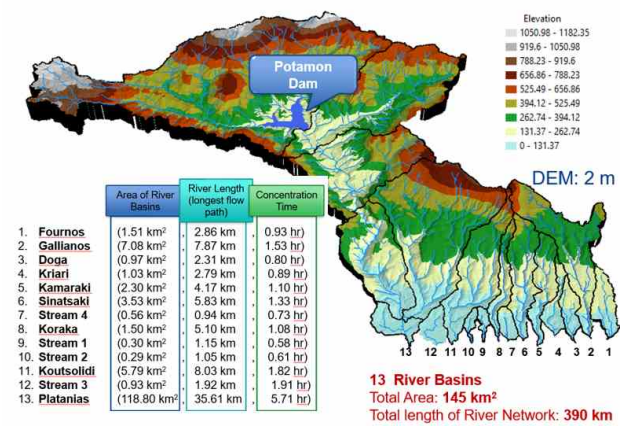

		Area of River Basins	River Length (longest flow path)	Concentration Time
1.	Fournos	(1.51 km²)	2.86 km	0.93 hr)
2.	Gallianos	(7.08 km²)	7.87 km	1.53 hr)
3.	Doga	(0.97 km²)	2.31 km	0.80 hr)
4.	Kriari	(1.03 km²)	2.79 km	0.89 hr)
5.	Kamaraki	(2.30 km²)	4.17 km	1.10 hr)
6.	Sinatsaki	(3.53 km²)	5.83 km	1.33 hr)
7.	Stream 4	(0.56 km²)	0.94 km	0.73 hr)
8.	Koraka	(1.50 km²)	5.10 km	1.08 hr)
9.	Stream 1	(0.30 km²)	1.15 km	0.58 hr)
10.	Stream 2	(0.29 km²)	1.05 km	0.61 hr)
11.	Koutsolidi	(5.79 km²)	8.03 km	1.82 hr)
12.	Stream 3	(0.93 km²)	1.92 km	1.91 hr)
13.	Platanias	(118.80 km²)	35.61 km	5.71 hr)

Figure 6-11: River basins and river network of Rethymno case study along with their primary characteristics

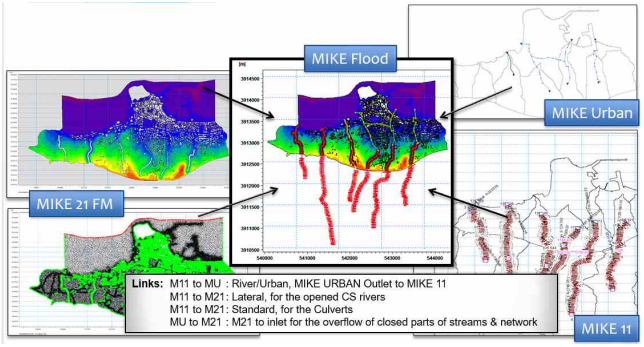

Figure 6-12: Schematic of integrated modelling framework for the simulation of urban floods

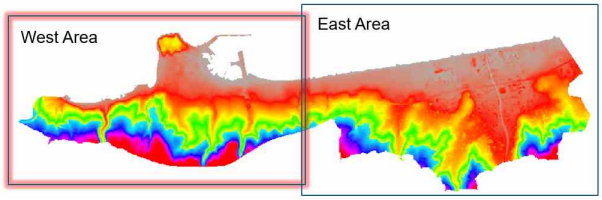

Figure 6-13: Division of area under study in two parts for the inland modelling process

Figure 6-14: Conceptual model of Area 1 as presented through the WebLP interface (mesh elements in green triangles with different size based on desired spatial resolution, parts of rivers with closed cross sections in dashed blue lines, cyan rectangles are manholes of subsurface network through which interactions between surface runoff and flow in subsurface networks is enabled, blue continues lines represent the parts of physical channels/rivers with open cross sections and red lines stands for the cross sections derived from DEM)

Different approaches were tested too, in order to create faster simulations. For further informaltion on how those models were set up readers should refer to Deliverable 4.2 under Rethymno case study section.

One of the precipitation event which has been used as catchment loads in model set ups, was the one recorded on November 10th, 1999 (127.4 mm in total, 100 mm fell in 2 hrs time period), since it had major impacts to cityôs functions and services. The simulation period for the aforementioned event lasts 12 hours with a time step varying based on model setup versions. Further, while trying to be consistent with the work described in the Flood Directive, a precipitation event of 100 years return period was also simulated, which is considered to be of medium frequency. For each scenario several outcomes were derived during normal run complete of models. Those are: maximum water depth (meter), time at maximum water depth (second), maximum current speed (meter/second), time at maximum current speed (second), duration above threshold (second), surface elevation (meter), still water depth (meter), total water depth (meter), U velocity component (meter/sec), V velocity component (meter/sec), P flux (meter^3/sec/m), Q flux (meter^3/sec/m), CFL number (HD) (undefined).

Additional outcomes might also be defined and exported during simulations. Based on the above results, indicative maps of the most important components of hazard assessment have been produced based on simulations of the recorded precipitation event of 1999 (Figure 6-15**Error! Reference source not found.** - Figure 6-18**Error! Reference source not found.**). Further, the map of maximum water depth based on the ourcomes of simulation of a 100 years return period precipitation event has been created (Figure 6-19**Error! Reference source not found.**). Since Rethymnoôs Old Town, was one of the areas that were more at risk at the west part of Rethymno throughout the years, an inset map has been created for enhanced presentation and visualisation of results.

Taking a closer look at the maps, it is apparent that Arkadiou street and several parts of the Old Town of Rethymno are more suscepible to physical stressors. Those areas correpond to numbers (3), (4), (5), (6) and (7) of Figure 6-3 and

Table 6-1 of section 6.1, i.e. modelling results are conistent with the areas at risk as identified by local stakeholders. In terms of the maximum water depth, several parts of the Old Town of Rethymno are inundated based on results of the historic flood event. The maximum water depth ranged mostly between 0.2 m to 0.6 m. Specifically, at the area along Arkadiou street, the water depth values were betwenn 1.0 m to 1.5 m at most of the parts, whereas at the area of museum (4) the maximum water depth was even higher and almost equal to 1.6 m (Figure 6-15**Error! Reference source not found.**). The same pattern in spatial variability of water depth is being noticed for the 100 year precipitation event with the difference that more parts are inundated with water of depth around 0.6 m and that Arkadiou street received values of water depth that ranged between 1.5 m and 2 m at most of its parts (Figure 6-19**Error! Reference source not found.**). Another flood problem that local stakeholdars had identified and was later confirmed through the modelling work, was the overlow of Sintsaki stream during high discharges (10). The maximum water depth that was derived from the historic flood event reached the high value of 3.0 m. Even though this value was conisered too high, the terrain morphology (dem data) confirmed the existance of low elevetations values compared with the

surroundings that led to the formation of such high values of water depth. The maximum water depth of almost all parts of the urbanised sections of area 1 was recorded around 12:00 -13:00 hr which is justified by the fact that at 12:00 the step accumulated precipitation of the simulated event received the maximum value of 12.5 m and at 12:20 the value 11.5 (second maximum) (please refer to Figure A-0-1 of Annex 1). Maximum values of water depth were recorded at the end of simulation for some areas surrounded by bouilding polygons since difficulties in drainage processes have been occurred and the water was considered to be trapped (Figure 6-16**Error! Reference source not found.**).

Having defined the value of 0.5 m as threshold value of maximum water depth in model's set up, above wich duration of indundation was worth having as an outcome, the map of Figure 6-17**Error! Reference source not found.** was produced. It is worth mentioning that duration of inundation has a significant role in the formation of flood risk in general. For the case of Rethymno, during the first minute of simulation the defined threshold was exceeded for all inland parts since precipitation was uniformly applied and distributed on the terrain, but lasted less that a minute. At the areas where the highest values of water depth were recorded, the durations were longer than 1 hr or even exceeed 11 hours at Arkadiou street.

The velocities that were derived from simulations was another flood characteristic of primary imporantance that was assessed within hazard estimation. Most of the maximum current speed values ranged between 0.1 to 0.5 m/s. At some parts of the Old Town the recorded values were between 0.5 m/s and 1m/s, whereas once more the highest values of velocities were recorded at Arkadiiou street, i.e. values of 1.0 m/s to 2.0 m/s.

Even though results and later maps have been produced for part of the coastal area too, description and comments have been provided only for the inland part where flood hazard and risk has impact to people's life and properties.

The lack of recoreded discharge data or the actually flood extent of previous flood events formed one of the challenges faced within the PEARL work, since no data was available for calibration purposes. Trying to overcome this difficulty, researchers utilised the knowledge and information gained by stakeholders in terms of Rethymno's flood problem. Specifically, the results of model simulations were assessed and were compared to the areas that were identified by stakeholders which are considered to be more at risk. As anticipated the areas that were related to fluvial and pluvial flooding based on stakeholders testimonies were in aggrement with the areas more susceptible to floods based on the results of the simulated events. Considering the weakness of the hydrondynamic module to simulate the physics of the overtopping phenomena, the areas that area being inundated due to overtopping have not been confirmed yet through the modelling work but it is planned to be tested during the last year of project. Samewise, comparison of exported results with stakeholders risk perception will be made for Area 2.

Apart from precipitation loads, the coupled urban models have been set up in order to simulate storm events related to the coastal pressures. Until now, two storm events have been simulated using the 2D hydrodynamic components of MIKE models. Those are the event on January 27th, 19:00, 1961 (end of simulation January 31st, 23:00, 1961) of North Direction, category 4 and the one starting on March 1st, 3:00, 2027 (ends on March 4th, 2:00, 2027) of North direction and category 5 (Table 0-11**Error! Reference source not found.**). During set up of those scenarios, profile series of water surface have been extracted from hydrodynamic coastal results and used as boundary conditions for the urban modelling. Unfortunately while running those simulation, they gave no inundation to the inland area which is justified by the fact that the hydrodynamic component is incapable of simulating overtopping phenomena during of which volumes of water intrude the adjacent zones of port facilities and inundate part of the Old Town. Therefore, new simulations are currently being set up in order to use as point source the resulted discharges from overtopping estimation and simulate their propagation is space through the 2D hydrodynamic component of inland models.

Except for the simulations that have already been completed, additional ones will be performed in order to simulate different hydro-meteorological scenarios that stakeholders would like to have available and examine through the WebLP platform of WP5. The simulations will be performed for Area 2 too. Scenarios of failure of infrastructures are also planned be examined e.g. dam breach of Potamon dam, as well as the impact of different urban growth scenarios. By running a CA model modified and enhanced within PEARL by NTUA, different land use will be provided affecting roughness values, hence, altering possibly the flood phenomena (Deliverable 6.2).

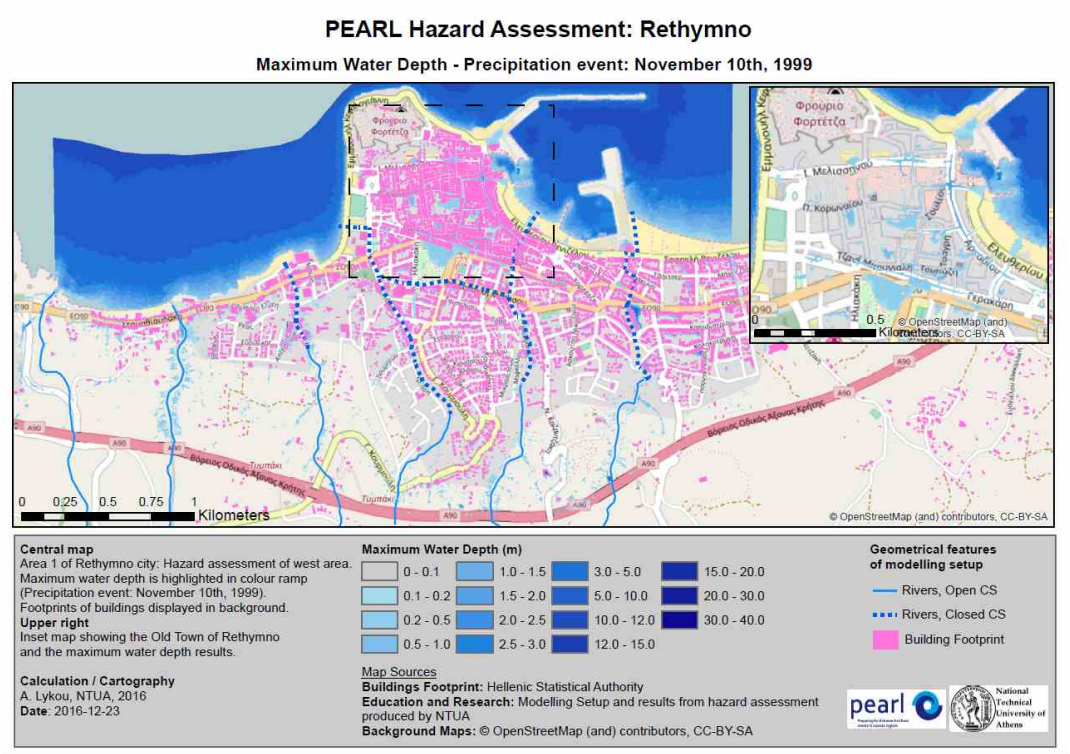

Figure 6-15: Maximum water depth for Area 1 of Rethymno (results from simulation of recorded precipitation event on November 10th, 1999)

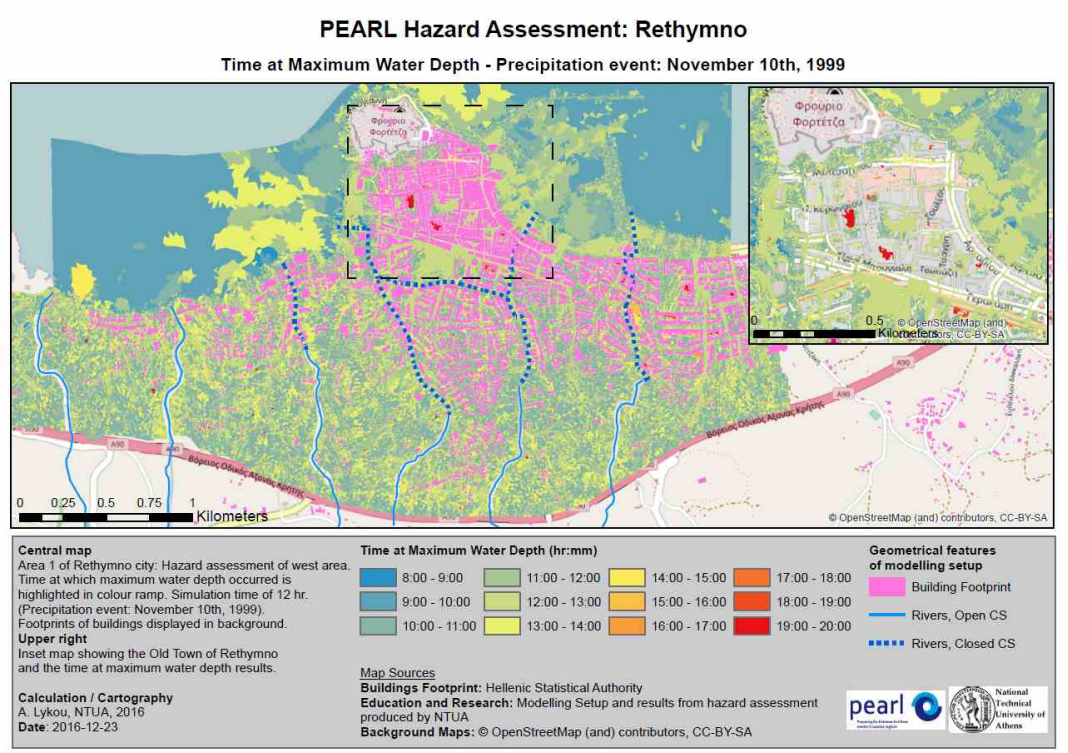

Figure 6-16: Time at maximum water depth for Area 1 of Rethymno (results from simulation of recorded precipitation event on November 10th, 1999)

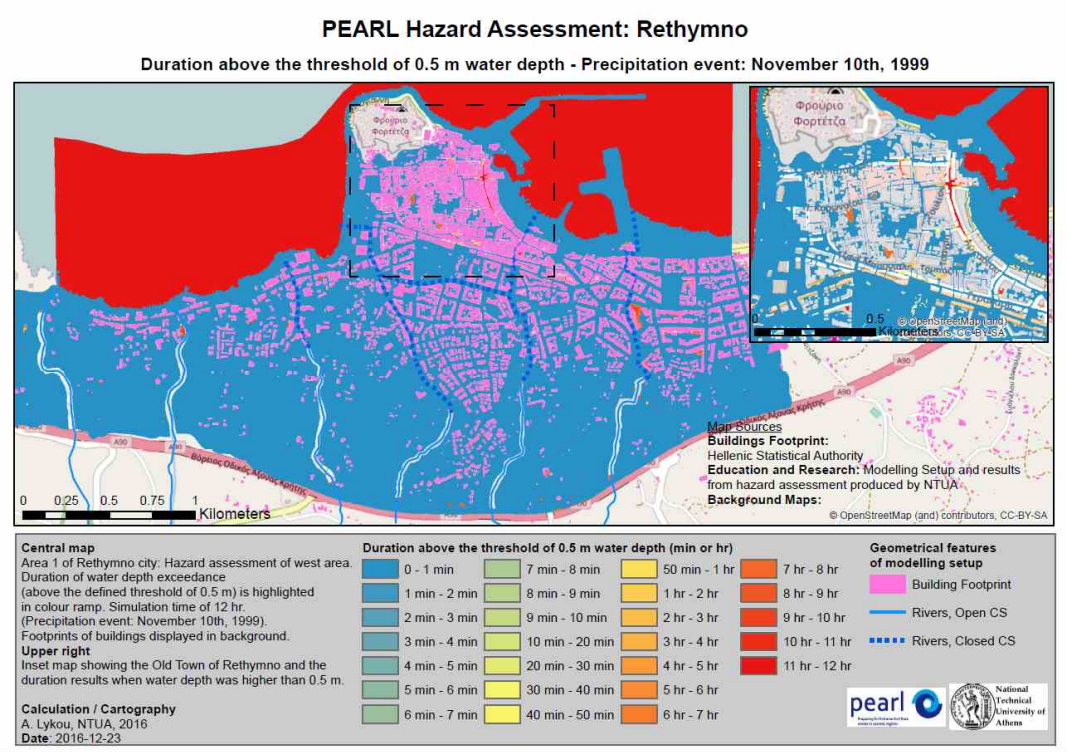

Figure 6-17: Duration of depth above threshold for Area 1 of Rethymno (results from simulation of recorded precipitation event on November 10th, 1999)

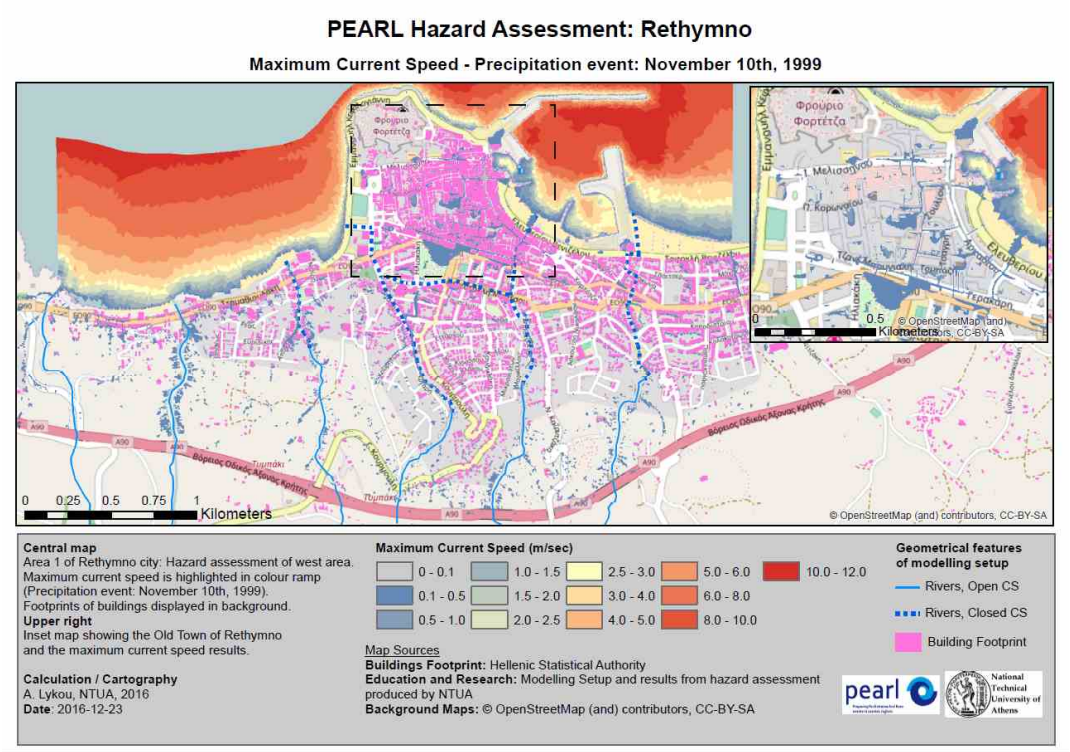

Figure 6-18: Maximum current speed for Area 1 of Rethymno (results from simulation of recorded precipitation event on November 10th, 1999)

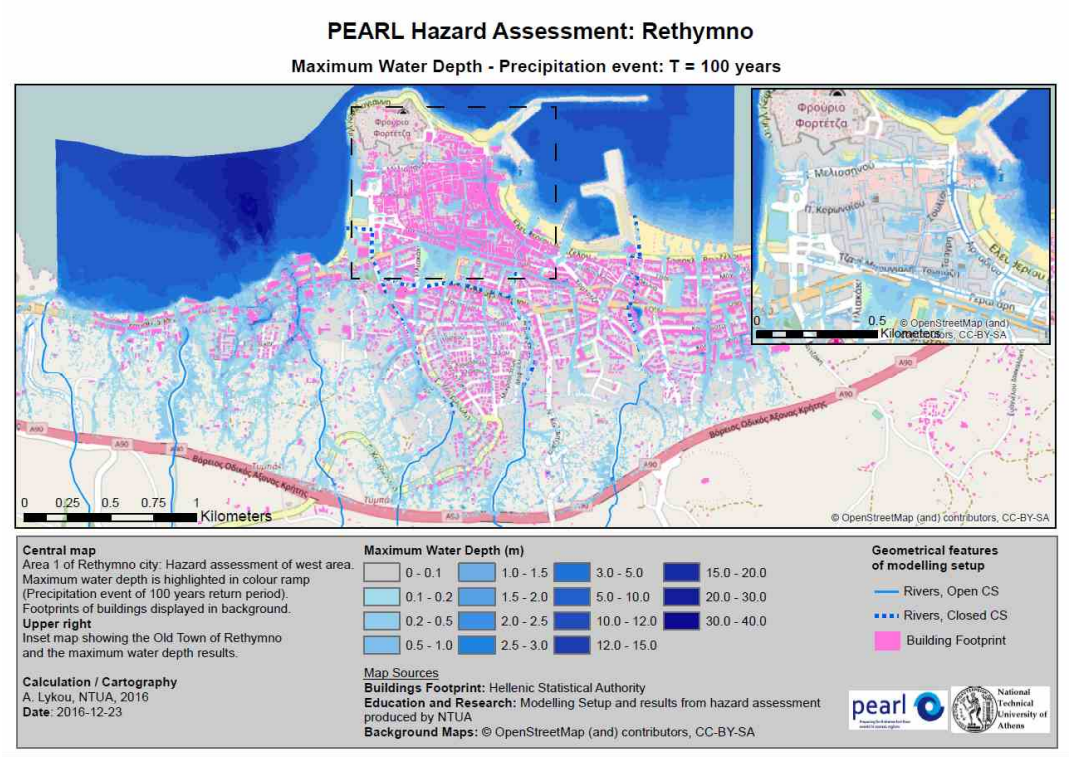

Figure 6-19: Maximum water depth for Area 1 of Rethymno (results from simulation of a precipitation event of 100 years return period)

6.3 Data collection and analysis for vulnerability asssessment

For the spatial vulnerability assessment, vulnerability has been defined on the basis of three components: *susceptibility*, *coping capacity* and *adaptive capacity*, which have been defined within the PEARL context and thoroughly described in vulnerabilityôs framework report (Sorg, Birkmann, Feldmeyer, & Medina Pena, 2016). Specifically within PEARL, the aim was to assess the social vulnerability of each case study, hence in Rethymno, by applying the suggested framework and adapting it based on data availability, assumptions and local conditions. Based on this modular structure of the framework, the three basic concepts are being divided into several parts in order to achieve a general and a more holistic picture of the current situation and case studiesô conditions in terms of extreme hydro-meteorological events vulnerability. The aggregation of various components into a single vulnerability index allowed to draw conclusions at a one glance by summarising everything in one index while applying the below formula (F.1) and present its spatial variability on a map.

$$\text{Vulnerability} = \frac{1}{3}\,(\text{Susceptibility} + \text{Lack of Coping} + \text{Lack of Adaptation}) \quad \text{(F.1)}$$

For the calculation of vulnerability, the lack of coping and adaptive capacity was incorporated, in order to assess all factors/indexes affecting the societal vulnerability. For the calculation of those factors, several indicators have been defined and eventually assessed based on the availability of geospatial data and spatially explicit statistical data of Rethymno.

The raw data for the calculation of indicators was extracted by several sources such as the Hellenic Statistical Authority[7] (after signing confidentiality agreements), the Technical and Planning Department of Rethymnoôs Municipality and open access databases (e.g. http://geodata.gov.gr/). The base maps used for cartography and presentation of results were taken from Open Street Map, ESRI ArcGIS.

The geospatial data used for the analysis or the creation of maps and representation of results were:

- Boundary of river catchments (.shp)
- Boundary of last flooding event as produced during hazard assessment (.shp)
- Administrative boundaries of Rethymno case study (.shp)
- Boundaries of censusôsectors (.shp)
- Boundaries of blocks (.shp)
- Boundaries of buildings (.shp)

The spatially explicit statistical data were consisted of three basic categories as collected during Census 2011 which are the below:

- Statistical data concerning individuals/citizens available at block scale
- Statistical data concerning households available at block scale
- Statistical data concerning buildings available at sector scale

The vulnerability assessment was conducted on the smallest possible scale i.e. block scale since the majority of data was available at that spatial scale. Especially for the calculation of indicators concerning buildings states or conditions (such as 4.1 and 4.2 of Figure A2-0-1 of Annex 2**Error! Reference source not found.**), considering the limitations of data properties while this data was available at sectors scale an assumption was made. More specifically, researchers made the assumption that every block that lies within a sector will inherit the properties of the corresponding sector. The city of Rethymno is divided into 608 blocks and 39 sectors, as presented in Figure 6-20, for which vulnerability assessment was conducted.

[7] Official Website of the Hellenic Statistical Authority: http://www.statistics.gr/en/home/

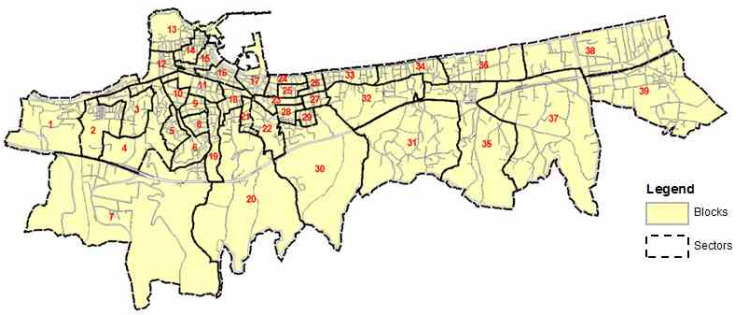

Figure 6-20: Bocksôand sectorsôboundaries used for the vulnerability assessment of Rethymno

All calculations were performed either in MS Excel based on raw data or extracted after queries in ArcGIS while using/building SQL expressions and then imported in excel sheets. Finally, the results of calculations were linked to ArcGIS shapefiles for the creation of maps and their representation in space.

The indicators predominately were calculated as ratios ranging from 0 to 100, either due to their definition or after performing min-max normalization of the indicatorsôvalue in order to transform them into dimensionless variables and make them comparable. For the fields missing or for the fields which were divided by ñ0ò, ñ9999òvalue was used which indicated ñNo dataòfor those entries. ñNo dataòentries were filtered and excluded from further calculations. In more detail, if for example one variable was defined as the average of two different indicators one of which had ñNo dataò value, then the indicator received ñNo dataò value too for that specific entry.

A graphical representation of sub-indexes (susceptibility, lack of coping and adaptive capacity) along with their components has been provided in Figure A2-0-1**Error! Reference source not found.**, Figure 0-2 and Figure 0-3. The indicators that were taken into consideration for the calculation of the overall index of the vulnerability have been highlighted, whereas the ones that could not be estimated due to insufficient data have been grey-shaded. Additionally, the weighting of each indicator and index has been provided. In fact all variables were considered equally important as presented in the below figures. Thorough analysis of each variable along with the assumptions made for their estimation is outside the scopes of this deliverable. It is highly important though to note that for the calculation procedure of vulnerability, the lack of coping and adaptive capacity was incorporated in order to assess factors which increase the societal vulnerability. Therefore, one has to keep the direction of the sub-indicators in mind. For example during the calculation of indicator 6.1 i.e. the average size of households, the households having more members were considered to be less vulnerable since there are more people to assist the more elderly members, the children or the disabled persons. Likewise, for the calculation of indicator 10.2, the population not having access to the internet was considered more vulnerable and was taken into account for the index estimation.

After the calculation of each indicator for the block scale, the three sub-indexes were estimated and finally the overall vulnerability index. For their spatial display and the creation of maps, the quantile method was used for 5 classes of vulnerability (Very High, High, Medium, Low, and Very Low). Based on quantile method of data classification, each derived class has the same number of cases. A second version of the Vulnerability map has also been produced after performing min-max normalization of resulted values, so that the newly derived values of vulnerability will range from 0 to 100. In this way, the map will be immediately comprehendible for further discussions with Rethymnoós stakeholders during the last LAA meeting which will take place towards the end of the project.

Additionally to the general vulnerability framework that has been applied in Rethymno, a household survey was conducted by IREUS team at the end of 2015 for the purpose of gaining insights into the vulnerability patterns of the exposed households. The extended vulnerability

assessment approach, which is planned to be applied during the last year of the project, will incorporate findings from the related household survey in Rethymno by combing statistical data provided by Census 2011 and information on household level derived from door to door interviews with citizens. The enhanced vulnerability method will follow Genoaôs example and will be reported in the update version of the current document to be submitted during the last year of the project.

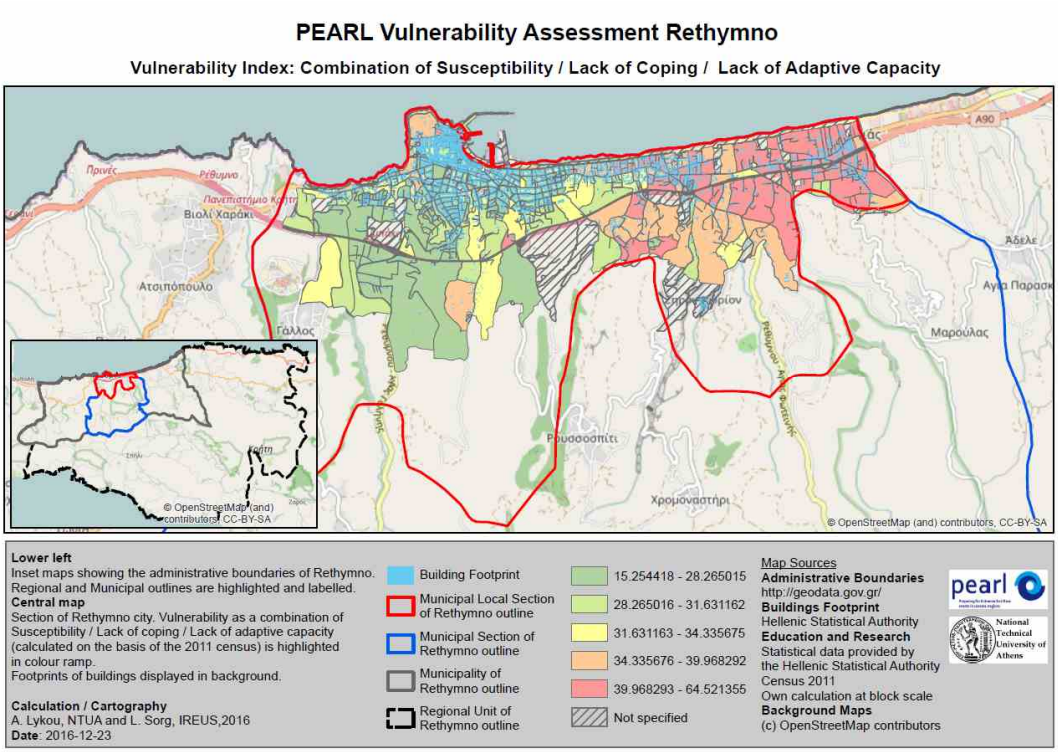

Figure 6-21: Vulnerability map of Rethymno case study (analysis was conducted at a block scale)

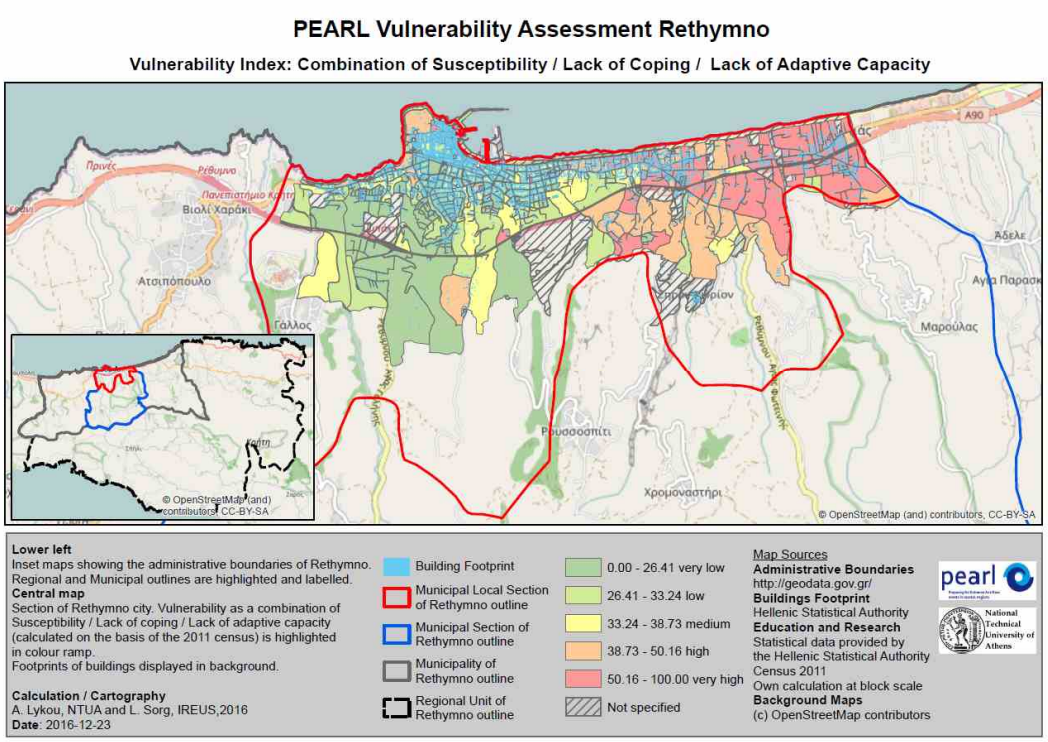

Figure 6-22: Vulnerability map of Rethymno case study (analysis was conducted at a block scale, values were normalised)

6.4 Risk assessment

Flood risk assessment within PEARL and specifically for Rethymno case study has been implemented by using the traditional approach i.e. risk has been defined as the combination of hazard and vulnerability through a local quantitative approach (Cardona, 2012). First step in the quantification of flood risk is the computational flood modelling based on which hazard has been defined. By using the sophisticated computational models described in section 6.2.2 i.e. hydrological and coupled hydraulic 1D-2D models, characteristics of flood events were simulated and different results were exported e.g. water depth, velocities, durations, etc. (Figure 6-15 - Figure 6-19). Main physical characteristics of the historical flood event of 1999 were assessed and different maps were produced that were later utilised within risk assessment.

Primary step in hazard map construction and eventually flood risk assessment was the classification of hazard in three intensity levels i.e. Low, Medium and High by taking into consideration the values and spatial variability of the two main characteristics of floods, the maximum water depth (Figure 6-15) and the velocities (Figure 6-18). Even though duration has a significant role in hazard formation, the short duration of flood phenomena and inundated zones in Rethymno, led to the neglect of duration results during hazard estimation. Following the methodology described by Vojinovic et al. (2016) and Cançado, Brasil, Nascimento, and Guerra (2008), the two aforementioned parameters were used to evaluate flood hazard a man is exposed to.

Table 6-1 indicates the three intensities used for the classification of flood hazard employed in the study area. Initially, the value of 1.5 m maximum water depth and 1.5 m/s velocity were used for the separation of the second and the third class, but local conditions, citizens risk perception and the ranging of values in results led to the selection of the below classification (Table 6-2). The above selection was also based on the graphical representation of the flood hazard zone and manageability perception of the communities in terms of flood water depth and duration described by Peters-Guarin, McCall, and van Westen (2012). Considering the flood preparedness and local conditions of Rethymno along with the fact that 1 m water depth is up to the waist of a moderate's people height, the 1 m water depth was considered to be more representative for the definition of Rethymno's extremes.

Table 6-2: Hazard classification based on maximum water depth and velocity values

Hazard (class)	**Depth** (m) / **Velocity** (m/s)
High	D > 1.0 m **or** V > 1 m/s
Medium	0.5 m ÒD Ò1.0 m **or** 0.1 m/s ÒV Ò1.0 m/s
Low	0.1 m ÒD < 0.5 m **or** 0.1 m/s ÒV < 0.5 m/s

For the vulnerability assessment, as described in section 6.3 of the current document, the framework developed by Sorg et al. (2016) was implemented. Within this framework, of equal importance and components of vulnerability are the *susceptibility* i.e. the likelihood of suffering harm, the *lack of coping* i.e. the lack of capacities for dealing with direct impact and the *lack of adaptation* i.e. the lack of capacities for long-term change (Sorg et al., 2016). The vulnerability assessment conducted at a block scale and encompassed indicators and indices techniques (Cardona, 2012). The indicators were estimated based on available data and took into account several aspects of an urban system such as demography, poverty and income, medical

service, information, education, gender equity, etc. Figure A2-0-1, Figure 0-2 and Figure 0-3 summarise the indicators that were used in its aspect of vulnerability along with their weighting. The maps of vulnerability that were eventually produced are being presented under **Error! Reference source not found.**

Figure **6-21** and Figure 6-22.

Following the procedure described in Vojinovic et al. (2016) under the traditional approach to flood risk assessment, the combined risk assessment was fulfilled by multiplying the map of vulnerability with hazard maps. First, the classes of hazard (low, medium and high) where ñtranslatedòinto scores by setting the values 0.33, 0.66 and 1 respectively in each class (Figure 6-23). Likewise, the values of vulnerability were normalised between 0 to 1 (Figure 6-24). After having produced the above maps, the final flood risk map of Area 1 of Rethymno was produced with values ranging from 0 to 1. Scores of risk lower than 0.25 were considered for areas of low risk, scores between 0.25 and 0.45 were given to areas of medium risk and the areas with scores greater than 0.45 were considered as high risk zones (Figure 6-25). While looking at the flood risk map, most of the areas in the west part of Rethymno are considered of low vulnerability whereas as anticipated in parts of the Old Town of Rethymno the risk is considered of medium scale. Specifically, at Arkadiou Street where hazardôs characteristics (water depth, velocity and duration) received higher values, the risk scores ranged from 0.25 to 0.40. Only very few points appeared to have higher values or risk ranging from 0.4 to 0.6.

The low values of risk are justified due to the low hazard scores that were formed based on the 1999 event, despite the values of vulnerability. The precipitation event was considered to be of return period lower than 100 years. As already stated, during the last year of PEARL project, additional result are planned to be produced since different scenarios will be examined for which risk assessment will be conducted too.

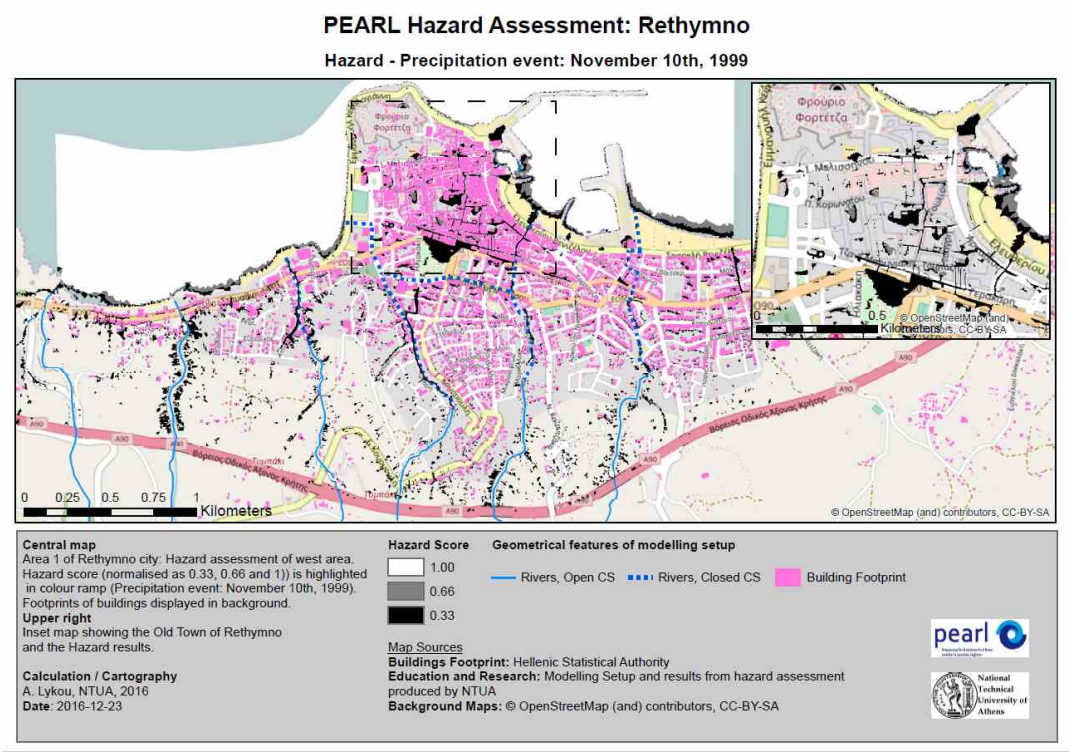

Figure 6-23: Hazard map for Area 1 of Rethymno (results from simulation of recorded precipitation event on November 10th, 1999)

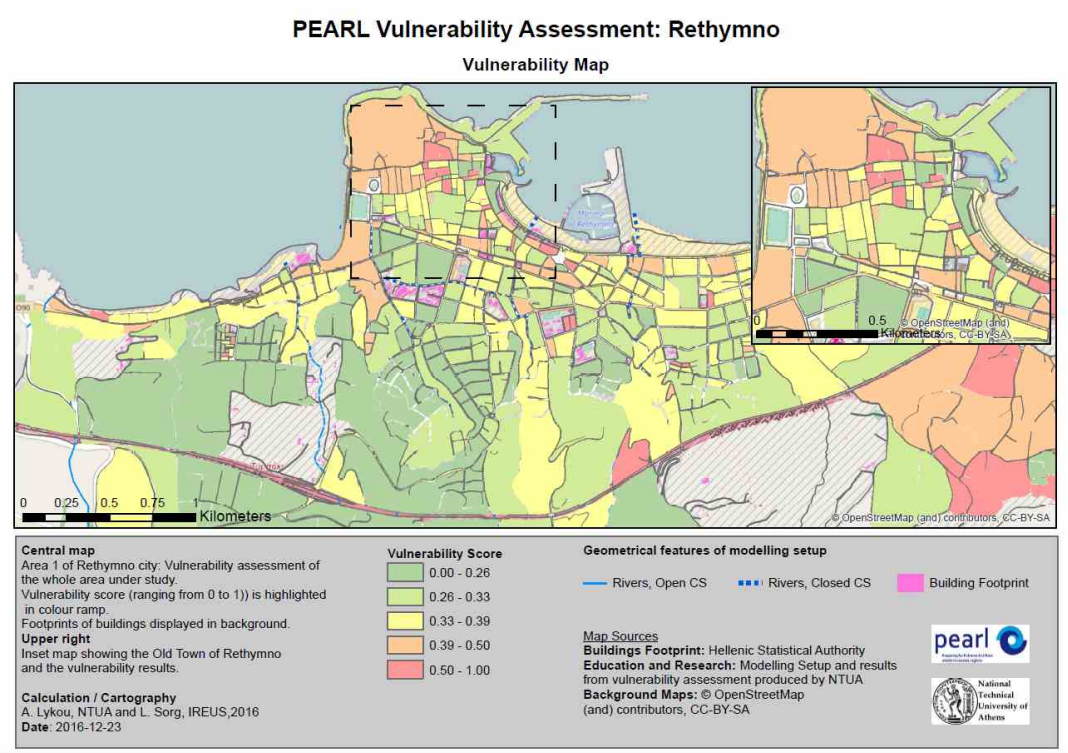

Figure 6-24: Vulnerability map zoomed at Area 1 of Rethymno (normalised values ranging from 0 to 1)

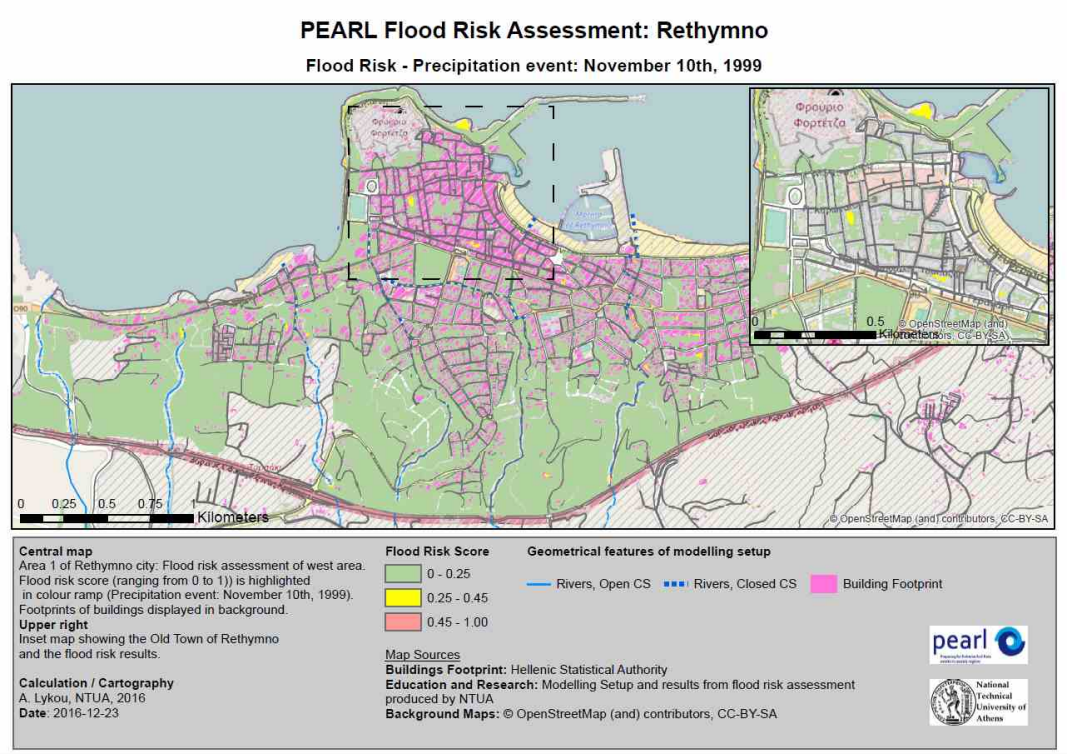

Figure 6-25: Flood risk map for Area 1 of Rethymno (results from simulation of recorded precipitation event on November 10th, 1999

6.5 How risk analysis benefit local stakeholders

Risk perception and communication along with its individual components i.e. hazard and vulnerability are considered to be key issues in flood risk management and critical for effective adaptation and disaster risk management (Cardona, 2012). For the case study of Rethymno, the aim, among others, was to reach different audience accessed through the LAA members in order to make risk comprehensible while improving their awareness on flood related issues and encourage them to act towards the formation of a city better flood prepared. The process in meeting the above goal was gradual while building a close collaboration with local authorities on a solid base.

Local authorities and different groups of active citizens have been reached within PEARL project through several technical meetings and LAA workshops and citizens actual risk perception has been gained after a door to door survey conducted by IREUS. Being consistent with the DoW of PEARL, local stakeholders were officially informed about the project and its objective during the 1st LAA workshop (Gourgoura P. et al., 2015). They were engaged into several activities, working groups and round tables during of which facts were established, flood problems and related flood defence infrastructures were identified and common pictures were created among LAA members and researchers. During the 2nd LAA workshop, the results of the risk perception household survey were presented to them and comparison of citizens and authoritiesô risk perception was achieved through a round table. Key outcomes were the necessity of awareness raising activities while authoritiesô individual responsibility was highlighted and the recognition of lack and essentiality of Early Warning System and evacuation plans for floods for the city of Rethymno. Additionally, stakeholders assessed the resilience of their city through the use of the PEARL KB FRI tool (Deliverable 5.2) and formed different hydro-meteorological, failure of infrastructure and urban growth scenarios that they would like to have examined through the modelling work (Gourgoura P., Lykou A., & Koutiva I., 2016). Building gradually the awareness of flood related issues for Rethymnoôs authorities, they were also encouraged to act by utilising the products of PEARL (KB, online FRI tool, WebLP, Water Detective, etc.) and to organise the first LAA action on awareness raising activities. After having comprehended the physical processes and how citizens actions affect the evolution of flood risk, a voluntary clean-up of a stream is planned to be conducted by the Municipality on spring 2017, aiming at informing and educating citizens based on experiential evidence.

Comprehensive picture and information will be given to Rethymnoôs authorities during the last LAA meeting which will take place towards the end of PEARL when all aspects of hazard, vulnerability and risk will be presented to them while seeking their points of view on every aspect and the creation of common images. The final risk analysis, the actions and points of view of the formed LAA group will deliver the actionable roadmap that Rethymno city really needs while utilising all PEARL products developed to assist food management and decision making processes.

Apart from the above described work, the collaboration of local authorities with the pearl team and the integrated modelling framework has also delivered some tangible benefits to Rethymnoôs stakeholders. Specifically, being familiar with the overtopping flood problem and the damaged caused to the windward breakwater of port facilities, PEARL team re-evaluated the cross section of the existing breakwater under climate change scenarios, taking into account related data that are predicted for up to 2050 about changes of the dominant wave, the storm surge and the sea level rise. Based on armour stability, toe stability and admissible average overtopping discharges, different solutions were examined**Error! Reference source not found.**. The performance of each solution was assessed based on the above mentioned criteria and the upgrading cost of each solution was also estimated. The results are presented in Figure 6-26 and the proposed solution is highlighted with bold fonts i.e. adding a berm alternative was suggested. The produced results were given to the Port Authority of Rethymno in order to have them available during the design of repair works of the windward breakwater.

Cross section		Armor damage		Toe damage N_{od}		Average overtopping		Cost (€/m)
		Design	2050	Design	2050	Design	2050	
Existing breakwater	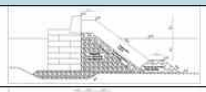	8.74	8.74	2.76	2.47	5.914	7.465	
Adding an extra armor layer on the front slope	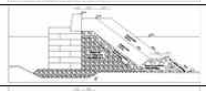	8.74	8.74	1.57	1.42	1.865	2.354	5392.00
Adding a berm	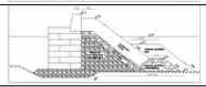	**8.74**	**8.74**	**0.62**	**0.57**	**1.346**	**1.889**	**1288.00**
Proposed Project design Municipal Port Authority of Rethymno, 2015		3.64	3.64	4.69	4.17	1.396	1.964	13992.00

Figure 6-26: Performance of the existing breakwater & the proposed alternative upgrading solutions along with estimated upgrading cost

6.6 References

Archontakis D. (2013). *The Old Town of Rethymno: from a run down gheto to growth leverage of Rethymno*. Rethymno.

Cançado, V., Brasil, L., Nascimento, N., & Guerra, A. (2008). *Flood risk assessment in an urban area: Measuring hazard and vulnerability*. Paper presented at the 11th International Conference on Urban Drainage, Edinburgh, Scotland, UK.

Cardona, O. D., M.K. van Aalst, J. Birkmann, M. Fordham, G. McGregor, R. Perez, R.S. Pulwarty, E.L.F. Schipper, and B.T. Sinh. (2012). Determinants of risk: exposure and vulnerability. In: Managing the Risks of Extreme Events and Disasters to Advance Climate Change Adaptation [Field, C.B., V. Barros, T.F. Stocker, D. Qin, D.J. Dokken, K.L. Ebi, M.D. Mastrandrea, K.J. Mach, G.-K. Plattner, S.K. Allen, M. Tignor, and P.M. Midgley (eds.)]. A Special Report of Working Groups I and II of the Intergovernmental Panel on Climate Change (IPCC) (pp. pp. 65-108). Cambridge University Press, Cambridge, UK, and New York, NY, USA,.

De Michele, C., Salvadori, G., Passoni, G., & Vezzoli, R. (2007). A multivariate model of sea storms using copulas. *Coastal Engineering, 54*, 734-751.

Dolan, R., & Davis, R. E. (1992). An intensity scale for Atlantic coast northeast storms. *Journal of Coastal Research, 8*(4 (Autumn, 1992)), pp. 840-853. doi: http://www.jstor.org/stable/4298040.

Dolan, R., & Davis, R. E. (1994). Coastal storm hazards. *Journal of Coastal Research*(SI 12), 103ð 114. doi: http://www.jstor.org/stable/25735593.

Friederichs, P., & Thorarinsdottir, T. L. (2012). Forecast verification for extreme value distributions with an application to probabilistic peak wind prediction. *Environmetrics, 23 (7)*, 579-594.

Gilleland, E., & Katz, R. W. (2006). *Analyzing seasonal to interannual extreme weather and climate variability with the extremes toolkit*. Paper presented at the 18th Conference on Climate Variability and Change, 86th American Meteorological Society (AMS) Annual Meeting.

Gourgoura P., Lykou A., & Koutiva I. (2015). PEARL 1st Stakeholder Workshop in Rethymno (01 & 02 October 2015) Report.

Gourgoura P., Lykou A., & Koutiva I. (2016). PEARL 2nd Stakeholder Workshop in Rethymno (07 & 08 June 2016) Report.

Hellenic Statistical Authority. (2011). Census. Retrieved accessed on 21 December 2015, from http://www.statistics.gr/

Li, F., van Gelder, P. H. A. J. M., Ranasinghe, R., Callaghan, D. P., & Jongejan, R. B. (2014). Probabilistic modelling of extreme storms along Dutch coast. *Coastal Engineering, 86*, 1ï 13. doi: http://dx.doi.org/ 10.1016/j.coastaleng.2013.12.009

Makropoulos C., Tsoukala V., Lykou A., Chodros M., Manojlovic N., & Vojinovic Z. (2014). *Improving resilience against extreme and rare events in coastal regions: an initial methodological proposal - The case study of the city of Rethymno*. Paper presented at the ADAPTtoCLIMATE International Conference, Nicosia, Cyprus.

Mendoza, E. T., Trejo-Rangel, M. A., Salles, P., Appendini, C. M., González, J. L., & Torres-Freyermuth, A. (2013). Storm characterization and coastal hazards in the Yucatan Peninsula. *Journal of Coastal Research*(65), 790-795.

Peters-Guarin, G., McCall, M. K., & van Westen, C. (2012). Coping strategies and risk manageability: using participatory geographical information systems to represent local knowledge. *Disasters, 36*(1), 1-27. doi: 10.1111/j.1467-7717.2011.01247.x

R Core Team. (2015). R: A language and environment for statistical computing [Press release]. Retrieved from http://www.R-project.org/

Rangel-Buitrago, N., & Anfuso, G. (2011). An application of Dolan and Davis (1992) classification to coastal storms in SW Spanish littoral. *Journal of Coastal Research*(64), 1891ð 1895.

Sorg, L., Birkmann, J., Feldmeyer, D., & Medina Pena, N. (2016). PEARL Vulnerability Assessment approach carried out by IREUS in Work Package 1, Concept Note, Version 2.

Tsoukala V., Chondros M., Kapelonis Z., Martzikos N., Lykou A., Belibassakis K., & Makropoulos C. (2016). An integrated wave modelling framework for extreme and rare events for climate change in coastal areas the case of Rethymno, Crete. *Oceanologia, 58*(2). doi: doi:10.1016/j.oceano.2016.01.002

Vojinovic, Z., Hammond, M., Golub, D., Hirunsalee, S., Weesakul, S., Meesuk, V., . . . Abbott, M. (2016). Holistic approach to flood risk assessment in areas with cultural heritage: a practical application in Ayutthaya, Thailand. *Natural Hazards, 81*(1), 589-616. doi: 10.1007/s11069-015-2098-7

Annex 1 of Rethymno Case Study

Results of the average wave height, period and duration for each storm class are given in the following tables (Table 0-1 - Table 0-6) for each direction N, NE, NW and for two periods: 1960– 2000 (past climate) and 2000– 2100 (future climate).

Table 0-1: Classification of Storm Events for North Wind direction and for the time period 1960-2000

Storm Class	Significant Wave Height [m]		Peak Period [s]			Energy [m² h]			Duration [h]	Events
	max	mean	min	max	mean	min	max	mean	mean	
I	3.12	2.20	5.53	9.67	7.24	37.03	135.38	84.34	16.62	65
II	4.09	2.40	5.25	9.16	7.51	137.14	269.91	198.58	32.60	127
III	4.18	2.57	5.71	9.25	7.68	274.26	440.87	335.13	47.72	75
IV	5.26	2.92	4.84	10.36	7.98	456.61	981.40	629.25	68.45	65
V	6.31	3.46	5.28	10.82	8.39	1173.10	1862.63	1491.27	111.86	14

Table 0-2: Classification of Storm Events for Northeast Wind direction and for the time period 1960-2000

Storm Class	Significant Wave Height [m]		Peak Period [s]			Energy [m² h]			Duration [h]	Events
	max	mean	min	max	mean	min	max	mean	mean	
I	2.82	2.13	5.31	7.93	7.08	37.01	105.83	66.86	14.23	31
II	2.88	2.30	5.90	9.45	7.37	122.66	213.85	168.04	30.60	15
III	3.45	2.53	6.11	8.16	7.43	239.86	310.29	274.20	40.50	4
IV	4.15	2.93	5.85	9.02	7.88	361.34	442.05	411.76	44.25	4
V	4.29	2.99	6.27	9.09	7.92	504.73	698.02	582.86	60.75	4

Table 0-3: Classification of Storm Events for Northwest Wind direction and for the time period 1960-2000

Storm Class	Significant Wave Height [m]		Peak Period [s]			Energy [m² h]			Duration [h]	Events
	max	mean	min	max	mean	min	max	mean	mean	
I	3.02	2.17	6.56	8.97	7.69	39.02	93.41	60.95	12.15	20
II	3.55	2.38	5.45	9.15	7.56	113.66	154.41	134.89	22.36	11
III	3.80	2.58	4.74	9.48	7.89	173.55	204.20	191.25	26.25	4
IV	4.38	2.88	4.62	10.34	8.35	273.85	287.91	280.88	30.00	2
V	4.24	3.19	6.19	9.64	6.19	404.12	404.12	404.12	36.00	13

Table 0-4: Classification of Storm Events for North Wind direction and for the time period 2000-2100

Storm Class	Significant Wave Height [m]	Peak Period [s]	Energy [m² h]	Duration [h]	Events

	max	mean	min	max	mean	min	max	mean	mean	
I	4.28	2.29	3.97	9.66	7.41	36.12	273.25	126.91	22.91	877
II	2.87	2.41	7.12	8.52	7.77	281.80	451.11	366.46	61.50	2
III	5.92	2.89	4.51	11.12	7.98	522.81	1026.32	716.39	79.25	127
IV	6.76	3.25	5.06	11.07	8.23	1076.35	2188.10	1362.44	118.37	35
V	7.68	3.77	6.62	11.30	8.61	2868.74	3865.89	3367.31	211.50	2

Table 0-5: Classification of Storm Events for Northeast Wind direction and for the time period 2000-2100

Storm Class	Significant Wave Height [m]		Peak Period [s]			Energy [m² h]			Duration [h]	Events
	max	mean	min	max	mean	min	max	mean	mean	
I	2.47	2.16	6.47	7.57	7.17	53.74	94.97	72.67	15.00	4
II	2.99	2.30	5.47	8.08	7.27	131.00	201.65	162.91	29.53	32
III	3.68	2.52	5.50	8.98	7.47	209.09	359.70	271.12	40.24	29
IV	3.98	2.69	5.80	8.95	7.62	378.86	598.96	464.12	60.35	17
V	4.62	2.93	5.21	9.26	7.77	670.08	883.05	747.09	80.25	4

Table 0-6: Classification of Storm Events for Northwest Wind direction and for the time period 2000-2100

Storm Class	Significant Wave Height [m]		Peak Period [s]			Energy [m² h]			Duration [h]	Events
	max	mean	min	max	mean	min	max	mean	mean	
I	3.27	2.14	4.32	9.26	7.25	35.67	73.57	52.56	10.76	41
II	3.86	2.30	4.95	10.67	7.65	78.64	119.10	98.12	17.18	22
III	4.34	2.40	4.66	10.87	7.89	123.50	173.22	146.55	23.55	20
IV	3.78	2.57	4.11	9.70	8.06	187.30	336.04	234.80	33.43	14
V	3.66	2.90	8.89	9.12	8.89	530.33	530.33	530.33	60.00	21

Results of estimation of Hs with Extreme Value Theory are being provided below:

Table 0-7: The significant wave height and the peak spectral period for each direction

Direction	F_{eff} [m]	t_d [s]	U_{10} [m/s]	H_s [m]	T_p [s]
NE	150208	46043	19.10	4.08	8.03
N	176593	90508	19.10	4.33	8.28
NW	113795	23967	19.10	3.57	7.49

Table 0-8: Return level estimations applying the GEV distribution.

Return level [years]	H_s [m]	T_p [s]
25	5.13	8.98
50	5.21	9.06

Table 0-9: Different scenarios for deep water waves

Wave Scenarios	H_s [m]	T_p [s]	Method Description
1	4.33	8.28	SMB
2	5.13	8.98	Extreme Value (25 years)
3	5.21	9.06	Extreme Value (50 years)

Table 0-10: Results xbeach for the most vulnerable profiles in common

Profile	Storm scenario 1-N direction		Storm scenario 2-N direction	
	maxRu (m)	**Inland distance flooding (m)**	**maxRu (m)**	**Inland distance flooding (m)**
1	1.1	125	2	140
6	1.2	40	2.3	45
10	1.6	35	1.8	115
12	2.1	35	2.3	50
	Storm scenario 3-NW direction		**Storm scenario 4-NE direction**	
Profile	**maxRu (m)**	**Inland distance flooding (m)**	**maxRu (m)**	**Inland distance flooding (m)**
1	0.9	15	3.5	160
6	0.8	30	2.3	60
10	0.7	25	2.8	165
12	0.8	25	4.2	145

Table 0-11: Distinguished storm events for the coastal simulations

Date and time	Wave height (m)	Period (s)	Direction	Duration (h)
27/01/1961 19:00	2.01-4.61	6.71-9.28	North	104
12/02/1960 00:00	4.59-5.61	9.27-10.72	North	44
01/03/2027 03:00	2.46-4.95	7.84-9.53	North	72
01/11/2020 21:00	2.07-2.65	6.78-8.95	Northeast	24
12/01/2005 12:00	2.43-3.03	7.41-8.16	Northwest	39

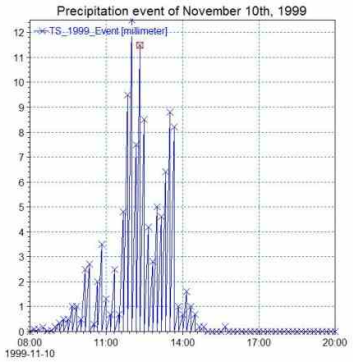

Figure A-0-1: Time series of simulated precipitation event of November 10th, 1999

Annex 2 of Rethymno case study

In the current annex, the modular structure of the Vulnerability Framework applied in Rethymno is being displayed in the following pictures (Figure A2-0-1, Figure 0-2, Figure 0-3), along with the indicators used for the calculation of each component of vulnerability and their weighting.

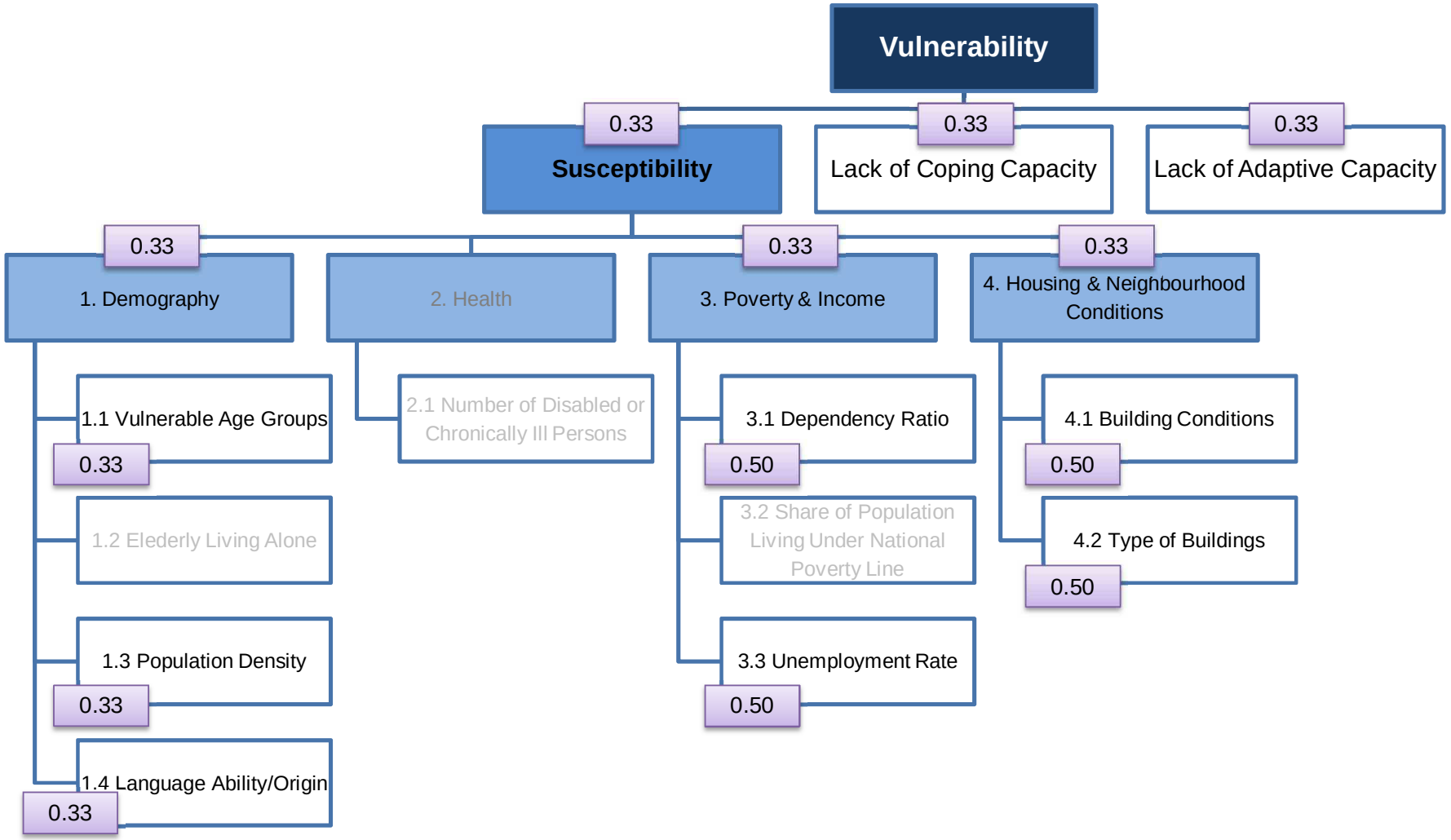

Figure A2-0-1 Modular structure of the Vulnerability Framework, indicators used for susceptibility calculation and their weighting (adopted from report of the PEARL Vulnerability Framework)

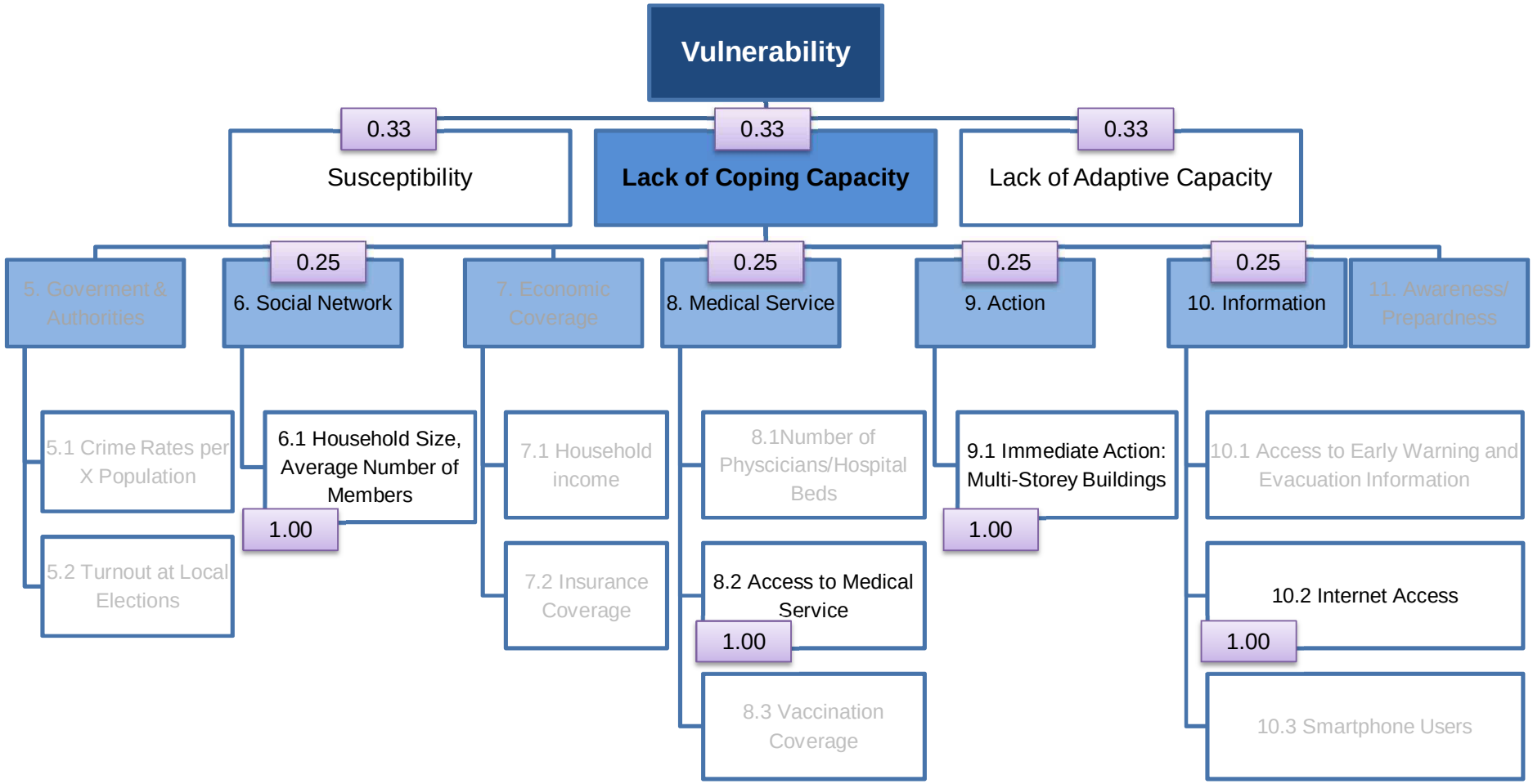

Figure 0-2: Modular structure of the Vulnerability Framework, indicators used for lack of coping capacity calculation and their weighting (adopted from report)

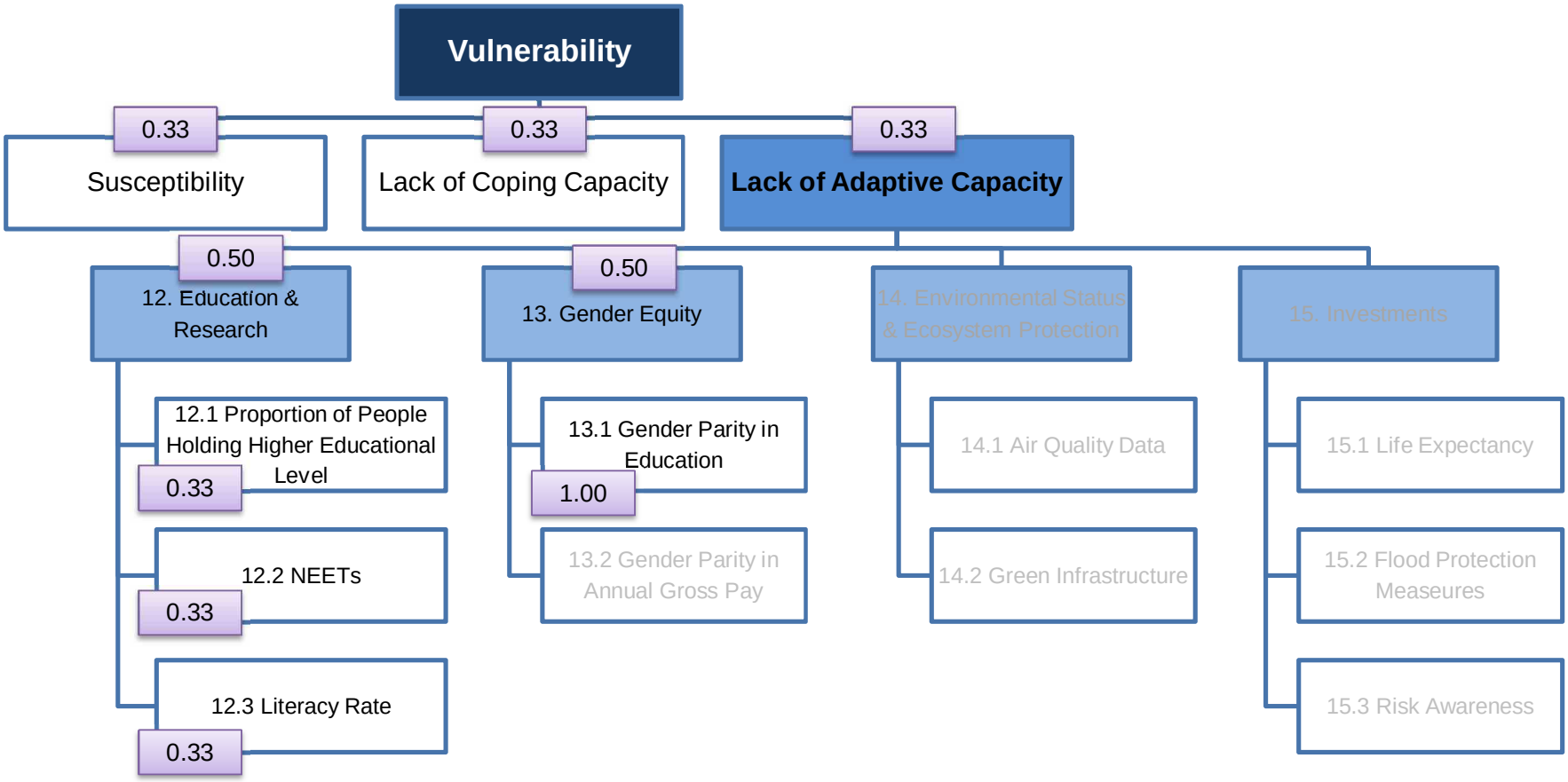

Figure 0-3: Modular structure of the Vulnerability Framework, indicators used for lack of adaptive capacity calculation and their weighting (adopted from report)

7 Case Study Chantellailon-Plage, France

7.1 Description of the study area

The two cities of the Charente-Maritime department, ñLes Boucholeursò is a district of Châtelaillon-Plage located on the limit of Yves. District count approximately 600 houses and have an important activity in oyster and mussel farming.

Figure 7-1: Initial case study area Les Boucholeurs, Chantellailon-Plage, France

The Atlantic coast is threatened by storm surges and potentially by the sea level rise. Those events could contribute to the failure mechanisms of the embankments and could generate some important water level on the rear part of this area, which is lower that the coast line itself.
This was the case on 27th-28th February 2010, when Xynthia Storm reaches the French Atlantic coast. The Charente-Maritime department was highly affected by this events which generated ú 1,4 billions of damages and 53 fatalities in France (2 on the site ñLes Boucholeursò). After this event, in the hurry, the place ñLes Boucholeursò was designed as one of the mainñBlack Areaò where all the houses should be destroyed. This impacted local community a lot due to their farming activities and living places.

Further discussions as well as strong participation of local stakeholders changed the marking ñBlack Areaò into ñOrange or Yellow Areaò. Currently the new strategy for this area is created. This relates to reconstruction on the embankment system. After this event, a large plan of protection measures was launched with some structural works: creation of breakwater, reinforcement of dikes, etc.

At the beginning of the project, the protection plan is ongoing but not all the protection measures were achieved.

One of the main challenges of the project is to help stakeholders to quantify the effects of the protection plan and allow some preliminary reflexions about the future measures which could be interesting to implement in the future to increase the resilience of the city. IN addition the case study area is enlarged to the whole city Châtelaillon-Plage.

7.2 Data collection and analysis for hazard asssessment

Xynthia modelling is done using TELEMAC software. For this case study, the initial situation is the situation before Xynthia event. The main data collected to build the coastal flooding model are:

- The bathymetry of the Atlantic coast taken from some existing models in this area
- The topography of the landside comes from a LIDAR survey made
- The dike profile along the coast line
- The location of breaches during the Xynthia event.
-

Artelia use the modelling tools TELEMAC-2D and TOMAWAC to study the coastal submersions.
TOMAWAC, software which belongs to the TELEMAC chain, calculates the swell, the waves resulting in a sea level overvalue.

TELEMAC-2D is a two dimensional hydrodynamic model which solves the Shallow Water Equations (also named Saint-Venant equations) with the Finite Element Method (FEM) or the Finite Volume Method (FVM). A computation mesh (not necessarily uniform) of triangular elements allows the refinement on the sensitive area of the study in order to obtain more precise results. TELEMAC-2D is applied for river and maritime hydraulics.

Moreover, several phenomena can be simulated with this software such as: the propagation of long waves, taking into account non-linear effects, the influence of Coriolis force, of meteorological factors: atmospheric pressure and wind, turbulence, dry areas in the computational domain: intertidal flats and flood plains, treatment of singular points: sills, dikes, pipes, é ..
TELEMAC can handle the modelling from few square kilometres (very local and local scale) to several square kilometres (regional scale).

The model of coastal submersion simulation is built on a grid and the calculation is done on every points of the mesh. At a regional scale the aim is to see if the coast will be submerged and the global impacts. Then, there is no need to implement in the model all the complexities of the reality such as buildings.

The following figure represents the mesh used for the Xynthia simulation. The cell size depends on the details wanted in the results. Thus, the number of calculation points increases in city localization.

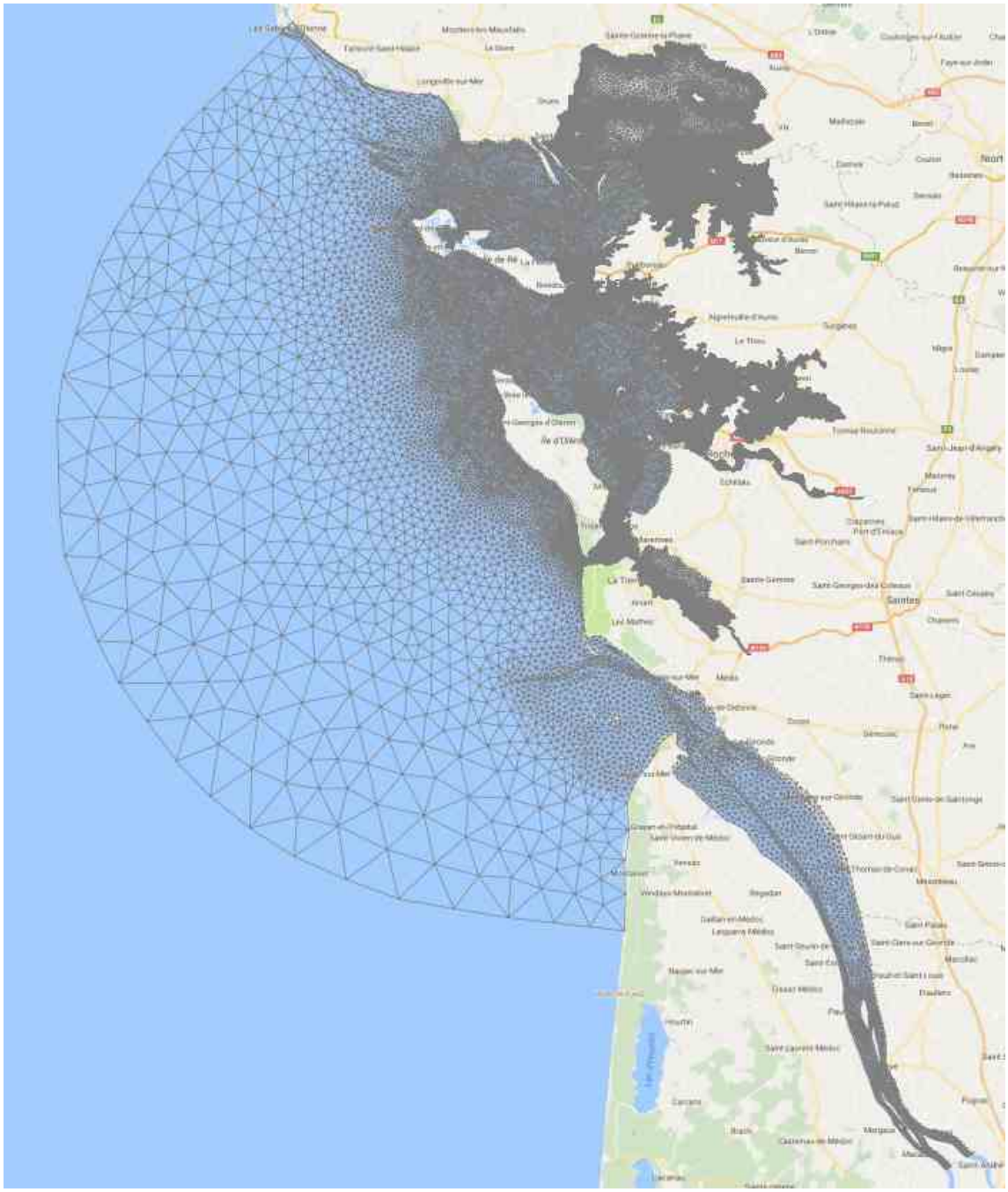

Figure 7-2: Developed mash for simulation of Xynthia event, Chantellailon-Plage, France

However, the change in scale in the model will influence the mesh. Indeed, if the studied area is focused on a very local part (e.g. Les Boucholeurs) as in the following figure, it becomes important to take into account all the infrastructures such as roads, culverts, buildings etc. to recreate realistic flows. Thus, the calculation around these elements needs to be more precise. It is conveyed by more points of calculation carefully placed in these areas.

Figure 7-3: Developed mash over the infrastructure and roads, for Xynthia event, Chantellailon-Plage, France

The calibration and validation event on this area is the Xynthia storm. This is the most important recent event here. In 1999, another large storm event reached France but due to a different wind direction, the most impacted area was located on the Gironde estuary.
The following figures present comparison at the tide gauges of La Rochelle - La Pallice, Rochefort, Le Verdon, La Cotinière and Royan, between the records during this storm and the results of model integrating the astronomical tide and the influences of the surge offshore, the wind and the swell. The theoretical tidal obtained with the 2D on the same period model is also draw to illustrate the importance of surges generated at the coast for the hydro meteorological parameters associated with this storm.

It appears from the analysis of these charts the following remarks:

- The evolution of water observed in tide of La Rochelle - La Pallice is very well represented by the model. There is a slight shift in the flow before the peak of the event,
- The model underestimated the level of the peak to the tide of Rochefort. The phase observed for the tide is similar to that observed for the astronomical tide,
- The tide gauge of Le Verdon is not exploitable for the peak of the Xynthia event. The exploitable period of the registration shows the good representation of the evolution of the water for the model,

- For the tide of La Cotinière model underestimated about 25 cm the maximum water level observed in the storm Xynthia. A temporal shift is also observed for this tide,
- Data of Royan tide gauge is not consistent with data of Le Verdon, despite a near location on banks of the Gironde estuary.
-

Despite the low number of exploitable data, the model allows to precisely represent the maximum water level measured at the tide of La Rochelle - La Pallice. Outside the main study area, the model correctly represents the evolution of the water level, without offering such high level of precision.

On the study area, the model represents accurately the influence of the hydro meteorological parameters on the evolution of the water level (on maritime side).

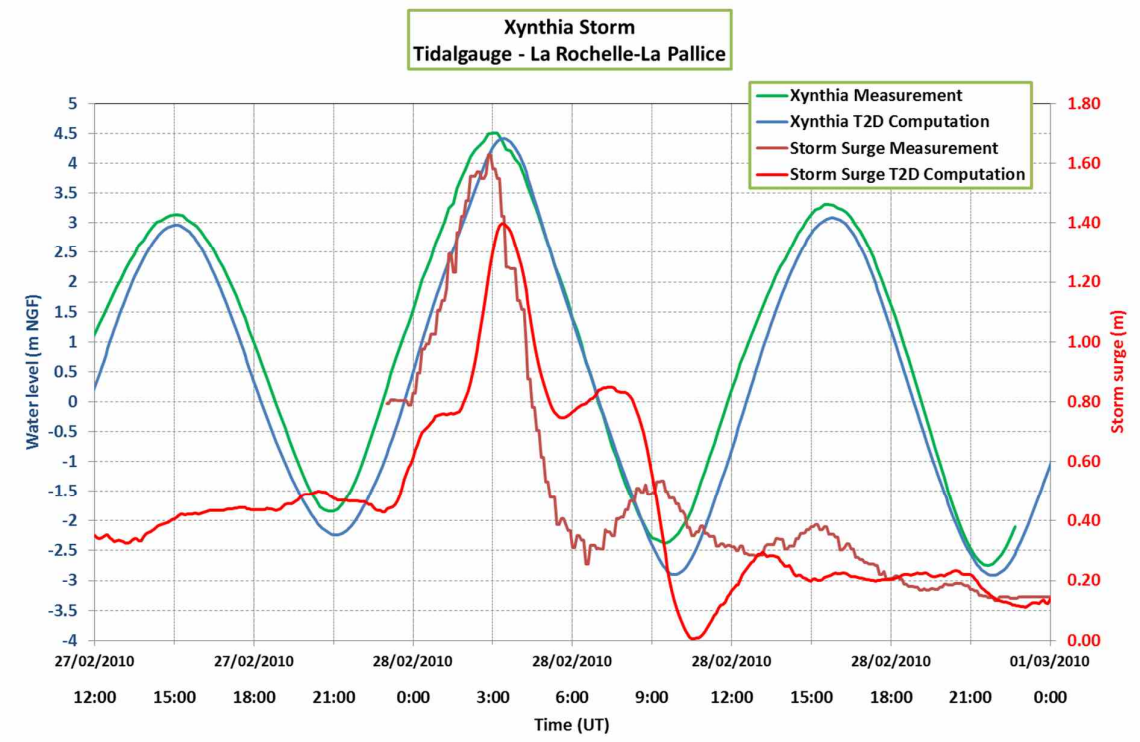

Figure 7-4: Tidal gauge la Rochele - La Pallice, France

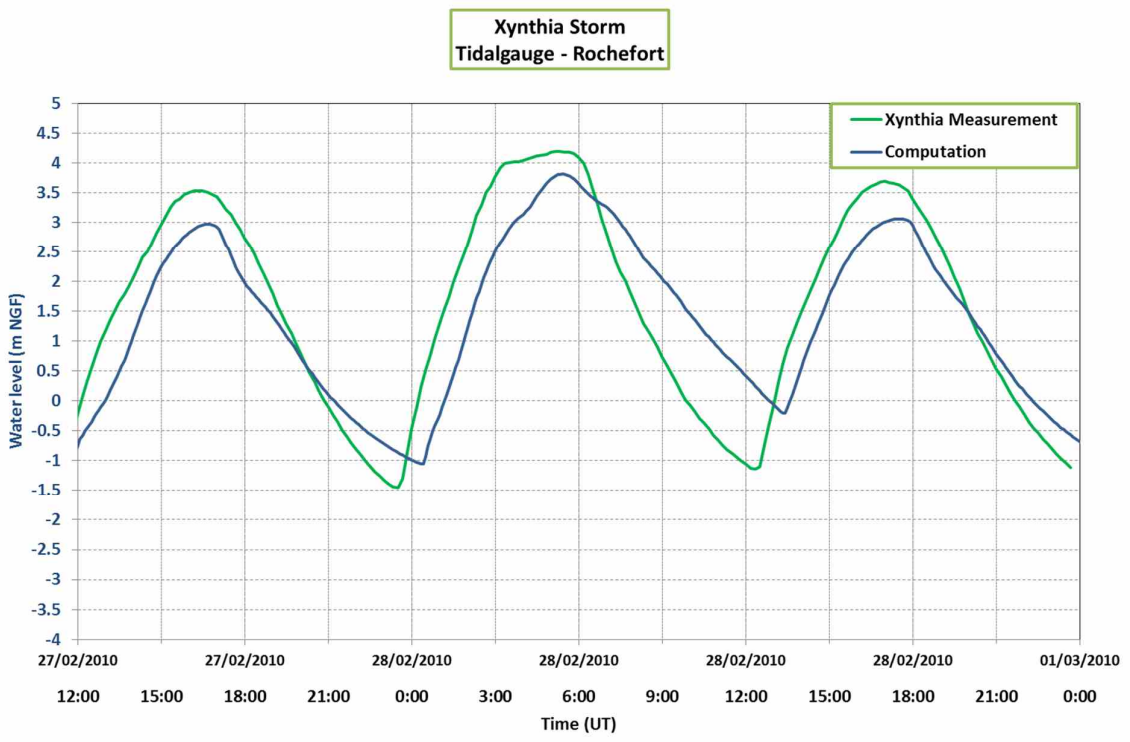

Figure 7-5: Tidal gauge Rochefort, France

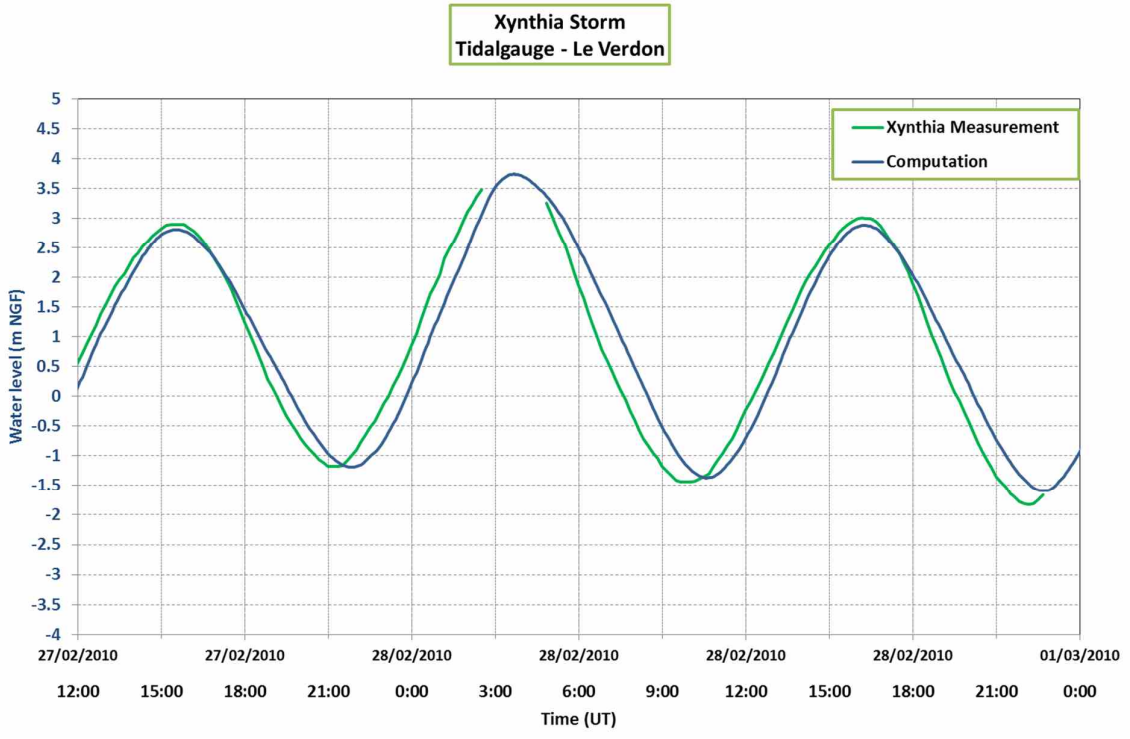

Figure 7-6: Tidal gauge Le Verdon, France

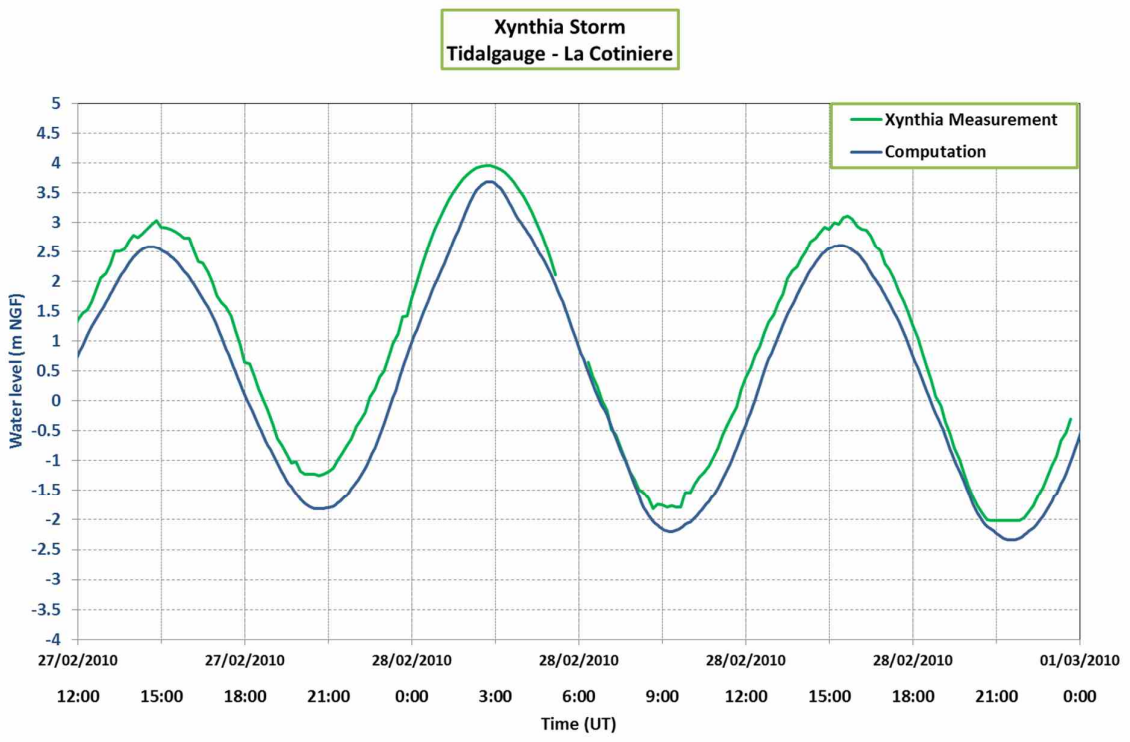

Figure 7-7: Tidal gauge La Cotiniere, France

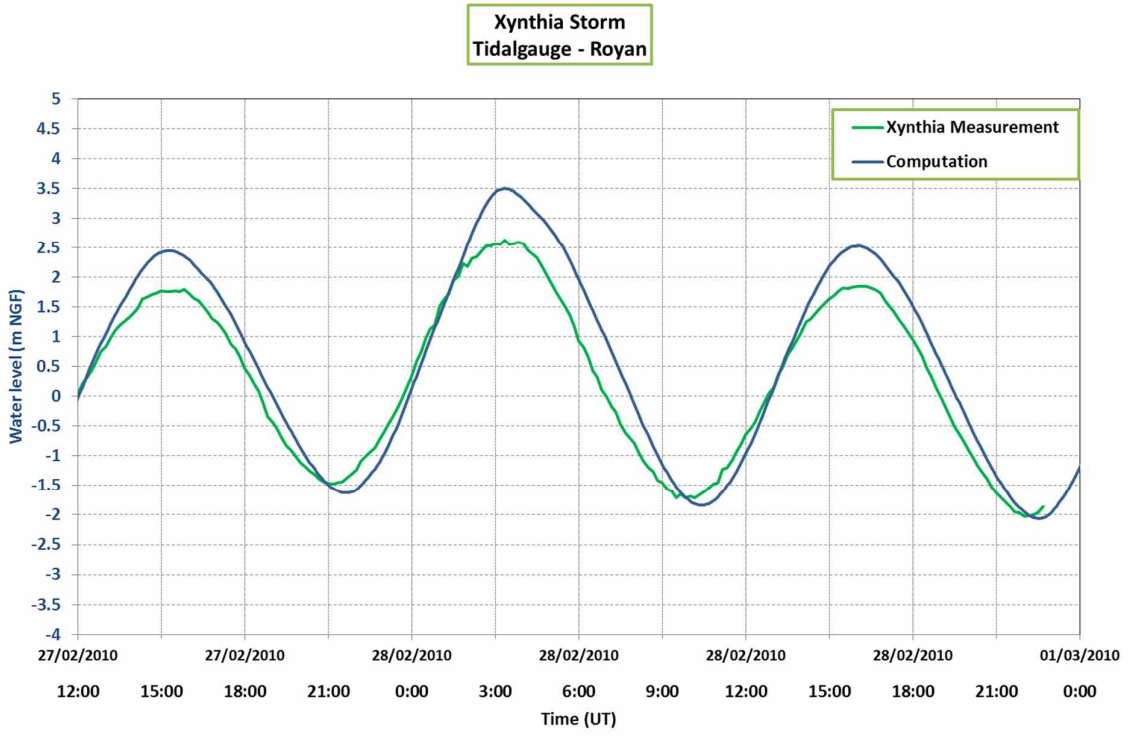

Figure 7-8: Tidal gauge Royan, France

The calibration of the model in the land behind the dikes, for Xynthia storm, is made by spatial comparison between the results of computation and:

- The limit of the area inundated or submerged determined in a previous study[8].
- The water marks identified in the same study,
-

For this analysis of the representation, by the model, of flows on the land part, the configuration of protection has been modified from that currently observed. The level of protections has been puts at their level before Xynthia, on Charon and Yves sectors. Indeed, on these sectors, protections have been reconstructed with a higher level after the storm.

To properly represent the water volumes on the land part, ruptures and destruction of protection works have also been integrated in the model. These failures have been defined on the basis of the study.

The outline of the flooded areas is well represented by the model as it could be seen on the following figures for La Rochelle and Chatelaillon-Les Boucholeurs

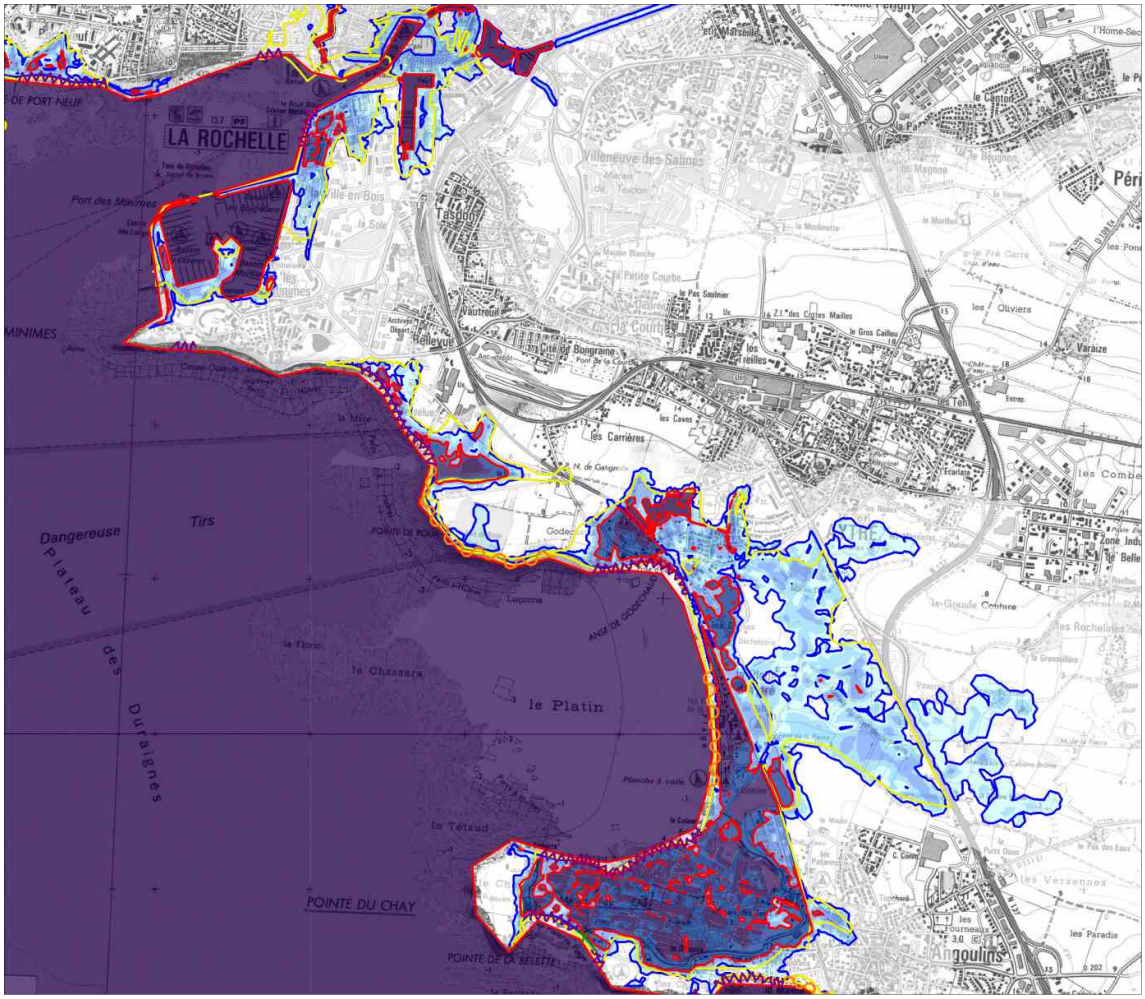

[8]Eléments de mémoiresur la tempêteXynthia du 27 et 28 Février 2010 en CharenteMaritime, Rapport d'étude Artelia pour la DirectionDépartementale de Territoires et de la Mer de la Charente-Maritime, Aout 2010, unpublished

Figure 7-9: Resulting flood map for Xynthia event, France

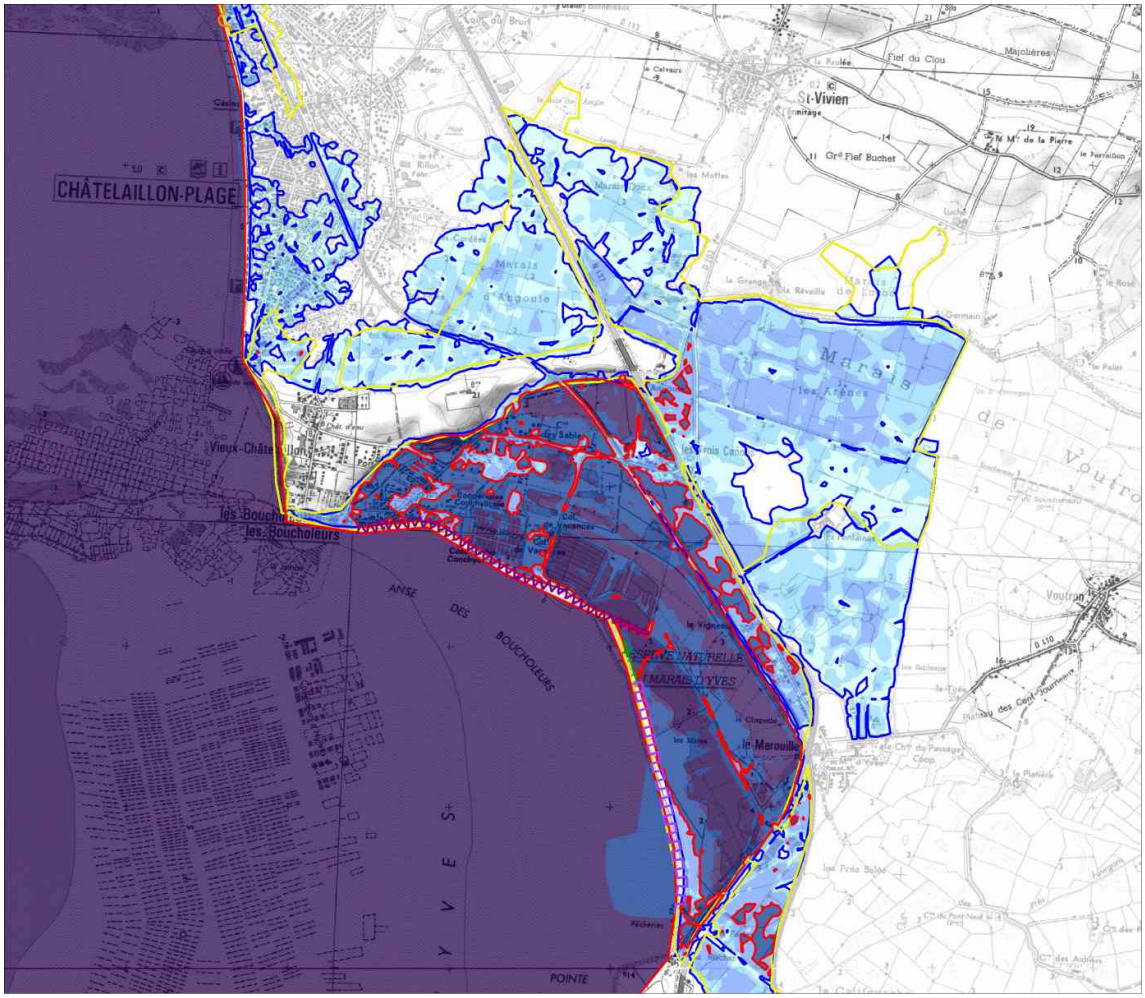

Figure 7-10: Resulting flood map for Xynthia event, Chantellailon-Plage, France

And finally, the following table presents, by communal territory, a summary of the differences between the observations and the results of the modelling.

At the end, more than 400 watermarks were able to face the results of the model on the study area. Despite the great disparity of information, the model provides a mean absolute deviation about 25 cm from the observations on this area.

The model correctly represents the maximum water levels on all the study area.
We could note that on the low areas behind the protections, the time of failure is an important control for the dynamic of filling and by consequence for the maximum water level observed.

Table 7-1: Watermarks used for model calibration

Cities	Water marks				
	Total number	***Number used***	***%***	***Mean deviation***	***Absolute mean deviation***
Andilly	2	2	100	-0.03	0.24
Angoulins	33	32	97	0.09	0.13
Aytré	44	43	98	0.04	0.20
Charron	35	35	100	-0.01	0.22
Châtelaillon	64	54	84	-0.17	0.23
Esnandes	26	26	100	0.15	0.21
La Rochelle	111	86	77	-0.43	0.52
L'houmeau	18	17	94	-0.14	0.16
Marans	7	6	86	-0.02	0.17
Marsilly	18	17	94	-0.06	0.22
Nieul	37	35	95	0.03	0.16
Saint Ouen d'aunis	1	1	100	0.00	0.00
Villedoux	2	2	100	-0.04	0.04
Yves	53	53	100	-0.03	0.16
Total	**451**	**409**	**91**	**-0.11**	**0.26**

For the exploitation of the model, an event similar to Xynthia but with an increase of the mean sea level of 20cm will be considered. This event which is designed to take in account the effect of the climate change is now used as the reference event for local marine submersion studies.
We used 3 different configuration of the protection system:

- The actual situation with all the already planned protection system
- The same situation with some potential breaches in the protection system. This event is the legal event.
- The situation before Xynthia

7.3 Data collection and analysis for vulnerability asssessment

Data used for vulnerability assessment is taken from National Institute for Statistics and Economy studies (INSEE). While creating the framework for vulnerability the data availability is crucial. The framework for vulnerability is defined in order to have vulnerability mapping in Esri software. Based on available information about buildings following attributes are available:

- Building type - urban function
- Building height

Vulnerability assessment takes into account *population vulnerability, socio-economic vulnerability and vulnerability of build environment*. This was chosen in order to have possibility to have spatial representation of results. Each vulnerability parameter has associated impact element.
Impact elements taken into account for population vulnerability (PV) are:

- PV_1 - population density,
- PV_2 - number of children, senior citizens, invalids,
- PV_3 - gender and

- PV_4 - mean income

Based on requirement we obtained data from INSEE in the form of tables. For this analysis impact elements or weights are defined arbitrary. Calculation of population vulnerability based on available data is done using relation below.

$$PV = w_1 PV_1 + w_2 PV_2 + w_3 PV_3 + w_4 PV_4$$

Where values for the weights are:

- w_1=0.25
- w_2=0.15
- w_3=0.25
- w_4=0.35

$$PV = 0.25 PV_1 + 0.15 PV_2 + 0.25 PV_3 + 0.35 PV_4$$

Calculated value for population vulnerability is 4.8. Since we did not used population data available for each building this value will be assigned to overall vulnerability.

Socio-economic vulnerability (SE)

Disasters affect assets through direct damages and the flow for the production through indirect damages. Hence, the socio-economic dimension suffers from both direct and indirect losses. Since we want to have vulnerability mapped only direct losses will be considered for this analysis. Predefined vulnerability levels are form 1 to 5 where level 5 corresponds to high vulnerability and level 1 to very low vulnerability. The different vulnerabilities are assigned to existing urban functions. The values are presented in the tale below.

Table 7-2: Assigned vulnerability levels for urban function mapped for case study

Urban functions		Vulnerability level
1	Housing	5
2	Education	4
3	Food	4
4	Working	5
5	Safety	5
6	Leisure	2
7	Religion	2
8	Health	5
9	transportation	4
10	railway	3
11	mixte	5

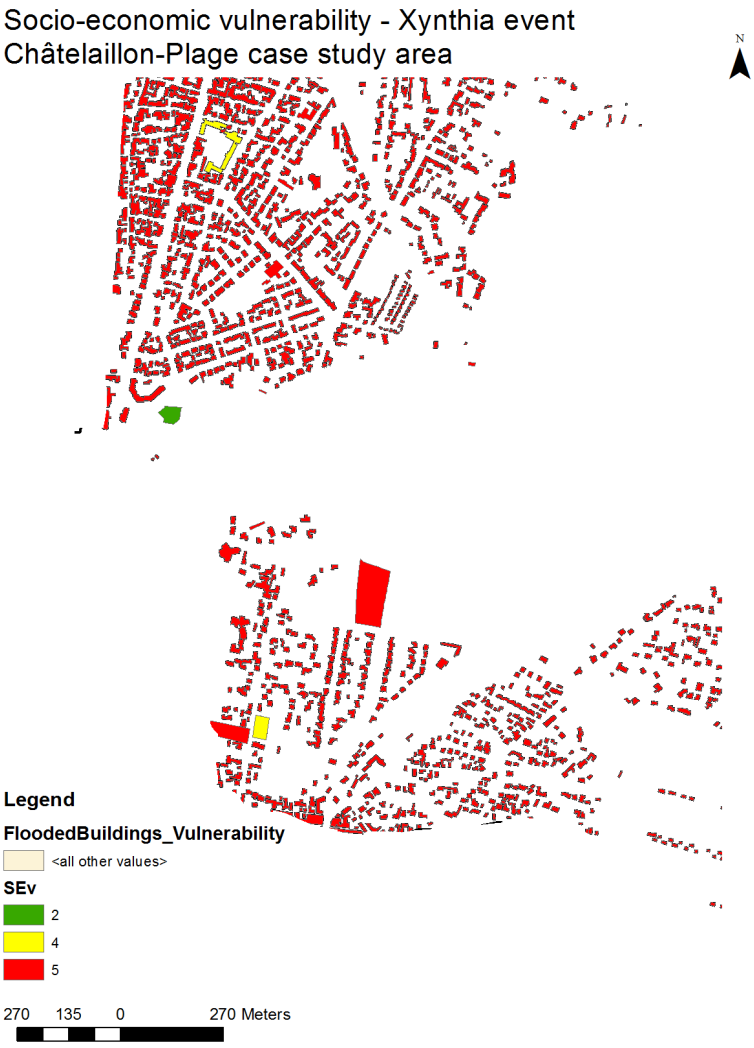

Figure 7-11: Socio-economic vulnerability mapped, for Xynthia event, Chantellailon-Plage, France

Overall vulnerability is presented with the relation below

$$V = V_{SE} + V_{PH}$$

Following this the vulnerability is calculated for each building in the case study area. The maps below show vulnerability mapping for the Xynthia event in Chantellailon-Plage.

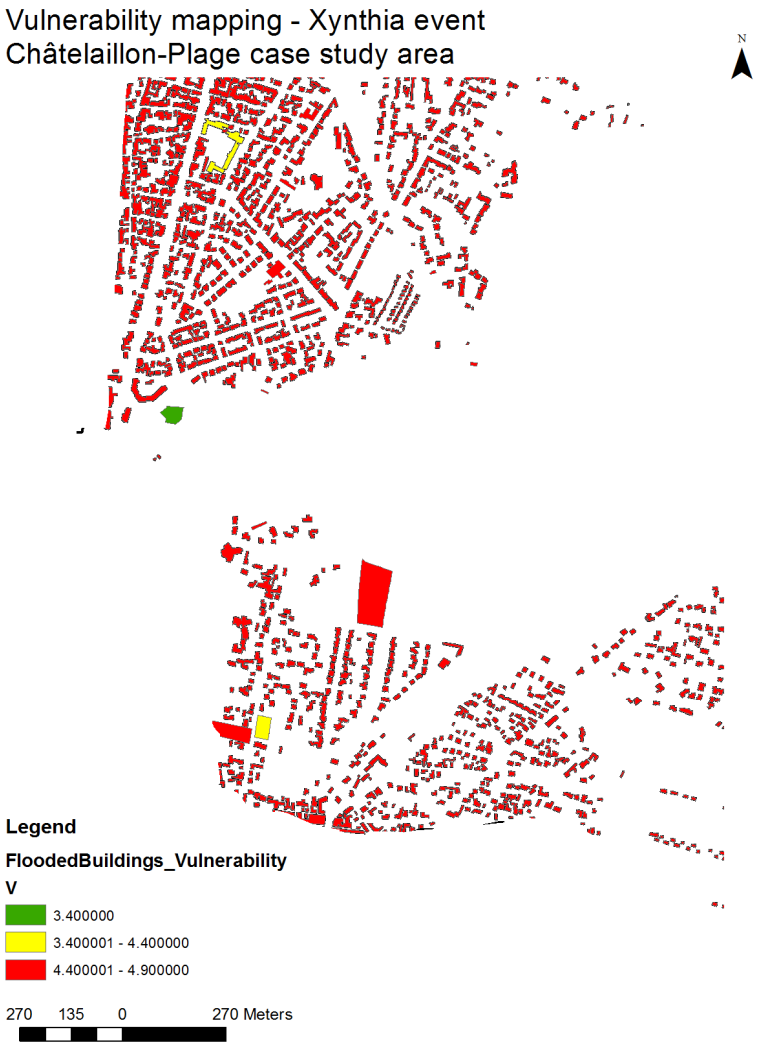

Figure 7-12: Vulnerability mapping for Xynthia event, Chantellailon-Plage, France

Hazard mapping

Based on different flood depth the following classes are defined and the case study area is covered.

Table 7-3: Defined zones for hazard mapping

Flood depth	Vulnerability level	
0	1	Zone 1
0.2	2	Zone 2
0.5	3	Zone 3
1	4	Zone 4
5	5	Zone 5

Figure 7-13: Hazard mapping (zoning) for Xynthia event, Chantellailon-Plage, France

7.4 Risk assessment

Numeric value of risk is calculated as a product between vulnerability and hazard and divided by five.

$$R = \frac{V \times H}{5}$$

R is representing risk with the value range from 1 to 5 where 5 is high risk and value 1 is low risk.

Figure 7-14: Risk map of cases tudy area for Xynthia event, Chantellailon-Plage, France

In addition the direct damages are calculated for each building with respect to existing hazard mapping. Based on available data the following parameters are needed.

- calculated area for each building
- flooded building classified
- depth damage curves
-

Flooded building are classified in GIS software are presented as layer. Depth damage curves are used from CORFU project. These curves are developed based on research with respect to different depth and different urban functions. Depth damage curves (figure below) are also adapted to the rearranged land use. Since the land use is represented through different urban functions, therefore the created depth-damage functions are following the same procedure.

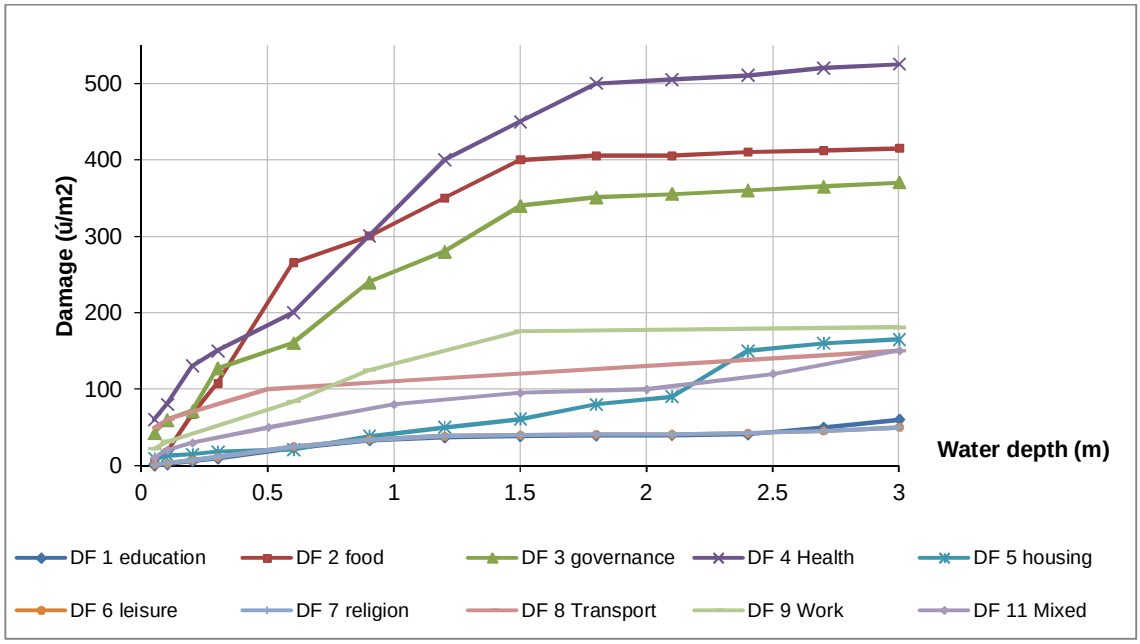

Figure 7-15: DDC applied for direct damage assessment for Xynthia event, Chantellailon-Plage, France

Direct damages are calculated in GIS evaluating the damage expressed in Euros per building. Three scenarios are applied for different flood maps.

Table 7-4: Different scenarios for direct damage assessment for Xynthia event, Chantellailon-Plage, France

Scenario 1	Xynthia	Xynthia	event
Scenario 2	X20_2016_ssBreches_classesH	Xynthia + 20cm	just overtopping possible
Scenario 3	X20_2016_PPR_classesH	Xynthia + 20cm (PPR)	with braches based on the rulles within PPR

Based on the calculations following results show that for scenario 1 1346 buildings are flooded with total direct damage of ú14,974,616.91.

Table 7-5: Direct damages for Scenario 1

Urban Function	Number	Total Damage (Euro)
Education	2	€ 60,567.44
Food	3	€ 705,871.11
Governance	1	€ 36,293.48
Health	0	€ -
Housing	1315	€ 12,948,886.09
Leisure	2	€ 45,647.40
Religion	0	€ -

Transport	0	€ -
Working	9	€ 257,268.28
Mixed	14	€ 920,083.11
Sum	1346	€ 14,974,616.91

For scenario 2 1553 buildings are flooded with total direct damage of €10,693,836.89.

Table 7-6: Direct damages for Scenario 2

UF	Number	Total Damage (Euro)
Education	2	€ 60,567.44
Food	2	€ 453,626.34
Governance	1	€ 36,293.48
Health	0	€ -
Housing	1513	€ 8,789,795.58
Leisure	2	€ 56,943.22
Religion	1	€ 5,010.28
Transport	1	€ 34,862.60
Working	18	€ 588,899.61
Mixed	13	€ 667,838.35
Sum	1553	€ 10,693,836.89

Within scenario 3 have 1722 flooded buildings with total direct damage of ú 21,311,024.79.

Table 7-7: Direct damage for Scenario 3

UF	Number	Total Damage (Euro)
Education	2	€ 94,941.18
Food	3	€ 705,871.11
Governance	5	€ 317,389.19
Health	0	€ -
Housing	1660	€ 17,795,886.84
Leisure	2	€ 56,943.22
Religion	1	€ 5,010.28
Transport	1	€ 34,862.60
Working	34	€ 1,380,037.26
Mixed	14	€ 920,083.11
Sum	1722	€ 21,311,024.79

Mapping of direct damages for different scenarios is done within GIS.

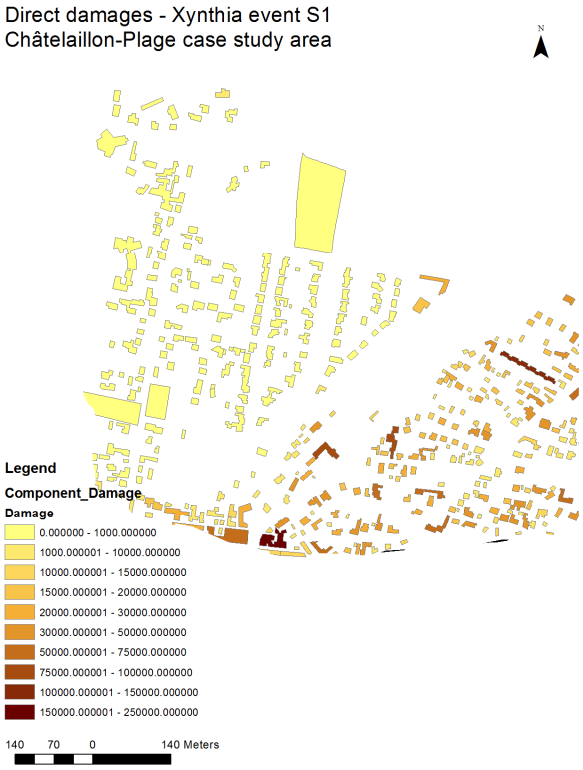

Figure 7-16: Direct damages mapped for S1, Xynthia event, Chantellailon-Plage, France

Figure 7-17: Direct damages mapped for S2, Xynthia event, Chantellailon-Plage, France

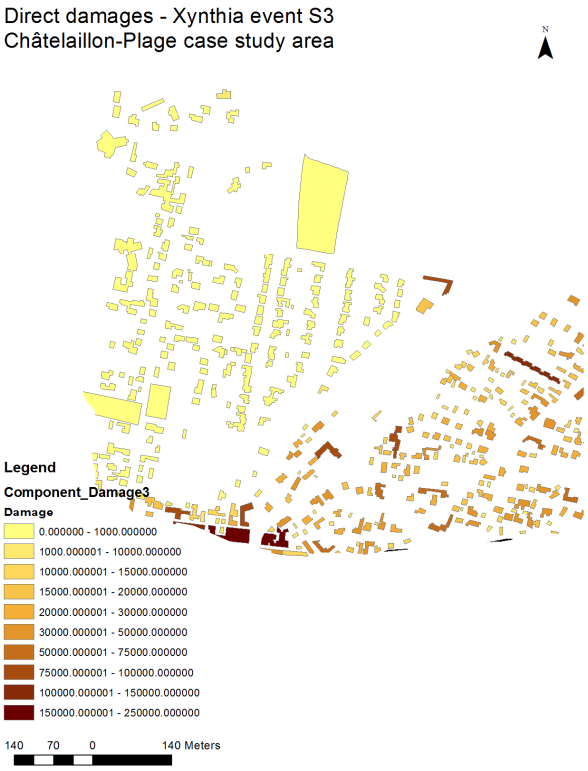

Figure 7-18: Direct damages mapped for S3, Xynthia event, Chantellailon-Plage, France

7.5 How risk analysis benefit local stakeholders

Work done by now is presenting our analysis regarding flood modelling, direct damage, vulnerability, risk and resilience assessment, where mapping within GIS is arranged to enchase communication between key stakeholders. In the experience gained during meeting with the stakeholders in the case study area the maps present very good way of presentation. In this way we are able to show on the map each building in the case study with calculated direct damage based on the flood map and available depth damage curves. Also for each building the vulnerability, risk and resilience level is evaluated. This helps a lot in the communication with stakeholders and as a part of decision making process.

8 Case Study Taiwan

8.1 Description of the study area

Taiwan, located at the central west of Pacific Ocean, has coastline of 1600 km and 23 million populations. The location is within one of the typhoon-prone area in the world. There are 3.5 typhoons approaching Taiwan in an annual average and the number of typhoons per year is increasing to 5.5 in the recent decade. Typhoons bring strong wind, extreme waves, high water level (storm surge) and heavy rain. These phenomena increase risks for the coastal area. According to records, the maximum hourly precipitation reached 300 mm, and the maximum one-day precipitation reached 1748 mm, which is 93.4% of the world record. Extreme wave which has wave height of 23.9 m was also measured during typhoon Krosa (2001) and a storm surge caused by typhoon Chebi (2001) reached 0.94 m. Due to the combined effect of extreme precipitation, river characteristics and topography of Taiwan, coastal flooding becomes one of the main nature hazards of Taiwan. The Water Resources Agency (WRA) of Taiwan reported that approximately 3000 buildings are damaged by floods annually, with an associated loss of approximately 400 million USD, which is approximately 4.6 times more than the loss caused by fire damage in Taiwan. In addition to extreme precipitation during typhoons, the river characteristics and topography of Taiwan are important factors that lead to flooding. The rivers in Taiwan are short and have steep slopes that exceed 1/100 in upstream reaches and 1/200~1/500 in downstream reaches. Concentrated rainfall in short and steep river basins generates rapid flow increases and flow peaks.

Tainan coast is the study area. Located at south-western of Taiwan, Tainan city is bordered by the Taiwan Strait to the west (Figure 1). It is the oldest city with more than 80% of the population lives near the coast. In 2016, Tainan City had a population of 1.9 million in its 37 districts. The total area of Tainan is 2200 km^2, with an average population density of 860 residents/km^2. However, the population density in the Tainan urban area is 4500 residents/km^2. Tainan has frequently flooded in the past. The floods that occurred in Tainan City were generally induced by multiple factors, including rainfall which exceeds the drainage system capacity, a poor condition of the drainage system, flood defense failure, rising sea level due to high tides and/or storm surges, and urbanization. According to historical records, several typhoons, such as Morakot in 2009 and Kongrey in 2013, have hit Taiwan. These typhoons were accompanied by abundant rainfall that caused serious damage, especially in Tainan. More than 300 projects have been implemented in Tainan City to prevent flooding over the past 10 years, but these projects have not solved the problem. Tainan City is selected as the study area not only because of its significant urban development but also because rainfall is the dominant factor that influences flooding.

Six rivers run through Tainan: the Bajhang River, Jishui River, Jiangjun River, Tsengwen River, Yanshui River and Erren River (from north to south). Midwestern Tainan is an alluvial plain of the Yanshui River and Tsengwen River, with a few hills and mountains distributed in the east. The only river that runs through the urban area of Tainan is the Yanshui River, with a length of 41.3 km and a watershed area of 340 km^2. The coastline of Tainan City is 63.7 km.

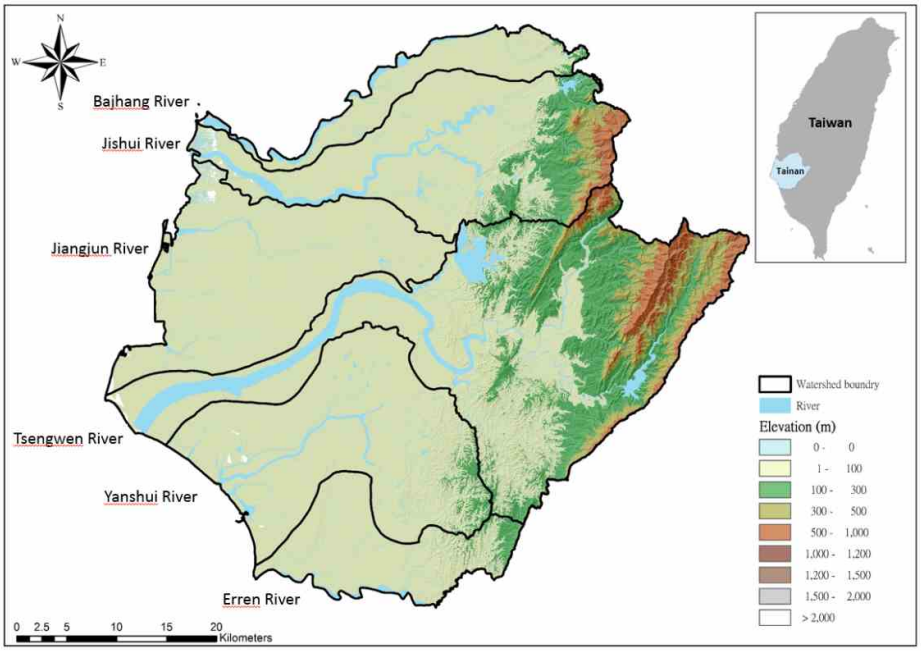

Figure 8-1 Location, river distribution and topography of Tainan City, Taiwan.

8.2 Data collection and analysis for hazard assessment

Flooding in urban areas has become a growing priority for city managers and disaster risk prevention agencies, and those communities that are situated in the coastal zone are further threatened by storm surges and rising sea levels. Tainan city used to flood frequently, therefore flood prediction, prevention, and mitigation are essential and a construction of flood inundation map (FIM) is beneficial for the purpose. Such maps offer valuable means to enhance our understanding of local flood risks.

8.2.1 *Data*

Large amount of different data were used for constructing a FIM. The lack of adequate flood observations during flooding events represents a great challenge in producing reliable flood models. Development of a FIM needs geographical and hydrological data as well as historical records, operating rules of sluices and reservoirs and reports of regulation projects, as shown in Table 1.

Table 8-1. List of data required for development of a flood inundation map.

Geography	Hydrology	Others
• DEM	• Rainfall	• Historical flooded extent and depth
• Aerial image	• Discharge	• Operating rules
• River/drainage cross section	• Water level	• Regulation reports
• Reservoir	• Tide level	
• Hydraulic structures	• Wave	
• Sewer system		
• Coastal dyke		
• Sea bathymetry		
• Land use condition		

The digital elevation model (DEM) is generated by LIDAR with spatial resolutions 40 x 40 m for hillside fields and 5 x 5 m for low-lying areas. River cross-sectional shape includes all six rivers in Tainan with interval of 300 m in non-urban areas and of 20 m in urban areas. Data of hydraulic structures and instruments including 4335 rainwater drains (open channel) and 4335 underground rainwater sewer system were collected. These data include shapes and elevations of the systems as well as locations and lengths. Other structures or hydraulic instruments including 1206 sluice gates, 955 bridges, 81 river dykes, 13 reservoirs, 38 ponds or detention basins, 380 pumping stations are also included (see Figure 2).

Moreover, satellite and aerial images are also used to divide or adjust the sub-watersheds, which were defined according to rainwater drainage or sewer systems. Land use conditions were collected to identify the land roughness and derive the flow behaviour. More than 45% of the land in Tainan city is used for agriculture and only 35% of Tainan City comprises villages or urban areas. Rainfall records from 37 rainfall stations that have recorded hourly rainfall for more than 20 years were used. The river level and discharge data are mainly used for calibration of the 1D hydrodynamic model. Tidal data are used for a storm surge analysis and as the downstream boundary of the river in the 1D hydrodynamic simulation. Wave data (height, period, and direction) and 200 m resolution bathymetry data are used for the run-up analysis together, especially during the typhoon period. Finally, data from historical flood events, including flood depths and flood extents, over the past 10 years were collected for model calibration and validation purposes.

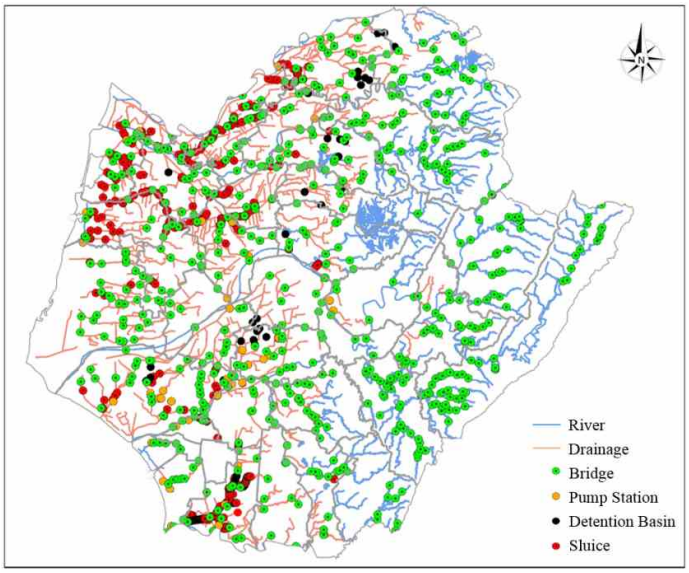

Figure 8-2 Network of river, drainage and hydraulic structures in Tainan City, Taiwan.

8.2.2 *Extreme event analysis*

River runoff is the driver of flood simulations, and it is assumed to be mainly generated by precipitation. The occurrence and quantity of runoff are dependent on the characteristics of the rainfall event. Annual maximum rainfall depths for durations of 6, 12, 24 and 48 h were obtained using historic hourly data from 37 rainfall stations in Tainan with records of longer than 20 years. The rainfall depths for recurrence intervals of 2, 5, 10, 25, 50, 100, 200 and 500 years are derived for the corresponding durations. The analysis results for the Tainan rainfall station were shown in Table 2. The results of the frequency analysis were used to develop the relationship between rainfall intensity (or depth), duration, and frequency (or return period) at all sites and to create IDF (Intensity–Duration–Frequency) curves which used to estimate rainfall intensity according to assumed duration and return period. Horner's equation is used to fit the IDF curves in this study.

The other event that was analyzed is storm surge. A storm surge is usually characterized as an abnormal rise in water level generated by a storm, over and above the predicted astronomical tide. In this study, the High Water of Ordinary Spring Tide (HWOST) is used as the base tide height. The maximum storm surges derived from 105 typhoons from 1980 to 2013 are obtained by numerical simulation. The heights of storm surge on the Tainan coast were estimated for return periods of 2, 5, 10, 25, 50, 100, 200 and 500 years, as shown in Table 2.

Table 8-2 Results of frequency analysis on rainfall and storm surge and calibration of the coefficients of Horner formula at Tainan Station.

	Duration (h)	Return Period (Years)							
		2	**5**	**10**	**25**	**50**	**100**	**200**	**500**
Rainfall (mm)	6	131	179	207	240	262	283	302	326
	12	177	237	273	314	343	370	396	428
	24	203	289	347	419	473	526	579	650
	48	229	329	395	479	541	602	664	745
Storm surge (m)		1.45	1.50	1.57	1.67	1.74	1.80	1.87	1.96
Horner formula coefficient	a	1143	1131	1062	959	888	827	776	721
	b	39.6	31.1	21.9	9.5	0.7	−7.1	−14.0	−21.8
	c	0.66	0.61	0.58	0.54	0.51	0.49	0.47	0.44

8.2.3 *Methodology*

Physically-based computational model SOBEK which was developed by Deltares (https://www.deltares.nl/en/) was used in the present work. One-dimensional (1D) hydraulic flow model was used to simulate flows in drainage channels. R-R (Rainfalli Runoff) model in areas with elevations higher than 100 m, which are defined as highland areas. Runoff routing to downstream areas (elevation < 100 m) was performed using 1DFLOW (Rural and Urban). When the runoff rates exceed the capacity of the river channel, the two-dimensional (2D) Overland Flow module takes over computations and simulates the propagation along the floodplain.

The parameters of the SCS Runoff Curve Number Method were set in the R-R modules for each watershed. The cross-sectional shapes of rivers, regional drainage systems and properties of sewers and hydrologic structures were used as inputs into the hydraulic model. Simulations were carried out separately in each watershed due to computational limitations. ArcGIS software was used to divide the drainage basins based on the DEM characteristics. The drainage basins were corrected according to satellite and aerial images when the auto-division results were biased.

8.2.4 *Model calibration and validation*

Records from historical flood events were used to calibrate and validate the model. Two indicators, Probability of Detection (POD) and Scale of Accuracy (SA), are used to assess the model performance. The optimal simulation performance is achieved when both POD and SA approach 100%. A 60% value for both POD and SA is required. To correct the flooded depth, the bias associated with simulated and observed peak flood depths should be lower than 0.2 m.

Four historical flood events caused by typhoons were used for model calibration, and two additional events (one typhoon and one rainstorm) were used for model validation. The model calibration results shows that the POD is higher than 70% (maximum 88.1% for Typhoon Fanapi flood simulation) and the SA is higher than 60%. The performance of validation suggest that the POD is 75% and SA is 62% for the typhoon event and the POD is 83% and SA is 68% for the rainstorm event. This quantitative assessment is satisfactory, however, an improvement is dedicated to work on.

8.2.5 *Flood Inundation Maps*

FIMs are designed to represent the possible flood conditions under various rainfall scenarios. Two types of rainfall scenarios were assumed: one with topography-based cumulative rainfall (CR) and the other with periodic rainfall (PR). Topography-based cumulative rainfall assigns rainfall amounts for various rainfall durations, but the amounts depend on topography. The rainfall amount in highland areas is 2.1 times higher than in the low-lying areas. The type of periodic rainfall is based on rainfalls of several return periods for various durations. Thirty-four scenarios consisting of quantitative and periodic rainfalls were assumed. To consider the effect of the sea, another eight scenarios with simultaneous rainfall and storm surge events were assumed for various return periods and 24-h durations. In total, 42 scenarios were used to produce the FIMs in the present work.

Figure 3 shows the FIMs with 100-year rainfall and durations of 6 and 24 h. These rainfall scenarios with different return periods are similar to those of cumulative rainfall, but they are presented differently to satisfy different requirements. Flooding began to occur in the coastal area (elevation < 1 m) for low-intensity rainfall events. The flooding is due to low-lying land in the coastal area. When the rainfall intensity increases, the flood extent expands due to the influence of low-lying areas. However, when the rainfall intensity increases, the flood extent reaches elevation > 10 m in some areas because the river discharge capability decreases due to tidal chokage. Figure 4 shows the results of various scenarios. The flood extents of a 100-year rainfall event for durations of 6, 12 and 24 h (scenario codes PR-6-100, PR-12-100 and PR-24-100) are overlapped, as is the influence of the storm surge (PR-24-100S). The most extreme scenario (100-year rainfall for 24 h) triggered severe floods, especially in the southern Tainan region (right-panel of Figure 3); however, the storm surge considerably affected low-lying areas in the western part of Tainan City.

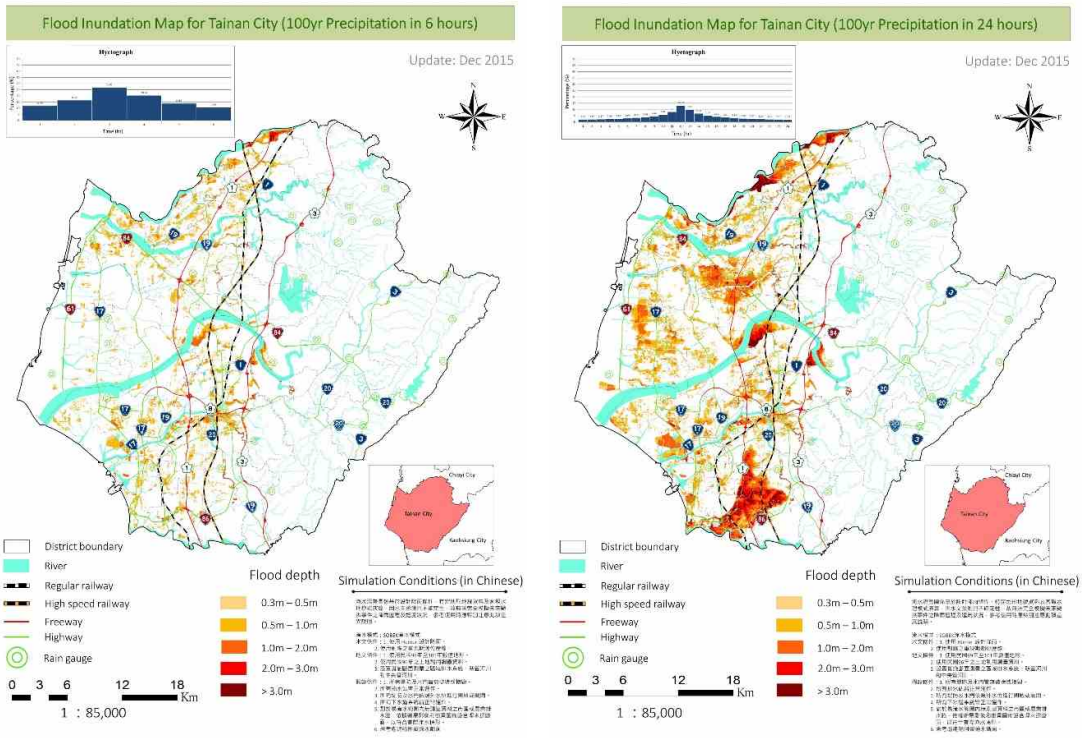

Figure 8-3 Productions of flood inundation map for Tainan City under conditions: (Left-panel) 100-year rainfall for 6 h (PR-6-100); and (Right-panel) 100-year rainfall for 24 h (PR-24-100).

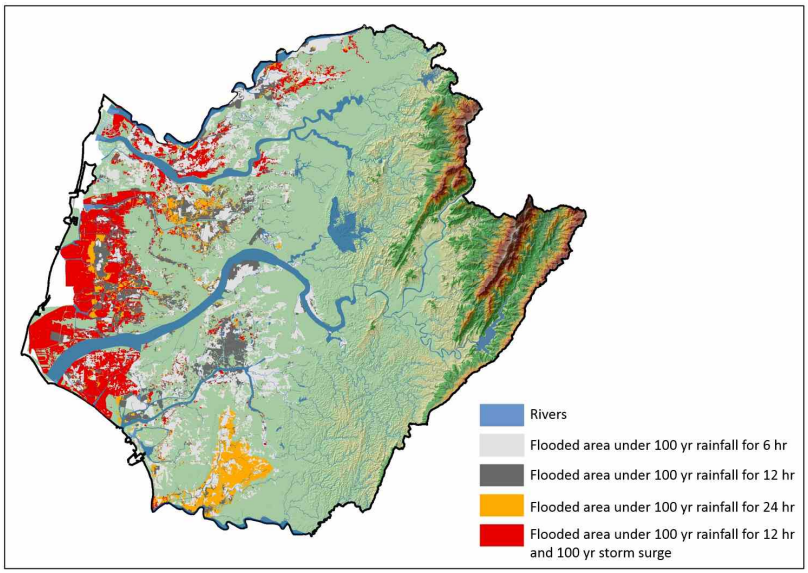

Figure 8-4 Overlap of the flooded area under various scenarios.

8.3 Data collection and analysis for vulnerability assessment

This study adopted the indicators of coastal vulnerability that were established by United National Environment Programme (UNEP, 2005). These coastal vulnerability index (CVI) is a function of five indicators (equation (1)). These indicators are population density in coastal area (*PD*), probability of natural disaster incidents (*ND*), forest cover (*FC*), geographic exposure (*GE*), and human development index (*HDI*).

$$CVI = (PD + ND + (1 - FC) + GE - (HDI)) \quad (1)$$

The indicators are standardised by equation (2) before being substituted into equation (1).

$$\text{index} = (X - X_{min})/(X_{max} - X_{min}) \quad (2)$$

Here, X indicates the data value for X indicator and the subscript of min and max represent minimum and maximum of that indicator, respectively. The calculated CVI is standardised and classified into three classes. When CVI is higher than 0.1 and lower than 0.5, the vulnerability is moderate. On the other hand, if CVI is above 0.5 or below 0.1, the study area has high or low vulnerability.

According to classification of UNEP, the CVI at Taiwan is 0.517 which is one of the most vulnerable countries in the world. Therefore, a local coastal vulnerability assessment was proposed. The local coastal vulnerability is a combined effect of three evaluated factors. In total, there are ten parameters were used in this assessment (Table 3). According to the proposed CVI, the vulnerability is classfied into five scales, which are extreme high ($CVI > 36$), high ($20 < CVI \leq 36$), moderate ($12 < CVI \leq 20$), low ($7 \leq CVI \leq 12$) and extreme low ($CVI < 7$).

The coastal vulnerability map of Taiwan using the proposed factors is plotted as Figure 5. In general, the western coast is more vulnerable than the eastern coast. Extreme high vulnerable suburbs are mainly located at middle- and south-western coast. This is due to the higher vulnerability of environmental factor (e.q. sandy coastline) and of social-ecomomical (e.q. higher development). It can also be found in the map that the coastline of Tainan is classified to has moderate vulnerability.

Table 8-3 Evaluated factors for vulnerability analysis.

Evaluated factor	Vulnerability evaluation parameter
Physical Factor	1. population density 2. fundamental protection facilities
Environmental Factor	1. coastal morphology 2. mean wave height (m) 3. mean tidal range (m) 4. coastal erosion 5. coastal geology sensitive area 6. rate of land subsidence (cm/yr)
Social-Economical	1. Human Development Index 2. Fundamental facilities: harbor, aquaculture, lifelines areas

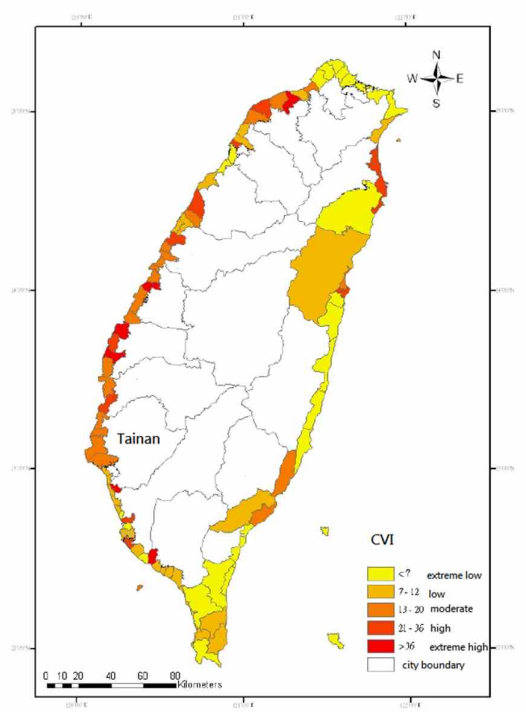

Figure 8-5 Coastal vulnerability map

8.4 Risk assessment

According to International Strategy for Disaster Reduction (ISDR), the definition of risk can be written as Risk = Hazard * Vulnerability. Impact on coastal area of sea-level rising due to climate change at the end of the 21st century was assessed. Different sea-level rising scenarios were adopted and the possible submerged areas can be seen in Figure 6. From the figure, it can be seen that large portion of Tainan city could be submerged in the scenarios in both scenarios, especially southern Tainan (bottom panels of Figure 6). The higher the sea level rise, the larger the area could be submerged.

Based on the coastal vulnerability map that obtained from previous section (Figure 5), the risk map of Taiwan coastline was established and shown in Figure 7 (scenario of 1.4 m sea-level rising).

Similar to vulnerability map, the western coast has higher risk than the eastern one. Southwestern coastline of Taiwan has the highest risks which might be caused by sea-level rising and Tainan city was classified with moderate risk. From the risk map of sea level rising, we can know that higher attention and protection are needed for area with higher risks, i.e. southwestern coastline of Taiwan.

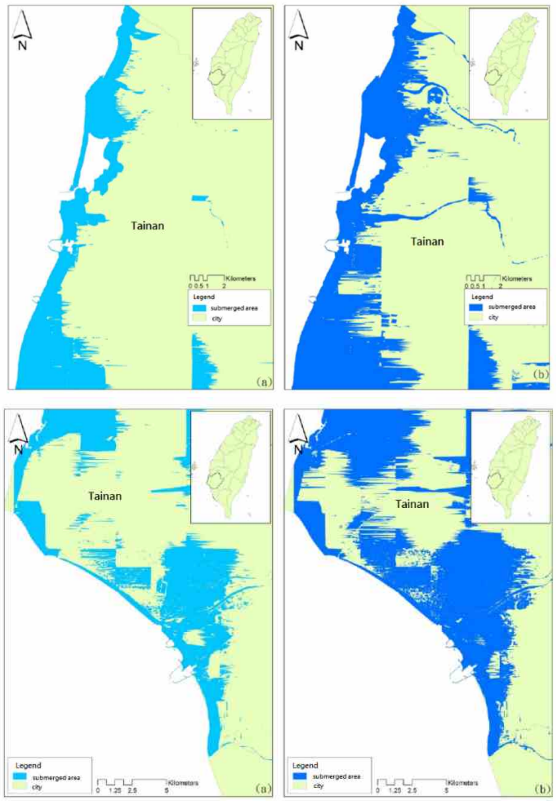

Figure 8-6 Maps of submerged areas due to sea-level rising. (a) rise 0.5 m (b) rise 1.4 m. Top panels are northern Tainan and bottom panels are southern Taiwan.

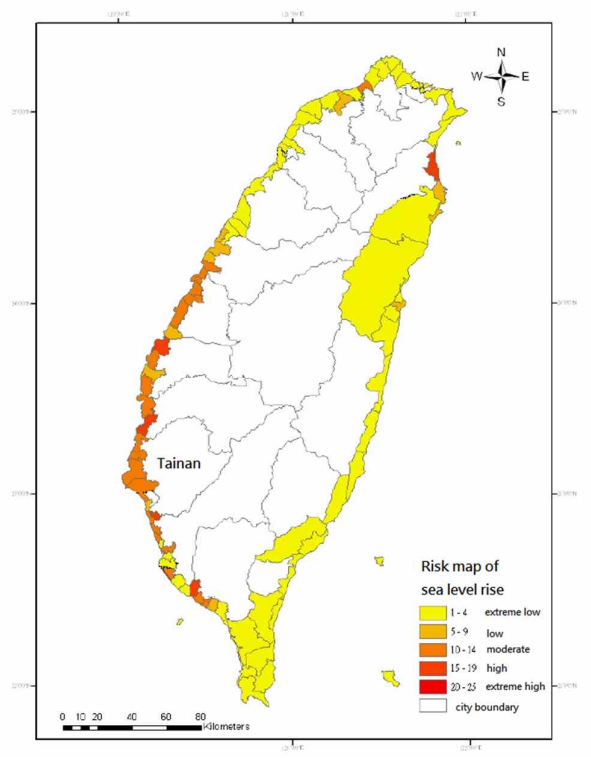

Figure 8-7 Risk map of sea level rise of 1.4 m

8.5 How risk analysis benefit local stakeholders

The works on the development of FIM for Tainan area involved stakeholders throughout the entire process, including at least two stakeholder meetings. One was held during the model simulation stage, and the other was held when the FIMs were produced. The participants of both meetings included FIM producers (the Water Resources Agency in the central government), groups that provided FIM development and technical support (university professors), first-line managers (Water Resource Bureaus in the local government), and public users (local residents). The objective of the first meeting which was held during the model calibration stage of flood simulation was to decrease the uncertainty in records of historical flood events based on inputs from local residents and their memories/perceptions and personal records. This information was very useful in the calibration process. The second meeting was held when all FIMs were produced. It educated the first-line managers and local residents regarding the conditions, results and uncertainty of FIMs. Additionally, that meeting provided information on web search systems, and users provided feedback to improve the FIMs. This was the first time that all stakeholders were present in the meeting and they all participated actively in the development and application of FIMs.

9 Case Study ï St Maarten

9.1 Description of the study area

9.1.1 *Location, social and economic features*

Sint Maarten is a constituent country of the Kingdom of the Netherlands as of 10/10/10. It encompasses the southern third of the Caribbean island of Saint Martin, while the northern two-thirds of the island constitute the French overseas collectivity of Saint-Martin. Its capital is Philipsburg. Its population is 40917 on 34 km^2 . Sint Maarten is located at the northern end of the Leeward Islands at 18.4^{0}N and 63.4^{0}W with a coastline of 364 km, see Figure 9-1

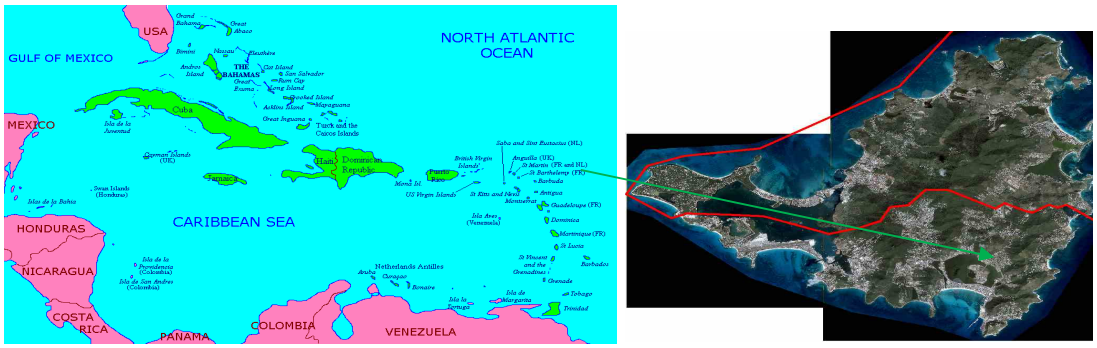

Figure 9-1 Location of St Maarten

The general climate of the island usually varies from a relatively dry season (January-April) to a rainy season (August-December), with moderate winds from the east to northeast. Showers normally occur during the late afternoon, as local effects of heating, humidity, etc. combine. Additionally, temperatures usually remain around 27^{0}C with the warmest month being August. The tropical nature of the island extends into seawater temperatures of around 27.2^{0}C, while skies typically range between mostly clear to partly cloudy.

9.1.2 *Main challenges that affect the case study*

Being located in the North Atlantic Ocean, Sint Maarten has been subject to hurricanes for many years. The Atlantic Tropical Cyclone Season runs from June 1st up to November 30th. Almost every year at least one tropical cyclone occurs within a range of 100 miles and on the average once every 4-5 years hurricane conditions are experienced in the island. The most recent hurricanes to cause considerable damage to the island were the hurricanes Omar (2008), José (1999), Lenny (1999), Georges (1998), Luis (1995), Marilyn (1995), Hugo (1989), Donna (1960) and Dog (1950). The damage estimated with hurricane Dog was about US$ 70.000, without loss of lives. Hurricane Donna left a quarter of the island homeless and killed seven people. However, the damage caused by Hurricane Luis was extensive. The total damage due to Hurricane Luis was estimated to be approximately 1 billion US dollars (direct and indirect). Over 80% of all construction (residential, businesses, churches, hotels and schools) sustained serious damage or had been completely

destroyed. Nearly all power and telephone lines were damaged and out of operation which left the island for several days without communication with the rest of the world.

Apart from the above mentioned hydro-meteorological hazards, the stormwater catchments and streams on Sint Maarten have several unique characteristics that contribute to the severity of flood-related impacts, Figure 9-2 shows photographs during and after a flooding event due to heavy precipitation. Urban environments are usually situated on low-lying areas, with little consideration for stormwater drainage, and as such are subject to flash flooding (i.e. inland flooding) from surrounding hills or extreme rainfall events due to hurricanes

Those areas close to the sea (such as Philipsburg) are very vulnerable to inundation due to high water levels resulting from storm surge. Typically, the localised flooding due to inadequate stormwater drainage system happens almost every time it rains. In residential areas, the streets are usually narrow due to inadequate development control mechanisms and as such they represent a limiting factor for further enlargement of stormwater channels.

Figure 9-2 Flooding after heavy precipitation

9.2 Data collection and analysis for hazard assessment

The analysis of rainfall data and the necessary information for hazard assessment is provided from previous studies done in St Maarten by UNESCO-IHE. St Maarten is prone to flood hazards from two different sources or drivers. 1. Coastal flooding due to the passing of hurricanes and tropical storms and 2. Inland flooding due to heavy precipitation and the morphological characteristics of the island, some catchment have steep slopes and short streams draining to the sea.

The coastal system was modelled to investigate the surge impact of three hurricanes that made an impact on Sint Maarten in the past.

For the inland flooding hydrological and hydraulic models were used to support the identification of hazards from inland floods (i.e. pluvial and flash floods).

9.2.1 *Coastal flooding data sources*

Bathymetric data of the study area for the hurricane simulation was sourced from General Bathymetric Chart of the Oceans (GEBCO). The Shuttle Radar Topography Mission (SRTM30) data are largely used for land data. In order to undertake simulations in the region that are more focused on Saint Martin island another bathymetry dataset was developed. This bathymetry data was prepared by combining detailed land and ocean datasets. The land data were derived from a 10m grid LiDAR (light detection and ranging) measurement, whereas a shallow water bathymetry in the south coast of Sint Maarten was developed using a method based on the Support Vector Machine

(SVM) algorithm. Two datasets were merged to develop the shallow water bathymetry - sonar and satellite datasets.

Hurricane Model

The two-dimensional hydrodynamic modelling software MIKE21[9] was used to simulate the hurricane-related processes. The Cyclone Wind Generation in WIND Tools of MIKE21 Toolbox provided the facility to generate travelling cyclone wind fields. It allows users to compute wind and pressure data due to a tropical cyclone (hurricane). Hurricane Omar was modelled in a previous study and has been used as an input to test some of the models being develop in PEARL.

Hurricane Omar

Hurricane Omar was a strong hurricane that took an unusual southwest to northeast track through the eastern Caribbean Sea during October, 2008. Early on 16 October, Omar reached its peak intensity with winds of 215km/h and a barometric pressure of 958mb. The remnants of Omar persisted until 21 October at which time it dissipated to the west of the Azores.

Hydrodynamic (Surge) simulation

MIKE 21 Flow Model can be used to simulate a wide range of hydraulic and related items, including coastal flooding and storm surge. The GEBCO bathymetry was used for the MIKE21 model set up of hurricane Omar. The initial surface elevations and boundary conditions used in the model set-up reflect the pressure field that follows the wind imposed on the model. The stress generated on the water surface by wind was included in varying both in time and space with values given through the result file generated in the hurricane simulation. The screen shots were taken when the eye of the hurricanes reached the vicinity of Saint Martin island.

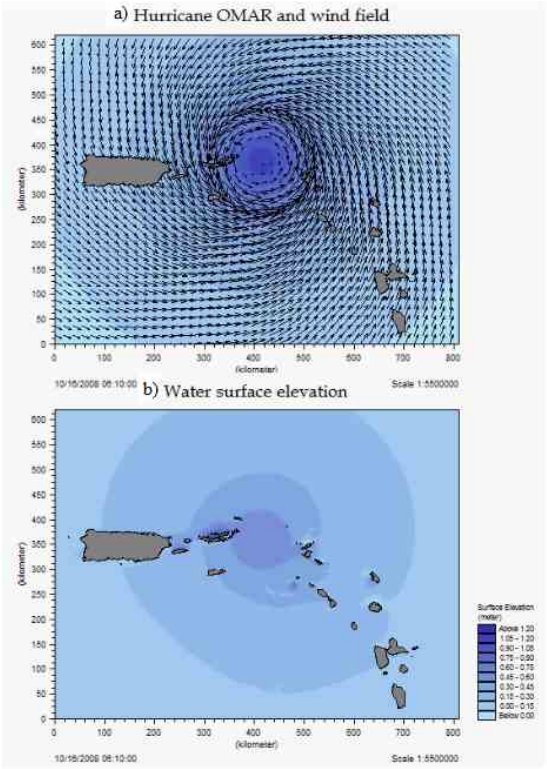

Figure 9-3 a) Hurricane Omar wind field, b) Water surface elevation (surge level) due to Hurricane Omar.

[9] http://www.dhisoftware.com/Products/CoastAndSea.aspx

Then the surge simulation using the higher resolution bathymetry was carried out to gain better understanding of storm surge in the vicinity of Saint Martin. The simulation for Hurricane Omar showed a storm surge of around 0.9m.

9.2.2 *Inland Flooding data sources*

A hydrological model for the study area was set up using MIKE 11 modelling software.[10] MIKE 11 offers a unique possibility to simulate catchment runoff using simple empirical rainfall-runoff methods. For St Maarten the unit hydrograph module (UHM) that simulates the runoff from single storm events based on the unit hydrograph technique was used. The UHM includes different loss models (constant, proportional) and SCS method for estimating storm runoff.

Catchment Delineation

Contour line maps were used to develop a Digital Terrain Model (DTM) of the Island. This DTM has a 10m spatial resolution. On the basis of this DTM, the catchment and sub-catchment delineation process was undertaken (Figures 3.1).

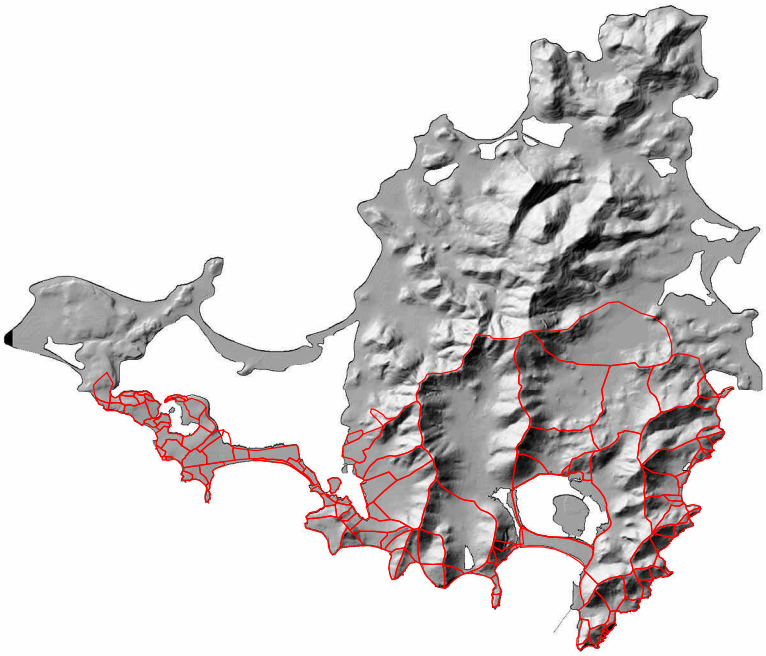

Figure 9-4 Model catchment areas (red line depicts the catchment boundaries).

Since the main purpose of hydrologic modelling is to produce the stormwater runoff by each of the sub-catchments, the next task was to define the stream network and to identify the area with runoff converging to each and every stream. The streams presented in Figure 3.3 have been surveyed and agreed with the local stakeholders to be used in all modelling work and subsequent reporting of results.

[10] http://www.dhisoftware.com/Products/WaterResources/MIKE11.aspx

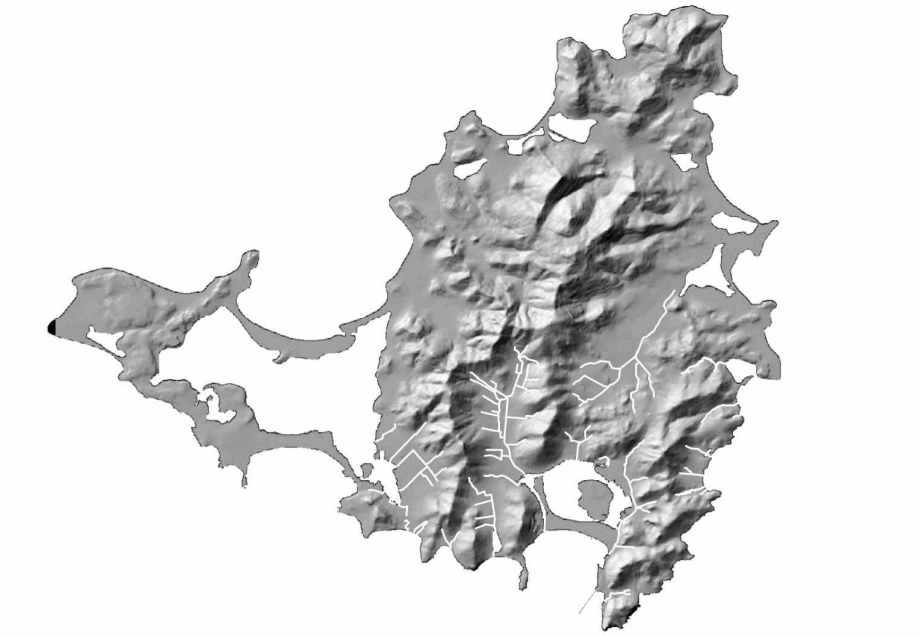

Figure 9-5 Model stream network (white line).

For the sub-catchment discharge calculation, the time-area curve method was used. The hydrographs generated for each rainfall event are calculated using the unit hydrograph of the sub-catchment and applying the principle of superposition. The curve number (*CN*) used in the SCS method depends on the soil type, the land use and the antecedent moisture condition (AMC) at the start of the storm. *CN* varies between 0, resulting in no runoff, and 100 which generates an excess rain equal to the rainfall. For natural catchments normally *CN* is between 50 and 100. The *CN* of sub-catchments applied in this study was identified based on the land use and the soil type.

Rainfall analysis

The lack of spatially continuous and accurate long-term precipitation datasets over Sint Maarten is a limitation to perform adequate analysis to cover all areas. The use of available data from Princes Juliana Airport together with the available data from the French side of the island was insufficient and it was necessary to merge this data with the data from other nearby regions in order to undertake the hazard assessment. To calculate the intensity-duration-frequency (IDF) curves for Sint Maarten, it was necessary to make a correlation with other islands where such curves have been already developed on the basis of actual data. The available IDF curves were sourced from Raizet11 (Guadeloupe) and also from St Croix12 (US Virgin Islands). The maximum precipitation in 24 hours for these two islands is presented in Table 9-1 and by the graph shown in Figure 9-6.

[11] "Les ressòurces en eau de surface de la Guadeloupe sur la période 1961-1978"

[12] "Generalized estimates of Probable Maximum precipitation and rainfall-frequency data for Puerto Rico and Virgin Islands" published by the National Oceanic and Atmospheric Administration

Table 9-1 Maximum precipitation in 24 hours

T (year)	2	10	50	100
Juliana Airport	82	168	243	275
Raizet	100	183	253	287
St Croix	102	178	254	318

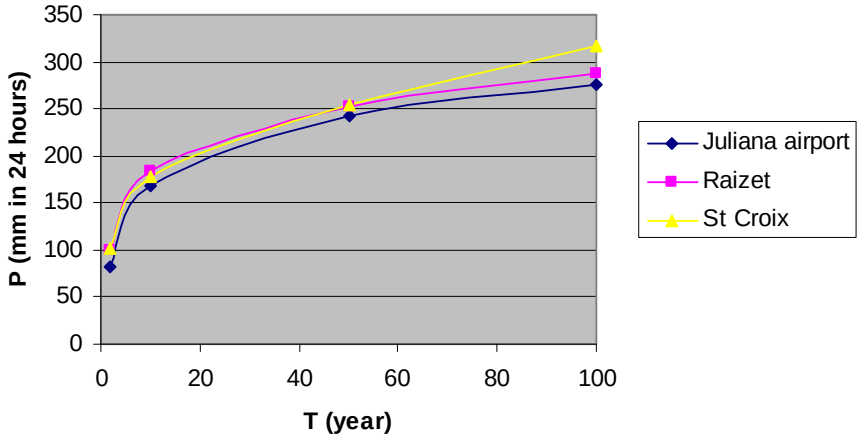

Figure 9-6 Maximum precipitation in 24 hours (Princess Juliana Airport, Raizet and St Croix)

From the analysis of Raizet data it was concluded that due the orographic similarity between the two islands, the IDF curves from Raizet could be applied to Sint Maarten. The IDF curves for Sint Maarten were derived by multiplying the intensity which corresponds to the maximum precipitation in 24 hours with the ratio of the IDF curves in Raizet. The calculated values are presented in Table 9-2 and by the graph shown in Figure 9-7.

Table 9-2 Intensities (mm/hr) for the return periods and the durations considered

Duration (hours)	Return period (years)					
	2	5	10	20	50	100
0.1	108.3	152.8	181.8	176.3	199.9	219.5
0.25	77.2	107.3	126.7	139.6	169.1	184.0
0.5	56.6	81.6	99.1	115.0	128.8	141.8
1	36.1	52.4	62.4	76.4	90.3	99.7
2	23.0	30.0	41.3	48.1	56.7	63.2
3	16.4	24.9	30.3	35.8	42.3	47.0
6	9.8	14.6	18.4	20.7	24.0	26.8
24	3.4	5.6	7.0	8.3	10.1	11.5

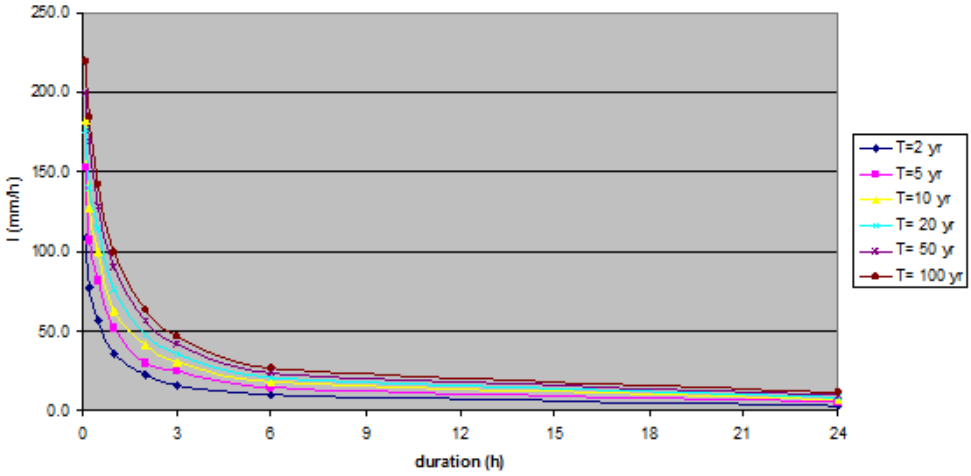

Figure 9-7 Sint Maarten IDF curves

The values of the rainfall depth derived from the IDF curves for Sint Maarten are presented in Table 9-3.

Table 9-3 Rainfall depth (mm) for different duration and return periods

Duration	T=5 yr	T=10 yr	T=20 yr	T=50 yr	T=100 yr
30 min	41	50	58	64	71
1 h	52	62	76	90	100
2 h	60	83	96	113	126
3 h	75	91	108	127	141
6 h	88	110	124	144	161
24 h	134	168	200	243	275

Hydraulic modelling

The hydraulic modelling was carried out by coupling the one-dimensional (1D) MIKE11 and the two-dimensional (2D) MIKE21 flow models. The two modelling packages were integrated into a single, dynamically coupled modelling system through MIKE FLOOD.[13]

The coupled 1D-2D simulations were carried out for five return periods (see Table 9-3). For these simulations, the 1h duration precipitation depths were considered. As an example, Figure 9-8 shows the flood depth and extent model results in case of the 1 in 100 year storm for the existing conditions.

[13] http://www.dhisoftware.com/Products/WaterResources/MIKEFLOOD.aspx

Figure 9-8 Flood depth and extent of the 1 in 100 year storm in existing scenario

While widespread flooding occurs in several parts of the island, the coupled hydrodynamic model results indicate that the most vulnerable area, with the most serious flooding, is the Cul De Sac catchment area. Residential areas in this catchment are predominantly situated on low-lying areas, with little consideration for stormwater drainage and as such are subject to flash flooding from surrounding hills, or extreme rainfall events such as direct thunderstorms. The drainage channels are inadequate to convey excess rainfall-runoff due to the limited capacity, obstructions and the morphological rising of the streambed and as such are not able to convey anything larger than 5 or 10 year rainfall event. Since the large contributing areas are steep, with some vegetation coverage, any rainfall is likely to cause erosion and landslides. The streets are usually narrow and as such represent a limiting factor for further enlargement of stormwater channels.

Historical flood information indicates that during small rainfall events typical impacts would include temporary disruption to transportation systems and other inconveniences related to the life on island. During the heavy rainfall events, especially those caused by hurricanes, the large-scale flooding can cause a widespread damage to the residential and commercial areas and even loss of human lives. The information related to hazard assessment has been used to test some of the models being develop in the framework of PEARL.

9.2.3 *Flood Hazard Assessment*

Flood hazard assessment is the evaluation of general negative consequences of floods. It relies on several parameters such as depth of flooding, duration of flooding, flood wave velocity and the rate of rise of flood water level. In the present study, flood depths and flood velocities were used as main variables for the assessment of flood hazards on Sint Maarten. The following numerical values have been applied to reflect different hazard categories:

- **Low hazard** - depth < 0.4m, and velocity < 0.5m/s (still just suitable for cars)

- **Medium hazard** - depth < 0.8m, velocity < 2 m/s, and velocity x depth < 0.5 (still just suitable for heavy vehicles and wading by able bodied adults)

- **High hazard** - depth < 1.8 m, velocity < 3m/s, and velocity x depth <1.5 (still just suitable for light construction like timber frame, brick veneer, etc.)

- **Very high hazard** - velocity > 0.5m/s and < 4m/s, and velocity x depth < 2.5 (still just suitable for heavy construction like steel frame, concrete, etc). Not acceptable for places of assembly or critical institutions.

- **Extreme hazard -** greater than very high significant flowpath development, considered unsuitable and likely to adversely impact flood levels. Unsuitable for light construction. Not acceptable for places of assembly or critical institutions.

9.2.4 *Vulnerability analysis*

In Sint Maarten the previous studies considers the vulnerability analysis of critical buildings (and to a certain extent road infrastructure). The first step in this analysis was to identify and locate all critical buildings on the island. The database of about 200 critical buildings was developed and sorted in relation to the facility type. Table 9-4 gives an overview of different facility types.

Table 9-4 Types of buildings

ID	Facility Type
1	Airport
2	Automotive
3	Banking
4	Commercial Centre
5	Education
6	Fuel Depot
7	Governance and Public Services
8	Health Care
9	Insurance
10	Lodging
11	Religious
12	Utilities

A geodatabase in ArcGIS was created and all buildings including those critical ones were incorporated. This database was developed to store basic information of facilities such as: Type, Name and Address of Facility, Shelter (this refers to emergency shelters), Designated (to select whether or not the specific building has being officially designated as shelter), Vulnerability of the building (this was assessed in relation to the habitable floor heights and the strength of the building to withstand impacts of inland and coastal floods) and Photos (a photo ID). Once the geodatabase of total buildings was created, fieldwork was conducted in order to identify the physical condition of buildings and the potential damage that can be incurred in case of flood events. The categories used for these two parameters are shown in Table 9-5.

Table 9-5 Categories of Vulnerability

Category	Vulnerability	
	Flood Height	Physical Condition
1	Low	Weak
2	Intermediate	Intermediate
3	High	Solid

Buildings made of wooden walls or other light structures (including light roof structure) are considered to be weak and highly vulnerable. On the other hand, buildings with concrete or brick walls and are in good condition (including solid roof structure) are considered to be solid and having low vulnerability.

The method used in the vulnerability assessment is based on a reclassification of data into a common scale (see Table 9-6).

Table 9-6 Reclassification of Vulnerabilities

Category	Vulnerability			
	Flood Height	Reclassified Value	Physical Condition	Reclassified Value
1	Low	1	Weak	5
2	Intermediate	3	Intermediate	3
3	High	5	Solid	1

The higher the reclassified values presented in Table 9-6, the higher the vulnerability of buildings is. After the reclassification, the two fields were summed to obtain the combined vulnerability as shown in Table 9-7.

Table 9-7 Final Categories of Combined Vulnerability

Category	Vulnerability	
	Class	Range
1	Low	0 - 2
2	Medium	2 - 4
3	High	4 - 6
4	Very high	6 - 8
5	Extreme	8 - 10

9.2.5 *Flood risk analysis*

In the previous studies, the notion of risk expressed as $R = H \times V$ was applied. Once the hazard and vulnerability class ranges are determined, multiplying these ranges for the respective classes will give the risk class ranges. In terms of the risk to critical buildings, Table 9-8 shows the classification that was applied in the flood risk assessment.

Table 9-8 Final risk assessment categories

Category	Hazard Range	Vulnerability Range	Risk Range (Hazard x Vulnerability)	Class
1	0 - 2	0 - 2	0 - 4	Low
2	2 - 4	2 - 4	4 - 16	Medium
3	4 - 6	4 - 6	16 - 36	High
4	6 - 8	6 - 8	36 - 64	Very high
5	8 - 10	8 - 10	64 - 100	Extreme

Figure 9-9 shows the flood risk to critical buildings in Sint Maarten island.

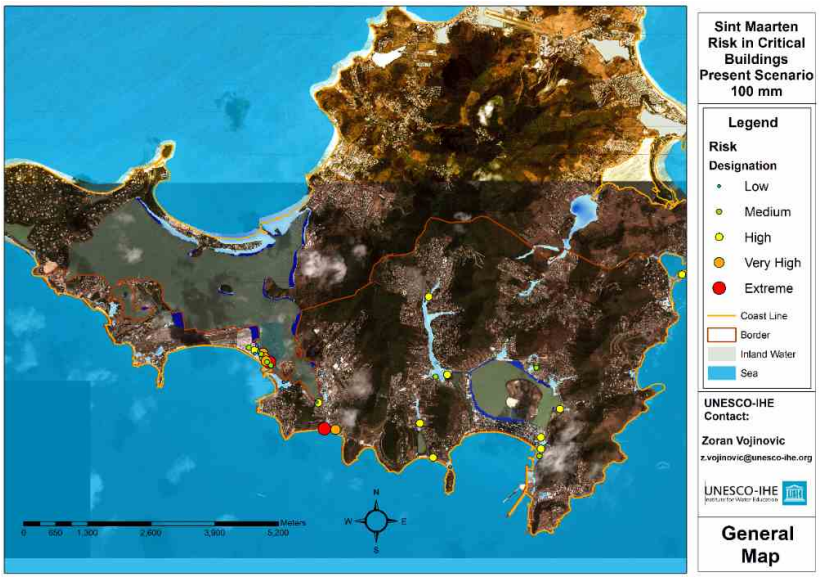

Figure 9-9 A map showing an example of a risk assessment result.

9.2.6 *Holistic Flood risk assessment*

The Risk Root Cause Analysis for St Maarten followed the methodological approach laid out in PEARL Deliverable 1.1. The research is based on individual, expert interviews with stakeholders, where the aim was to capture as diverse a set of views about disaster causation as possible through interviews with multiple stakeholder types. 22 interviews were conducted between July and November 2015, the majority face-to-face interviews but also telephone interviews with those whom it was not possible to meet during fieldwork on the island. The researcher ósnowballedô out from interviews with initial contacts provided by other PEARL researchers to generate a wider field of interviewees.

The interviews were in-depth, typically lasting 1-2 hours each. The interviews centred on actor behaviour pre-, during and post- flooding events as well as eliciting stakeholder opinions about the broader causes of specific disaster events on the island. The interview structure adapted the broad PEARL Risk and Root Cause Analysis Framework ï which displays root causes acting on risk across the inter-acting physical, governance, socio-economic and perceptions, values and beliefs domains ï for the context - for example, seeking to understand the impact of changes in governance on the island in 2010 on risk management.

The Root Cause Analysis highlights, although it does not make explicit, many of the inter-connections across the physical, socio-economic and governance domains and pathways that give rise to risk. This has been reported in deliverable 1.3. The information from the Root Cause Analysis has been used as an input in the description of the Agent-Based Modelling work in a format that highlighted the actors, actor-relationships and underlying institutions conforming the current flood ósystemô In conjunction, the outcome of the interviews also provides a timeline of policy measures and the underlying motivation for relevant policies.

Information from the Root Cause Analysis method was used for the development of agent-based models (ABM) which are part of the PEARL Holistic Risk Assessment Framework. For work package 3 there are two ABMs in PEARL developed at UNESCO-IHE. The first one focuses on the interaction of floods, humans and their built environment as drivers of hazard, vulnerability and exposure. The drivers are the institutions which in model terms are expressed in terms of institutional statements. For example, land use planning can be a driver of exposure and institutional statement derived from this driver could be ñLand owners must not construct new buildings (or houses) if their land is located 25m from the waterfront.ò The ABM in this study addresses long-term institutions related to prevention and mitigation and recovery phases of the disaster management cycle. The second ABM focuses on the short-term, operational and management related to the preparation and response phases of the disaster risk management cycle. These are connected to flood early warning and evacuation processes. A summary of the on going research results for the evacuation ABM is provided in the following section.

The findings of the RRCA were used to formalise the concepts based on the MAIA framework. Institutional statements are extracted and coded from RRCA outputs based on the methods described in (Basurto et al., 2009; Watkins and Westphal, 2015).Concept formalization is an iterative process which continues until the problems formulated and systems identified are well captured in MAIA structures (Ghorbani, 2013). The following tables show examples of the different structures of MAIA and the formalization.

Table A. Social structure

Name	Property	Personal value	Information	Possible role
Households	- Wealth - Level of risk to take - Risk awareness - Insurance - Building plan	- Safety	- Zoning policy - Beach policy - Hillside policy - Building ordinance - Insurance policy	- Land owners
Businesses	- Asset - Profit - Level of risk to take - Risk awareness - Insurance - Building plan	- Profit maximization - Safety	- Zoning policy - Beach policy - Hillside policy - Building ordinance - Insurance policy	
VROMI	- Budget - Enforcement - Fine	- Safety		- Permit - Inspection

	- New Project

Table B. Institutional structure

Name	Attributes (roles)	Deontic type	aIm	Condition	Or else	Type
Building code	Land owners	must	elevate new house/building by 0.2 m	any location and any time	fined	Rule
Beach policy	Land owners	must not	build houses/building	within 25 m from the coast line	fined	Rule
Flood risk management	New Project department	may	Construct or maintain FRM measures	If flood leads to casualty		Norm
Flood risk management	Businesses		fund FRM measures	if measures protect asset		Shared strategy

Table C. *Physical structure*

Name	Property	Type	Behaviour	Affordance
Building (residential or business or public)	- Location - Elevation - Building function - Floor height - Flooded - Damage	- Private	- Flooded - Damaged	- Constructed - Maintained
Drainage channels (pipes)	- Location - Cross-section - Physical condition - Design discharge	- Public	- Damaged	- Constructed - Maintained
Hazard triggering factors (precipitation, storm surge)	- Return period	- Public		- modelled
Flood map	- Depth - Extent	- Public		
FRM measure	- Type	- Private/Public	- Damaged	- Constructed - Maintained

Development of the Institutional ABM

The development of ABM for the Sint Maarten FRM case study started before the RRCA field work and interviews took place. The initial model was developed using the NetLogo simulation environment (Wilensky 1999). Model inputs are obtained from desk studies and previous UNESCO-IHE studies on the island. In this model setup, there were two types of agents: businesses and ordinary residents. Businesses construct commercial buildings (e.g., hotels) and residents build residential houses. The institutions incorporated in that preliminary model were based solely on the Hillside policy. Businesses build in mild slopes and low lying areas, especially along the coast (to attract more tourists) whereas residents have more flexibility to build their houses on the island. However, since the land use zoning in the island defined higher elevations for nature, it is not allowed to build in elevations higher than 200m. In the model, the buildings, whether commercial or residential, represent the owners. Early simulation result presented in Figure 9-10 shows that commercial buildings (yellow coloured) aggregate more along the coast. On the other hand, residential housings (brown ones) concentrate on the hilly areas. The modelling exercise shows the

potential of ABMs in showing emergent phenomenon, which in this case is location of different types of buildings, from simple institutions.

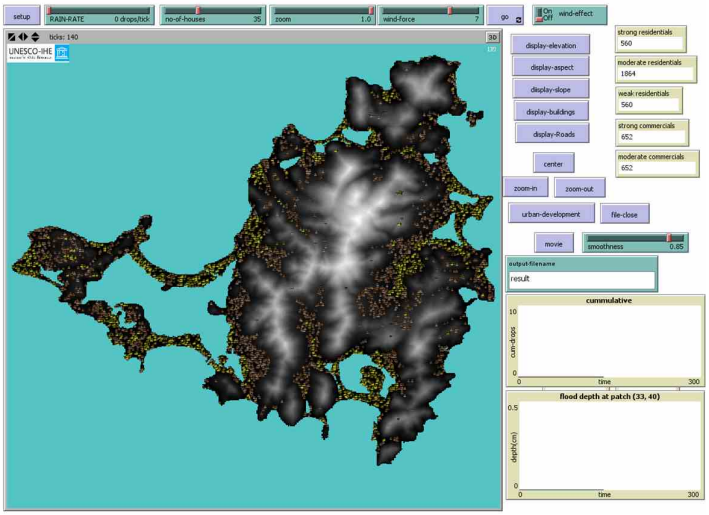

Figure 9-10 Building Pattern Result in the NetLogo visualization **environment**

After the RRCA was performed, more agents and institutions were identified and hence the ABM was expanded. To simulate the co-evolution of the human-flood systems and the FRM dynamics better, the modellers identified the need to couple the ABM with a flood model. In addition to a more realistic representation of the flood system, coupling a flood model with the ABM provides a platform to test the different FRM policy implementations (e.g., enlarging channel cross-sections and constructing new detention basins). However, NetLogo was found to be limited in the coupling process, especially running the flood model executables and manipulating input-output files. Therefore, the modellers changed the modelling platform to Repast Simphony (North et al., 2013), a Java based ABM environment.

The coupled institutional ABM ï flood model being developed in PEARL focuses on long-term institutions related to prevention and mitigation and recovery phases of the disaster management cycle. The following preliminary result (Figure 9-11-11) shows an increase in the number of flooded houses (i.e., ticks 2, 7, 10, 13 and 17) for the same return period of rainfall (i.e., 5 year). The reasons for this can be increase in flood extent and new buildings constructed in flood plains. In the first case, increase in percentage of impervious surfaces because of construction of new buildings resulted in more runoff being generated from the same rainfall intensity. That, in turn, would create much flood covering larger extent. In the second case, most of the new buildings might not obey zoning regulations and not elevate their house.

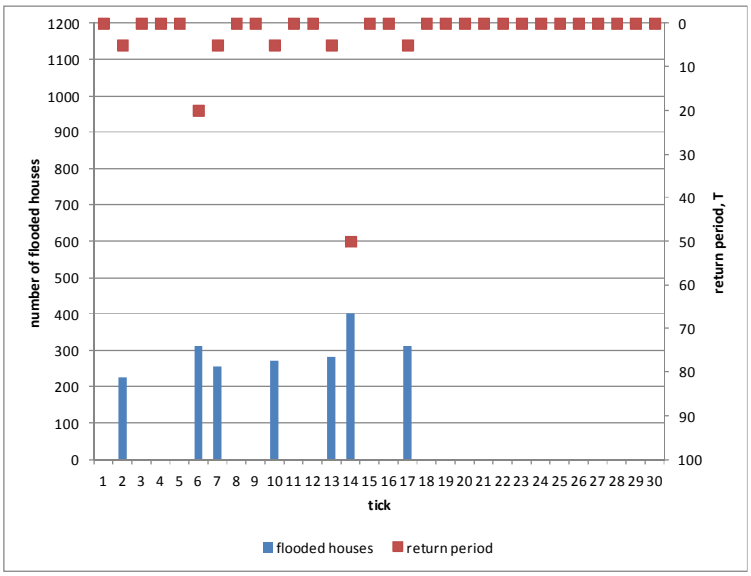

Figure 9-11. Results of a simulation for 30 years of the coupled model ABM and flood risk assessment

Remarks

This research developed and proposed a modelling framework to better represent and simulate the coupled human-flood system. The elements discussed in the human subsystem are agents and institutions that shape agentsôdecisions, actions and interactions. This subsystem is modelled using ABMs as they provide a functionality to represent heterogeneous agents and their institutions. The dynamic link between the two subsystems happens through the urban environment. The coupled ABM-flood modelling method permits to incorporate and model the physical changes made by ñhumansò on the urban environment every time step and assess how that change the flood risk in time. The methodology aims to capture the complex interaction of humans and their urban environment with flood, to simulate feedbacks and co-evolution of the coupled subsystems.

The application of the model in St Maarten, modelling human-flood interaction using coupled ABM-flood models helps to understand the system. In addition, it can be used to investigate possible future directions in flood risk management. The coupled model can also help us to study how levels of exposure (i.e., number of assets-at-risk), flood hazard (i.e., flood magnitude and extent) and vulnerability (i.e., propensity to be affected) change with change in human behavior (i.e., policies and their implementations). The outcomes that we expect from the modellings include the level of risk, in terms of assessed impact, as a way to measure the effectiveness of formal and informal institutions, and types of measures favored, or not, in an urban area based on the social, economic, political, and governance factors.

Strength and limitations of the framework

The strengths as a modelling framework include its functionality to test different policy options. This is better than a simple scenario analysis of structural and non-structural measures as it is also possible to test agentsôbehaviors (reaction) with different constraints and other informal institutions at the same time. The coupled ABM-flood model shows flood risk as a function of time by incorporating implementations that change flood hazard, exposure and vulnerability. This gives a

comprehensive view of flood risk than computing risk from flood event based on a single historical (unchanged) urban environment condition.

One of the limitations of the framework is that modelling two subsystems which are made of other complex subsystems requires lots of data. Adding more subsystems also requires to have a balance between better representations of a system and developing a complicated model, which results are difficult to track and interpret. Another limitation, related to modelling, is that flood model input-output files change depending on the type of software used. This can be a big issue especially when commercial software packages using binary formats are used.

Flood impacts on road transportation using microscopic traffic modelling technique

The impact of extreme hydro-meteorological events on transportation is twofold ï coming from rainfall events and flooding of the road network. First, the extreme weather conditions lead to reduced maximum speed limits (Keay and Simmonds, 2005). As different streets in the network have different speed limits, the atmospheric conditions will define a proportionate speed reduction in each link. The decrease of speed limit will be driven by the intensity and the duration of the rainfall event and it will reduce road capacity before the flood has even occurred. Thus the flood impacts will start evolving in a transportation system, which already has reduced capacity due to heavy rainfall intensities.

Different combinations of intensities of rainfall and storm surges are simulated to produce the time varying flood characteristics. The consequent flood intensities in terms of flood extent, depth and propagation determine whether a street in the road network is going to be closed for traffic. This closure will affect the overall road capacities, the trip definition and the route assignment components of the traffic model

Traffic simulation with SUMO

The SUMO software (Behrisch et al., 2011) has been used to create a basic model, so that the proposed methodology can be tested. The traffic model was limited by the reduced availability of transportation measurement data, but it is believed there are sufficient data to further test the methodology. The model uses the traffic network of the whole island of St Maarten, which is rather large for conventional microsimulation network (total area 87 km2 and nearly 80 000 inhabitants). For example, when 30 cm of flood depth was used as a criterion for street closure, 268 streets in the whole network were identified to be closed and the traffic through them should be rerouted. From a traffic modelling point of view, the road network was going to suffer from 268 accidents, whose temporal characteristics depended on the propagation of the flood. In SUMO terms, each of these accidents had to be represented independently and this posed a problem when multiple scenarios were going to be modelled and discussed. Therefore, to simplify the problem, the test simulations focused on the cul de sac area. The following setting was used to setup the sumo model and some screenshots of the results are showed in Figure 9-12.

- Simulated 5000 vehicles for 3 hours (10 800 seconds)
- A vehicle is inserted each second for the first 5000 seconds of the simulation
- Once the vehicle reaches its destination, it disappears from the network
- The street closures are from 300-5000 s simulation time

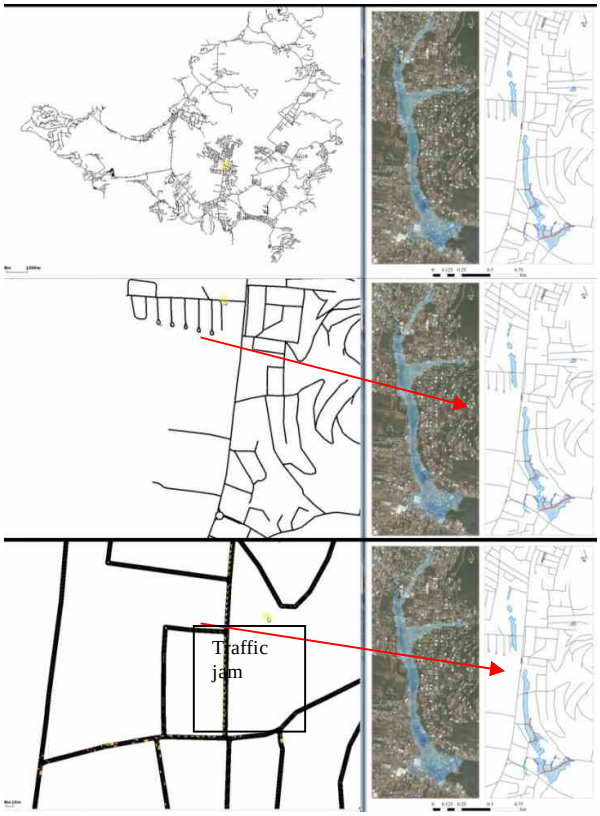

Figure 9-12 Results Sumo model generating traffic jam due to 1:100 year floods

Due to the lack of traffic data, modelling different vehicle classes and purposes of trips are reliant purely on assumptions. However, different vehicle classes can give valuable input, when traffic delays or cancellation of trips are monetized. This is currently represented by the activity based traffic demand model, which generates trips according to synthetic data about population and locations of big employers, schools and shops. However the preliminary results are showing a drop in the amount of running vehicles, which are the ones generating a traffic jams. Figure 9-13 shows the profile of running vehicles over simulation time.

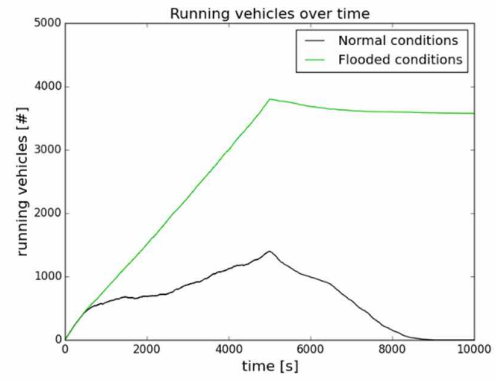

Figure 9-13 running vehicles over time

The results can be summarized as follows:

In terms of travel time

- Å 720 hours of additional travel time (78% increase from the normal scenario)
- Å 1951 vehicles have increase in travel time (57 % of the overall vehicles)
- Å 444 vehicles experienced delays mode than 30 min

In terms of travel distance

- Å 1369 vehicles rerouted (41 %)

In terms of vehicles being indirectly affected

- Å (%vehicles with longer travel time) ï (% vehicles travelled longer distance) =

57%-41%=16% indirectly affected by slower traffic

Remarks

This research presents a novel methodology for assessing flood impacts on traffic. Micro-simulation traffic models are starting to be used to approach that problem, even though only a microsimulation model can capture the dynamics of both the natural and social-technological sphere. The impacts of adverse weather conditions on traffic have been studied in detail, but have never been previously integrated with flood events. This methodology combines the joint impacts of both adverse weather conditions and accumulated floods to road transportation.
Traffic measurements are needed to verify and calibrate the parameters used in the SUMO model to ensure the modelling results can represent the traffic conditions properly. Cost assessment model of travel delays also needs to be adjusted to regional specifications of salaries in Sint Maarten.

The use of Agent Based Models for climate change adaptation and development of large-scale evacuation strategies for flood risk mitigation

This research explores the use of Agent Based models to test different evacuation and communication strategies as a measure for climate change mitigation in cities under threats from floods and flood related disasters. The ABM model was used to evaluate different evacuation strategies in order to minimize risk and to prove the feasibility of new warning dissemination tools. In this context, the following steps were followed: i) creation of a framework to classify human behaviour under extreme hydro-meteorological events. ii) evaluation of ABM to simulate different scenarios for city evacuation under extreme hydro-meteorological events. iii) integration of ABM and GIS for risk assessment management. iv) testing of new technologies for warning dissemination to reduce risk and exposure.
For this proof of concept ABM a total of 6046 agents were initialized using the residential buildings layer. The model was set up to run for an entire week from Monday to Monday and as a start of the simulation it was selected 04:00 hrs. At the beginning of the simulation every agent select a destination and start its movement towards it, which is chosen based on the individualõs classification (Table 1) and according to the day and the time of the day for each agent, going from home to work, leisure, school and so on (see **Error! Reference source not found.**). Into the ABM a hurricane[14] based flood was introduced to test the evacuation capabilities of the agents as full 2D hydrodynamic model. Additionally, in order to explore and evaluate how the provision of warning information can

[14] Hurricane Omar in 2008 was used for this test.

affect the evacuation response and behaviours under extreme hydro-meteorological as a result of climate change, 4 different runs or scenarios were set up in the ABM:

- **Baseline scenario:** The agents evacuate according with the initial set of rules of the ABM, no new information is given to the agents in how to evacuate and the evacuation will be performed based on the "existing" knowledge of the agent.
- **Scenario 1:** A message with the warning and evacuation was sent at the same time to all the population in the island.
- **Scenario 2:** A message with the warning and evacuation was send gradually to all the population in the island, known as stage evacuation.
- **Scenario 3:** A message with the warning and evacuation was sent only to those inhabitants that reside and/or work in the areas to be expected be affected by the hazard event.

Figure 9-14 (a) presents the initial model running and (b) shows the flood coming into the island and agents already in the evacuation process. And Figure 9-15 presents the metrics or performance of each scenario.

(a) (b)

Figure 9-14 Screenshots ABM Sint Maarten.

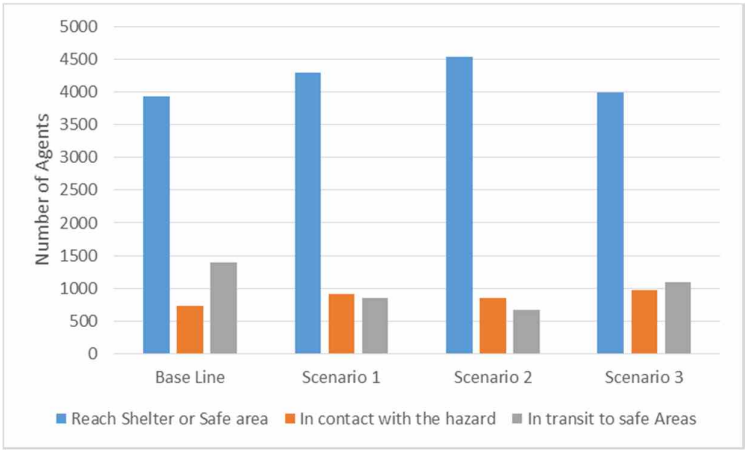

Figure 9-15. ABM Preliminary Results.

Remarks

This experiments explores and demonstrated the feasibility of using ABM to test large scale city evacuations under an extreme flood threat such as a hurricane and also to test different evacuation strategies and has the potential of becoming a powerful tool for operational risk management purposes such as: Determination of evacuation patterns, identification of critical infrastructure, can be used to identify the need to improve existing emergency locations (i.e. number of beds, food storage, etc). This ABM has the potential to test different communication strategies before and during the flooding event is unfolding, to test the effects of warning lead time, the effects of formal and informal communication in the overall performance of an evacuation, etc.

The preliminary results of this research are part of an ongoing effort to enhance the preparedness of European cities at coast location. The next steps in the research is to develop further the ABM including more detail and complex cognition model in order to adjust the behaviour in a more realistic way. The ABM model will be also expanded to include all the inhabitants of the island and more dissemination warnings will be tested in order to gain more insights on evacuation processes to help planner, decision makers and authorities to improve the emergency plans for real cities and to have a final effect on saving lives due to floods in Coastal cities.

References

Alves, A., Sanchez, A., Vojinovic, Z., Seyoum, S., Babel, M. and Brdjanovic, D., 2016, Evolutionary and holistic assessment of green-grey infrastructure for CSO reduction, Water 2016, 8, 402; DOI:10.3390/w8090402.

Basurto, X., G. Kingsley, K. McQueen, M. Smith, and C. M. Weible (2010), A Systematic Approach to Institutional Analysis: Applying Crawford and Ostromôs Grammar, Polit. Res. Q., 63(3), 523ï 537, doi:10.1177/1065912909334430.

Behrisch, M., Bieker, L., Erdmann, J., Krajzewicz, D., 2011. SUMO - Simulation of Urban MO-bility - an Overview. Presented at the SIMUL 2011, The Third International Conference on Advances in System Simulation, pp. 55ï 60.

DHI, 2007. MIKE FLOOD Modelling of Urban Flooding, A Step-by-step training guide.

Fraser Arabella, 2016. PEARL Risk and Root Cause Analysis Brief: St Maarten, Dutch Caribbean.

Fraser Arabella and Sorg Linda. (2016). Deliverable 1.3: Risk and Root Cause Assessment (RRCA) Methodology and Applicability. PEARL project.

Ghorbani, A., P. Bots, V. Dignum, and G. Dijkema (2013), MAIA: a Framework for Developing Agent-Based Social Simulations, J. Artif. Soc. Soc. Simul., 16(2), 9, doi:10.18564/jasss.2166.

Keay, K., Simmonds, I., 2005. The association of rainfall and other weather variables with road traffic volume in Melbourne, Australia. Accid. Anal. Prev. 37, 109ï 124. doi:10.1016/j.aap.2004.07.005

Keller, R.J., Mitsch, B.F., 1992. Stability of Cars and Children in Flooded Streets [WWW Document]. URL http://search.informit.com.au/documentSummary;dn=696127213419517;res=IELENG (accessed 1.5.15).

North, M. J., N. T. Collier, J. Ozik, E. R. Tatara, C. M. Macal, M. Bragen, and P. Sydelko (2013), Complex adaptive systems modeling with Repast Simphony, Complex Adapt. Syst. Model., 1(1), 3, doi:10.1186/2194-3206-1-3.

Ostrom, E., R. Gardner, and J. Walker (1994), Rules, Games, and Common-pool Resources, University of Michigan Press, Ann Arbor, MI, USA.

Rossman, L. A., 2010. Storm water management model user's manual, version 5.0. Cincinnati: National Risk Management Research Laboratory, Office of Research and Development, US Environmental Protection Agency.

Shand, T.D., Smith, G.P., Cox, R.J., Blacka, M., 2011. Development of Appropriate Criteria for the Safety and Stability of Persons and Vehicles in Floods [WWW Document]. URL http://search.informit.com.au/documentSummary;dn=317612923491163;res=IELENG (accessed 1.6.15).

Teo, F.Y., Xia, J., Falconer, R.A., Lin, B., 2012. Experimental studies on the interaction between vehicles and floodplain flows. Int. J. River Basin Manag. 10, 149ï 160. doi:10.1080/15715124.2012.674040.

UNDP. (2012). Flood Risk Reduction: Innovation and technology in risk mitigation and development planning in Small Island Developing States: towards floor risk reduction in Sint Maarten. United Nations Development Programme (UNDP).

USEPA, 2013. Case Studies Analyzing the Economic Benefits of Low Impact Development and Green Infrastructure Programs. Washington, DC.

Vojinovic, Z., 2015. Floor Risk: The Holistic Perspective. IWA Publishing.

Watkins, C., and Westphal, L.M. (2015). People Donît Talk in Institutional Statements: A Methodological Case Study of the Institutional Analysis and Development Framework. Policy Stud. J. 44, S98ï S112.

Wilensky U. (1999). NetLogo. https://ccl.northwestern.edu/netlogo/. Centre for Connected Learning and Computer-Based Modelling, Northwestern University, Evanston, IL, USA.

10 Case Study Ayuttahaya, Thailand

10.1 Description of the study area

10.1.1 *Location, social and economic features*

The historic city of Ayutthaya lies in an island on the Chao Phraya River in Thailand and is at risk of flooding. In 2011, much of the island was inundated following heavy monsoon rainfall over a period of 3-4 months that affected much of Thailand. The historic city of Ayutthaya was an important centre for trade and diplomacy, and its remains has been designated a UNESCO World Heritage site, covering much of the island. Understanding the flood risk to the city and its cultural heritage is a challenge as their value cannot be easily evaluated in monetary terms.

The flood risk to the historic city was assessed by combining estimates of hazards and vulnerability. A community based (or participitory) approach to flood risk assessment was developed and applied in the island. The hazard is estimated through an understanding of the flooded depths. A coupled 1D-2D hydraulic model was used to simulate the flood events of 2011 to produce a flood map with information on the depth of inundation. This model was calibrated and validated to provide confidence of its reliability. The vulnerability was estimated through an approach which takes into account the physical, social, economic and cultural dimensions of vulnerability.

The city of Phra Nakhon Si Ayutthaya is located approximately 70km north of Bangkok, in the Chao Phraya River valley. The location is shown in Figure 10-1.

Figure 10-1 Location of Ayutthaya Island. Approximately one third of the island is protected by UNESCO as a World Heritage Site (WHS).

Ayutthaya Island covers around 720 ha and has a population of over 40,000 people. The city is located within Phra Nakhon Si Ayutthaya district, which is in the Phra Nakhon Si Ayutthaya province. The total area of the World Heritage property is 289 ha and its boundaries are also depicted in Figure 1. The Historic City of Ayutthaya was inscribed on the World Heritage List, since it bears "a unique or at least exceptional testimony to a cultural tradition or to a civilization which is living or which has disappeared" (UNESCO, 2013).

10.1.2 *Main challenges that affect the case study*

Ayutthaya Island is susceptible to fluvial flooding (where river flow exceeds the channel and defence capacity) and pluvial flooding (resulting from extreme intense rainfall, exceeding the capacity of drainage). Additionally, storm surges in the Bay of Thailand can cause increased water levels. The root causes of flooding were identified as the terrain topography in the Chao Phraya River basin, extreme hydro-meteorological conditions, and the lack of proper risk mitigation policies and measures.

To date Ayutthaya Island has experienced two devastating flood events, in 1995 and 2011. During the 2011 flood event the entire island was inundated and the water depth at certain location exceeded two metres. Some images of the flooding are presented in Figure 10-2. The 2011 flood event was caused by a series of consequent tropical storms in the Indian Ocean and lasted longer than one month.

Figure 10-2 The 2011 flood event in Ayutthaya. The entire island was inundated for longer than four weeks.

The 2011 extreme flood event

In late June 2011, heavy rainfall combined with multiple tropical storms happened throughout the extended rainy season, resulting in Thailand's most severe flooding in the last 50 years. Figure 10-3 shows the monthly rainfall totals for 2011, which was above average for the 7 months prior to the floods.

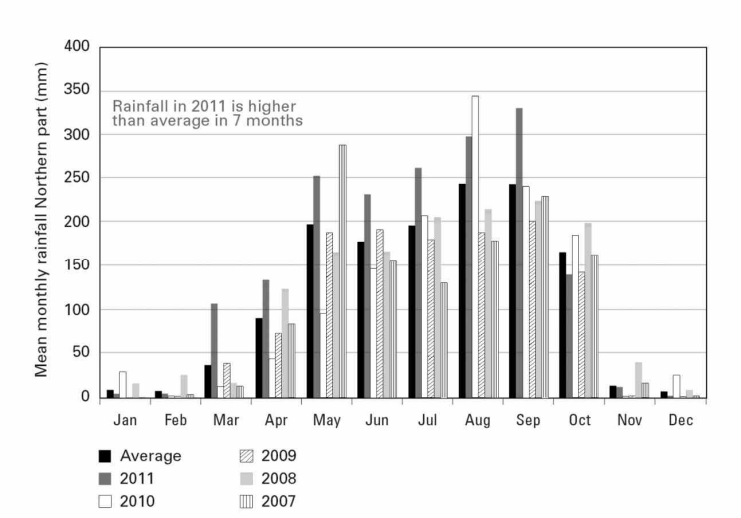

Figure 10-3 Comparison of monthly rainfall in the northern part of Thailand

In mid 2011, heavy rainfall occurred in the North following by a series of monsoons and tropical storms. It started with the arrival of Tropical Storm Haima on June 24-26, followed by Tropical Storm Nock-Ten on July 30 to August 3, accelerating the severity of rainfall across the northern, northeastern, and central parts of the country. The rainfall and floods were again reinforced by Tropical Storm Haitang on September 28, followed by Tropical Storm Nalgae on October 5-6, and Tropical Depression Twenty-four (see Figure 10-4).

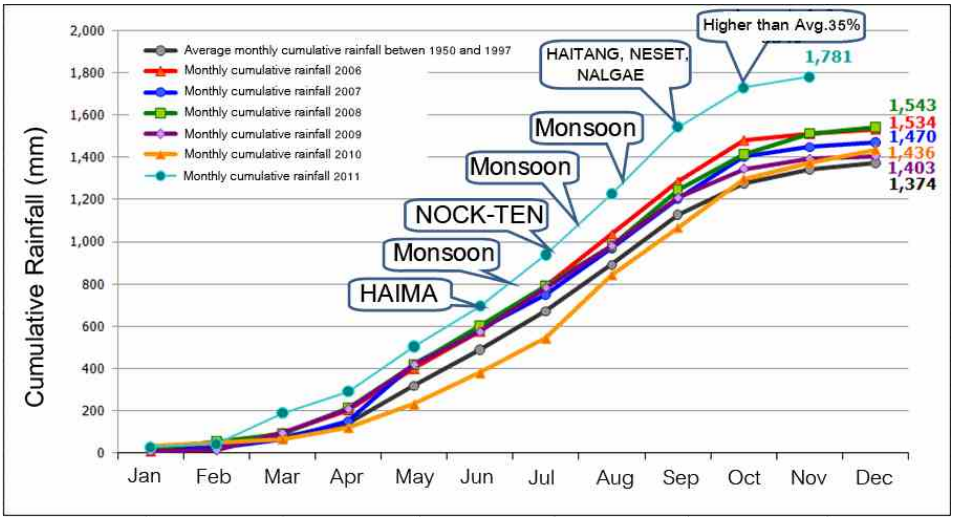

Figure 10-4 Cumulative rainfall and storm events in 2011

When two major dams in the North, the Bhumibol and Sirikit Dams, nearly reached their capacity, they began to discharge excess water. Consequently, more than ten major flood-control structures breached, leading to perfect conditions for severe flooding. The floodwaters flowed southward towards rivers and then traversed through floodplains. 65 of 77 provinces were affected by high flood levels. The total damage-costs were USD 46.5 billion. Over the next two years and beyond, the

rehabilitation and reconstruction costs were estimated at USD 50 billion (GFDDR, 2012). Thailand's economic growth in the fourth quarter of 2011 contracted considerably, reducing GDP growth from 2.6% to 1.0%. Overall, the flooding affected more than 13 million people, and at least 813 fatalities nationwide were reported.

Amongst all the flooded provinces, Ayutthaya Province had the highest numbers of fatalities with 97 deaths. For almost two months, flooding caused damage across the whole province, inundating several governmental offices, public-service buildings, and major industrial estates located near the city. Complex urban areas and historical sites were drowned. In the UNESCO World Heritage Site of Ayutthaya Historical Park (AHP) alone, the damage costs were estimated at USD 22.8 million (Toyoda et al, 2012).

After flooding in 2011, several flood mitigation plan have been proposed for Chao Phraya River basin. During the event of 2011, the capacity of Chao Phraya River at Ayutthaya was about 1,500 cms but the total inflow on 4 Oct. 2011 was about 3,300 cms, which led to significant flooding. Figure 10-5 illustrates the lack of capacity in the current system of rivers and canals around Ayutthaya.

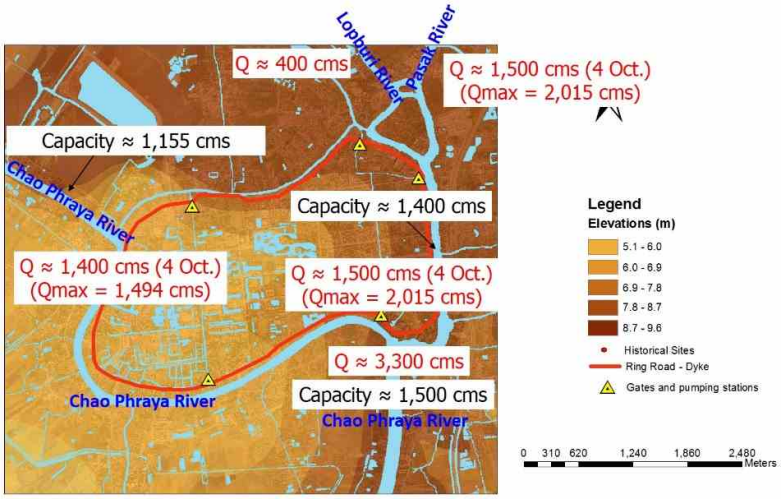

Figure 10-5 Schematization of the capacity of rivers and canals for the flooding event of 2011

Due to the significant amount of water to be transported the studies or developed plans consider mitigation measures at two level of interventions at regional and local scale.

The regional mitigation measures have been identified for the scope of this study. These include an Ayutthaya bypass channel with a capacity of 1,200m3 and the Chainat-Pasak canal with a capacity of 1,000m3. Local mitigation measures include increasing retention/detention pond areas, reviving ancient canals, and increasing the dike height (around the U-Thong Road which runs along the edge of the island).

The main flood management issues in the present situation can be summarized as follows:

- Inadequate drainage capacities;
- Poor condition of natural floodways and retentions;
- Rivers are confined (no room for expansion);
- Many natural floodways and retentions have been deteriorated.
- The main flood protection of Ayutthaya's island is a ring-road which serves as a dike.

10.2 Hazard Modelling and Analysis

10.2.1 *Data availability and sources*

The availabe data set that were used for the research activities is presented in Table 10-1.

Table 10-1 Available information and data sets

Data set	Description
DEM	10 x 10m resolution grid Ÿ resampling to 20 x 20m.
Hydrological Data	Max. Annual Discharges, water levels and rainfall TS.
Land Use	Cultural, Residential and Agricultural areas.
Location of Cultural Assets	Heritage Sites, Non-Heritage Sites.
Chao Phraya 1D Model	Existing model from previous study.
Existing Plans of Mitigation Measures	Projects being studied to reduce flooding.
River Geometry and Hydraulic Properties	XS data, profiles, roughness coefficients, etc.
Flood Protection / Drainage System Data	Elevation and location of dikes.

The hazard component was determined from a simulation of the 2011 flood event. A coupled 1D-2D numerical model using the DHI MIKE FLOOD software was developed to investigate the propagation of excess floodwater from the 1D river model (using DHI-MIKE11) to the 2D floodplain model (using DHI-MIKE21) for the study area.

The domain of the 1D numerical model (see Figure 10-6a) represents the flow dynamics of the lower Chao Phraya Riverbasin (lower CPR) starting from the downstream of Nakorn Sawan province (called the Lower CPR Domain). Another sub-domain of the 1D model (see Figure 10-6b) is focused on Ayutthaya Island (called Ayutthaya Domain) which is the main focus of this study. All 1D numerical setups and calibrations were facilitated by the Asian Institute of Technology (AIT) in Bangkok.

1D modelling setup for the 'Lower CPR Domain' model.

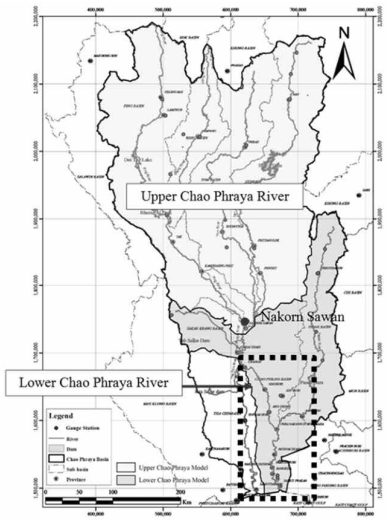

(a)

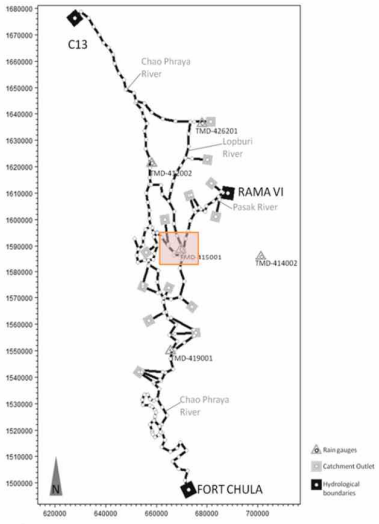

(b)

Figure 10-6 (a) the boundary scheme of the 1D numerical model at lower CPR (map sources: Punya Consultant, 2009), (b) the boundary scheme of the coupled 1D-2D model marked on the 1D model layout.

The time-series of rainfall from five weather stations (see Figure 10-7) recorded by the Thai Meteorological Department (TMD) were used as a boundary condition for a lumped and conceptual catchment rainfall-runoff (hydrological) model using NUM in DHI-MIKE11.

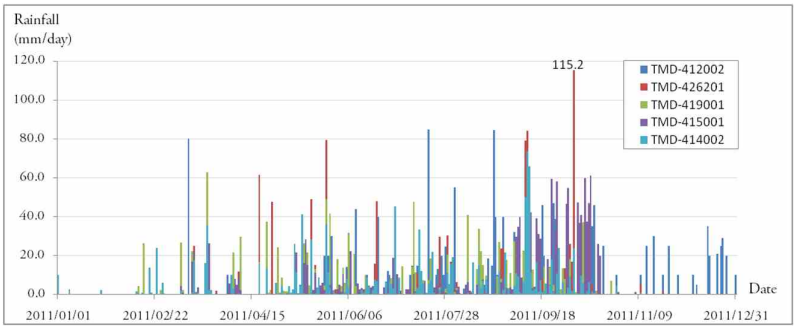

Figure 10-7 Rainfall time-series recorded by five TMD stations

The computed discharge at station C13 (see Figure 10-8), the regulated discharges of Rama-VI dam (see Figure 10-9) collected by the Royal Irrigation Department (RID), and the tidal levels at Fort Chula (see Figure 10-10) collected by the Hydrographic Department of the Royal Thai Navy were used as the boundary conditions to the lower CPR domain model.

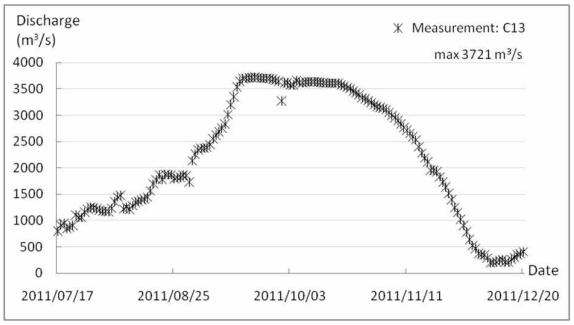

Figure 10-8 Time-series of discharges at Chaophraya River C13

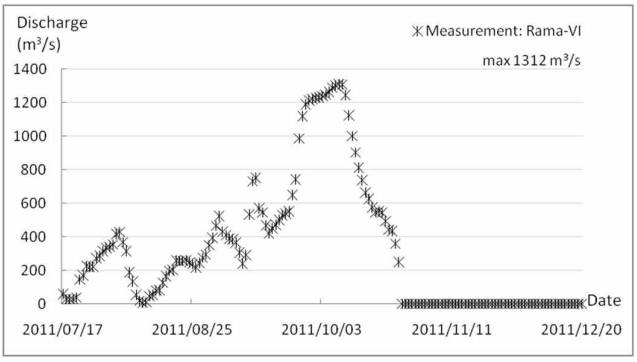

Figure 10-9 Time-series of discharges at Pasak River Rama-VI

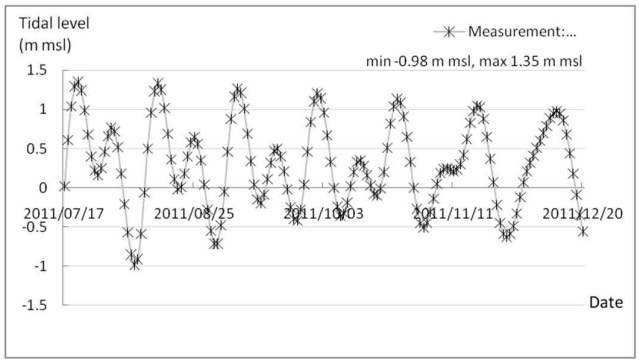

Figure 10-10 Time-series of tidal levels at Chula fort

1D modelling setup for 'Ayutthaya Domain' model

The total length of river modelled is 52 km (see Figure 10-11) surrounding the island by four channels: Chao Phraya River, Pasak River, Lopburi Rive, and Maung Canals. A Manning friction coefficient of 0.02 was applied uniformly to the constructed 1D river networks and following the criteria defined by Chow (1959).

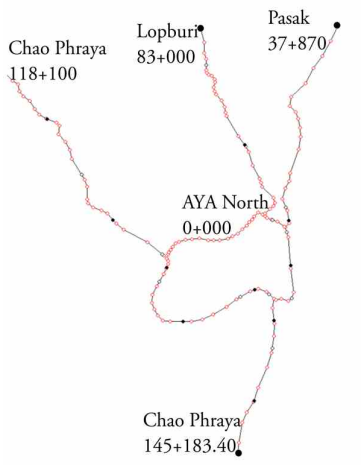

Figure 10-11 1D model layout of the Ayutthaya domain and its boundary chainages

From the Lower CPR simulations, the time series of discharge and water level were transposed, which have then been used as input boundary setups for the Ayutthaya Domain. The boundary conditions were: the discharge and water levels (see Figure 10-12 and 10-13) of Chao Phraya River, the discharge of Pasak River (see Figure 10-14), and the discharges of Lopburi River (see Figure 10-15). However, the model was recalibrated with observed data of discharge and water level at C.35 and S.5 station in the year 2011 by adding site flow at Chao Phraya and Pasak as the boundary conditions.

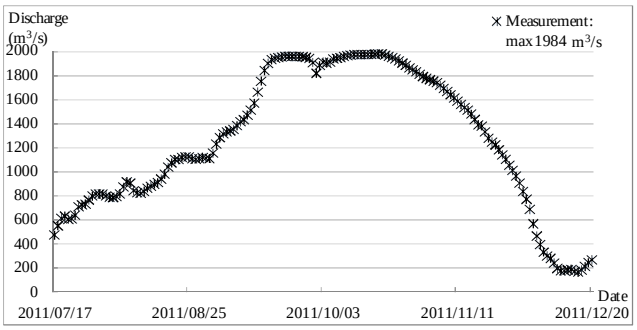

Figure 10-12 Computed time-series data of discharges at chainage 118+100 of Chao Phraya River

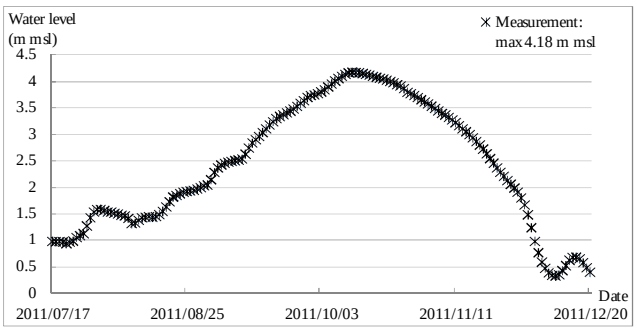

Figure 10-13 Computed time-series data of waterlevel at chainage 145+183.40 of Chao Phraya River

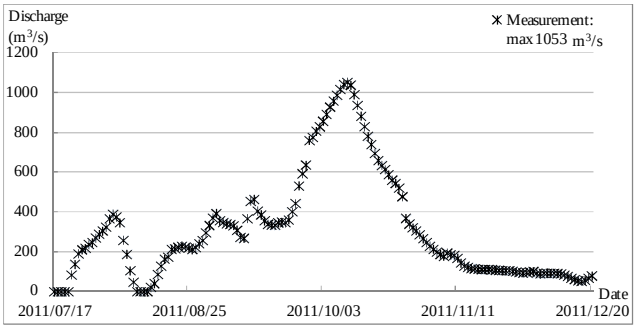

Figure 10-14 Computed time-series data of discharges at chainage 37+870 of Pasak River

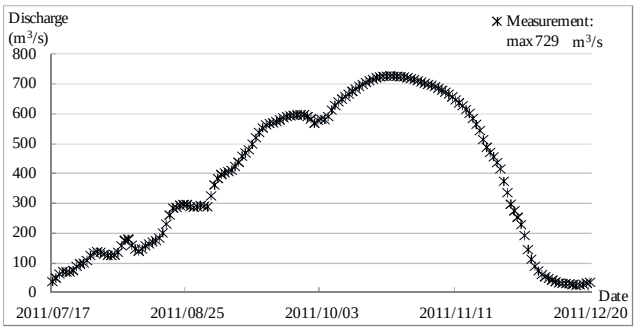

Figure 10-15 Computed time-series data of discharges at chainage 83+000 of Lopburi River

Coupled 1D-2D modelling setup

A coupled 1D-2D model of Ayutthaya was developed to investigate the propagation of excess floodwater from the 1D channels: Chao Phraya Rivers, Pasak, Lopburi, and Maung Canal into the 2D urban area, using the DHI MIKE Flood software.

The 1D model setup was described in the previous section. For the 2D model setup, a 20 m resolution aerial LiDAR DEM was used as the bathymetry input data. The simulation setting of the drying depth is 0.01m and the flooding depth is 0.02m. A Manning's coefficient of 0.033 was used following an earlier study by Keerakamolchai (2014). The time step is 5 seconds with a simulation period from 1 July to 30 November 2011. The schematization of the coupling models is shown in Figure 10-16.

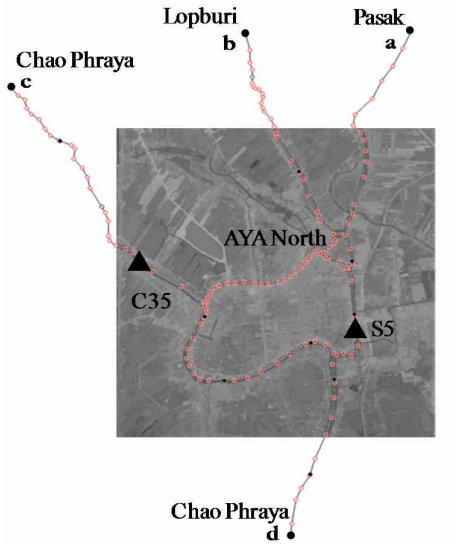

Figure 10-16 A coupled 1D-2D modelling setup.

Validating simulation models

The 1D component of the model was calibrated using observed discharge data at two locations (Station C35 at the Chao Phraya River and Station S5 at the Pasak River). Two metrics are used to quantify the agreement between the modelled and observed daily discharge and river stage (level). The first is the coefficient of determination (R^2). The second is the Root Mean Square Area (RMSE)

the indicators are presented in Table 10-2. Figure 10-17 shows the simulated and observed discharges (a) and river stages (b) at Station C35. Figure 10-18 shows the simulated and observed discharges (a) and river stages (b) at Station S5.

Table 10-2 R^2 and RMSE values to measure agreement between observed and measured discharge and rive level at river stations C35 and S5.

	Discharge		Stage	
Station	R^2	RMSE (m^3/s)	R^2	RMSE (m)
C35	0.98	152	0.99	0.45
S5	0.99	56	0.97	0.55

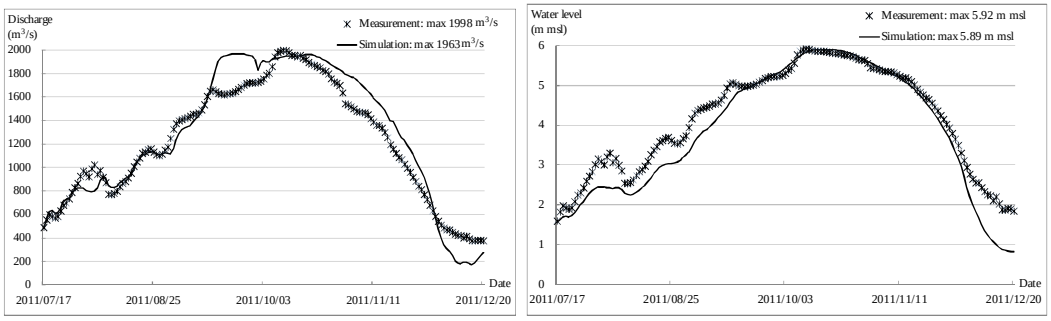

(a) (b)

Figure 10-17 Validation of computed results and measurements at C35 station on Chao Phraya River: (a) discharges, (b) water levels.

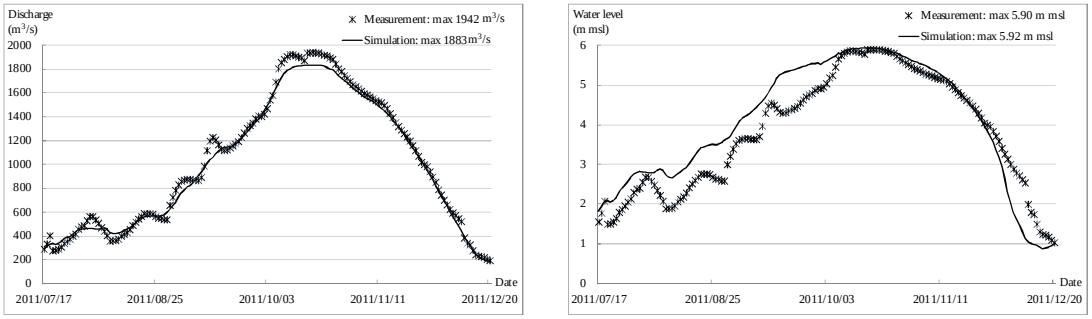

(a) (b)

Figure 10-18 Validation of the computed results and measurements at S5 station on Pasak River: (a) discharges, (b) water levels.

At the C35 station on Chao Phraya River, the coefficient of determination (r2) of discharges in the simulation was 0.98 with the root mean square error (RMSE) differed from the measurements by 152 m3s-1 (see Figure 10-17a). Whereas, the r2 of water level in the simulation was 0.99, the RMSE was 0.45 m msl (see Figure 10-17b). At the S5 station on Pasak River, the coefficient of determination (r2) of discharges in the simulation was 0.99 with the RMSE was 56 m3s-1 (see Figure 10-18a). Whereas, the r2 of water level in the simulation was 0.97, the RMSE was 0.55 m msl (see Figure 10-18b).

The validation of the 2D component of the model was carried out using flood depths in the Ayutthaya area; The Manning's roughness values were adjusted so as to match simulated and observed flood

extents and depths on the island. The average recorded flood depth is approximately 2.0 m while the computed average flood depth was 1.97 m.

Hazard is defined based on the depth of inundation alone. Floodwater velocities in the site are known to low (less than 1 m/s) and can be neglected. A body of research is available about the relationship between flood characteristics and negative consequences, such as the threat to human life (Penning-Rowsell, 2005; Jonkman et al., 2008; Peters-Guarin et al 2012). In this research, threshold depths of < 0.5m, 0.5-1.5m, and >1.5m were used to define the flood hazard as low, medium and high respectively.

Hazard maps

Hazard was defined based on the depth of inundation. Floodwater velocities are known to be very low, less than 1 m/s, and can be neglected. In this research, threshold depths of < 0.5m, 0.5-1.5m, and >1.5m, were used to define the flood hazard as low, medium and high respectively. The results from the MIKE FLOOD model were used to assess hazard, using the simulation of the 2011 flood event. The depth of inundation is used as the parameter to identify the level of hazard as described previously. The resulting hazard map is presented in Figure 10-19.

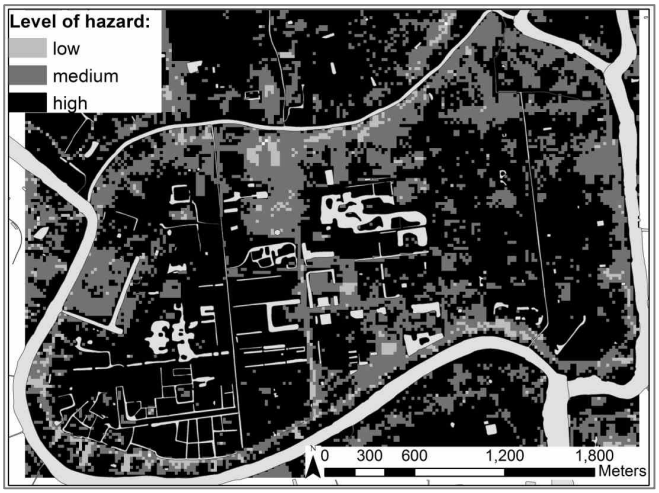

Figure 10-19 Flood hazard map of the extreme flood event in 2011. The levels of hazard are identified based on threshold values of 0.5, 1.5 meters depth of inundation.

10.3 Vulnerability Data and Analysis

Public involvement is critical in the flood risk assessment process and the development of a disaster risk mitigation plan. Communities living within the study area and other stakeholders know much about the flooding and the capacities required to cope with a disaster. Thus, a range of activities were organised in Ayutthaya in order to exploit local knowledge and to contribute to building capacity among stakeholders. The identified stakeholders included organisations at different levels in the governmental hierarchy ranging from local government, through national government and international organisations.

The vulnerability of the island and its communities to flooding in the existing situation (before the application of any mitigation) is assessed following a multidimensional approach.

10.3.1 *Physical dimension*

Four types of building-use were differentiated for the physical vulnerability assessment on Ayutthaya Island: residential buildings, cultural properties, critical infrastructure and roads. For each type of buildings appropriate parameters were defined that affect the degree of potential damage from flooding.

The results of the categorisation and assigning of vulnerability classes are summarised in Figure 10-20.

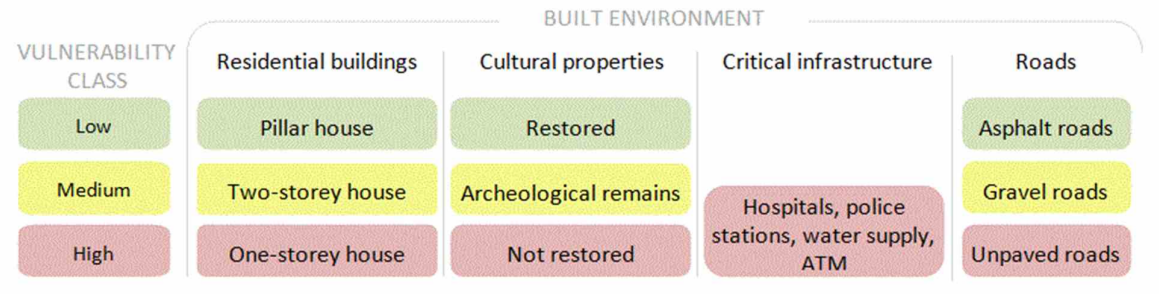

Figure 10-20 Categorisation of build environment into different classes of vulnerability

Critical facilities were identified during the group mapping exercise with community representatives. People pointed out the importance of structures such as hospitals, schools and the university (potential evacuation centres), and some active templates. Moreover, people highlighted that in case of a flood event ATMs do not function which causes serious problems, as people are unable to access cash.

10.3.2 *Social dimension*

The community was chosen as the appropriate scale for assessing social vulnerability. It was determined that Ayutthaya consisted of 33 unique communities through consultation with the director of the Public Affairs Department, Ayutthaya Municipality. A methodology originally developed by the United Nations University was introduced to develop indicators for social vulnerability assessment. In summary, indicators are identified that can measure qualities of the community of interest and their relationship with vulnerability. Data should then be collected to put values against these indicators. These values can be normalised between 0 and 1, and then combined by weighting the importance of the separate indicators, to form a composite index value. Finally, these values can be mapped. In this study, 22 indicators were selected that covered 8 categories (see Table 10-3).

Table 10-3 Parameters and indicators for assessment of the social dimension of vulnerability at a community level.

Parameters	**Indicators**
Susceptibility	
1. Health risks caused by floods	1. Injuries, water-borne diseases caused by floods 2. Access to medical services
2. Vulnerable groups	3. Existence of people with special needs 4. Availability of social support

3. Flood effect on income/livelihood	5. Income lost 6. Access to basic needs during a flood
4. Flood effect to property	7. Type of housing 8. Flood protection measures 9. Property insurance 10. Building conditions
Capacities	
5. Flood awareness	11. Awareness about flood risk 12. Availability and accessibility of flood risk information
6. Flood preparedness	13. Early warning system 14. Emergency response plan 15. Leadership
7. External support	16. Capability to receive support from local authority 17. Capability to receive support from NGOs
8. Community cohesiveness and education	18. Social network 19. Flood effect on psychological health 20. Literacy and education 21. Cultural participation and spirituality 22. Sense of community and belonging

A questionnaire was developed with 42 multiple choice questions to ascertain the values for each indicator. The questionnaire was presented during Focus Group Discussions (FGDs) with approximately 180 representatives from 30 communities.

10.3.3 *Economic dimension*

The analysis of the economic dimension of vulnerability is intended to understand the capacity of the local economy to cope with or adapt to a disaster. The economic dimension of vulnerability was assessed by analysing the response of businesses to flooding during the event and afterwards, in the recovery period. Business Continuity Management theory was used to assess economic vulnerability. Here, a business is considered resilient to flooding if it implements a business continuity plan (PACE, 1998). The vulnerability of a given economic activity was assessed by considering the following parameters:

1. Duration of complete shutdown of the business due to a flood event;
2. Duration of reduced business activity caused by a flood event; and
3. Operational capacity during reduced activity.

20 semi-structured interviews were completed with representatives of business owners in order to evaluate a set of parameters for economic vulnerability. Interviewees were asked to answer questions based on their experience from the 2011 flood event. The economic vulnerability score was calculated using the following equation:

$$VS = I * T_{sd} + I * T_d * C_d,$$

Where: **VS** denotes vulnerability score, I denotes income level before the 2011 flood event, **Tsd** denotes the duration of complete shutdown [months], **Td** denotes the duration of reduced activity [months], and **Cd** denotes operational capacity during downsizing phase [portion in comparison to normality].

Seven business sectors were identified (non-tourist accommodation, non-tourist goods and foods,

non-tourist transportation, tourist accommodation, tourist food and drink, tourist services and tourist transportation). Based on threshold scores of 0-2, 2-4, and 4-6, economic vulnerability was assessed as low, medium, or high. The interviewers went door-to-door to collect data about flood experiences in 2011 and to directly observe some evidence of the damages, such as water stains from previous floods, and broken furniture.

10.3.4 *Cultural dimension*

The cultural dimension of vulnerability was differentiated from other dimensions to capture the effect of flooding on cultural values embodied in various properties. Cultural values include the historical, spiritual, aesthetic, social and other intrinsic values that constitute the cultural significance of a property (Torre, 2002; Vecvagars, 2006). These values can be associated with different attributes of a cultural property, such as its location and setting, materials, form and shape (UNESCO World Heritage Centre, 2012). The level of cultural vulnerability was assessed by considering the *significance* and *sensitivity* of the cultural assets in areas exposed to flooding. Both of these characteristics can be assessed qualitatively. The significance was assessed by consultation with the responsible government department and local community. Each property was assessed on a scale of 1 to 5, where 1 indicates that a property is not culturally significant, and 5 represents very high cultural significance.

The sensitivity of each property was assessed on a scale of 1 to 4, where 1 indicates low sensitivity to floodwaters, and 4 represents high sensitivity. The assessment was completed using expert opinion.

Archaeological remains that are considered significant because of the nature of the materials used in the structure, and where those materials could be damaged or compromised by floodwaters, were assessed as being highly sensitive to flooding. Table 10-4 shows the matrix to define the vulnerability of cultural buildings.

Table 10-4 Matrix to define a level of vulnerability for cultural properties

		Score of property sensitivity			
		low	medium	medium-high	high
Level of property significance	very low	low	low	low	medium
	low	low	low	medium	medium
	medium	low	medium	medium	high
	high	medium	medium	high	high
	very high	medium	high	high	high

10.3.5 *Vulnerability Assessment*

The data collected on each dimension of vulnerability were analysed and mapped in a GIS environment, with vulnerability ranging low (1) to high (3).

Physical vulnerability was assessed using the methodology described previously. *Social vulnerability* was calculated for each of the identified 33 communities, by combining the scores from 8 variables,

using the weights shown in Figure 10-21.

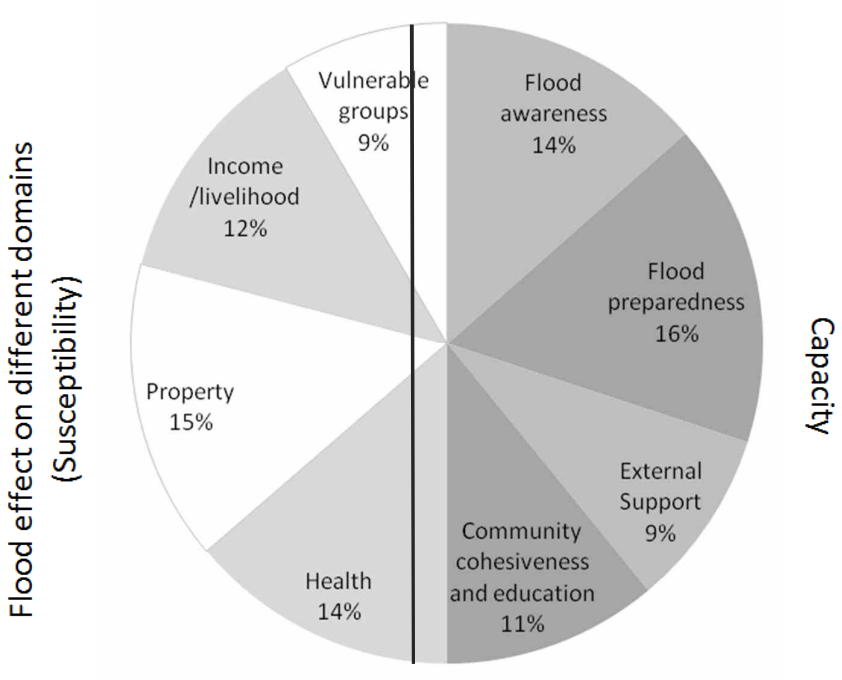

Figure 10-21 A set of eight parameters to assess social dimension of vulnerability at the community level. The percentage indicates the weight of each parameter into overall vulnerability score.

Economic zones were identified through the field work and the level of vulnerability for each type of economic activity was evaluated using three parameters described previously. Vulnerability scores were calculated for seven business sectors (Table 10-5).

Table 10-5 Scores of economic vulnerability for each type of business.

Type of businesses	Shutdown phase [months]	Reduced business activity [months]	Operational capacity during reduced activity [portion in comparison to normality]	Vulnerability score
Non-tourist: accommodation	1	2	0.9	2.8
Non-tourist: goods stores and food	1	3.5	0.2	1.7
Non-tourist: transportation	1.5	2.5	0.2	2.0
Tourist-oriented: accommodation	2.0	3.7	0.7	4.6
Tourist-oriented: food and beverage	3.7	4.0	0.2	4.6

Tourist-oriented: services	2.0	1.5	0.4	2.6
Tourist-oriented: transportation	2.5	3.0	0.8	4.9

Finally, the map of the cultural dimension of vulnerability captures the vulnerability of intangible values embodied within cultural properties (e.g. historic, symbolic, social, spiritual, aesthetic values). The level of cultural vulnerability was identified as a product of the significance of cultural property and its sensitivity to flooding.

Figure 10-22a depicts the footprints of the buildings and infrastructure and their associated levels of vulnerability. The estimated social vulnerability is mapped in Figure 10-22b. The results for economic vulnerability are mapped in Figure 10-22c and the results of the cultural dimension of vulnerability are mapped in Figure 10-22d.

A combined vulnerability map was created by weighting the scores from the separate four dimensions, following a survey at the final consultation workshop. However, because of political upheaval, only 8 participants attended this workshop. This number of participants was not deemed sufficient to obtain accurate results for the appropriate weights. It was therefore decided to give each of the four vulnerability dimensions equal weight. The combined vulnerability map is shown in Figure 10-22e

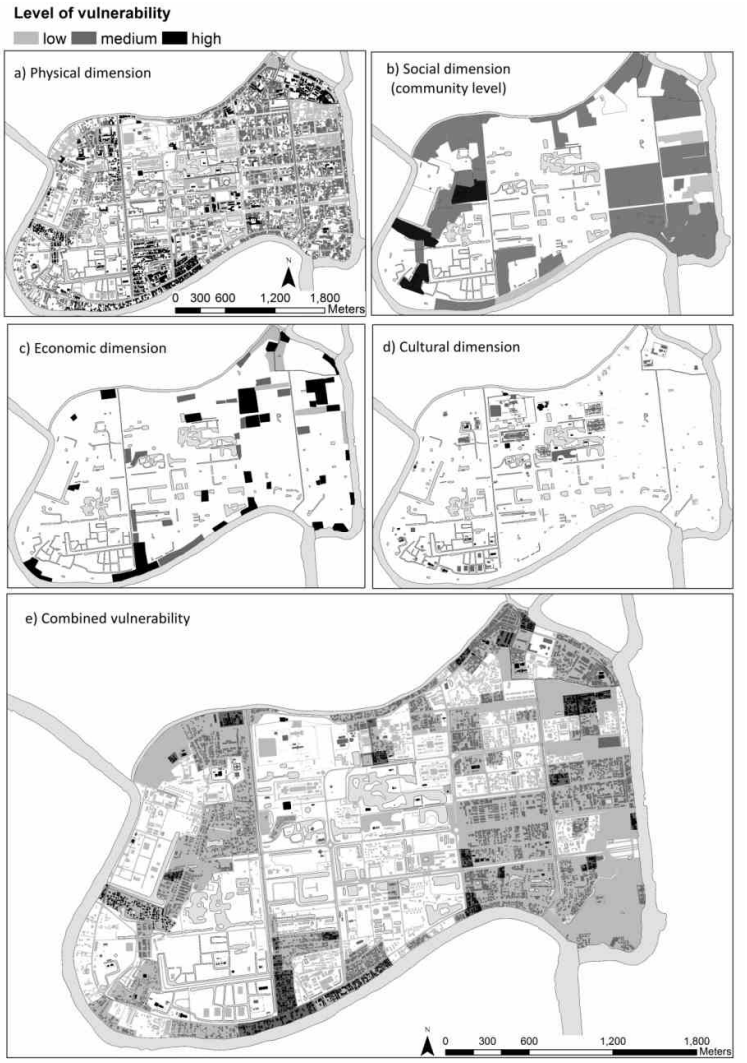

Figure 10-22 Vulnerability maps

10.4 Flood Risk Assessment

Methodologies for flood risk assessment have typically been based on the views and knowledge of experts, excluding the views of the community at large, while employing a technocratic or technocentric approach. The adverse effects of floods often entail far-reaching socio-economic and environmental implications, and may include loss of life and injuries, psychological effects, environmental degradation, and diminution of intrinsic values. Importantly, not all of the impacts can be expressed in monetary terms or other quantifiable units. Therefore, qualitative approaches can be employed to address these factors. The assessment of many of the aforementioned consequences is difficult through expert estimation alone. Therefore, participatory approaches, that facilitate the involvement of various stakeholders, including communities at risk, have been actively developed in recent years.

Vojinovic and Abbott (2012) consider stakeholder participation as a means for realising social justice in flood risk management. The purpose of stakeholder participation is to induce a change in the built

and managed environment that aligns with a positive change in the social environment. The same authors state that successful stakeholder participation requires the traditional engineering way of thinking to change into one where ideas emerge from social concerns and which serve humanity.

The approach used in the study area combined both quantitative and qualitative data and methods,. Traditionally, there has been a focus on using quantitative methods alone to assess risk. The assessment of flood hazard relies on the collection of physical data such as topography and land cover, and combines these with hydrological data to produce physical models of the hazard. The four dimensions of vulnerability are assessed using quantitative data. Physical and economic vulnerability is assessed in monetary terms. A statistical analysis of social and cultural data is conducted to assess vulnerability in those two dimensions.

A qualitative assessment of risk through an estimation of the hazard and vulnerability is conducted using local and expert knowledge to identify vulnerable assets, and questionnaires and workshops to gain knowledge on the expected hazards and the vulnerability of communities.

The quantitative and qualitative assessments are not carried out in isolation, and at each stage, the two assessments are informed by each other. For example, the risk analysis relies largely on quantitative data processing. However, this can be updated with information from stakeholders, and communicated to stakeholders through fora or other means.

10.4.1 *Risk Quantification*

The combined vulnerability hazard maps are raster files with values from 1 to 3, where 1 means low level of vulnerability/hazard, 2 means medium level, and 3 means high level. In order to produce a risk map the vulnerability and hazard raster files are multiplied. An example of a flood risk map produced for the extreme flood event similar to the 2011 flood event is presented in Figure 10-23.

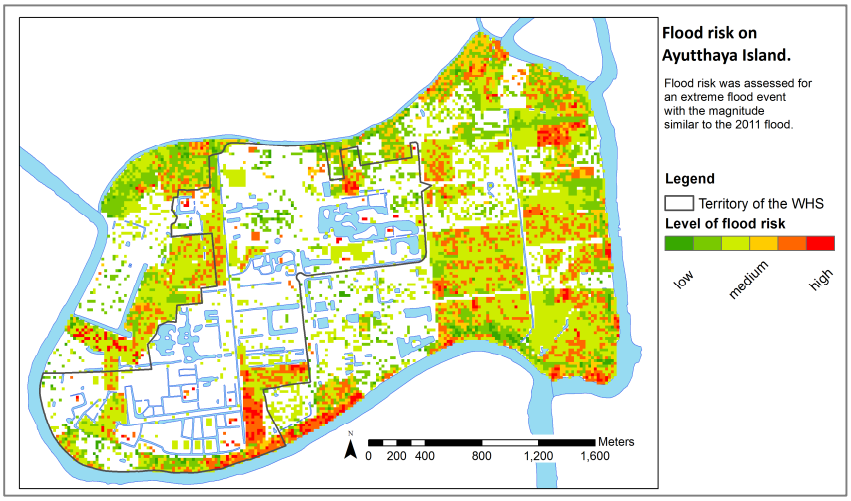

Figure 10-23 Flood risk map of Ayutthaya Island with the current state of flood protection

10.4.2 *Risk perception*

Data collection

A group mapping exercise was used to assess the perception of risk by local communities. Figure 24 presents photographs of this exercise. The facilitator of the exercise first provided an introduction to the concept of risk and then encouraged participants to share their feelings about flood risk in the area of their residence and to voice their thought process out loud. Afterwards, a group of 10-15 people worked together to create a map of the perceived risk for a given area. Participants were encouraged to express an agreed level of risk by colouring in a blank map. Three different colours were used to indicate areas of low, medium or high perceived risks, Figure 10-24.

Figure 10-24 The process and an output example of the group mapping exercise with community representatives.

The direct observations from the discussions demonstrated that from the outset participants tended to assign high level of risk for the entire island. The accompanying comments explain that: "We have an elevated road (U-Thong Road) but when a flood breaches this road, our island is turned into a basin. Inside the island, many roads are elevated to at least +.50 m, thus our small community in the low land area is like a puddle".

Data analysis.

All the information received was converted into a GIS format and a single risk perception map was created for Ayutthaya Island, as shown in Figure 10-25. Even though participants of each group were invited and encouraged to discuss and to colour the area of the Historic City of Ayutthaya, none of the groups did it. It was noticed, that participants were more interested in the areas of their own communities and did not show much interest in the World Heritage Site. Some participants commented that it is the responsibility of appropriate experts to judge the risk for the World Heritage Site and not local residents. Communities' representatives said that they were not aware of the vulnerability and condition, as well as the possible effects of flooding on the properties.

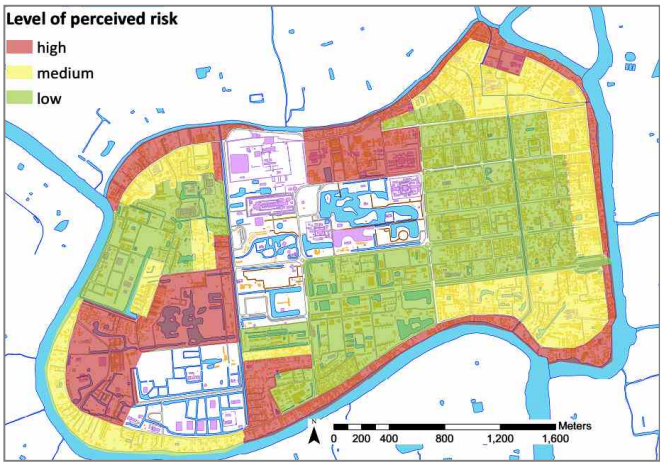

Figure 10-25 Risk perception map based on group mapping exercises.

10.4.3 *Risk Communication*

Characterization of communication means

A range of relevant flood risk related information was identified (e.g. flood magnitude, vulnerability level) which would aid communication in the project. Furthermore, various means and techniques could be employed for risk communication, such as maps, graphics, tables, and charts. Data to analyse the effectiveness of various means were gathered by direct observations during workshops and by questionnaires.

Perception of information from different means

The main objective of the investigation of risk communication means was to understand the ability of local residents and stakeholders to perceive and share information and knowledge through maps and other means. Figure 10-26 shows participants during the workshops.

Figure 10-26 Presentation of the model results to the stakeholders (left). Community representatives work with the satellite image at the municipality office (right).

Workshop activities demonstrated that local residents and stakeholders are able to share flood risk related information (e.g. flood magnitude of past events (duration, depths of flooding), vulnerable

areas, and history of flood events). The preferred means of communication by residents was orally, by telling stories. Participants could easily and precisely describe flood levels during past events at different places beyond their own community with this method.

Most of the workshop participants were literate and could read written materials or respond to questions in written form. However, it was noticed that residents had difficulty in interpreting information from maps and identifying locations. Residents preferred to receive illustrated information rather than written descriptions. For instance, they could easily understand the location when the references to local landmarks were used or photos of the places were provided. Residents talked about depths of inundation and described water levels above the ground, rather than mean sea level. Local units were used for spatial measurements instead of SI units. In contrast, local institutions and the key stakeholders preferred maps and statistical data, both as charts and graphs, as communication means. Table 10-6 summarizes the preferences of local stakeholder to different risk communication means.

Table 10-6 Matrix showing the level of information perception by different stakeholders from various communication means.

Type of information	Location		Depth of inundation			Vulnerabilities	
			Descriptive text				
Communication tool	Map	Descriptive text with references to local landmarks	Map	water level above the ground	water level above the mean sea level	Map	Statistic (tables, charts)
Local residents	-	++	-	++	-	-	+
Ayutthaya Municipality	+	++	+	++	+	+	+
Fine Art Department, Provincial office	+	+	+	+	++	+	++
Hydro- and Agro-Informatics Institute	++	-	++	-	++	++	++
Asian Institute of Technology	++	-	++	+	++	++	++
UNESCO Bangkok	++	-	+	+	+	++	++

"-" ð not possible to perceive information
"+" ð low or moderate level of information perception
"++" ð very good information perception

Preferable channels of information

150 copies of the questionnaire regarding the appropriate sources of flood related information were distributed at the community workshop. 94 completed copies were collected. The results are presented in Figure 10-27.

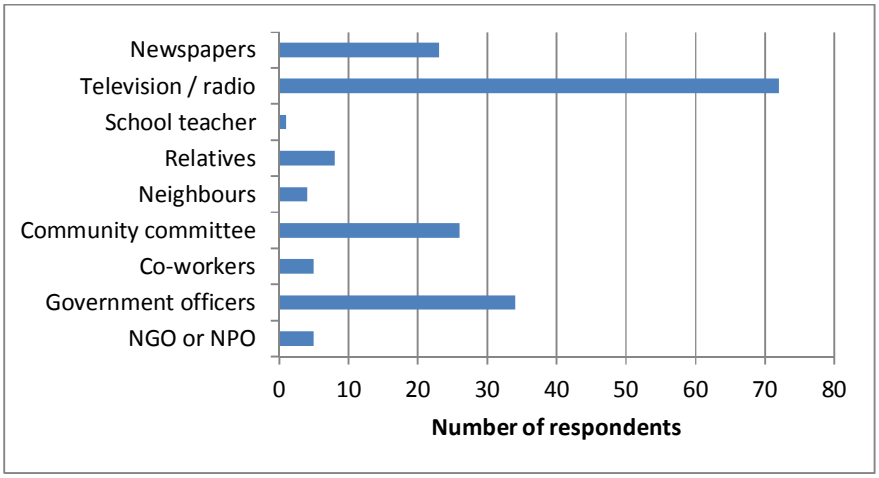

Figure 10-27 Use of different information sources in the context of risk communication among Ayutthaya residents[15]

The results show that 72 from 94 respondents (77%) preferred to receive flood risk related information through broadcast channels such as television or radio. Respondents indicated the timeliness of announcements and easy access as reasons for using these channels. The second most popular source of information was "newspapers", and 23 respondents (24 %) mentioned this medium. 53 respondents (56%) mentioned that they would first follow the news on a television or a radio, and then try to verify information using newspapers. 34 of 94 respondents (36 %) mentioned that information provided by the local government (Ayutthaya Municipality) is also essential. Residents pointed out that Ayutthaya Municipality has a responsibility to take care of local residents and respondents trust this source of information. Particularly, residents rely on the Municipality when information is needed to make a decision to evacuate. During the 2011 flood event, residents could find it difficult to evacuate without guidance from Ayutthaya Municipality.

The majority of the respondents were elderly people, therefore the internet was not considered to be a popular information channel. These residents usually do not use the internet. However, respondents mentioned that in case they need urgent information updates, they would contact younger friends, family members or acquaintances for support. Thus, respondents expressed an understanding of the benefits that the internet could provide in case of emergencies.

10.5 Assessment of scenarios

Differente scenarios can be proposed and assesed by analysing diffetent patterns of different drivers, for example urbanization or climate change. Flood mitigation scenarios can be implemented and evaluated in the hydraulic model by amending the model set up including its geometry and other parameters. The baseline scenario is the existing situation, referred to as Case 1. In this baseline situation (Case 1), the dyke that surrounds the island (U-Thong Road) is maintained at +5.30m, and no other mitigation measures is implemented.

[15] NGO refers to Non-Government Organisation, and NPO refers to Non-Profit Organisation

10.5.1 *Urbanization and land use changes in Ayutthaya*

Aiming at assessing the consequences of various scenarios within WP3, spatially based urban growth models which are able to address the future land change were used. For the development of this task Dinamica EGO (Soares et al, 2011) was used as a land use change model engine to simulate the different scenarios. Dinamica Ego is being used by different researchers to assess scenarios of urban growth (e.g, Pathirana, 2011, Sanchez A. et al, 2014, Sanchez A. , 2013, CORFU, 2014).

Land use maps were collected for Ayutthaya for different years. Depending on the study area these sets can be used to calibrate and validate the model. The following data was collected:

- Satellite Images from Google Maps.
- Shape Files (Buildings, Roads, Railways, Waterways, Places, etc).
- Web documents on case studies cities; both: general and flood related.

Figure 10-28 presents the results of the cellular automata model after calibration for Ayutthaya.

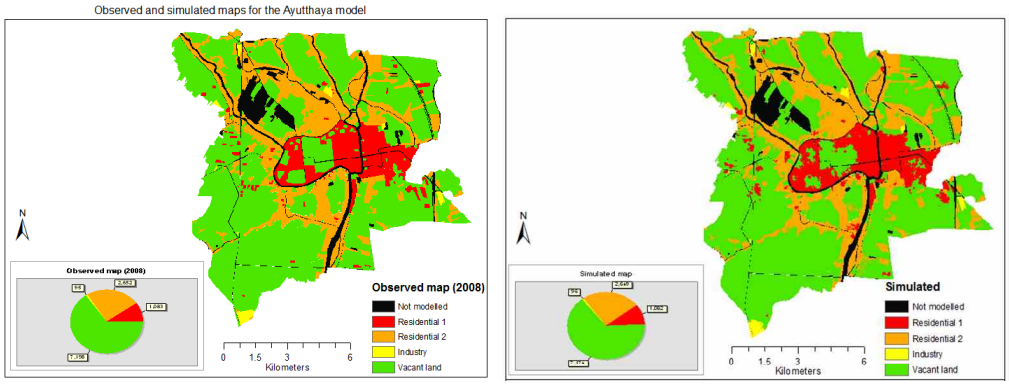

Figure 10-28 Observed and simulated land use map in Ayutthaya after calibration

The simulation of urban growth for the next 30 years allowed an opportunity to explore the possible outcomes of three defined possible scenarios namely, business as usual, sprawl and compact growth. Figure 10-29 shows the results for scenarios of future growth in Ayutthaya. Results show that significant growth would be experienced that have potential to cause gentrification around cultural heritage sites, impact the watershed hydrology, increase the fragmentation of landscapes, change demand for water supply and increase the costs of supplying basic water supply and waste water drainage services to new development areas as well as increase the demand and pressure for services around the areas of cultural heritage

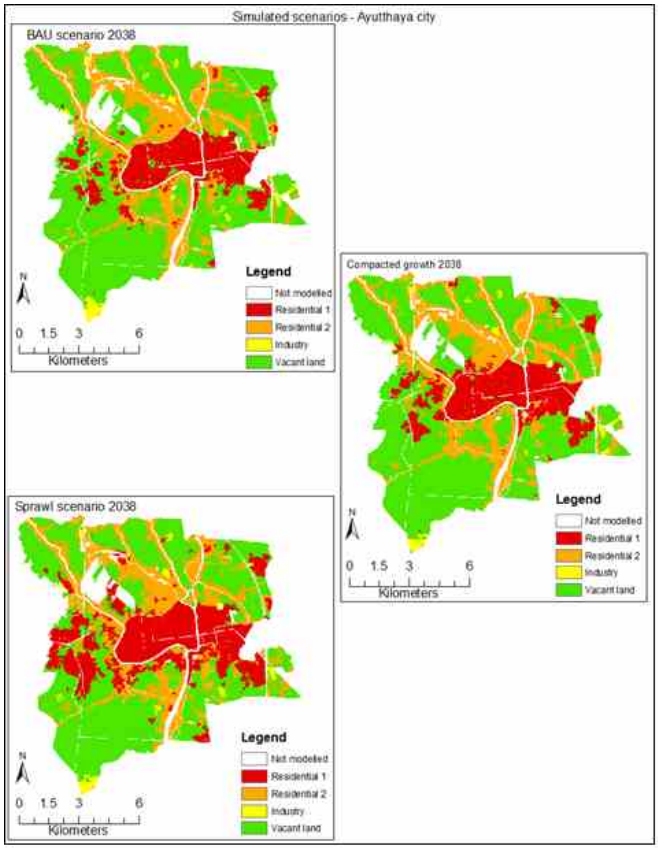

Figure 10-29 Assessment of scenarios of land use change for 30 years

10.5.2 *Flood simulations*

By using a 20 m resolution of LiDAR-DTM as topographic input data for the coupled 1D-2D modelling, a simulated result of the Case 1 scenario shows that the maximum floodwater depths were over 6 m msl in rivers and ponds. In Ayutthaya Island, the area of ~7.8 km^2 was inundated to a depth of approximately 2 m (see marked boundary in Figure 10-30) and the estimated flood volume is ~ 13 million m^3.

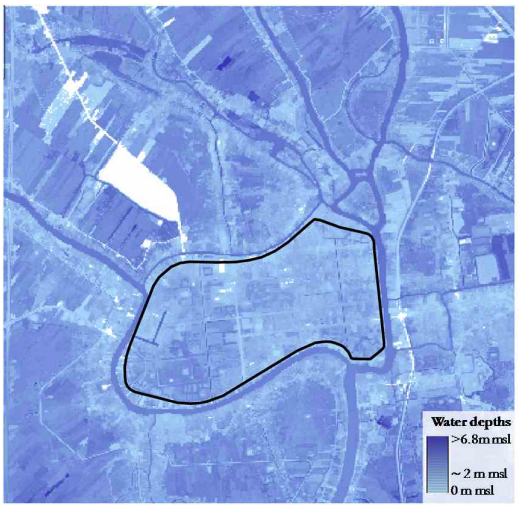

Figure 10-30 Maximum flood depths of the Case 1 scenario when using 20 m resolution of LiDAR-DTM as topographic input data for the coupled 1D-2D modelling

Once the hydrodynamic model has been calibrated and represents well the exisiting condition, it can be used to assess different scenarios and the effectiveness of proposed mitigation measures.

Multifunctional Detention Pond

The first proposed for flood risk reduction on Ayutthaya Island at the local level is the introduction of a system of retention and detention ponds. In order to define appropriate locations for the ponds, three maps were analysed, namely the existing drainage system, land-use, and topography, as shown in Figure 10-31. The locations of the proposed measures are illustrated in Figure 10-32. The lowest area of the Island is the best location for ponds to collect the water through gravity flow. Moreover, the land is vacant, and further development is feasible

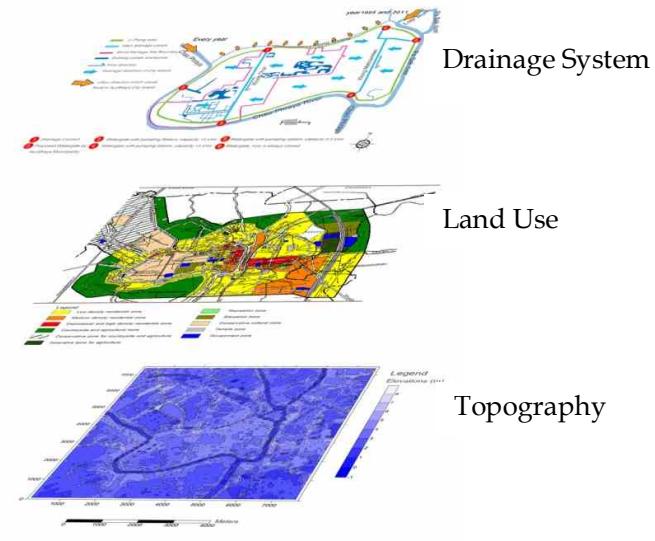

Figure 10-31 Area analysis to identify suitable location for the detention pond system.

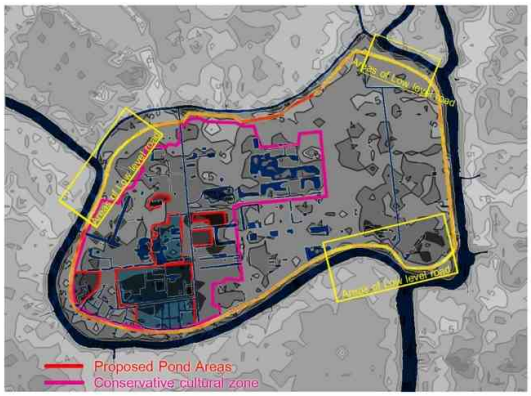

Figure 10-32 Proposed Pond Areas map

This measure includes increasing the pond capacity, establishing the detention pond areas and dredging of existing retention ponds. It is proposed to increase the depth of the existing retention ponds by 1-2 m as shown in Figure 10-33, thus it will increase the capacity of ponds from the existing 519,000m3 to 1,498,000 m3 .

Landscape design

The measures described above could be incorporated into a series of landscape plans to be assessed. For instance, one representation of the proposed water management system is shown in Figure 10-33 includes the revival of ancient canals and their connection to the existing drainage system. This measure improves the drainage system and alleviates flood hazard in the study area

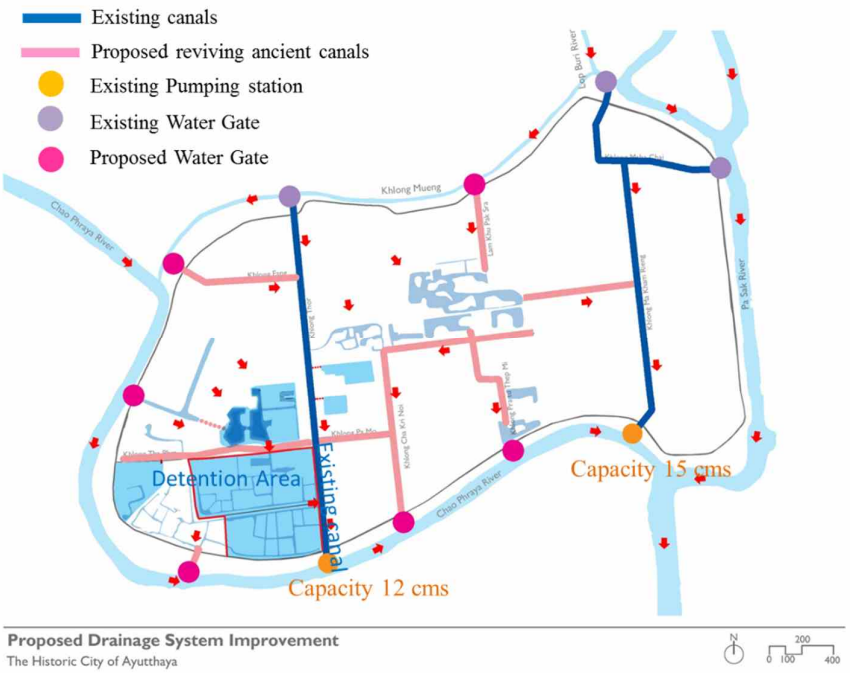

Figure 10-33 Proposed drainage system improvement for Ayutthaya Island.

Figures 10-34a and 10-35b show the behaviour of the system under flood and dry weather conditions respectively. The difference between these two is that the water is to be pumped out from the inland canal network to the Chao Phraya River during a storm or a flood event, and vice-versa during a dry period.

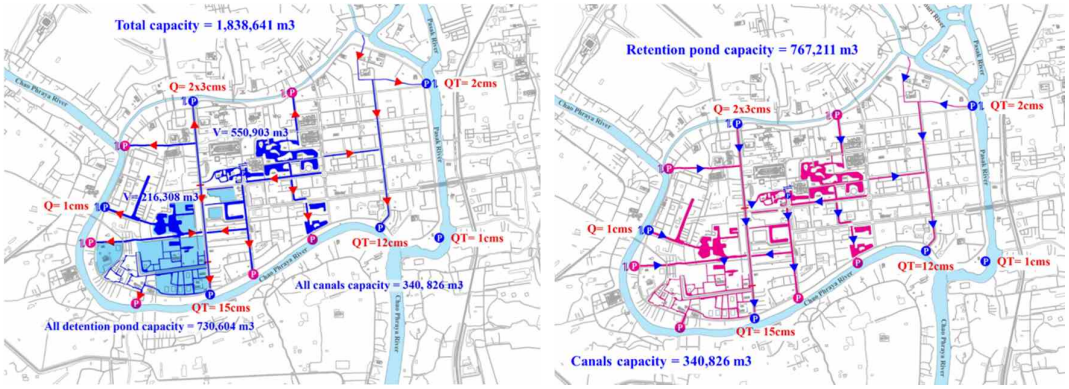

a. b.

Figure 10-34 Water management system during a. flood event and b. During dry period